UNIVERSITY OF LEICESTER

BIOANALYTICAL STUDIES ON THE ASSESSMENT OF VITAMIN D STATUS

Lewis Couchman

Department of Cancer Studies

Thesis submitted in accordance with the requirements for the degree of Doctor of Philosophy in Cancer Studies at the University of Leicester

2016

‘Whoever wishes to investigate medicine properly should proceed thus: in the first place to consider the seasons of the year.’

Hippocrates (circa 400 BC)

Bioanalytical Studies of the Assessment of Vitamin D Status

Lewis Couchman

Abstract

The most widely used and clinically accepted biochemical marker for assessing vitamin D status is the total serum 25-hydroxyvitamin D (25-OHD) concentration. In high-throughput clinical diagnostic laboratories, there is a trend towards the use of fully-automated clinical analysers for such assays. This means that immunoassays are commonly used, despite significant inter-assay variability due to varying concentrations of other related vitamin D metabolites and sample-to-sample matrix differences. It is important for clinicians requesting 25-OHD analyses to understand these issues and limitations, and where necessary to confront laboratories for details of analytical methods used. The availability of reference measurement procedures for 25-OHD based on liquid chromatography and tandem mass spectrometry (LC-MS/MS), whilst not intended for routine clinical sample analysis, should be utilised to improve assay harmonisation and reduce interlaboratory variability. The development of higher-throughput, semi-automated LC-MS/MS methods for routine application is also increasing due to recognition of the pitfalls of immunoassay-based methods for 25-OHD analysis, as well as the opportunity to individually measure multiple vitamin D metabolites. This thesis will discuss the reasons for ongoing 25-OHD assay variability, but will also discuss the novel application of LC-MS/MS to larger molecules related to the assessment vitamin D status. These include the analysis of parathyroid hormone (PTH) and PTH variants, and the three major isoforms of vitamin D binding protein.

Acknowledgements

I wish to thank my supervisors, Dr. Don Jones and Dr. Caje Moniz for their encouragement, advice, assistance and generosity throughout the completion of this work. I'd also like to acknowledge my laboratory colleague at King's College Hospital, Prof. Bob Flanagan for his invaluable input and advice, and for supporting my studies for the last 13 years. Thanks finally to all the staff in Clinical Biochemistry and Toxicology at King's College Hospital, London.

Special thanks also to my wife Katie, to Mum, and to Dad for their continued support, without which this would not have been possible.

Thank you all.

Contents

Chapter Two

Chapter Three

Chapter Four

Chapter Six

Chapter Seven

List of Tables

List of Equations

List of Figures

1.8. Plot of the influence of mobile phase velocity (*u*) on the A term (red), B term (green) and C term (blue) of the Van Deemter equation. Summation of the three terms gives the hyperbolic curve (black), from which the optimum mobile phase velocity (flow-rate) can be deduced.

1.9. The effect of particle size on column efficiency. Smaller particles provide increased efficiency due to (i) smaller particle size distribution (lower A term component) and (ii) reduced efficiency drop at higher mobile-phase velocities due to shorter diffusion paths (reduced effect on C term at increased flow-rates). The term UPLC was trademarked by Waters Corp. for their range of sub-2 µm packing materials. Figure adapted from Flanagan *et al*., 2007.

1.10. A schematic of a superficially porous particle with a 0.5 µm diffusion path and a fully porous particle of the same total particle size. The efficiency of superficially porous particles is increased compared to fully porous particles due to (i) the ability to reproducibly manufacture the particles, reducing the particle size distribution, a factor which lowers the van Deemter A term, and (ii) a reduced C term directly related to the shorter diffusion path. The increased efficiency (which can alternatively be realised by using smaller diameter fully porous particles) comes without an increase in pressure, since the total particle size remains constant.

1.11. HPLC tandem mass spectrometry of a peptide mixture using a triple quadrupole instrument Shown also in this example, an in-line ultra-violet (UV) detector. Precusor ions are isolated in the first quadrupole (Q1), fragmented in the collision cell (also a quadrupole), and specific product ions isolated in the third quadrupole (Q3). Pairs of Q1 and Q3 ion *m/z* values are called 'transitions', and many transitions are monitored during the chromatographic separation of a mixture of components when such instruments are operated in multiple reaction monitoring (MRM), or selected reaction monitoring (SRM) mode. Figure adapted from Hoofnagle & Wener, 2009.

1.12. Schematic of the ThermoFisher Scientific Q Exactive. Shown are (a) the ion source, (b) the isolation quadrupole, (c) the C-trap, used to focus ions prior to entering the Orbitrap, (d) the collision cell used to produce fragment ions in

transfer the retained compounds, via the tee-piece to dilute the contents of the elution loop, onto the analytical column. The valves then return to the positions shown in (a), the eluting pump is used to deliver a gradient to the analytical column, and the TurboFlow column can be washed. By switching Valve A only, the elution loop re-filled for the next injection.

2.2. Multi-channel LC-MS/MS ('multiplexing'). By selecting a data window based on the target analyte retention time, and a suitable window (e.g. ± 30 seconds), a selector valve is used to determine which of the four channels is in line with the MS. The MS detector therefore avoids collecting background signal, and can maximise throughput.

2.3. Mobile phase flow profiles through a column, demonstrating (a) a typical, laminar flow profile and (b) the 'flatter' flow profile with turbulent flow.

2.4. Example 3PLUS1^{TM} MassChrom 25-OHD calibration curves produces using the TFC-LC-MS/MS method. Shown are calibration curves for 25-OHD2 (left), and 25-OHD3 (right). Both calibration curved were constructed using the peak area ratio with that of 25-OHD3-D_6.

2.5. Example TFC-LC-MS/MS chromatograms. The extracted chromatograms on the left show (a) 25-OHD3, (b) 25-OHD3-D_6, and (c) 25-OHD2 from a Chromsystems 3PLUS1^{TM} Level 2 Calibrator, and the chromatograms on the right (d, e, and f) the equivalent chromatograms in a clinical sample.

2.6. Comparison of results (N = 195) between the Diasorin Liaison Total vitamin D immunoassay and TFC-LC-MS/MS methods. Shown are (top) scatter plot with linear regression statistics, and (bottom) Bland-Altman plot with 95 % limits of agreement (µg/L).

2.7. Comparison of results (N = 195) between the IDS iSYS vitamin D immunoassay and TFC-LC-MS/MS methods. Shown are (top) scatter plot with linear regression statistics, and (bottom) Bland-Altman plot with 95 % limits of agreement (µg/L).

2.8. Comparison of results (N = 136) between the Siemens Advia Centaur vitamin D immunoassay and TFC-LC-MS/MS methods. Shown are (top) scatter plot with linear regression statistics, and (bottom) Bland-Altman plot with 95 % limits of agreement (µg/L).

List of abbreviations

1,25-OHD	1α,25-dihydroxyvitamin D (total)
1,25-OHD3	1α,25-dihydroxyvitamin D_3
24,25-OHD	24,25-dihydroxyvitamin D (total)
24R,25-OHD	24*R*,25-dihydroxyvitamin D (total)
25-OHD	25-hydroxyvitamin D (total)
25-OHD2	25-hydroxyvitamin D_2
25-OHD3	25-hydroxyvitamin D_3
3-*epi*-25-OHD	3-*epi*-25-hydroxyvitamin D (total)
3-*epi*-25-OHD3	3-*epi*-25-hydroxyvitamin D_3
ALTM	All-laboratory trimmed mean
amu	Atomic mass unit (based on ^{16}O)
APCI	Atomspheric pressure chemical ionisation
APPI	Atomspheric pressure photo ionisation
BSA	Bovine serum albumin
CKD	Chronic kidney disease
CPB	Competitive protein binding (assay)
CRM	Charge residual model (in electrospray ionisation)
CRM	Certified reference material
CYP	Cytochrome P450
CV	Coefficient of variation (%)

D2	Vitamin D_2
D3	Vitamin D_3
D.A.R.T.s	Disposable automation research tips
Da	Dalton (the unit of mass defined as one twelfth of the mass of the monoisotopic form of ^{12}C)
DEQAS	Vitamin D external quality assessment scheme
DTT	Dithiotreiol
ECD	Electrochemical detection
EDTA	Ethylenediamine tetraacetic acid
eGFR	Estimated glomerular filtration rate
ELISA	Enzyme-linked immunosorbent assay
ESI	Electrospray ionisation
FAI	Free androgen index
FDA	(US) Food and Drug Administration
FGF-23	Fibroblast growth factor 23
FWHM	Full width at half maximum
Gc	Group specific component (see also 'VDBP')
GC	Gas chromatography
GC-MS	Gas chromatography-mass spectrometry
H	Length of chromatographic bed
HEPES	2-[4-(2-Hydroxyethyl)piperazin-1-yl]ethane sulfonic acid
HETP	Height equivalent of a theoretical plate

HPLC	See ‘LC’
HR-AM	High-resolution accurate mass (spectrometry)
IA	Immunoassay
IAA	Iodoacetamide
IEM	Ion ejection model (in electrospray ionisation)
IFCC	International Federation of Clinical Chemistry
IOM	Institute of Medicine
IQC	Internal quality control
IU	International units
IUPAC	International Union of pure and applied chemistry
kDa	Kilodalton (see also ‘Da’, Daltons)
kV	Kilovolts
LC	Liquid chromatography (or high-performance liquid chromatography, HPLC)
LC-MS	Liquid chromatography-mass spectrometry
LC-MS/MS	Liquid chromatography-tandem mass spectrometry
LD	Levenschtein distance
LD	Linkage disequilibrium
LLE	Liquid-liquid extraction
LX	Laminar flow (see also ‘TX’, turbulent flow)
MALDI	Matrix-assisted laser desorption ionisation
mg	Milligrams

mmol	Millimoles
MRM	See ‘SRM’
MS	Mass spectrometry
MS/MS	Tandem mass spectrometry. See also ‘MS^2’
MS^2	Tandem mass spectrometry
MSIA	Mass spectrometric immunoassay
m/z	Mass-to-charge ratio (mass = *m*, charge = *z*)
NBA	Nitrobenzoic acid
ng	Nanograms
NIST	National Institute of science and technology
nmol	Nanomoles
N_t	Plate number (number of theoretical plates)
PFP	Pentafluorophenyl
pmol	Picomoles
ppm	Parts per million
PTAD	4-phenyl-1,2,4-triazoline-3,5-dione
PTH	Parathyroid hormone
PTHrP	Parathyroid hormone-related peptide
Q1	First quadrupole (in a triple quadrupole MS)
Q2	Second quadrupole (collision cell, in a triple quadrupole MS)
Q3	Third quadrupole (in a triple quadrupole MS)

QconCAT	Quantitative concatenation
QQQ	Triple quadrupole
Re	Reynolds number
RIA	Radioimmunoassay
RMP	Refence measurement procedure
SHBG	Sex hormone binding globulin
SISCAPA	Stable isotope standards and capture by anti-peptide antibodies
SNP	Single nucleotide polymorphism
SPE	Solid-phase extraction
SRM	Selected reaction monitoring (or multiple reaction monitoring, MRM)
SRM	Standard reference material. See also 'CRM', Certified reference material
Th	Thomson (proposed unit for m/z)
TIC	Total ion current
TICE™	Tecan immobilised extraction coating
TFA	Trifluroacetic acid
TFC	Turbulent flow chromatography
TOF	Time of flight (mass spectrometry)
TSQ	Triple-stage quadrupole (see also 'QQQ', triple quadrupole)

TX	Turbulent flow (see also 'LX', laminar flow)
µg	Micrograms
µm	Microns
µmol	Micromoles
UPLC™	Ultra-high performance liquid chromatography (Trademark Waters)
UV	Ultra-violet
VDSP	Vitamin D standardization programme
VDBP	Vitamin D binding protein (Gc-globulin)
VDR	Vitamin D receptor
VIM	Valve interface module
v/v	Volume-to-volume

Chapter One

Physiology of vitamin D and introduction to analytical techniques

1.1. Historical background

Although rickets was first described as a medical condition as far back as 1650, it was not until the early 20th century that this bone disease, alongside other pathologies, was linked to dietary deficiencies in the 'vitamine' (Funk, 1911; Hopkins, 1912). Initially, the compound thought to be primarily associated with anti-rachitic properties was vitamin A, which had been isolated from butter fat and cod liver oil, and was shown to be beneficial to xerophthalmia and bone health in rat models (McCollum & Davis, 1913; McCollum, 1914; Mellanby, 1920). Following this, Hopkins reported that heating butter fat destroyed the ability to prevent xerophthalmia. However, McCollum found that whilst Hopkins experiments held true with regards the prevention of xerophthalmia, the anti-rachitic activity of vitamin A remained after similar heat-treatment of cod liver oil, and suggested that 'vitamin A' in fact consisted of two active entities, including the newly-discovered anti-rachitic factor which was called vitamin D (McCollum, 1918; Mellanby, 1924).

The discovery that vitamin D from dietary sources was useful for the prevention of rickets coincided with a second significant observation that the incidence of rickets mirrored the changing of seasons, and the exposure to ultra-violet (UV) light (Hess & Unger, 1921; Hess *et al.*, 1921). It was said that sunlight could cure rickets just as well as cod liver oil (Chick *et al*., 1923; Chick, 1924). It had also been observed that artificial sunlight, in the form of UV irradiation had similar benefits (Huldschinsky, 1919). A number of experiments followed in the next few years (Hume & Smith, 1924; Hess & Weinstock, 1924) which proved the existence of an unknown substance which, when exposed to UV irradiation, possessed anti-rachitic properties. However, it was not until the work of Adolf Windaus (1876-1959), arguably the foremost steroid chemist of the 1920s and 1930s, that the chemical in question was discovered to be the compounds we now know as 7-dehydrocholesterol, and that UV irradiation to the skin converted this chemical to vitamin D_3 (D3) *in vivo* (Holick*et al.*, 1980; Wolf, 2004). Such was the magnitude of this discovery, especially with regards public health and the reduced incidence of rickets in children, that Windaus was awarded the Nobel Prize in Chemistry in 1928 for 'the services rendered through his research into the constitution of the sterols and their connection with the vitamins' (Wolf, 2004).

1.2. Introduction

'Vitamin D' is a single term often used non-specifically to describe a *group* of seco-steroids primarily involved in the regulation of calcium and phosphate. In fact, circulating 'vitamin D' in human serum consists of a highly complex mixture of about 40-50 closely related compounds, of which the biological actions, clinical importance, and analytical relevance of only a relative few are understood (Zerwekh, 2008).

1.2.1. Nomenclature and structures

The most important and widely-studied compounds are vitamin D_2 (ergocalciferol, D2) and D3 (cholecalciferol). Both D2 and D3 can be found in foodstuffs such as oily fish, dairy products including eggs and whole milk, cereals and, nowadays, in a range of fortified food products and dietary supplements. Despite this, and even in countries where dietary intake of vitamin D is high, the majority of circulating vitamin D in humans comprises D3. Photolysis of the B-ring of 7-dehydrocholesterol (Figure 1.1) to pre-vitamin D_3 occurs upon skin exposure to UV B radiation (290-315 nm) from sunlight. Pre-vitamin D_3 then undergoes isomerisation under physiological conditions to form D3 (Holick, 1987; Holick, 2008). The conventional carbon-numbering system used for all vitamin D metabolites arises from those originally assigned to 7-dehydrocholesterol, as defined according to the International Union of Pure and Applied Chemistry (IUPAC) nomenclature for steroids (Figure 1.1). D2 differs slightly from D3 in structure, in that the D2 side chain has a double bond between carbon-22 and carbon-23 and a methyl group at carbon-24. The molecular weights of D2 and D3 are therefore 396.65 and 384.64 Da, respectively. For supplementation, doses can also be prescribed in International Units (IU). 1 IU is the equivalent of 0.025 µg of either cholecalciferol or ergocalciferol (i.e. 1 µg of either compound is 40 IU, Office of Dietary Supplements, available at www.ods.od.nih.gov). In this thesis, measured concentrations of vitamin D metabolites will be referred to using mass units (i.e. µg/L).

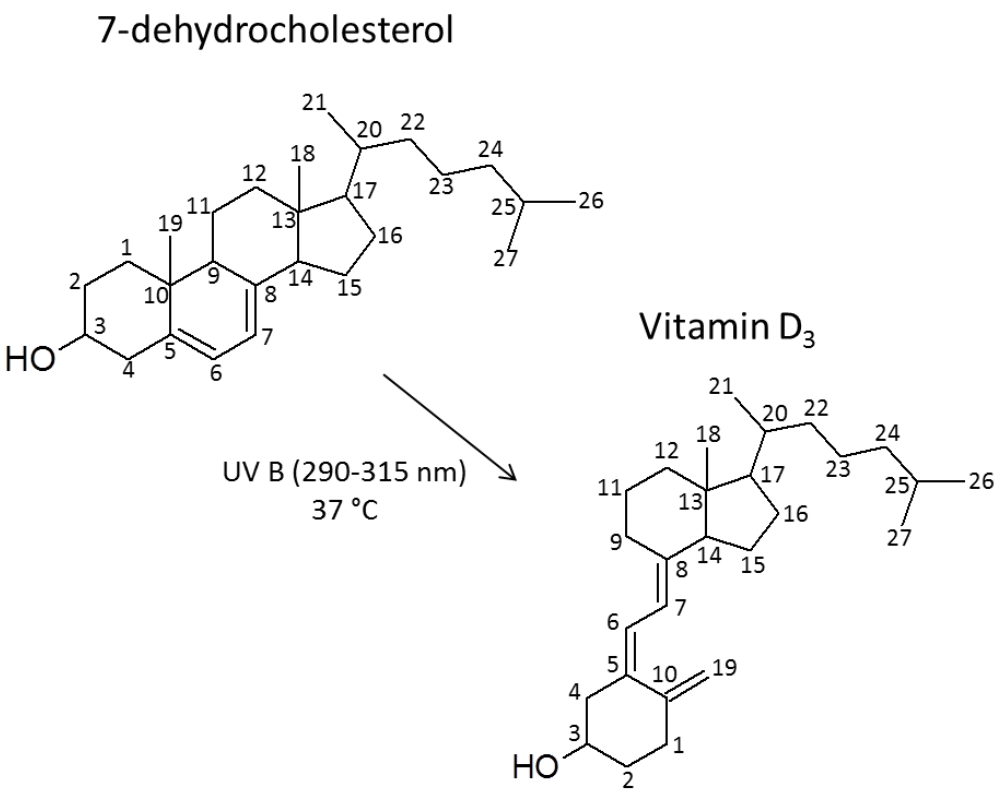

Figure 1.1. Photolysis of the B ring in 7-dehydrocholesterol under UV B irradiation to vitamin D_3 (via pre-vitamin D_3). Also shown is the IUPAC convention for carbon numbering of the vitamin D nucleus.

It is also important for vitamin D metabolites and their chemical derivatives to clearly specify stereochemistry. Side-chain hydroxylation, for example, can give rise to *R* and *S* isoforms, e.g. 24*R*,25-dihydroxyvitamin D_3 (24R,25-OHD3) and 24*S*,25-dihydroxyvitamin D_3 (24S,25-OHD3), and A-ring hydroxylation gives rise to epimeric alpha- and beta- products, e.g. 1α,25-dihydroxyvitamin D_3 (1,25-OHD3) and 3-*epi*-25-hydroxyvitamin D_3 (3-*epi*-25-OHD3).

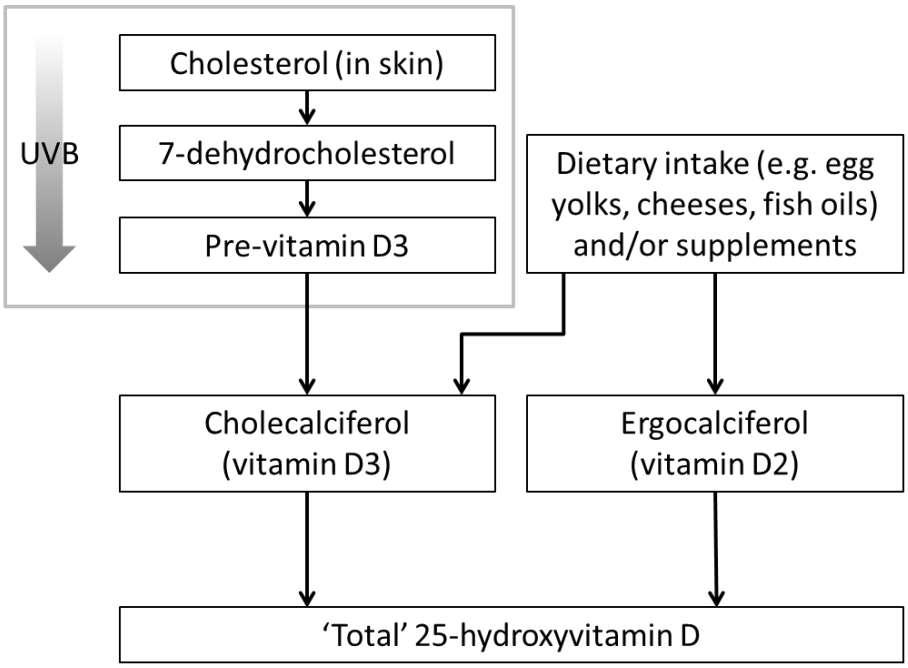

Figure 1.2. Summary of the production of vitamin D_3 via 7-dehydrocholesterol and UV B radiation in the skin, and dietary intake of vitamin D_2 and vitamin D_3.

1.2.2. Vitamin D metabolism and clearance

D2 and D3 can be considered as pre-pro-hormones since they require multiple-stage metabolism (or 'activation') in order to produce the biologically active compounds, which then exert their effects through interactions with vitamin D receptors at the tissue level. The conversion of D2 and D3 to their respective active states is a two-step hydroxylation process. Both compounds are firstly oxidised at the carbon-25 position to produce the pro-hormones 25-hydroxyvitamin D_2 and D_3, respectively (25-OHD2 and 25-OHD3). For clarity, these compounds are sometimes referred to as 25-monohydroxyvitamin D_2 and D_3, and 25-OHD3 is often called calcidiol. *In vivo*, this first hydroxylation of D2 and D3 takes place in the liver, and is catalysed primarily by cytochrome P450 2R1 (CYP2R1, 25-hydroxylase), and to much a lesser extent, or when concentrations are very high, by CYP27A1 and CYP3A4 (Jones, 2012). A human mutation in the CYP2R1 gene causes rickets (Cheng *et al*., 2004). Subsequently, the 25-OHD2 and 25-OHD3 are transported to the kidneys, bound primarily in the circulation to a specific vitamin D binding protein (Gc-globulin, VDBP), but also to serum albumin,

where the second hydroxylation (via 25-OHD-1α-hydroxylase, CYP27B1) at the carbon-1α position occurs (Jones *et al.*, 2012). As with CYP27R1, mutations in CYP27B1 have been shown to cause rickets (Fraser *et al*., 1973). This second hydroxylation step is stereospecific (i.e. 1α rather than 1β). The resulting 1α,25-dihydroxylated species (1,25-OHD) exert their biological activity with regards calcium homeostasis through interaction at vitamin D receptors (VDRs). The production of 1,25-OHD is a tightly-controlled, and dynamic process which takes place in response to small changes and fluctuations in concentrations of calcium and phosphate in the circulation. The function of CYP27B1 is up-regulated by parathyroid hormone (PTH), and down-regulated by fibroblast growth factor 23 (FGF-23). The concentrations of these active species are therefore (i) very low (pmol/L, ng/L), and (ii) fairly dynamic depending upon the time of sampling. In order to maintain appropriate concentrations of the active species, the inactivation and subsequent clearance of 1,25-OHD occurs via a series of hydroxylation and oxidation steps (Figure 1.3), known also as the carbon-24 oxidation pathway, which is catalysed by CYP24A1 (Jones, 2012). It is the action of this same enzyme which results in the production the 24R,25-OHD3, a potentially important metabolite which can be found in the circulation at concentrations 5-10 % of the serum 25-OHD3 (Jones, 2012). Alternative clearance pathways involving the production of lactone metabolites (Figure 1.4) have also been proposed. Whilst the biological function of the intermediates of the carbon-24 oxidation pathway remains to be elucidated, there are suggestions that these metabolites play a role in bone mineralisation (St. Arnaud, 2010). Further, mutations of CYP24A1 in humans have been implicated in idiopathic infantile hypercalcaemia (Schlingmann *et al*., 2011).

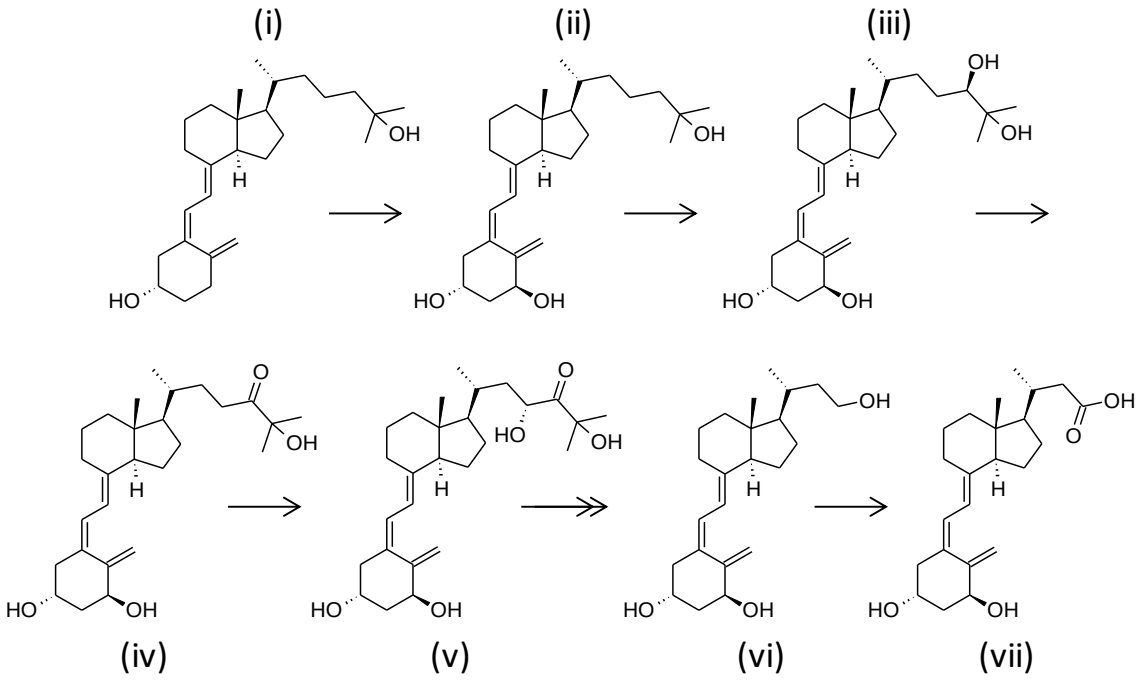

Figure 1.3. Inactivation and further metabolism of (i) 25-OHD3 and (ii) 1,25-OHD3 via the carbon-24 oxidation pathway intermediates (iii) 1α,24*R*,25-trihydroxyvitamin D_3, (iv) 1α,25-dihydroxy-24-*oxo*-vitamin D_3, (v) 1α,23*S*,25-trihydroxy-24-oxo-vitamin D_3, (vi) 1α-hydroxy-23,24,25,26-tetranor-vitamin D_3 and (vii) calcitroic acid. 25-OHD3 can also be directly metabolised to 24*R*,25-dihydroxyvitamin D_3 (not shown).

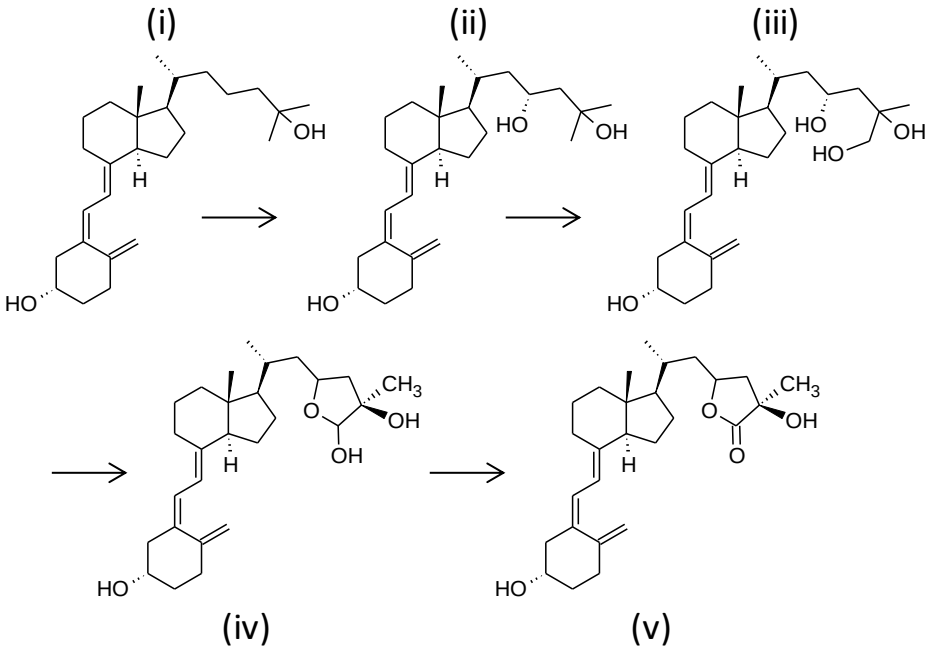

Figure 1.4. Cyclisation of (i) 25-OHD$_3$ via hydroxylation to (ii) 23*S*,25-dihydroxyvitamin D$_3$ and (iii) 23*S*,25,26-trihydroxyvitamin D$_3$, followed by reduction to (iv) 23,25,26-trihydroxyvitamin D$_3$ lactol and (v) 23,25,26-trihydroxyvitamin D$_3$ lactone.

1.2.3. Parathyroid hormone and calcium regulation

Calcium is the most abundant mineral in the body, constituting approximately 1 kg of the total body weight in an average adult (Figure 1.5). The vast majority of this (>99 %) is found in bone as hydroxyapatite, with the remainder found in the extracellular fluid, the gut, and the kidney (Aurbach *et al.*, 1992; Mundy & Guise, 1999). Aside from the structural role of calcium found in the skeleton, calcium is an essential mineral in (i) the release of neurotransmitters, (ii) muscle contraction and relaxation, (iii) a number of intracellular signalling processes, and (iv) as a co-enzyme in the coagulation pathway. In the circulation, plasma calcium exists as free (ionised) calcium (reference range 1.2-1.37 mmol/L), an albumin-bound fraction ('corrected calcium'), and complexed with citrate and phosphate. The reference range for total calcium is 2.2-2.6 mmol/L.

Parathyroid hormone (PTH) is a relatively small (84 amino acid) single-chain peptide synthesised by the parathyroid glands. It is one of the main calcitropic hormones responsible for the tight regulation of plasma ionised calcium (Aurbach *et al.*, 1992). The intact, active form of PTH (PTH1-84), is produced by the sequential cleavage of the initially translated peptide, pre-pro-PTH (115 amino acids), via pro-PTH (90 amino acids). Neither pre-pro-PTH, nor pro-PTH are detectable by immunoassay in plasma samples (Friedman, 2009). PTH1-84 is released into the circulation in response to low extracellular ionised calcium (Ca^{2+}), and is regulated by a classical negative feedback mechanism (Figure 1.6), mediated through calcium-sensing receptors found on parathyroid cells. Circulating PTH1-84 is rapidly cleared (plasma half-life approximately 2-4 minutes), being metabolised by both the liver and kidneys (Garrett *et al*., 2012).

Circulating PTH1-84 acts to increase plasma ionised calcium concentrations through several classically-described mechanisms (Cundy *et al*., 2008) mediated through interaction of the amino-terminal end of the PTH molecule with G-protein coupled PTH/PTH-related peptide (PTHrP) receptors. Firstly, PTH1-84 stimulates bone resorption by osteoclasts (the bone cells responsible for breaking down bone tissue) thus releasing calcium and phosphate from the bone. Secondly, PTH1-84 acts directly in the renal tubules to stimulate calcium reabsorption and inhibit phosphate reabsorption. Finally, PTH1-84 stimulates enzymatic 1-alpha-hydroxylation of 25-OHD

to 1,25-OHD in the kidneys. As mentioned, the active 1,25-OHD directly interacts with VDRs in the small intestine to increase calcium absorption.

PTH also has significant anabolic effects on bone formation when given at low-dose subcutaneously via stimulation of osteoblasts, the bone cells responsible for bone formation. For this reason PTH-based bio-therapeutic anabolic agents including recombinant forms of full-length PTH1-84, such as Preotact® (Nycomed), and truncated forms, for example recombinant PTH1-34 (Teriparatide®, Eli Lilly) are widely used clinically, sometimes in preference to traditional anti-resorptive treatments such as bisphosphonates, for the treatment of osteoporosis in post-menopausal women at risk of fracture (Pliener-Duxneuner *et al*., 2009; Mosekilde *et al*., 2011).

Clinically, PTH1-84 measurement is useful in the diagnosis of hyper- and hypocalcaemia, in the differentiation of primary and secondary hyperparathyroidism, for example related to parathyroid cancers, and in the prevention of bone mineral disorders in renal patients.

The calcitropic peptide hormone calcitonin exhibits short-term effects largely opposite to those of PTH1-84. Calcitonin is a 32-amino acid peptide, synthesised and secreted from the parafollicular cells in response to high plasma ionised calcium. Conversely, a fall in plasma ionised calcium inhibits calcitonin secretion. Primarily, calcitonin acts to reduce plasma ionised calcium by inhibiting osteoclast activity, but it has also been shown to inhibit the absorption of calcium in the small intestine, and to inhibit the reabsorption of calcium in renal tubular cells. As with parathyroid hormone, calcitonin (most commonly salmon calcitonin) is used therapeutically in the treatment of conditions which cause chronic hypercalcaemia, such as Paget's disease. However, calcitonin is thought to have little effect on chronic calcium homeostasis, since clinical observations have shown that neither calcitonin-deficient patients (e.g. athyroid patients), nor those with medullary thyroid cancer and excess calcitonin production experience alterations in calcium homeostasis (Mundy & Guise, 1999).

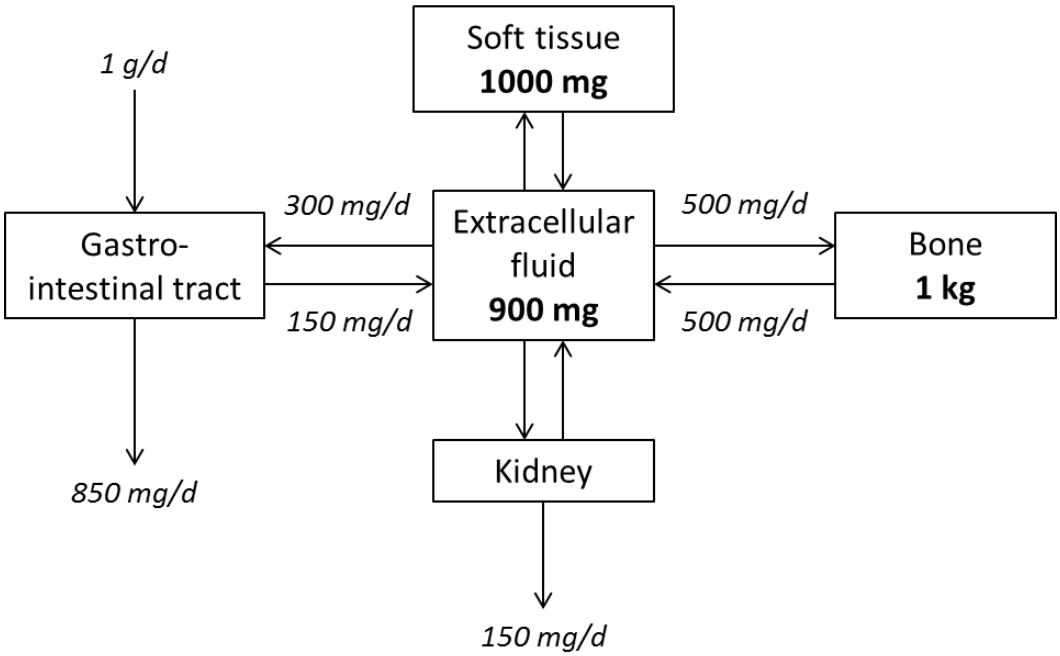

Figure 1.5. Typical calcium homeostasis in a healthy adult over a 24-hour period.

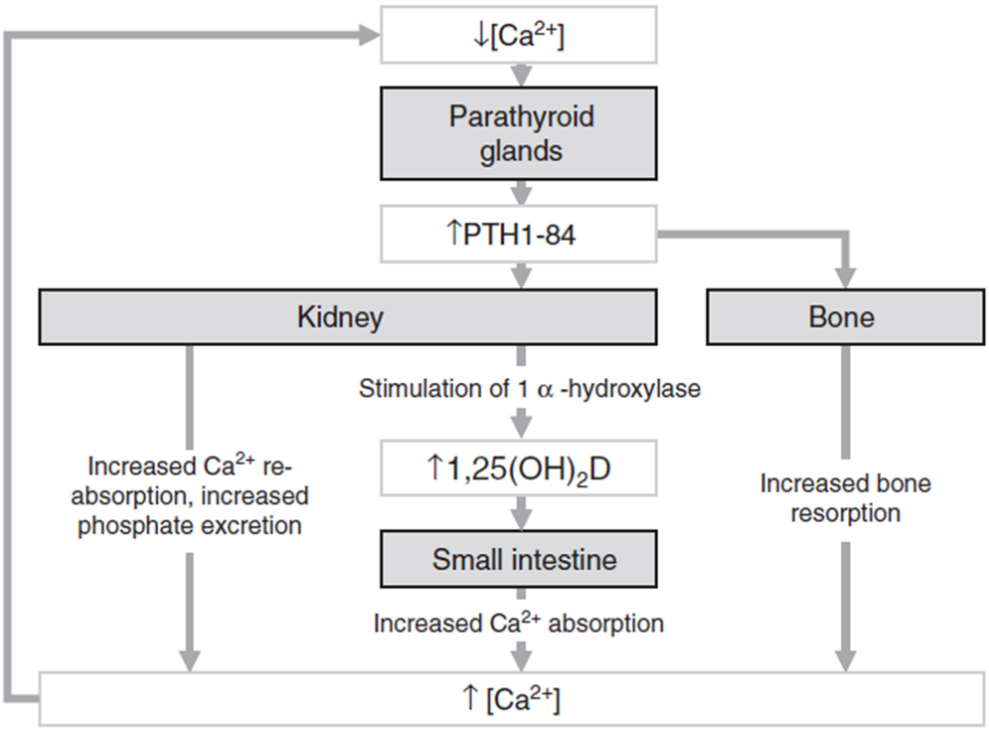

Figure 1.6. Physiology of calcium (Ca^{2+}) regulation via PTH1-84. PTH1-84 secretion is increased in response to low plasma ionised calcium, and acts to increase total 1α,25-dihydroxyvitamin D concentrations via stimulation of renal 1-α-hydroxylase, subsequently increasing calcium absorption from the gut. PTH1-84 also stimulates osteoclastic bone resorption, and directly increases renal calcium reabsorption.

1.3. Vitamin D status

An individual's vitamin D status defines whether they are vitamin D deficient, sufficient, or intoxicated (Holick, 2009). Hence dietary vitamin D intake/absorption, circulating concentrations of vitamin D metabolites, and the interaction of vitamin D metabolites and other hormones such as PTH, all play key roles in maintaining calcium homeostasis and defining one's vitamin D status. Since calcium is an essential mineral, it is involved in a number of vital physiological processes, as well as a number of pathophysiological states. Consequently, vitamin D sufficiency, or vitamin D repletion, is associated with optimal functioning for a number of physiological processes. As will also be discussed, vitamin D insufficiency, or deficiency, has been associated with a number of different pathologies, and vitamin D supplementation is more and more commonly advocated. In order to assess whether an individual is vitamin D replete or vitamin D deficient, a biochemical investigation to assess vitamin D status is required.

Currently, the most widely used and accepted biochemical marker for vitamin D status is the serum concentration of total 25-OHD (Holick, 2007). This is paradoxical, since 25-OHD itself is biologically inactive and, as has been discussed already, a large number of other vitamin D metabolites and hormones are involved in calcium homeostasis. The rationale for using this as the biomarker for vitamin D status, rather than total 1,25-OHD, the active moieties, is that 25-OHD is thought to represent the 'body store' of vitamin D. Compared to D2 and D3, which have very short half-lives in the circulation, 25-OHD has a half-life of 2-3 weeks (Holick *et al*., 2011; Vogeser *et al*., 2014). On the other hand, 1,25-OHD is found at much lower, and more dynamic, concentrations. Not only does this have analytical implications, but it is well recognised that the dynamic nature of 1,25-OHD concentrations makes correlation with clinical findings, or concentrations of other vitamin D metabolites, difficult. Indeed, serum 1,25-OHD is frequently normal, or even elevated in subjects with vitamin D deficiency, due to secondary hyperparathyroidism (Holick *et al*., 2011). Recently, Vogeser *et al*. (2014) reviewed the current approach to assessing vitamin D status. Given the complexity of this biological system, it is perplexing that only a single marker is so widely used to assess vitamin D status; clearly in some situations this approach is clinically useful, e.g. to confirm severe vitamin D deficiency. However, given that inter-individual variability

in vitamin D metabolism has been widely observed (e.g. mutations in enzymes involved in vitamin D metabolism, polymorphisms in VBDP), for large population-wide studies, and as a measureable outcome in randomised controlled trials, it may be more useful to measure a series of biomarkers to give a more complete picture of true vitamin D status.

1.3.1. Vitamin D sufficiency/deficiency and vitamin D supplementation

Vitamin D has in recent years become a public health concern. Despite a lack of consensus amongst world experts on either (i) the classification of individuals as deplete/replete based upon their 25-OHD concentration, or (ii) the best strategy and dosing regimen for vitamin D supplementation, the health concerns associating vitamin D deficiency with a wide range of pathologies has been extensively publicised, and vitamin D deficiency is considered to be a global pandemic (Holick, 2007; 2008).

1.3.1.1. Reference Ranges

The concentration of 25-OHD which constitutes sufficiency is still fairly widely debated, even amongst expert groups such as the Institute of Medicine (IOM, 2011; Ross *et al*., 2011) and the Endocrine Society (Holick *et al*., 2011). As of 2013, there was no international consensus on the 'normal' 25-OHD serum concentration. It is suggested by many experts in the field that optimal vitamin D status should be defined by a total serum 25-OHD concentration greater than 30 µg/L (Hossein-Nezhad & Holick, 2013; Heaney, 2013), and that the concentrations associated with deficiency are from 10-20 µg/L (Heaney, 2013; Bischoff-Ferrari*et al*., 2016). There is disagreement as to whether 20-30 µg/L is 'sufficient' (Rosen *et al*., 2012). Published guidelines issued following an international meeting of vitamin D experts held in Warsaw, Poland, in 2012 (Pludowski *et al*., 2013) concluded that (i) vitamin D deficiency should be defined as a concentration of 25-OHD less than 20 µg/L, (ii) concentrations of 25-OHD between 20-30 µg/L were 'suboptimal', and (iii) the target concentration for 25-OHD should be 30-50 µg/L, or even up to 100 µg/L. The latter of these suggestions, i.e. that higher concentrations of 25-OHD may be required in some individuals, was in agreement with

previous suggestions in the literature (Holick, 2007; Holick *et al*., 2011). In the UK, the National Osteoporosis Society issued summary guidelines in 2013 which recommended that individuals with a 25-OHD below 30 nmol/L (12 µg/L) should be considered deficient, that a 25-OHD from 30-50 nmol/L (12-20 µg/L) may be inadequate for some individuals, and that a 25-OHD greater than 50 nmol/L (20 µg/L) was sufficient (Aspray *et al*., 2014).

Most of the differences in opinion regarding what concentration of 25-OHD constitutes adequate vitamin D status arise from the fact that if certain insufficiency concentrations are assumed, very high proportions of the population would be classified as vitamin D deficient, despite a very high percentage of these individuals having no clinically observed bone disorders. Furthermore, although there are huge numbers of observational, or associative studies which provide data linking vitamin D deficiency to a diverse range of pathologies, there are very few high-quality randomised controlled trials relating these pathologies to vitamin D supplementation (Allan *et al*., 2016).

1.3.1.2. Supplementation strategies

Given the apparent prevalence of vitamin D deficiency, a number of clinical supplementation strategies have been reported in the literature. Since the vast proportion of circulating vitamin D metabolites arise from exposure to sunlight rather than via dietary intake, certain populations with lower exposure to UV B radiation are considered to require greater supplementation than others – this may be as a result of either geographical location, or ethnic, cultural, or social behaviour differences. Seasonal supplementation during winter months is advocated by some (Pasco *et al*., 2004; Vogeser *et al*., 2014).

Guidelines for vitamin D intake have been published by the Institute of Medicine (IOM, 2011, Ross *et al*., 2011), and the American Endocrine Society (Holick *et al*., 2011). Both of these documents can be considered an improvement on the preceding 1997 IOM document, which recommended just 200 IU/d for maintaining skeletal health – a dosage which is unlikely to increase 25-OHD concentrations to optimal levels (Bischoff-

Ferrari *et al.*, 2006). Although there is broad general agreement between the two guidelines, suggesting between 400-2,000 IU/d depending on age and sex, there are some significant discrepancies between these recommendations, which may reflect differences in the goals of the two groups – the IOM recommendations were intended for healthy individuals and the general population, whereas the endocrine society recommendations were aimed at individuals at risk of vitamin D deficiency (Rosen *et al*., 2012; Pramyothin & Holick, 2012). There are also a number of studies investigating the effect of large bolus doses (e.g. 50,000 IU two weekly, Demetriou *et al*., 2012; 300,000 IU, Turner *et al*., 2013) of D2 or D3 on vitamin D status.

1.3.1.3. Vitamin D toxicity

Vitamin D toxicity is rare (Rajakumar *et al*., 2013; Bell *et al*., 2013), but a few cases, mostly in children, are reported in the literature. One such case reports a 2-year-old boy who ingested a total of 2,400,000 IU of vitamin D in the form of 4 ampoules of vitamin D supplement drops (Raquiferol® D3) over a four day period (Barrueto *et al*., 2005). The recommended dose for this supplement was 2 drops per day, but the child was given 1 ampoule per day. The child presented with severe abdominal pain and biochemical tests revealed resistant hypercalcaemia. The peak serum calcium was 15.0 mg/dL (3.75 mmol/L), and 25-OHD peaked at 470 µg/L (1,175 nmol/L). After a two-week inpatient stay with administration of intravenous fluids, the child made a full recovery.

1.3.2. Vitamin D and pathology

It is known that severe vitamin D deficiency causes rickets in children and osteomalacia in adults (Holick, 2006; Holick, 2007). This finding fits with the very early observational studies of workers in this field in the 1920s. However, it appears that the actions of vitamin D are not limited to calcium homeostasis. More recently, vitamin D status (typically by surrogate measurement of 25-OHD, using any one of a number of analytical methods) has been linked to a much wider range of pathologies, and has been suggested (either directly or indirectly) to up- or down-regulate a large number

of gene functions. It has been shown that the VDR is almost ubiquitous, and is expressed in a wide variety of cells. For instance, vitamin D deficiency has been associated with predicting cancer risk (Hollis *et al*., 2013) and cancer mortality (Bjelakovic *et al*., 2014), slowing the growth of tumours (Ray *et al*., 2012), cardiovascular disease (Ng *et al*., 2013), neurological and psychological disorders and diabetes (Mitri *et al*., 2011; Alam *et al*., 2012), amongst others. A common clinical presentation related to vitamin D deficiency is proximal myopathy (Rasheed *et al*., 2013). Indeed, very large epidemiological studies (Bjelakovic *et al*., 2014a) on >95,000 participants, mainly comprising elderly women, have shown that D3 supplementation decreased all-cause mortality.

1.4. Analytical techniques

Analysis of vitamin D metabolism, especially in the context of a clinical laboratory, requires an understanding of a few key analytical techniques. The techniques described briefly in this section will be referred to and discussed in more detail throughout this thesis.

1.4.1. Immunoassay

Immunoassay (IA) is a technique in which analyte(s) are measured using an antibody, or antibodies, raised against the target analyte. The first IAs were radioimmunoassays (RIAs) described by Yalow and Berson in the 1960s (Yalow & Berson, 1960). IAs are today very commonly used in clinical laboratories for a wide range of tests, using a variety of sample matrices. A number of different IA systems are available, with many now built into fully-automated laboratory systems to enable rapid production of results. Generation of signal in IAs to allow analyte detection and measurement is achieved using chemical labels, or 'tags' such as radioactive, colourimetric, fluorescent, chemiluminiscent, or electrochemiluminescent labels. Depending on the assay format, the analyte concentration is either directly, or inversely proportional to the generated signal. Broadly, IAs may be split into two categories – separation IAs, or heterogeneous IAs, which involve one or more separation step during the analytical procedure (e.g. for washing steps or prior to detection), and non-separation IAs, or homogeneous immunoassays where no such separation steps are used (Dinis-Oliviera, 2014). A common example which demonstrates the principal of immunoassay is enzyme-linked immunosorbent assay (ELISA). ELISAs themselves have a number of formats, one of which is the 'sandwich ELISA', illustrated in Figure 1.7.

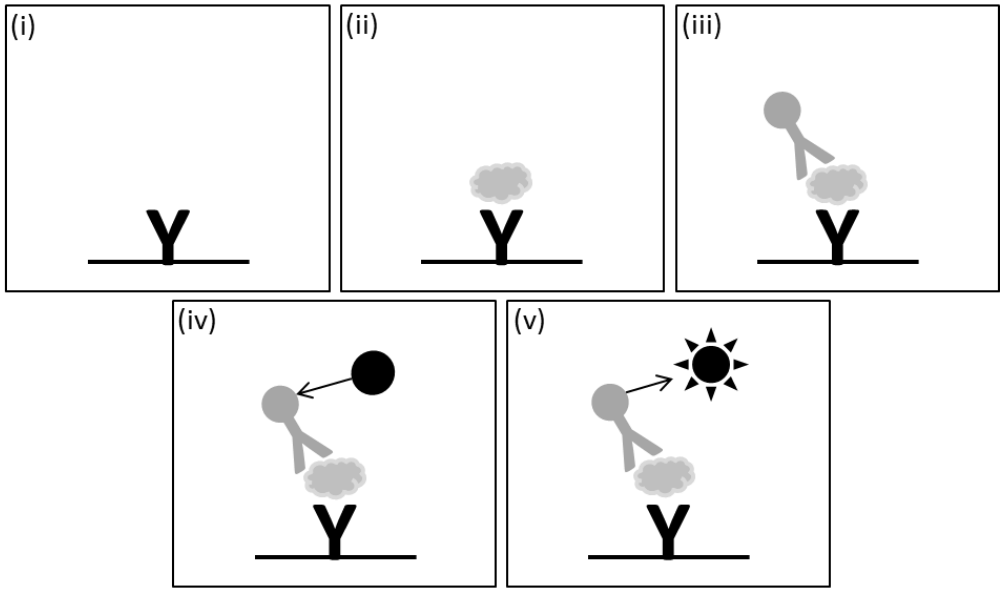

Figure 1.7. Schematic of a 'sandwich' ELISA. (i) An anti-analyte antibody is coated to the wall of a tube or the well of a microtitre plate. (ii) The sample containing an unknown amount of analyte is added, and binds to the antibody. (iii) A second anti-analyte antibody is added to the well, and forms the 'sandwich' with the captured analyte. The second antibody is labelled with an enzyme that catalyses a reaction which produces a detectable product. (iv) The enzyme substrate is added. (iv) The product of the enzyme reaction is measured, typically using absorbance of light at a specific wavelength.

1.4.2. Liquid chromatography

Liquid chromatography (LC) is an extremely widely used analytical technique for the separation of components in mixtures. Although 'chromatography' in its earliest form is arguably traceable back to the 1800s and the separation of dyes using filter paper (Touchstone, 1993), it was the work of Tswett in the early 1900s on plant pigments using open tubular columns (Tswett, 1906), and more recently the Nobel prize-winning work of Martin and Synge in the mid-20th century which enabled the more widespread adoption of this analytical tool with the development of silica gel-based partition chromatography for the separation of amino acids (Synge, 1939; Martin & Synge, 1941). Partition chromatography separates solutes based on their partition coefficients between the two phases in the chromatography system.

A key concept in chromatographic separations, especially for complex mixtures, is that of efficiency. The more efficient a chromatographic system, the greater the resolving power, and hence the ability to separate compounds. A measure of chromatographic efficiency is the number of 'theoretical plates' or 'plate count' of a column – this is a theoretical number, the concept for which originates from industrial distillation column methods using bubble-cap trays. The greater the plate number, the more efficient a chromatography system. Directly related to the plate number (N_t) and the length of the chromatographic bed (H), is the 'height equivalent to a theoretical plate' (HETP), which is calculated as shown in Equation 1.1.

Equation 1.1. Calculation of the number of theoretical plates.

$$Nt = \frac{H}{HETP}$$

1.4.2.1. Band broadening

The kinetic parameters of a mobile phase passing through a chromatography column (i.e. the linear velocity, μ) influence the efficiency of the system as a whole. The term 'band broadening' is used to describe the combined effects of these parameters with respect to the efficiency of a system. Optimal chromatographic efficiency is achieved by minimising factors which cause band broadening. In the 1950s, van Deemter studied the factors which contribute to band broadening, and derived an equation (Equation 1.2) for modelling band broadening and chromatographic efficiency (HETP) with respect to the linear velocity of the mobile phase (van Deemter, 1956).

Equation 1.2.The van Deemter equation.

$$HETP = A + \frac{B}{\mu} + C\mu$$

The van Deemter equation combines three factors which contribute to band broadening. The 'A term' is a constant with respect to flow rate, and is related to the Eddy diffusion, or flow path, of the mobile phase through the column. The A term can therefore be reduced by using small, tightly-packed, and evenly-sized particles. The 'B term' describes the diffusion coefficient, or dispersion, of the solute and is inversely proportional to the flow rate. The B term is reduced by increasing the flow-rate, and also by minimising the system dead volume. The 'C term' describes the resistance to mass transfer between the mobile and stationary phase (the dispersion of analytes into and out of the pores in packed columns), and is directly proportional to the flow rate. When plotted, the three terms combine to reveal a hyperbolic curve in which the minimum HETP (i.e. the maximum efficiency) corresponds to an optimum mobile phase velocity (Figure 1.8).

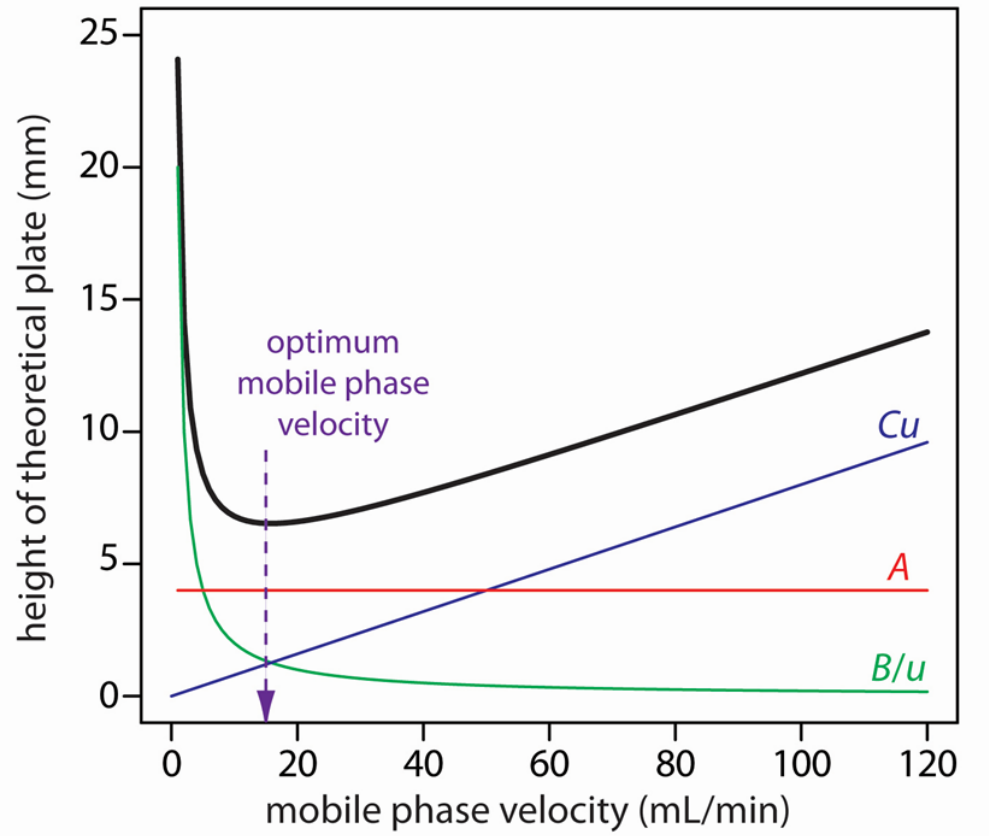

Figure 1.8. Plot of the influence of mobile phase velocity (u) on the A term (red), B term (green) and C term (blue) of the Van Deemter equation. Summation of the three terms gives the hyperbolic curve (black), from which the optimum mobile phase velocity (flow-rate) can be deduced.

The theoretical approach towards chromatographic separations described by Van Deemter has led to the development of novel LC technologies to improve efficiency such as (i) small particle packing materials, and (ii) superficially porous particles (Figures 1.9, 1.10).

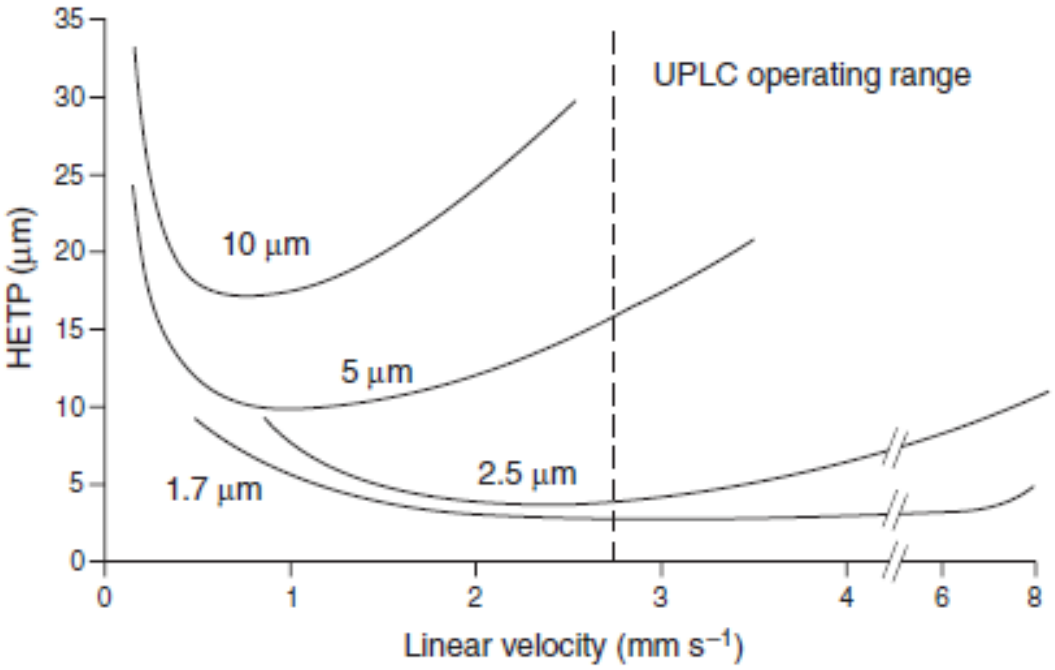

Figure 1.9. The effect of particle size on column efficiency. Smaller particles provide increased efficiency due to (i) smaller particle size distribution (lower A term component) and (ii) reduced efficiency drop at higher mobile-phase velocities due to shorter diffusion paths (reduced effect on C term at increased flow-rates). The term UPLC was trademarked by Waters Corporation for their range of sub-2 µm packing materials. Figure adapted from Flanagan *et al.*, 2007.

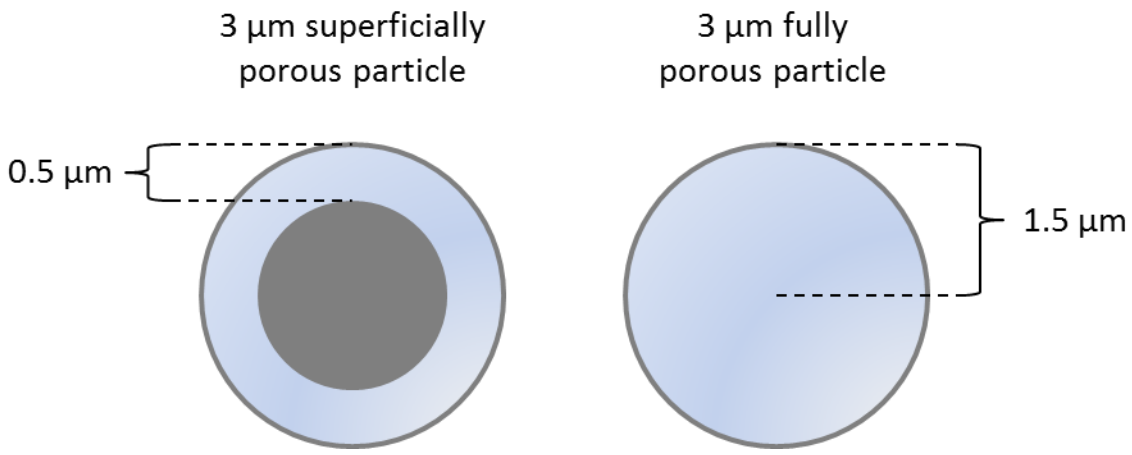

Figure 1.10. A schematic of a superficially porous particle with a 0.5 µm diffusion path and a fully porous particle of the same total particle size. The efficiency of superficially porous particles is increased compared to fully porous particles due to (i) the ability to reproducibly manufacture the particles, reducing the particle size distribution, a factor which lowers the van Deemter A term, and (ii) a reduced C term directly related to the shorter diffusion path. The increased efficiency (which can alternatively be realised by using smaller diameter fully porous particles) comes without an increase in pressure, since the total particle size remains constant.

1.4.3. Mass spectrometry (liquid chromatography-mass spectrometry)

Mass spectrometry (MS) is a technique in which ions are produced in an ion source (see following sections for different ionisation methods used in this thesis), and are then separated, or sorted, in a mass analyser based upon their mass (*m*) and charge (*z*), as a function of their mass-to-charge ratio (*m/z*).

MS is a powerful analytical technique for the identification of chemical species, since two compounds with different chemical formulae will produce different characteristic mass spectra. MS can also be carried out using multi-stage MS experiments. In such experiments, (precursor) ions are produced and sorted as in single-stage experiments, but are then fragmented to produce characteristic product ions, which can then be further analysed. A single fragmentation event followed by analysis of product ions is sometimes referred to as 'tandem MS' (or MS/MS, or MS^2), and requires hybrid instruments with two mass analysers (one for precursor ion sorting and one for product ion sorting) and a means of precursor ion fragmentation such as a collision cell. A number of mass analysers are available which can carry out such experiments. In this thesis, MS analyses were carried out using (i) triple quadrupole (QQQ) instruments (Figure 1.11) and (ii) hybrid quadrupole-Orbitrap instrumentation (Figure 1.12). Both instruments use quadrupole ion filters which consist of four parallel rods, ideally hyperbolic in shape. Ions are filtered based on the stability of their trajectories in oscillating electric fields. The Orbitrap mass analyser was invented by Makarov in the early 2000s (Makarov, 2000; Hardman & Makarov, 2003). In the Orbitrap, ions are trapped in an orbit around a central spindle electrode, and oscillate axially at a frequency directly related to their *m/z* value. The measured ion frequencies are Fourier transformed to produce high-resolution mass spectra (Hu *et al*., 2005). In high-resolution MS, two key measures are (i) the measured mass error, and (ii) the observed resolution. These are calculated using experimental data from Equations 1.3 and 1.4, respectively.

Equation 1.3. Calculation of mass error.

$$Mass\ error\ (\Delta\ ppm) = \frac{(Measured\ m/z - Theoretical\ m/z)}{Theoretical\ m/z} \times 10^6$$

Equation 1.4. Calculation of mass resolution.

$$Resolution = \frac{m/z}{FWHM}$$

where FWHM is the full peak width (m/z units) at half-maximum height

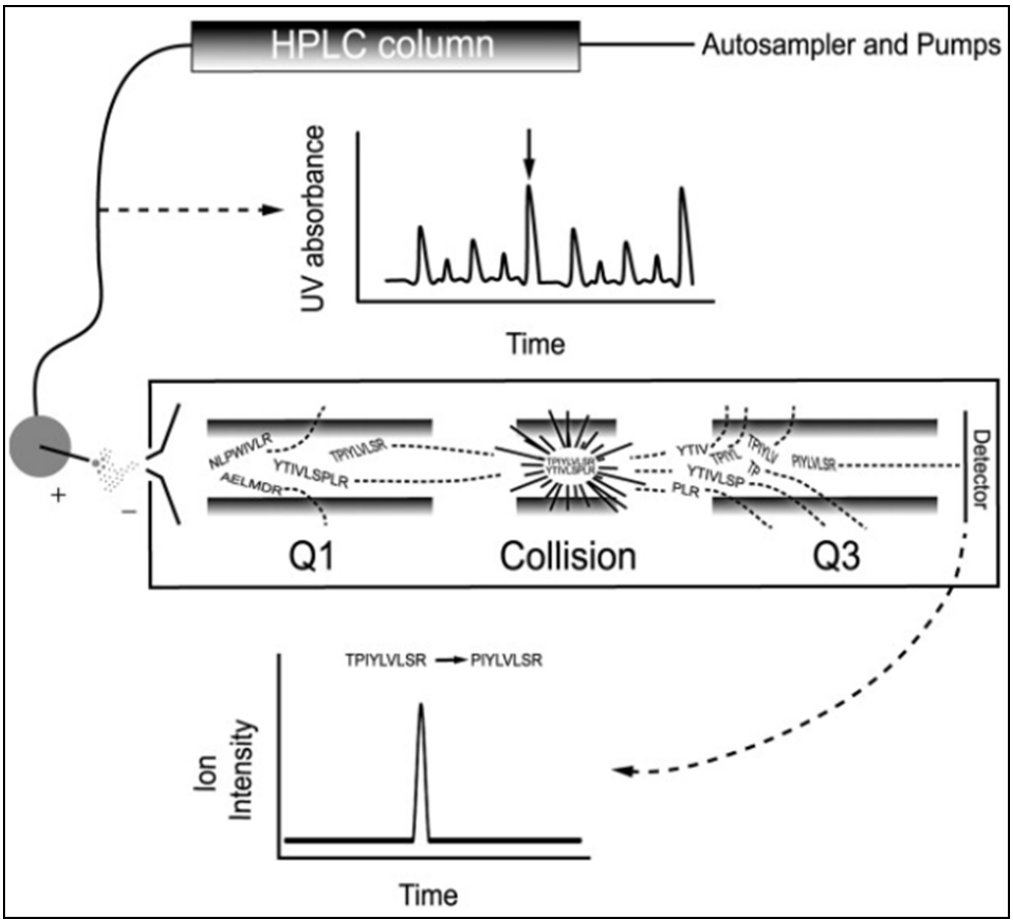

Figure 1.11. HPLC tandem mass spectrometry of a peptide mixture using a triplequadrupole instrument. Shown also in this example, an in-line ultra-violet (UV) detector. Precusor ions are isolated in the first quadrupole (Q1), fragmented in the collision cell (also a quadrupole), and specific product ions isolated in the third quadrupole (Q3). Pairs of Q1 and Q3 ion *m/z* values are called 'transitions', and many transitions are monitored during the chromatographic separation of a mixture of components when such instruments are operated in multiple reaction monitoring (MRM), or selected reaction monitoring (SRM) mode. Figure adapted from Hoofnagle & Wener, 2009.

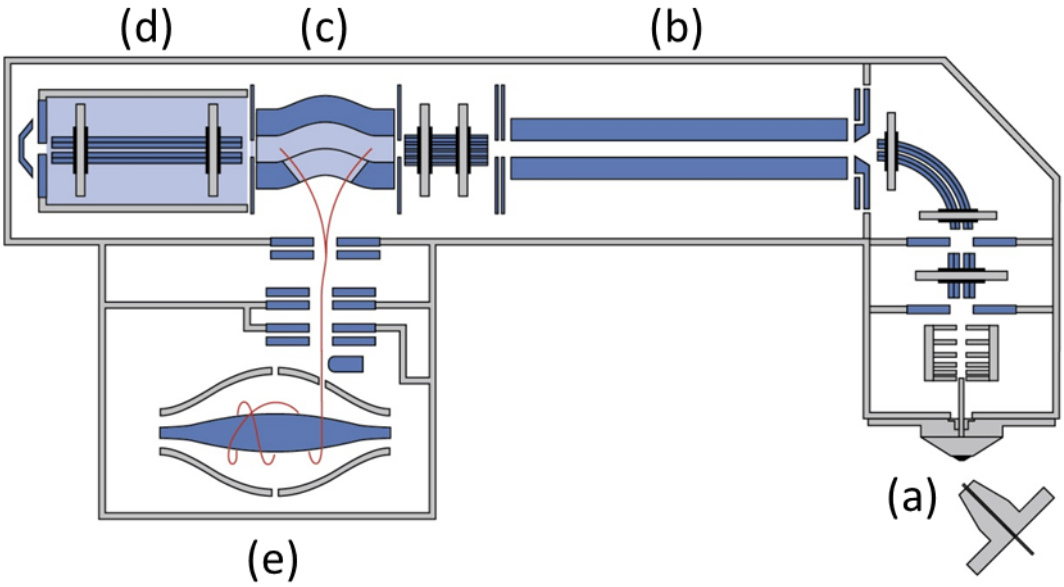

Figure 1.12. Schematic of the ThermoFisher Scientific Q Exactive mass spectrometer. Shown are (a) the ion source, (b) the isolation quadrupole, (c) the C-trap, used to focus ions prior to entering the Orbitrap, (d) the collision cell used to produce fragment ions in MS2 experiments, and (e) the Orbitrap mass analyser, showing an approximate ion trajectory about the central spindle electrode.

1.4.3.1. Electrospray ionisation

Prior to MS analysis, compounds must be ionised in the ion source of the MS instrument. The history of MS dates back to the turn of the 20th century with the work of Aston and Thomson, but it was the more recent work of Dole and co-workers in the 1960s (Dole, 1968), and latterly Fenn and co-workers (Fenn *et al.*, 1989) and the development of 'soft' ionisation techniques such aselectrospray ionisation (ESI) which has enabled MS to be far more widely applied for the analysis of biomolecules (Figure 1.13), and especially proteins and peptides. John Fenn was awarded the 2002 Nobel Prize for this work.

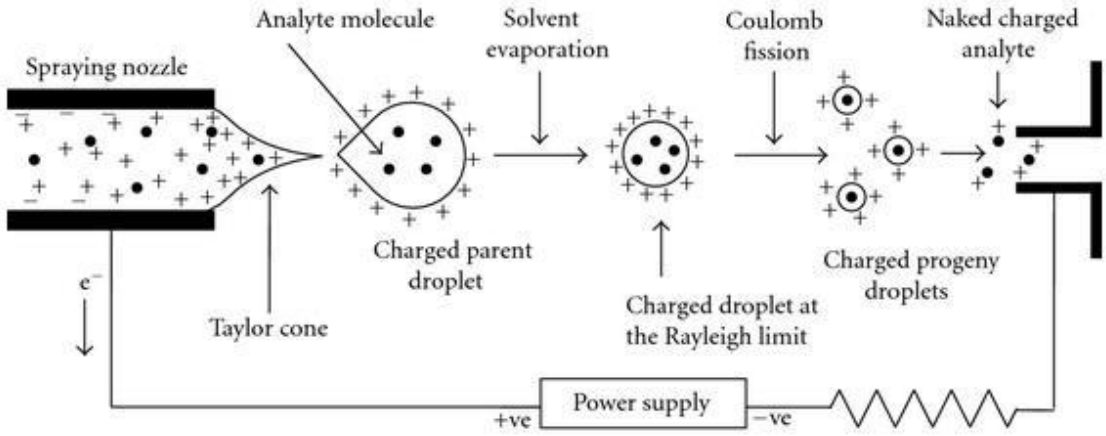

Figure 1.13. Schematic of the electrospray ionisation (ESI) process.

There are two primary models which are used to describe the process of ESI – the ion ejection model and the charge residual model (Wilm, 2011; Konerman *et al*., 2013). For both, eluent flow from the LC column enters a metal capillary held at an electrical potential (typically 1-5 kV), causing distortion of the liquid and subsequent formation of a Taylor cone as the flow exits the capillary. From the Taylor cone, a mist of charged droplets are emitted, which undergo rapid desolvation with the assistance of heat and desolvating gas (nitrogen) flow(s). As droplets shrink, the density of charge increases to the point at which the repulsive force between ions exceeds the surface tension of the droplet (the Rayleigh limit). At this point, ions are released from the small nano-droplets via one of the two mechanisms described below –the ion ejection model (IEM), which is thought to dominate in the ESI of small molecules, or the charge residual model (CRM), which is thought to predominate for larger peptides and proteins. In the IEM, as droplets shrink, the electric field of the droplets is sufficiently high to overcome the surface tension, and cause ejection of small (typically protonated) solvated ions from the droplet surface. The CRM is widely accepted as the preferred model for large molecule such as proteins (Konerman *et al*., 2013). In the CRM, droplets shrink to the point where each nano-droplet contains a single analyte molecule. As the final solvent layer vanishes, the charge of the droplet is transferred to the analyte.

1.4.3.2. Protein mass spectrometry

MS is an extremely useful tool for protein identification and analysis, especially so when used in combination with LC. Until the 1990s and the advent of protein MS (proteomics), sequencing proteins was reliant upon large amounts of purified protein and the use of Edman degradation sequencing. However, this was time-consuming and costly, and did not always guarantee successful sequence assignment (Steen & Mann, 2004).

The first step in a protein mass spectrometry experiment is typically to digest the protein into a series of so-called 'proteotypic' peptides. For subsequent analysis of peptides using LC-MS, the ionisation method of choice is ESI. Proteotypic peptides are usually doubly protonated during the electrospray ionisation process to produce $[M+2H]^{2+}$ precursor ions as the major species. The 2^{+} charge state is observed experimentally in spectra by a 0.5 Da spacing between isotopes of a precursor ion *m/z* (as shown in Figure 1.14 for the peptide LPDATPTELAK). Peptides which are greater than 15 amino acids in length and peptides with additional basic residues such as histidine (His, H), which can also be protonated, may form $[M+3H]^{3+}$ species (Steen & Mann, 2004). Larger peptides or small proteins produce more complex spectra with multiple charge states, e.g. insulin, hepcidin, and PTH (Figure 1.15).

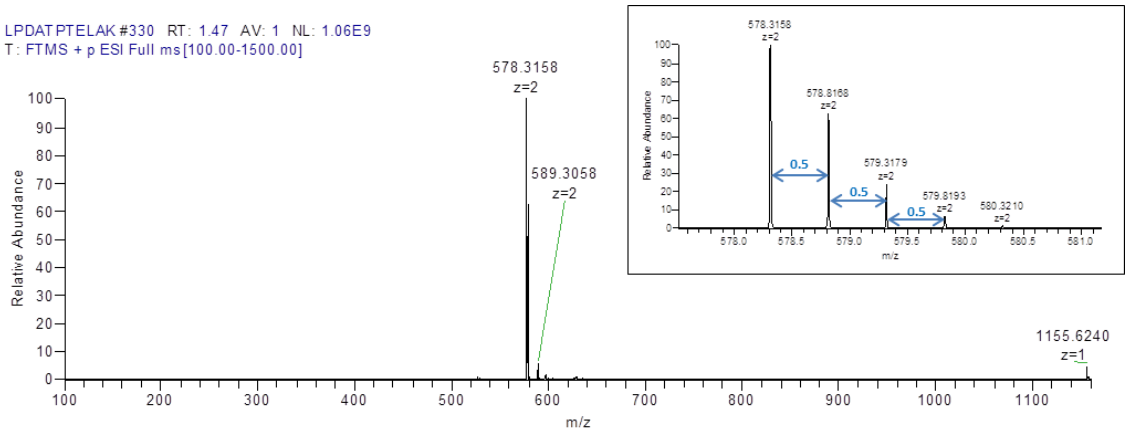

Figure 1.14. Precursor ion spectrum for the peptide LPDATPTELAK. The signal intensity for the doubly charged peptide (*m/z* 578) is significantly greater than for the singly protonated peptide (*m/z* 1,155). Shown inset is the isotope spacing for the doubly charged peptide. Data were collected via loop-injection of a solution of LPDATPTELAK (custom-synthesised, ThermoScientific), prepared in 0.1 % (*v/v*) aqueous formic acid, using a Q Exactive MS, operating in full-scan mode (70,000 resolution, 100-1,500 *m/z* scan range).

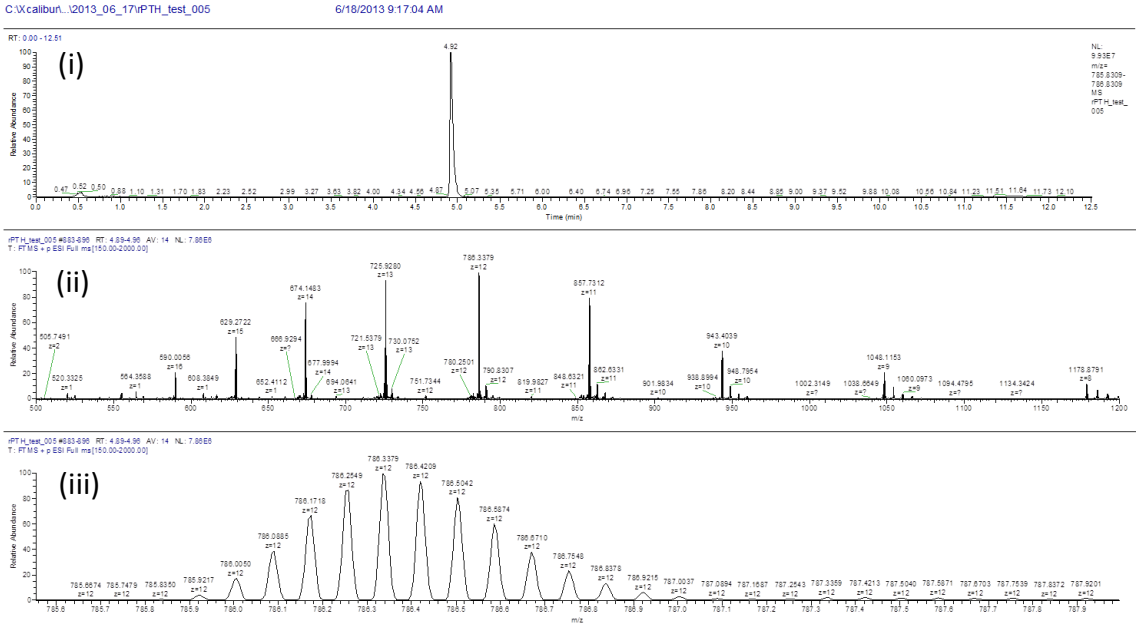

Figure 1.15. Example intact PTH (PTH1-84) HR-AM spectra. Shown are (i) the chromatographic peak for the protein, (ii) the charge state distribution of the protein – charge states from $[M+8H]^{8+}$ through to $[M+16H]^{16+}$ were observed, and (iii) the isotopic distribution of the most abundant charge state, $[M+12H]^{12+}$.

In tandem MS experiments, fragmentation patterns of peptide precursor ions provides an extremely useful tool for (i) identifying peptide sequences (*de novo* sequencing) and (ii) developing selective and specific targetted peptide assays. The amino acid composition (Table 1.1) of the peptide imparts a specific precursor ion *m/z* value. Fragmentation of precursor ions occurs in a relatively predictable manner, to produce characteristic product ion spectra in which peaks are identified according to the Roepstorff-Fohlmann-Biemann nomenclature (Roepstorff & Fohlman, 1984; Steen & Mann, 2004, Figure 1.16). Of the a, b, c and x, y, and z ions formed, the b- and y-ion series are the most informative and usually the most abundant, as these product ions are the result of fragmentation at the amide bonds between sequential amino acids. As shown in Figure 1.16, the b-ion series are product ions formed in which the charge remains on the N-terminus side of the peptide, and y-ion series are those product ions with a C-terminal charge.

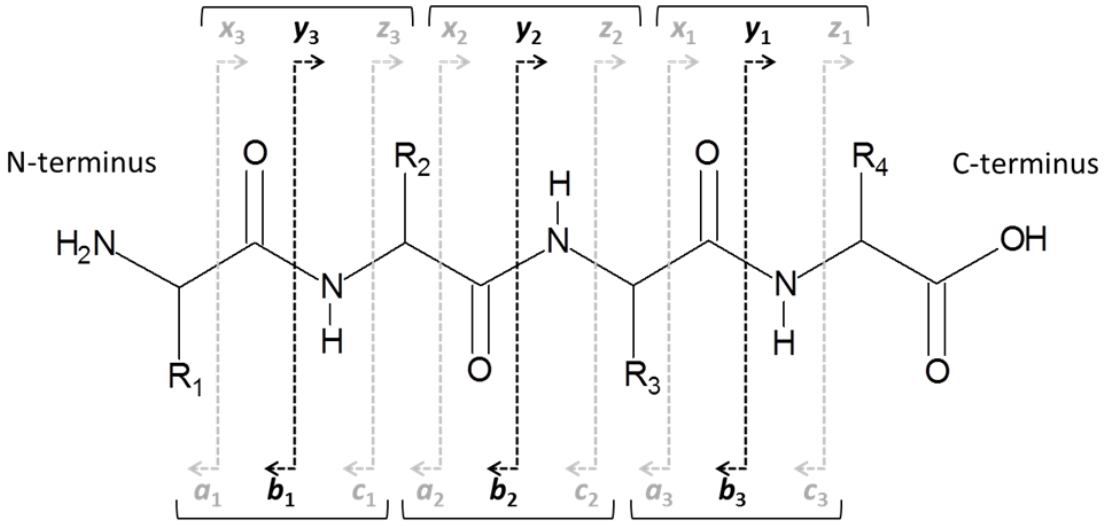

Figure 1.16. Fragmentation and nomenclature of peptide product ions according to the Roepstorff-Fohlmann-Biemann system (Roepstorff & Fohlman, 1984).

Amino acid	Amino acid structure	Amino acid	Amino acid structure
Alanine **(Ala, A)**	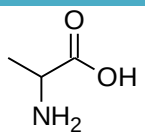	**Leucine** **(Leu, L)**	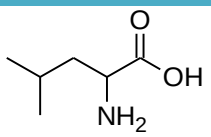
Arginine **(Arg, R)**	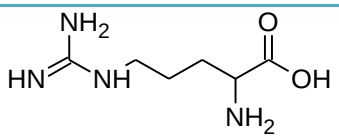	**Lysine** **(Lys, K)**	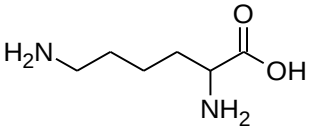
Asparagine **(Asn, N)**	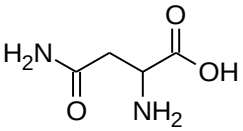	**Methionine** **(Met, M)**	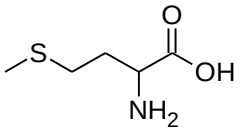
Aspartic acid **(Asp, D)**	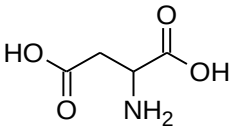	**Phenylalanine** **(Phe, F)**	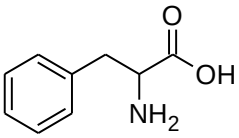
Cysteine **(Cys, C)**	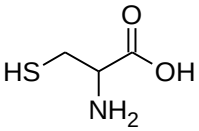	**Proline** **(Pro, P)**	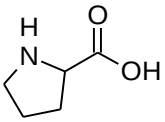
Glutamic Acid **(Glu, E)**	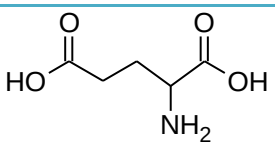	**Serine** **(Ser, S)**	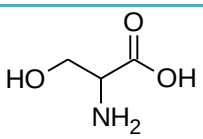
Glutamine **(Gln, Q)**	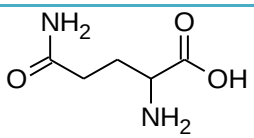	**Threonine** **(Thr, T)**	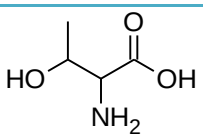
Glycine **(Gly, G)**	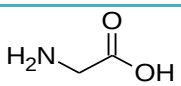	**Tryptophan** **(Trp, W)**	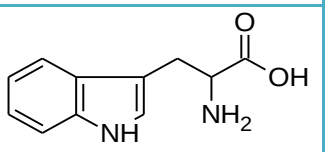
Histidine **(His, H)**	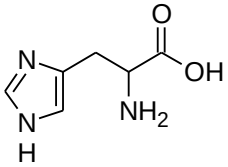	**Tyrosine** **(Tyr, Y)**	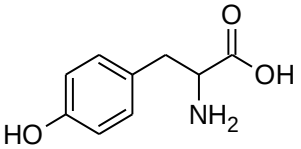
Isoleucine **(Ile, I)**	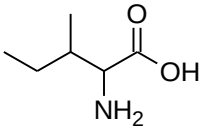	**Valine** **(Val, V)**	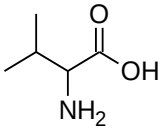

Table 1.1. Amino acid structures and standard abbreviations.

A peptide MS^2 spectrum consists of a mixture of product ions formed as a result of the precursor ions fragmenting at different bonds (Figure 1.17). The difference between sequential b- and y-ion *m/z* values corresponds to the monoisotopic mass of the amino acid (Table 1.1), hence the ability to use tandem MS for peptide sequencing. Furthermore, due to the relatively predictable pattern of fragmentation observed for peptides, a number of software packages are available to predict *in silico* the likely product ions (usually b- and y-ion series) for a given precursor ion sequence. As with the fragmentation of non-peptide small molecules, additional product ions (sometimes called 'satellite fragments' when referring to peptide MS^2 spectra – Steen & Mann, 2004) are observed in the MS^2 spectra of some peptides due to further loss of, for example, water (H_2O) or ammonia (NH_3) moieties.

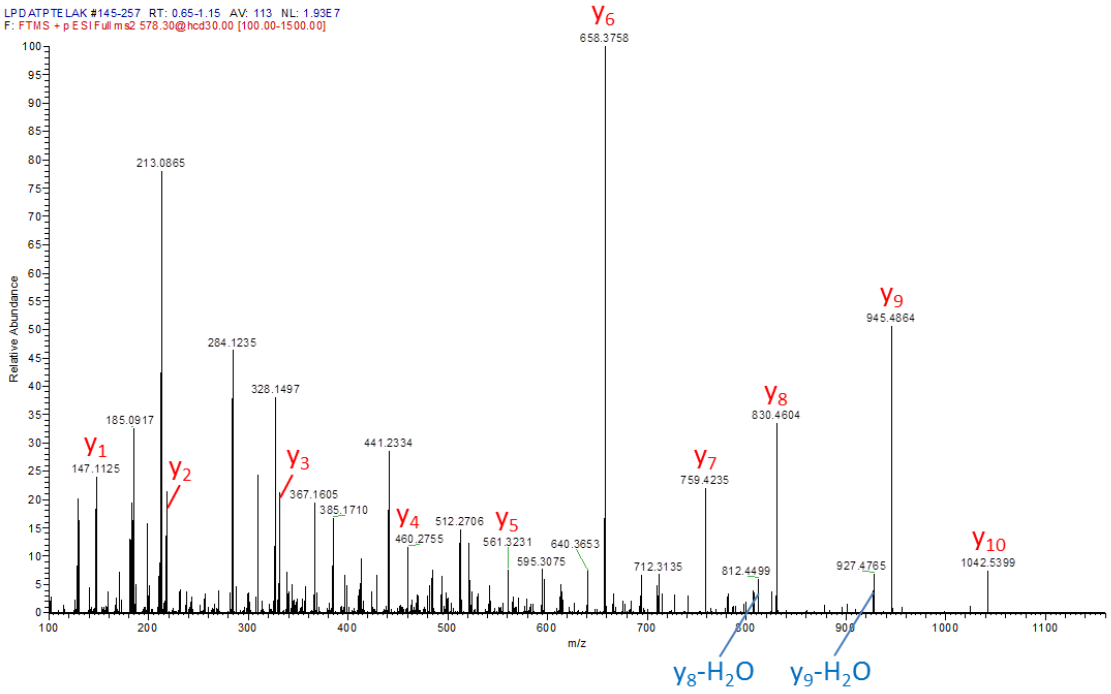

Figure 1.17. Averaged product ion (MS^2) spectra for the peptide LPDATPTELAK. Spectra collected during infusion of a solution of LPDATPTELAK (in 0.1 % *v/v* aqueous formic acid). Scan range 100-1500 m/z, normalised collision energy 30, 4.0 Da quadrupole isolation width for precursor ion (578.3 *m/z*, $[M+2H]^{2+}$).

Once MS and MS^2 spectra are obtained for the peptides of a digested target protein, either experimentally (e.g. from discovery experiments) or from on-line resources for known protein sequences, these data can be used to build LC-MS/MS methods. For large proteins, there may be dozens of candidate peptides, and hundreds of possible *m/z* transitions which could be used. Specific peptides and *m/z* transitions are typically selected based on a number of criteria, including (i) MS response (i.e. MS ionisation efficiency), (ii) chromatographic performance, (iii) intensity of product ions, (iv) specificity of m/z transitions, and (v) presence of peptides containing modified and/or modifiable amino acids (Picotti and Aebersold, 2012). The translation process from protein sequence data to targeted LC-MS/MS method is summarised in Figure 1.18.

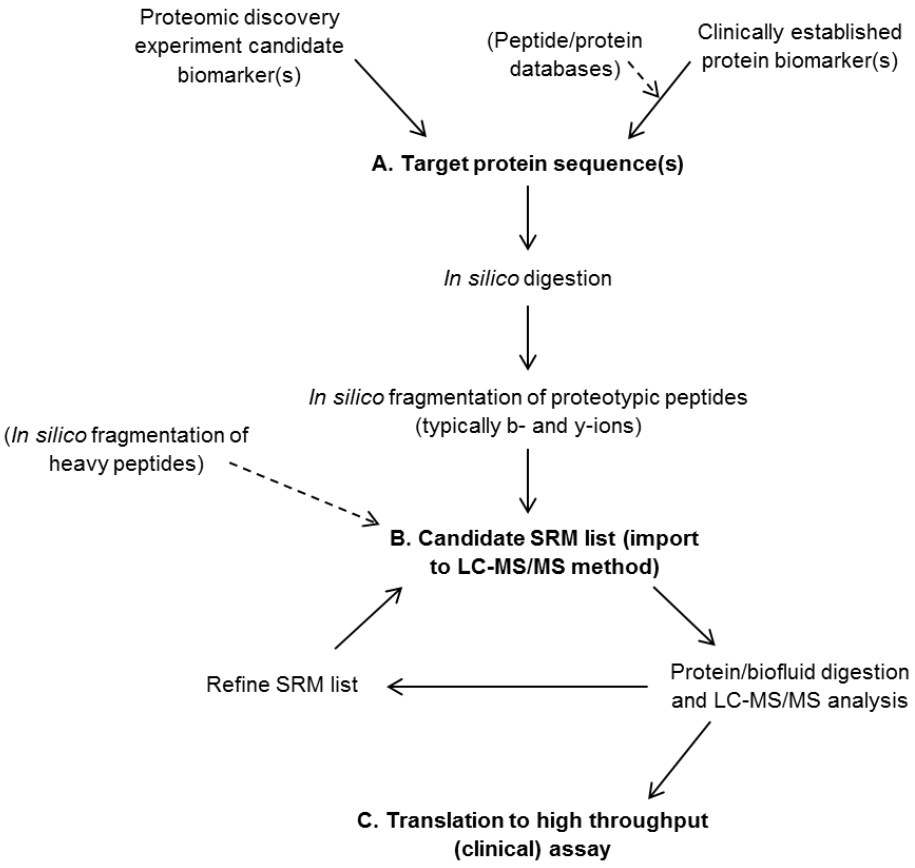

Figure 1.18. Schematic showing the process for selecting proteotypic peptides for a targeted protein LC-MS/MS assay.

1.4.3.3. Atmospheric pressure chemical ionisation

In atmospheric pressure chemical ionisation (APCI), ionisation occurs via a series of chemical reactions and subsequent charge transfer within the discharge region of a corona needle (Figure 1.19). Since the ionisation occurs in the gas phase, APCI benefits from (and can withstand) higher LC flow-rates when used in conjunction with high temperatures, and is suited to analytes which (i) do not readily ionise in solution and/or (ii) are highly polar. Typically, steroids are cited as compounds which may ionise better by APCI than by ESI. APCI tends to only form singly charged ion species (either protonated or other adduct ions related to the eluent composition), and so this technique is not used for protein MS.

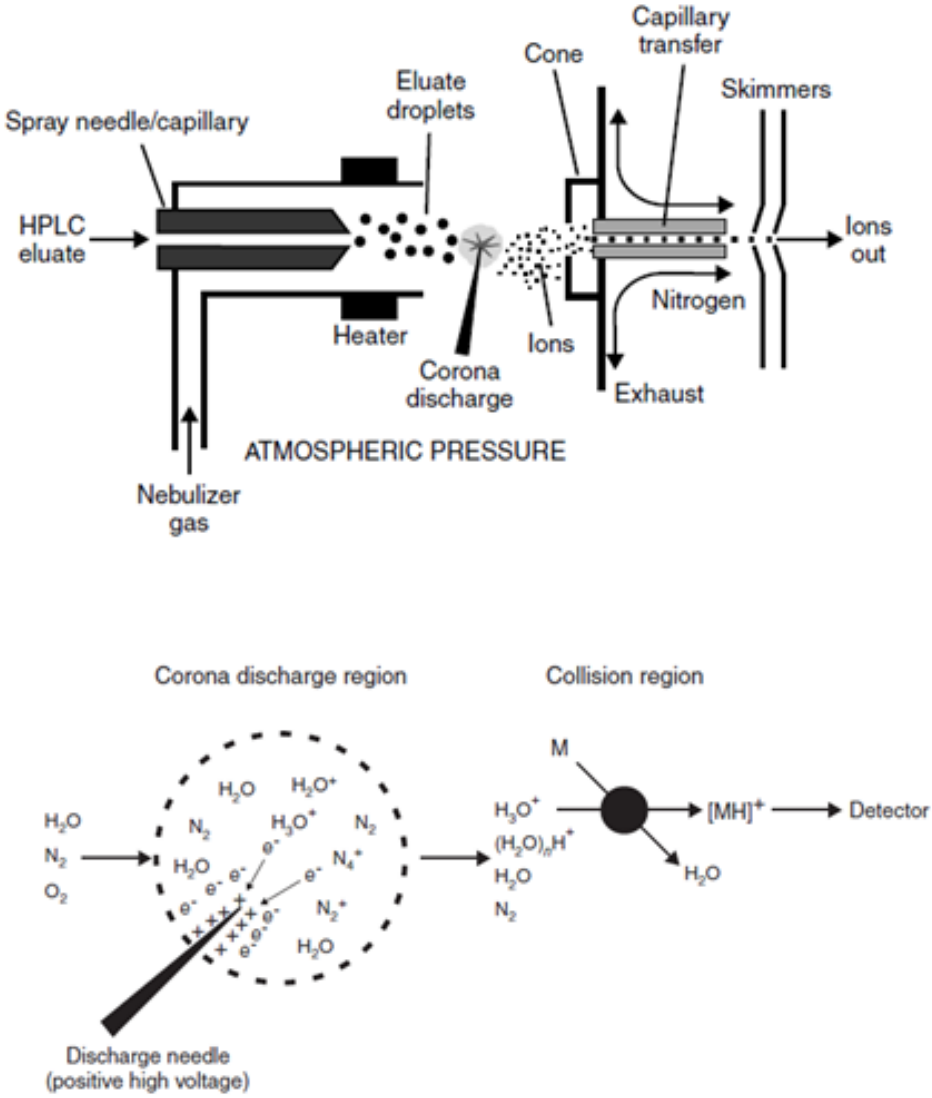

Figure 1.19. Schematic of an atmospheric pressure chemical ionisation (APCI) source (top), and the chemical ionisation process within the corona discharge region surrounding the discharge needle.

1.5. Current analytical methods for analysis of 25-OHD

1.5.1. Analysis of 25-OHD

The analysis of 25-OHD is highly complex (Carter, 2012). The analysis of total serum 25-OHD as a marker of vitamin D status is complicated by a number of factors, including (i) the presence of a large number of structurally-related metabolites, (ii) the fact that vitamin D metabolites in circulation are tightly bound to VDBP, (iii) the fact that vitamin D is an endogenous compound, and a truly representative blank matrix for use analytically is unavailable, and (iv) a large number of analytical methods are available to choose from. International proficiency testing of all 25OHD assays has been available through the vitamin D external quality assessment scheme (DEQAS) since 1989. The scheme was established in response to several studies in the mid to late 1980s indicating poor performance of 25OHD assays (Carter *et al*., 2004; Binkley *et al*., 2004). Testament to the success of the scheme are (i) the increase in the number of participants from just 25 in 1989 to approximately 1,100 (October, 2014) (Carter *et al*., 2015), and more importantly (ii) an overall reduction in the all-method inter-laboratory precision (% CV) from 32 % in 1994, to 15.3 % in early 2009 (April and July distributions only – Carter *et al.*, 2010). The vitamin D standardization programme (VDSP) has also been established to promote the standardisation of laboratory measurement of total 25-OHD, in order to improve clinical and public health practice worldwide (Binkley *et al*., 2014).

Measurement traceability has become increasingly important in clinical laboratories in recent years to aid efforts for method harmonisation (Binkley *et al*., 2014). For the analysis of 25-OHD, standard reference materials (SRMs) are available via the National Institute for Science and Technology (NIST). The first SRM (SRM972) was replaced by the current SRM (SRM972a), and consists of four levels (4 x 1 mL) of frozen human serum with assigned values for a range of 25-OHD metabolites, including 24*R*,25-OHD3 and 3-*epi*-25-OHD3.

1.5.1.1. Immunoassays for 25OHD

Immunoassay-based techniques superceded the competitive protein binding (CPB) assays of the 1970s (Haddad *et al*., 1971) for measuring vitamin D metabolites, and have been widely available since the first RIAs for total 25-OHD developed in the mid 1980s (Hummer et al., 1984; Hollis & Napoli, 1985). With increased automation, the development of enzymatic and chemiluminescent assays, and the incorporation of these assays into fully-automated analysers and track-based laboratory systems, they are still commonly used around the world in clinical laboratories for 25-OHD analysis.

However, as will be discussed in some detail in this thesis, IAs for 25-OHD are limited in their ability to specifically detect and measure any of the individual circulating species, and are therefore subject to significant interferences (Ong *et al*., 2012; Su *et al*., 2014). As will also be discussed, there are concerns with immunoassays regarding the influence of VDBP (Heijboer *et al*., 2012; Carter & Phinney, 2014).

1.5.1.2. HPLC for 25OHD

Early CPB assays have previously showed the benefits of chromatographic separation of vitamin D metabolites, not only from one another, but also from matrix components and interferences. The use of HPLC with UV detection to resolve vitamins D and their metabolites was first reported in the 1970s (Jones & DeLuca, 1975; Ikekawa & Koizumi, 1976), and a method reporting the use of HPLC-UV following extraction from human plasma published in 1978 (Jones, 1978). Despite by today's standards being a very complex, time-consuming analytical workflow involving extraction of relatively large plasma volumes, multiple columns and eluent systems and pre-purification by fractionation, this early work clearly demonstrated and recognised the importance of being able to isolate and independently assay 25-OHD2 and 25-OHD3. Electrochemical (ECD), rather than UV detection has also been reported for the analysis of 25-OHD (Masuda *et al*., 1997; Nurmi *et al*., 2013), though it seems both UV and ECD have been superceded by MS detection.

1.5.1.3. LC-MS and LC-MS/MS for 25OHD

LC-MS has been used for the analysis of 25-OHD since the early-1990s (Watson *et al*., 1991). MS detection offers increased sensitivity when compared to UV methods, and the ability to distinguish 25-OHD2 and 25-OHD3 by their different *m/z* values means that chromatographic resolution of these two compounds is not a pre-requisite. Single-stage LC-MS has been used for 25-OHD analysis, but showed lower sensitivity than MS/MS, and was more prone to matrix effects (Bedner & Phinney, 2012). LC-MS/MS is the recommended method for 25-OHD analysis by the National Health and Nutritional Examination Survey (NHANES) and the UK Food Standards Agency National Diet and Nutrition Survey (NDNS) (Yetley *et al*., 2010; de la Hunty *et al*., 2010). The reference method for 25-OHD carried out by NIST uses LC-MS/MS (Tai *et al*., 2010). As of 2013, all DEQAS samples are now assigned 'target' values using the NIST method (Carter *et al*., 2015).

1.5.1.4. Other methods for 25OHD

Gas chromatography-MS (GC-MS) methods have been used for the analysis of steroids in biological samples for many years. GC-MS has been applied to the analysis of vitamin D metabolites, but is a lengthy process requiring extraction and derivatisation (De Leenheer & Cruyl, 1978; Coldwell *et al*., 1988).

1.6. Aims of the thesis

Since 'vitamin D deficiency' is considered so prevalent in the population, and has been linked to such a diverse range of pathological conditions, it is clear that the biochemical assessment of vitamin D status is essential for further understanding the role of vitamin D metabolites in our physiology and pathphysiology.

The hypothesis of this thesis is to investigate the application of novel analytical methods to study not only 25-OHD, but other possible components to use for the assessment of vitamin D status, in order to improve their use for clinical diagnosis.

25-OHD has been used for many years, and will continue to be the primary biochemical marker of vitamin D status. In Chapter Two, a method for the measurement of 25-OHD using turbulent flow chromatography will be developed and compared to some commercially available immunoassay methods. Results will be compared according to current guidance on 25-OHD concentrations for vitamin D status classification. The benefits of automation for the analysis of 25-OHD using LC-MS/MS in high-throughput clinical laboratories will also be discussed. The availability of reference materials and refernce methods for 25-OHD, as well as the ongoing work of DEQAS and the VDSP, have improved the inter-laboratory agreement in 25-OHD analysis. However, LC-MS/MS remains an 'open' analytical platform. For Chapter Three, the inter-laboratory variability in 25-OHD measurement will be investigated using questionnaire data to determine whether certain LC-MS/MS conditions are beneficial for accurate 25-OHD measurement.

The use of LC-MS/MS for protein and peptide analysis for clinical diagnostics is an extremely active area of research. Certainly, LC-MS/MS is an incredibly powerful tool for the analysis of such compounds and, compared to immunoassay, offers unique insights into protein heterogeneity, isoforms, and modified forms. Coupled with novel sample preparation methods such as immunoaffinity, even low abundance protein targets can potentially be investigated. In Chapter Four, the use of LC-MS/MS for the analysis of PTH will be investigated. In particular, the comparison of LC-MS/MS against PTH immunoassay will be investigated. As with 25-OHD, PTH immunoassays are subject to interference from structurally similar compounds in the circulation. In the

case of PTH, this involves truncated forms which are especially problematic in patients with poor or reduced kidney function.

There has also been a great deal of recent research regarding the analysis of VDBP. The reasons are two-fold – firstly, it has been suggestsed that variation in VDBP concentration may influence the analysis of 25-OHD by some homogeneous immunoassays, and secondly, there is interest in VDBP concentration itself as an adjunct to 25-OHD, in a concept similar to that of the 'free androgen index' which has been used for some years as a biomarker for androgen status. Analytically, these large proteins are usually analysed following proteolytic digestion. In Chapter Five, the same turbulent flow chromatography used for 25-OHD in Chapter Two will be investigated as a possible post-digestion analytical method for the measurement of target peptides. This approach, plus more novel approaches using rapid immobilised trypsin, will be discussed with reference to VDBP in Chapter Six.

Identification of proteins via tryptic peptides using MS is an extremely powerful tool. However, as with 25-OHD identification and quantification require entirely different approaches and considerations. In Chapter Seven, a novel approach to protein quantitation using non-human matrices as internal standards will be discussed.

To summarise, the thesis will look at the development of novel analytical techniques, applicable to high-throughput diagnostic laboratories, designed to measure those compounds which are currently used to assess vitamin D status (25-OHD), as well as consider how the same techniques can be modified to analyse other compounds related to vitamin D metabolism and physiology, which may serve as an adjunct to better assess vitamin D status.

Chapter Two

Development of high-throughput, and automated analytical techniques for the analysis of vitamin D metabolites using LC-MS/MS

2.1. Background

The biochemical assessment of vitamin D status must include the analysis of 25-OHD, either alone or in combination with other biomarkers (Seamans & Cashman, 2009; Holick, 2009). However, the analysis of 25-OHD is not straightforward (Carter, 2012). The use of LC-MS/MS for 25-OHD analysis should offer (i) increased analytical specificity when compared to immunoassay-based methods, and (ii) should account better for sample-to-sample matrix variability via the incorporation of an isotopically-labelled internal standard and removal of matrix components during sample preparation. Immediately advantageous is the ability to independently quantify 25-OHD2 and 25-OHD3.

However, another important concept for the development of a 25-OHD analysis suited to a high-throughput clinical diagnostic laboratory is analysis time, and the complexity of sample preparation procedures. As mentioned in the previous Chapter, it is not feasible for high-throughput clinical laboratories to adopt the time-consuming, manual, and therefore costly, methods used by certified reference laboratories such as that used by NIST (Tai *et al*., 2010). At King's College Hospital, London, the routine 25-OHD workload is approximately 3,000 samples per month, based on 2016 data. The analytical process for LC-MS/MS of 25-OHD includes both the sample preparation time, and the 'on-instrument' batch analysis time, each of which should be optimised for high-throughput workloads. There are a number of options for semi-automating common sample preparation procedures, and the on-instrument analysis time can be reduced through use of modern LC pumps and switching valves (e.g. to incorporate on-line sample preparation techniques) and column technologies.

2.1.1. Automated sample preparation

There are advantages of LC-MS/MS when compared to automated immunoassays and clinical analysers for many clinical assays (Hoofnagle & Wener, 2009). Key benefits are (i) the ability to multiplex, and hence simultaneously analyse dozens, if not hundreds of analytes (e.g. 25-OHD2 and 25-OHD3 in this case), (ii) the ability to analyse multiple different sample matrices on a single analytical platform, and (iii) the ability to rapidly

develop methods; immunoassays often require long lead times to generate sufficiently robust antibodies. However, current clinical MS processes, especially those related to sample preparation, tend to be manual process-driven (Zhang & Rockwood, 2015). A fully-automated total analytical workflow incorporating LC-MS/MS, i.e. from sample to result, with random access and bi-directional interfacing to laboratory information systems, akin to fully-automated clinical analysers, may still be some years away from realisation. However, currently available solutions towards semi-automating some of the key steps in the analytical process can be dramatically improved by automated liquid handling and on-line sample processing (Vogeser & Kirchhoff, 2011; Zhang & Rockwood, 2015). Automation of analytical processes for multiple samples simultaneously is a parallel automation process, e.g. simultaneous pipetting using 8-channel, 12-channel, or 96-channel pipetting stations, or 96-well plate mixing/centrifugation. On-line systems in which a process is automated for each sample within a batch can be termed a serial automation process, e.g. the automated valve-switching to allow the use of a preparative LC column and an analytical column in series for each sample within a batch. The two types of automation can be combined in a full LC-MS/MS automation process, for instance by using parallel automation for rapid sample preparation, followed by serial automation of further sample clean-up using an on-line sample preparation methodology.

2.1.2. Turbulent flow chromatography (TFC)

TFC offers efficient removal of potential interferences (Du & White, 2008), and fast analyses from biological fluids when compared with solid-phase extraction (SPE) or liquid-liquid extraction (LLE) procedures (Berna *et al*., 2004; Zhou *et al*., 2005; Morgan *et al*., 2010). For the analysis of plasma samples, endogenous phospholipids are recognized as a major cause of matrix effects. When compared with methanol-based protein precipitation alone, TFC has been shown to offer a significant (approximately 10-fold) reduction in the amount of phospholipids in the analysis of human plasma samples for metabolomic analysis (Michopoulos *et al*. 2010), and for enzyme assays (Liesener & Karst, 2005). However, a detailed study by Du & White (2008) concluded that phospholipids are not entirely removed by the TurboFlow column during sample

loading, but those that are retained can be selectively 'extracted' by careful choice of elution solvent during the transfer step and/or chromatographically resolved from compounds of interest during the second chromatographic stage.

Off-line handling of the sample is often limited to centrifugation to remove particulates (Zimmer *et al*., 1999) and dilution with internal standard(s) (Couchman *et al*., 2012), or protein precipitation to remove endogenous binding proteins (Bunch *et al*., 2009; Salameh *et al*., 2010). On-line sample analysis and transfer of analytes between columns is software-controlled through two 6-port valves, one with a custom rotor seal to allow the inclusion of a tee-piece, and most commonly using a 'Focus Mode' valve arrangement (Figure 2.1). Moreover, in the same way that automated SPE systems can be configured for minimum cycle times (Schellen *et al*., 2003), such systems are easily adapted to ensure maximal use of detector time through staggered, parallel methods in which samples are extracted whilst previous extracts are being analysed ('multiplexing', Figure 2.2). In this way, considerable savings in terms of time and solvent use can be achieved. In contrast with on-line SPE, however, the extraction columns are re-usable for several hundred injections (Zeng *et al*., 2004; Chassaing *et al*., 2005).

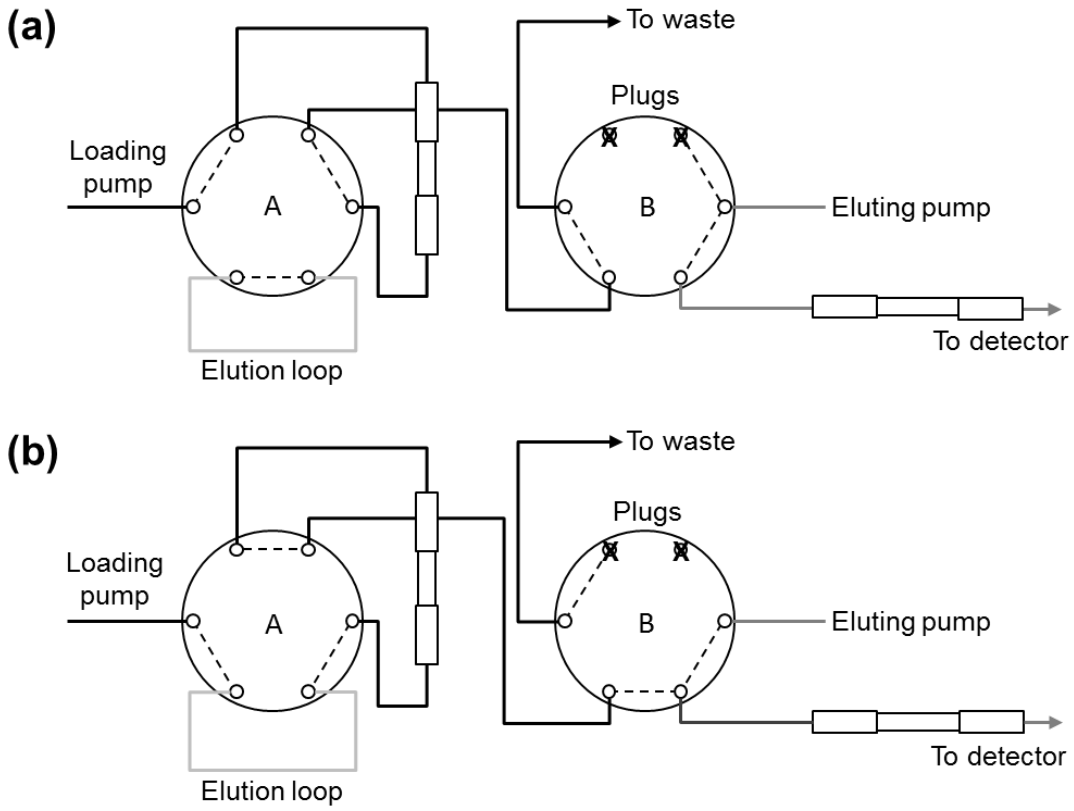

Figure 2.1. TurboFlow valve arrangement, showing two valves, A and B. Valve A uses a standard 6-port rotor seal, and Valve B has a customised rotor seal with an in-built tee-piece. Analytes are injected onto the TurboFlow column with the valves positioned as shown in (a), and unretained analytes and matrix components are diverted to waste. Both valves switch as shown in (b) to transfer the retained compounds, via the tee-piece to dilute the contents of the elution loop, onto the analytical column. The valves then return to the positions shown in (a), the eluting pump is used to deliver a gradient to the analytical column, and the TurboFlow column can be washed. By switching Valve A only, the elution loop re-filled for the next injection.

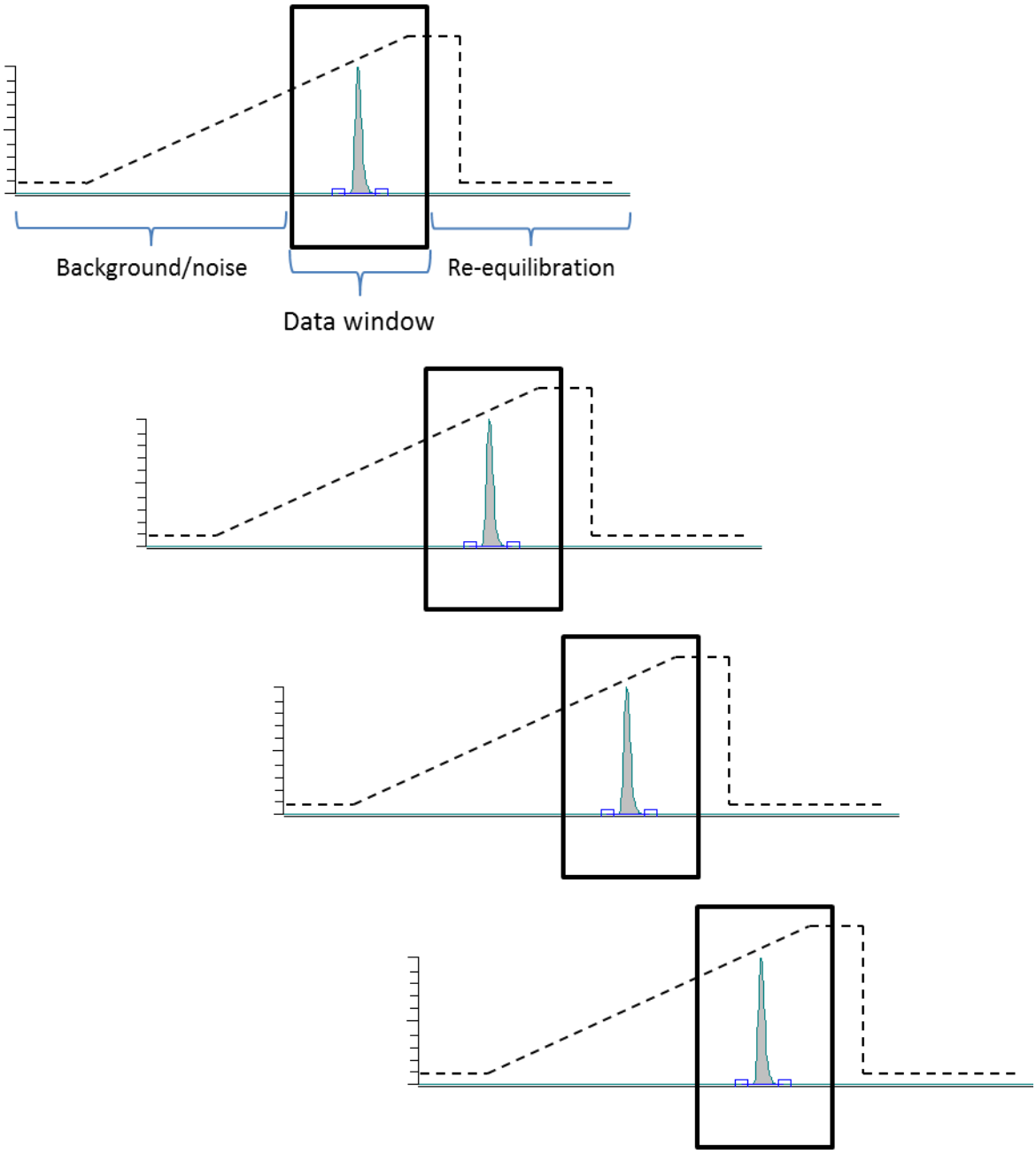

Figure 2.2. Multi-channel LC-MS/MS ('multiplexing'). By selecting a data window based on the target analyte retention time, and a suitable window (e.g. ± 30 seconds), a selector valve is used to determine which of the four channels is in line with the MS. The MS detector therefore avoids collecting background signal, and can maximise throughput.

2.1.1.1. Turbulent flow theory

With traditional HPLC columns, the factors that contribute to band-broadening and, therefore, column efficiency, were first described by van Deemter *et al.* (1956). The A-term of the van Deemter equation predicted that the efficiency of packed-bed columns would increase with (i) decreasing average particle size and (ii) increasing uniformity of particle sizes (particle size distribution). However, increased back-pressure, sometimes referred to as the 'pressure-drop', is associated with the use of such particles. The lack of robust pumping systems limited early HPLC methods to the use of columns packed with particles of 5–10 µm in diameter. The development of ultra high-pressure HPLC pumps and novel particle manufacturing techniques has meant that in the last 10 years or so, very small HPLC particles, often less than 2 µm in diameter, have become commonplace. As well as improved efficiency resulting from a reduced A-term of the van Deemter equation, the use of sub-2 µm particles also has an influence on the van Deemter C-term. Small, uniform particles have reduced interstitial spaces, meaning that mass transfer in both the mobile and stationary phases is more efficient, and is less influenced by increasing mobile phase velocity. This means that separations may be carried out significantly faster, without compromising on chromatographic efficiency.

It was first observed by Pretorius & Smuts (1966) using open tubular columns, that an alternative way to improve both the speed of analysis and the efficiency of mass transfer was to use turbulent, or inertial, rather than laminar flow. Under turbulent flow, the flow profile through a column is much flatter than under laminar flow conditions (Figure 2.3), resulting in less band broadening. This is also advantageous for reproducible, yet rapid step changes in the mobile phase composition flowing through a column. The convection motion (or Eddy currents) created under turbulence also results in more even mass transfer within the mobile phase. The flow-rate at which flow changes from laminar to turbulent can be estimated using critical Reynolds numbers (Re). For columns packed with uniformly spherical particles, it has been reported that the critical Reynolds number is between 1 and 10 Re, varying owing to the irregularly shaped particles (Quinn & Takarewski, 1999; Edge, 2003; Herman &

Edge, 2012). However, using packed-column, high-pressure systems (e.g. packed columns with 3–5 µm particles or smaller), the back-pressures associated with the flow-rates necessary to achieve turbulence are prohibitively high, both in terms of the pumping systems and the robustness of the particle architecture.

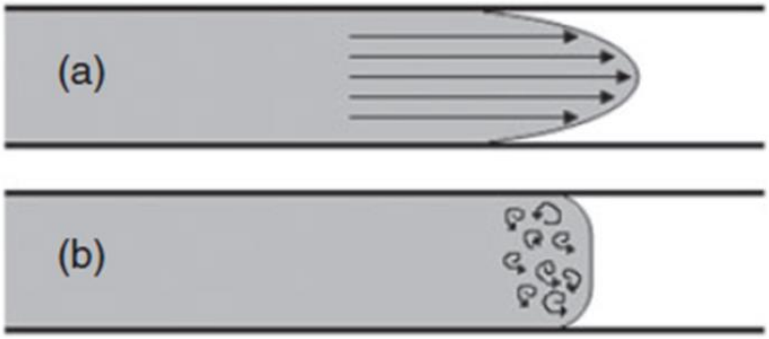

Figure 2.3. Mobile phase flow profiles through a column, demonstrating (a) a typical, laminar flow profile and (b) the 'flatter' flow profile with turbulent flow.

In the mid-1990s, by going against the convention of developing very small, reproducibly-shaped HPLC particles, Quinn and Takarewski observed some interesting findings when evaluating the van Deemter efficiency curves produced using columns packed with large (approximately 50–100 µm), irregularly shaped particles at increasing flow-rates. Using these particles, the back-pressures were sufficiently low to allow flow-rates that would generate turbulence, and it was observed that, at increasing flow-rates (and increasing Re values), column efficiency also increased (i.e. under turbulent flow, an unpredicted second van Deemter curve minimum was observed). The use of such packed columns (marketed as TurboFlow™ columns, at first via Cohesive Technologies, and later through ThermoFisher Scientific) at increased flow-rates was therefore patented in 1997 (US patent no. 5,919,368). At increased

flow-rates, it was also observed that the diffusion co-efficients of the solutes studied had a significant effect on retention. Larger macromolecules (e.g. proteins) in solution diffuse more slowly than smaller molecules (e.g. drugs/metabolites), and so may be excluded from the TFC column if the flow-rate is such that these larger molecules do not have time to diffuse into the pores of the particles and interact with the stationary phase chemistry. Under the same turbulent flow conditions, smaller molecules do have time to diffuse into and out of the pores, where they are either retained or eluted depending upon their affinity for the chosen bonded phase chemistry. A more detailed investigation into the relationship between flow-rate and molecular weight was recently reported by Herman & Edge (2012), who investigated the exclusion/retention of a range of nine proteins with differing molecular weights using a Cyclone™ TurboFlow column (50 x 0.5 mm i.d.). It was observed that, at neutral loading pH (pH 8.0, 5mmol/L aqueous ammonium formate), at a flow-rate of 1.0 mL/min, >99 % of proteins with a molecular weight greater than 15 kDa were excluded from the column. When the flow-rate was increased to 2.0 mL/min, the molecular weight exclusion 'cut-off' decreased to 8.7 kDa, as theory predicts. However, under acidic pH (0.1 %, *v/v*, aqueous formic acid, pH ~3.0), it was observed that almost all (>94 %) proteins with a molecular weight greater than just 1 kDa were excluded from the column. Although the exact mechanism for this phenomenon remains uncertain, and cannot be explained by the physical processes of turbulent flow alone, TFC is clearly a very efficient way of separating large matrix components, such as proteins, from smaller molecules. Therefore, it is in this area that TFC has found the most applications. For the analysis of small molecules (e.g. drugs, their metabolites, and some endogenous hormones) in biological matrices using traditional chromatographic techniques, the removal of matrix components is a necessary pre-analytical step. If not removed, high-molecular-weight matrix components quickly block the frits and pores of traditional HPLC columns, and have been shown to cause significant suppression of detector response in assays using LC-MS/MS. TFC columns, as well as efficiently removing large molecular weight interferences by the mechanisms described above, are less susceptible to blockage, owing to the large interstitial spaces. This therefore allows for the direct injection of biological fluids, providing they are free of particulate matter, for up to 1,000 injections (Edge, 2003). Compared with manual methods of sample

preparation, e.g. using solid-phase or liquid-liquid extraction, which are often time-consuming and therefore costly, TFC is simple to use, and highly amenable to automated, high-throughput workflows.

2.2. Aims

The work in this chapter describes the development of a novel method for the measurement of 25-OHD2 and 25-OHD3 using TFC-LC-MS/MS. The developed method was used to measure these compounds in clinical samples sent for routine 25-OHD analysis, and the results were compared against those produced for the same samples using three different commercially available immunoassay kits. Results for individual samples and results for the sample population as a whole were compared in terms of vitamin D status classification, using the following cut-off concentrations based on the report of Pludowski *et al.* (2013): less than 10 µg/L: severely deficient, greater than 10 µg/L but less than 20 µg/L: deficient, greater than 20 µg/L but less than 30 µg/L: sub-optimal, and greater than 30 µg/L: optimum.

Secondly, an automated protein precipitation sample preparation method was evaluated to assess the impact on batch analysis time for a busy UK clinical laboratory. The Chromsystems 96-well filter plate-based method was evaluated using a 96-channel automated liquid handling system and plate centrifuge. This was used in conjunction with the two-dimensional trap and analytical columns supplied in the Chromsystems MassChrom 25-OHD LC-MS/MS kit.

Thirdly, chromatographic methods for the resolution of 3-*epi*-25-OHD were developed using fused-core LC columns, with an emphasis on the total analysis time. The relative proportion of 3-*epi*-25-OHD3 was estimated in a small population of samples sent for routine analysis of 25-OHD. A rapid LC separation approach was also tested to attempt to futher speed up the separation of these two isobaric compounds.

2.3. Materials and methods

2.3.1. Chemicals and reagents

25-OHD2, 25-OHD3, 25-OHD3-D_6, 25-OHD3-D_3 and 3-*epi*-25-OHD3 were all from Sigma Aldrich (Poole, UK). Methanol and acetonitrile (LC grade) were from Rathburn (Walkerburn, UK). Isopropanol and acetone were from (BDH AnaLaR grade) were from VWR International (Lutterworth, UK). Additional control material from UTAK Laboratories (Tri-level Vitamin D Plus, UTAK, Valencia, CA, USA) were also used for the TFC-LC-MS/MS method.

Calibrators (6PLUS1™ and 3PLUS1™ 6-level and 3-level calibrator sets, respectively), internal quality control solutions (IQCs, bi-level) containing both 25-OHD2 and 25-OHD3, internal standard solution (containing 25-OHD3-D_6) and precipitation reagent were all from Chromsystems (Munich, Germany) as part of the MassChrom® 25-OH-Vitamin D2/D3 in serum/plasma LC-MS/MS kit (part number 62000). Nominal concentrations for Chromsystems calibrators and IQCs were traceable to the NIST SRM (SRM 972a). The 3PLUS1™ kit was used for the TFC-LC-MS/MS method, and the 6PLUS1™ kit, which became available later, was used for the automated precipitation method. Bi-level IQCs were used with both calibrator sets.

2.3.2. Materials and instrumentation

96-Well filtration plates, collection plates and plate seals were from Chromsystems (Munich, Germany). A Heraeus™ Labofuge™ 400 centrifuge (ThermoFisher Scientific) with 96-well plate rotor was used for plate centrifugation. For the non-TFC methodology for the automated sample preparation method, proprietary trap columns and analytical columns were from Chromsystems (Munich, Germany). TurboFlow™ columns (C18-XL, 0.5 x 50 mm) and Hypersil™ GOLD C18 columns for the TFC method without the resolution of the 3-*epi*-25-OHD3 (50 x 2.1 mm, 1.9 um and 3 um particle sizes) were from ThermoFisher Scientific (Runcorn, UK). For the development of the 3-*epi*-25OHD resolving method, Accucore™ pentafluorophenyl (PFP) columns (100 x 2.1 mm and 50 x 2.1 mm, both 2.7 um total particle size) were from ThermoFisher

Scientific (Runcorn, UK). Additionally, Poroshell™ guard cartridges (5 x 3.0 mm i.d., 2.7 um total particle size) were from Agilent Technologies (Cheadle, UK).

Multiple LC-MS/MS systems were used. For the TFC-LC-MS/MS methodology, an Aria Transcend TLX-II system was used, fitted with four Accela™ 600 quaternary pumps, valve-interface module (VIM), and CTC Pal autosampler. The MS was a TSQ Vantage™ (ThermoFisher Scientific, San Jose, CA) with interchangeable ESI/APCI ion sources. For the non-TFC methods, analysis was carried out on either (i) a Jasco HPLC system (including DG-2080 degasser, two PU-2085*Plus* binary pumps, AS-1550 autosampler, and CO-2067*Plus* column oven – all Jasco, Great Dunmow, UK) with a 3200 triple quadrupole MS with Turbo V ion source (Sciex, Warrington, UK), or (ii) an Agilent 1200 series LC system, consisting 1260 binary LC pump and degasser, 1290 Infinity II autosampler, and 6460 triple quadrupole MS with Jet-Stream ion source (all Agilent Technologies, Santa Clara, CA).

96-channel liquid handling for the automated 96-well filter-plate method was carried out using a Versette™ liquid handler (Thermo Scientific, Vantaa, Finland), equipped with a 96-channel 300 µL pipetting head and six moveable plate stages.

For the non-TFC method using automated precipitation, system eluents were used as supplied by Chromsystems (wash buffer, system eluents, auto-sampler wash buffer). For the TFC method, and for the evaluation of the 3-*epi*-25-OHD resolving method using rapid LC, eluents were prepared as follows: Eluent A was 0.1 % (*v/v*) aqueous formic acid, and Eluent B was 0.1 % (*v/v*) formic acid in methanol. For the TFC-LC-MS/MS method, the TurboFlow column wash was 'Magic Mix' (2:2:1, *v/v/v*, acetonitrile: isopropanol: acetone). Magic Mix was also used for the autosampler needle washing (Wash 2), along with a mix of Eluent A and B (40:60, *v/v*) as the other wash solvent (Wash 1).

MS/MS settings were separately tuned for each ion source and for each MS instrument used. In all cases, except for the investigation of a rapid chromatographic method for the separation of 25-OHD3 and 3-*epi*-25-OHD3, water-loss *m/z* transitions were avoided for quantitation, though were included for data acquisition (Table 2.1). For the investigation of the rapid epimer-resolving method, a methanolic equimolar mixture of

25-OHD3 and 3-*epi*-25-OHD3-D_3 was used to allow the assessment of peak overlap of the isobaric compounds. No in-source water-loss was observed (Agilent Jet Stream ion source), and for simplicity in the absence of sample matrix, water-loss transitions from the protonated precursor ions were used (*m/z* 401.3>383.3 and 404.3>389.3, respectively – Table 2.1).

2.3.3. Comparator methods

For the comparison of the developed TFC-LC-MS/MS method with automated immunoassay platforms, samples were additionally analysed using (i) the Diasorin Liaison® 25 OH Vitamin D TOTAL chemiluminescent immunoassay (in routine operation at King's College Hospital at the time of analysis), (ii) the Immunodiagnosticsystems (IDS) iSYS 25-Hydroxyvitamin D3 automated chemiluminescent immunoassay, and (iii) the Siemens Advia Centaur Vitamin D Total method (in current use at King's College Hospital at the time of writing). All assays were carried out from barcoded serum samples according to manufacturer's instructions. Samples were stored frozen (-20 °C) between analysis by each method, and analysed by all methods within a 4-month period. Statistical analysis of results was analysed using AnalyseIt™ software (version 2.30) within Microsoft Excel. Comparison of each method to the TFC-LC-MS/MS method was carried out using three pair-wise Bland Altman plots.

2.3.4. Clinical samples and controls

Samples sent for routine 25-OHD analysis (N = 195) were anonymised and analysed by four methods for the comparison study. Only a sub-set of the samples (N = 136) had sufficient volume to allow analysis by the fourth method, the Siemens Advia Centaur method. For investigation of the chromatographic methods for the separation of 3-*epi*-25-OHD3, additional portions of DEQAS samples 404 and 405 were kindly supplied by DEQAS. A further set of samples sent for routine 25-OHD analysis (N = 74) were anonymised and analysed by the epimer-resolving TFC-LC-MS/MS method to assess relative prevalence of the 3-*epi*-25-OHD3. These samples were not pre-selected based on age at time of sampling.

	Analyte	Q1	Q3	CE (V)	Additional MS settings
TSQ Vantage (APCI)	25-OHD2	395.3	269.1	17	*S-lens:* 95-110 V; *Scan width:* 0.025 m/z; *Collision pressure:* 1.5 mTorr; *Q1/Q3 resolution:* 0.7 FWHM *Discharge voltage:* 4.0 V; *Vaporiser temperature:* 380 °C; *Capillary temperature:* 280 °C; *Sheath gas:* 20; *Auxiliiary gas:* 10
			251.1	24	
			(377.1)	17	
	25-OHD3	383.3	257.1	16	
			229.1	19	
			(365.1)	13	
	25-OHD3-D_6	389.3	263.1	17	
			229.1	19	
Sciex API 3200 (ESI)	25-OHD2	395.3	269.1	28	*Dwell time:* 20-50 ms; *DP:* 50-55 V; *EP:* 4-6 V; *CEP:* 13-19 V; *CXP:* 3-4 V *Curtain gas:* 20.0; *Collision gas:* 3.0; *IonSpray voltage:* 5,000 V; *Temperature:* 350 °C; *Ion Source Gas 1:* 40; *Ion Source Gas 2:* 30
			251.1	40	
			(377.1)	30	
	25-OHD3	383.3	257.1	25	
			229.1	32	
			(365.1)	22	
	25-OHD3-D_6	389.3	263.1	25	
			229.1	32	
Agilent 6460 (ESI)	25-OHD3; 3-*epi*-25OHD	401.3	383.1	4	*Dwell time*: 20 ms; *Fragmentor voltage*: 106 V; *Cell accelerator voltage*: 4 V *Gas temperature:* 350 °C; *Gas flow:* 11 L/min; *Nebuliser:* 55 psi; *Sheath gas temperature:* 325 °C; *Sheath gas flow* 11 L/min; *Capillary voltage:* 5000 V; *Nozzle voltage:* 500 V
	25-OHD3-D_6	404.3	386.1	4	

Table 2.1. Summary MS/MS conditions for each of the three LC-MS/MS instruments used.

2.3.5. Sample preparation

Samples, calibrators, and IQC solutions (100 µL) were added to either a 1.5 mL centrifuge tube for the manual TFC-LC-MS/MS method, or were pipetted into wells of a 96-well filter plate for the automated method. This sample volume was used for all instruments and methods. For the manual TFC-LC-MS/MS method, internal standard solution was added (200 µL, 25 µg/L 25-OHD3-D_6 in acetonitrile), and the tubes were capped and vortex mixed (10 min) on a multi-tube vortex mixer. Supernatents (> 100 µL) were transferred using plastic disposable Pasteur pipettes into autosampler vials with glass inserts (300 µL volume) for analysis.

For the automated method, the precipitation reagent (25 µL) and internal standard solution (100 µL) supplied by Chromsystems were added from separate reagent troughs, the filter plate was covered with a plastic removable lid, and the well contents mixed (600 rpm orbital shaking, 10 min). The filter plates were placed on top of 96-well collection microplates, and supernatents were collected by centrifugation (2,000 g, 4 min). The collection microplates were sealed with adhesive plate-seals also supplied by Chromsystems, and the sealed plates were transferred to the autosampler for analysis.

2.4. Results and discussion

2.4.1. TurboFlow method

The summary valve switching proilfe for the optimised TFC-LC-MS/MS method is shown in Table 2.2. Absolute analyte recovery (without matrix present) on the C18-XL TurboFlow column was assessed by comparison of peak areas of a freshly prepared solution of 25-OHD2 and 25-OHD3 in Eluent starting conditions (20 % *v/v* methanol in deionised water with 0.1 % *v/v* formic acid), which was injected (i) in replicate (N = 3) onto the TurboFlow column followed by (ii) replicate injection directly onto the analytical column (N = 3) with the TurboFlow column bypassed. Mean recovery was 79 % for 25-OHD2 and 97 % for 25-OHD3. Calibration was linear (R^2> 0.99) for both analytes using the 3PLUS1™ Chromsystems calibrator kit (Figure 2.4) over the calibration ranges.

Intra-assay precision for 25-OHD3 was assessed by the replicate analysis (N = 5) of three sample pools containing 'low', 'medium' and 'high' concentrations of 25OHD (based on initial analysis using the Diasorin Liaison Total method). The precision (% CV) was 9.1 %, 6.0 % and 8.2 % at mean 25-OHD concentrations of 2.0, 17.0 and 46.0 µg/L, respectively.

Inter-assay precision was assessed by replicate analysis of the UTAK Tri-Level QC samples over 3 batches. The precision (% CV) for 25-OHD2 and 25-OHD3 respectively were 11.2 % and 6.2 % for Level I (10 µg/L both analytes), 5.7 % and 7.3 % for Level II (30 µg/L both analytes) and 9.8 % and 8.1 % for Level III (73 µg/L both analytes).

The lower limit of quantitation (LLoQ), taken as the mean concentration at which the precision (% CV) exceeded 20 %, was 1.0 µg/L and 0.7 µg/L for 25-OHD3 and 25-OHD2, respectively.

The retrospective analysis of 8 DEQAS samples was carried out as an additional evaluation of the performance of the TFC-LC/MS/MS result. Table 2.3 summarises the results, including the initial submitted results (Diasorin Liaison Total), and the all-laboratory trimmed-mean (ALTM) result reported by DEQAS.

		Loading pump (C18 XL)							Eluting pump (Hypersil GOLD C18)		
Step	**Time (sec)**	**Flow rate (mL/min)**	**%A**	**%B**	**%C**	**%D**	**Tee**	**Loop**	**Flow rate (mL/min)**	**%A**	**%B**
1	40	2.00	60	40	-	-	Out	Out	0.50	80	20
2	40	0.20	60	40	-	-	In	In	0.30	80	20
3	15	1.00	-	-	100	-	Out	In	0.50	80	20
4	15	1.00	-	-	100	-	Out	Out	0.50	25	75
5	25	2.00	-	-	100	-	Out	Out	0.50	15	85
6	20	2.00	-	-	100	-	Out	Out	0.50	5	95
7	20	2.00			100	-	Out	Out	0.50	-	100
8	21	2.00			100	-	Out	Out	0.50	-	100
9	20	2.00			100	-	Out	Out	0.50	80	20
10	20	2.00	-	100	-	-	Out	In	0.50	80	20
11	60	2.00	60	40	-	-	Out	Out	0.50	80	20

Table 2.2. Summary of the gradient elution and TurboFlow valve switching method.System eluents were as follows: (Loading/Eluting Pump Eluents A) 0.1 % (v/v) formic acid in deionised water, (Loading/Eluting Pump Eluents B) 0.1 % (v/v) formic acid in methanol, (Loading Pump Eluent C) 1+2+2 (v/v/v) acetone, acetonitrile and isopropanol ('Magic Mix').

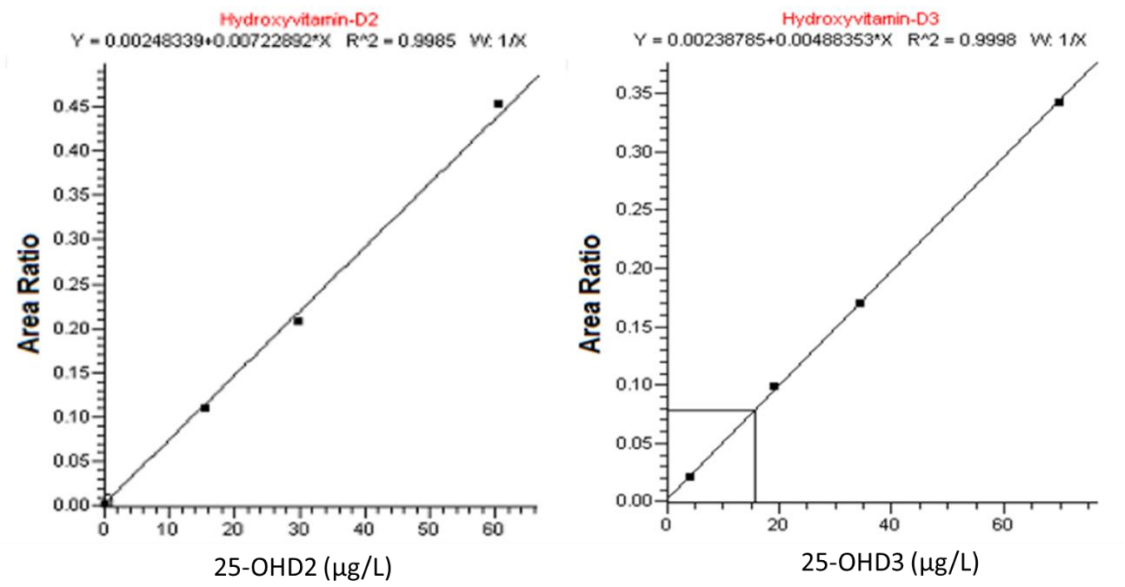

Figure 2.4. Example 3PLUS1™ MassChrom 25-OHD calibration curves produces using the TFC-LC-MS/MS method. Shown are calibration curves for 25-OHD2 (left), and 25-OHD3 (right). Both calibration curved were constructed using the peak area ratio with that of 25-OHD3-D_6.

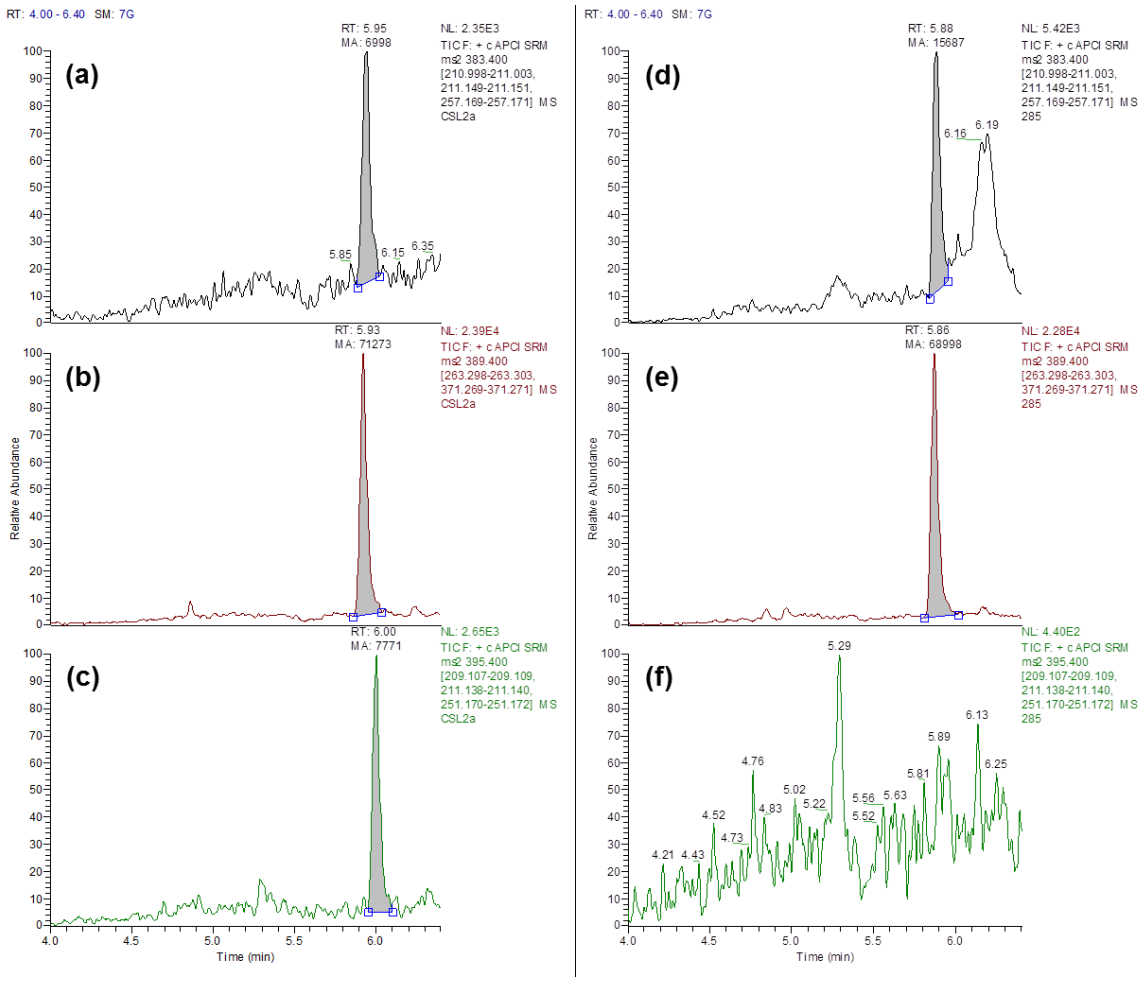

Figure 2.5. Example TFC-LC-MS/MS chromatograms. The extracted chromatograms on the left show (a) 25-OHD3, (b) 25-OHD3-D6, and (c) 25-OHD2 from a Chromsystems 3PLUS1™ Level 2 Calibrator, and the chromatograms on the right (d, e, and f) the equivalent chromatograms in a clinical sample.

	ALTM	Diasorin Liaison Total	TFC-LC-MS/MS		
	25-OHD (µg/L)	25-OHD (µg/L)	25-OHD3 (µg/L)	25-OHD2 (µg/L)	25-OHD (µg/L)
1	7.9	7.9	6.4	1.7	8.1
2	15.5	14.9	12.6	1.3	13.9
3	30.0	32.5	24.9	1.5	26.4
4	20.2	20.9	16.8	1.2	18.0
5	26.9	25.6	23.6	4.8	28.4
6	7.3	6.0	4.7	1.3	6.0
7	19.4	19.7	16.2	1.3	17.5
8	9.6	8.3	7.5	0.7	8.2

Table 2.3. Summary results for 8 DEQAS samples analysed by the routine Diasorin Liaison Total method and by TFC-LC-MS/MS. Also shown are the DEQAS all-laboratory trimmed-mean (ALTM) results.

2.4.2. Comparison of results

For the TFC-LC-MS/MS method in which 25-OHD2 and 25-OHD3 were independently quantified, a total 25-OHD was calculated for any samples in which 25-OHD2 exceeded the analytical limit of quantitation (1.0 µg/L). In cases where the 25-OHD2 was not detected, or was below the limit of quantitation, the 25-OHD3 concentration was taken as the total 25-OHD for the comparison.

2.4.2.1. TFC-LC-MS/MS vs Diasorin Liaison Total Vitamin D immunoassay

For the sample population as a whole, there was an overall correlation between the two methods (Pearson correlation = 0.877, R^2 = 0.77, Figure 2.6). The mean bias between the two methods (TFC-LC-MS/MS – Liaison) was -0.86 µg/L, suggesting the TFC-LC-MS/MS method gave, on average, slightly lower results that the Liaison. However, the 95 % limits of agreement (-11.58 to 9.86 µg/L) showed large variability between results for individual samples.

2.4.2.2. TFC-LC-MS/MS vs IDS iSYS Vitamin D immunoassay

As with the comparison to the Diarosin Liaison immunoassay, for the sample population as a whole there was an overall correlation between the two methods (Pearson correlation = 0.875, R^2 = 0.76, Figure 2.7). The mean bias between the two methods (TFC-LC-MS/MS – iSYS) was -3.04 µg/L, again suggesting the TFC-LC-MS/MS method gave, on average, slightly lower results that the immunoassay. Again, the 95 % limits of agreement (-13.88 to 7.81 µg/L) showed large variability between results for individual samples.

Despite similarities between the correlations of each of these immunoassays with the TFC-LC-MS/MS method, the correlation between the two immunoassay results was in fact worse than between each of the immunoassays and the TFC-LC-MS/MS method [R^2 = 0.68, mean bias (iSYS – Liaison) 2.18 µg/L, 95 % limits of agreement -10.53 to 14.88 µg/L].

2.4.2.3. TFC-LC-MS/MS vs Advia Centaur Vitamin D immunoassay

There was an overall correlation between the two methods (Pearson correlation = 0.831, R^2 = 0.69, Figure 2.8). The mean bias between the two methods (TFC-LC-MS/MS – Centaur) was -0.57 µg/L, suggesting the TFC-LC-MS/MS method gave, on average, slightly lower results than the Advia immunoassay. The 95 % limits of agreement (-11.90 to 10.76 µg/L) for all samples showed large variability between results for individual samples. However, there was a clear positive bias for the immunoassay at lower concentrations. Taking a sub-set of the samples, in which the measured 25-OHD (by TFC-LC-MS/MS) was less than or equal to 25 µg/L, the correlation between the methods was still apparent (Pearson correlation = 0.80, R^2 = 0.64), but the immunoassay showed a bias of almost 35 % [slope (95 % CI) of scatter plot 1.347 (1.152 to 1.542)].

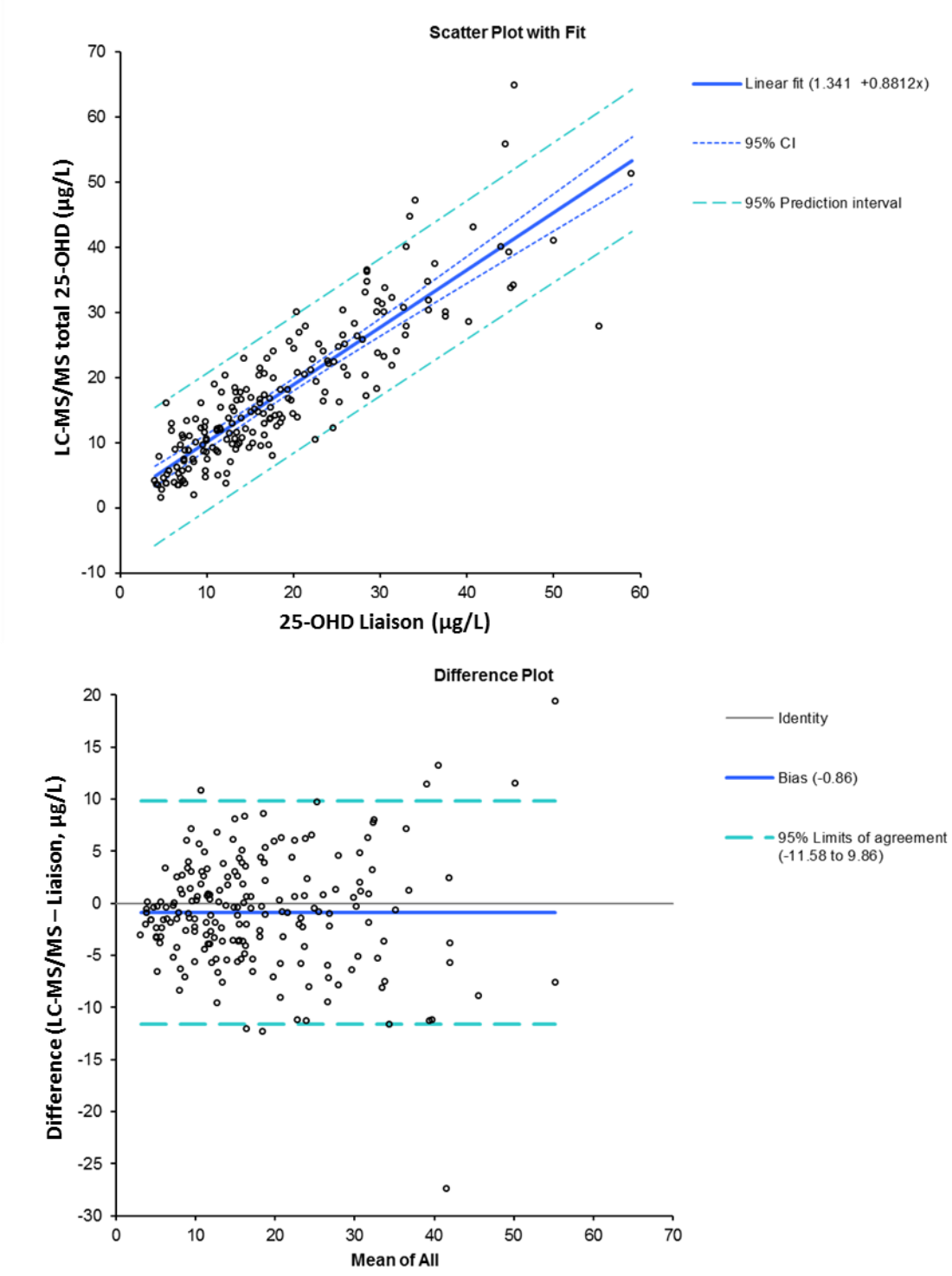

Figure 2.6. Comparison of results (N = 195) between the Diasorin Liaison Total vitamin D immunoassay and TFC-LC-MS/MS methods. Shown are (top) scatter plot with linear regression statistics, and (bottom) Bland-Altman plot with 95 % limits of agreement (µg/L).

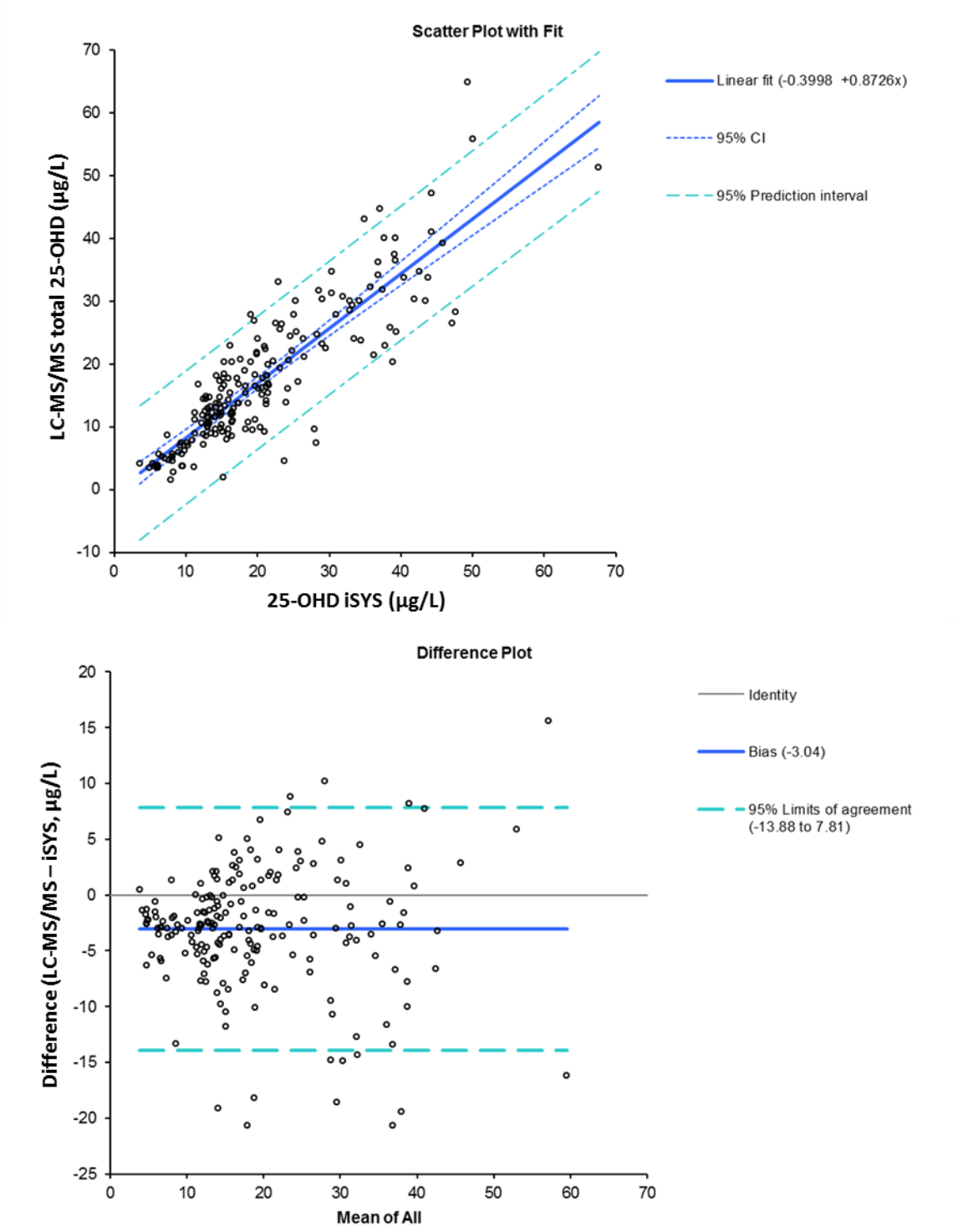

Figure 2.7. Comparison of results (N = 195) between the IDS iSYS vitamin D immunoassay and TFC-LC-MS/MS methods. Shown are (top) scatter plot with linear regression statistics, and (bottom) Bland-Altman plot with 95 % limits of agreement (µg/L).

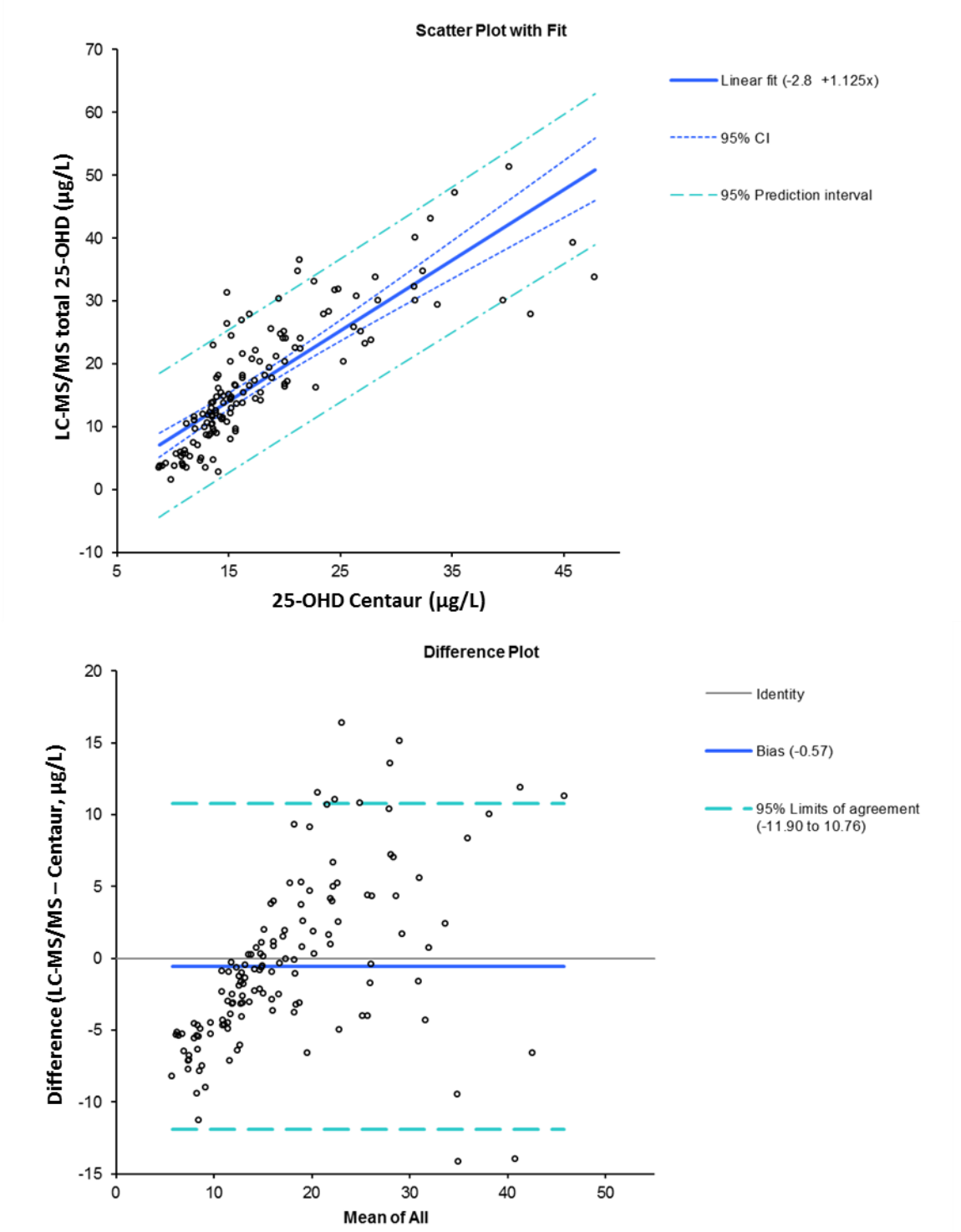

Figure 2.8. Comparison of results (N = 136) between the Siemens Advia Centaur vitamin D immunoassay and TFC-LC-MS/MS methods. Shown are (top) scatter plot with linear regression statistics, and (bottom) Bland-Altman plot with 95 % limits of agreement (µg/L).

2.4.2.4. Classification of vitamin D status and assessment of possible treatment outcomes

The data for vitamin D status classification based on the results from each of the four assays is summarised in Table 2.4. In general, the proportion of all patients classified as severely deficient, deficient, sub-optimal, or optimal were broadly similar for each assay, expect for a much lower proportion of patients with severe deficiency when analysed using the Advia Centaur methodology.

	TFC-LC-MS/MS N (%)	Diasorin Liaison N (%)	IDS iSYS N (%)	Siemens Advia Centaur N (%)
Total N	195	195	195	136
'Severe' deficiency (<10 µg/L)	52 (26.7)	48 (24.6)	26 (13.3)	5 (3.7)
'Deficient' (<20 µg/L)	75 (38.5)	78 (40.0)	88 (45.1)	94 (69.1)
'Sub-optimal' (<30 µg/L)	38 (19.5)	39 (20.0)	43 (22.1)	25 (18.4)
'Optimal' (≥30 µg/L)	30 (15.4)	30 (15.4)	38 (19.5)	12 (8.8)

Table 2.4. Summary data for patient samples analysed using each of four 25-OHD assays. Proportions of the total population are shown for each assay according to vitamin D status classification cut-off concentrations.

For individual samples, status classification discrepancies were observed depending upon which of the four assays results were used. For samples where the 25-OHD measured by TFC-LC-MS/MS was below 10 μg/L ('severe deficiency', N = 52), the immunoassays gave the following results. For the Diasorin Liaison, the mean 25-OHD for these samples was 9.0 μg/L, and 17 (33 %) samples had measured 25-OHD greater than 10 μg/L. For the IDS iSYS, the mean 25-OHD for these samples was 11.7 μg/L, and 26 (50 %) samples had measured 25-OHD greater than 10 μg/L. For the Advia Centaur, 35 sample results were available for this group; the mean concentration was 12.0 μg/L, and 30 (85 %) samples had measured 25-OHD greater than 10 μg/L.

For samples where the 25-OHD measured by TFC-LC-MS/MS was greater than 10 μg/L but less than 20 μg/L ('deficient', N = 75), the immunoassays gave the following results. For the Diasorin Liaison, the mean 25-OHD for these samples was 14.8 μg/L, 14 (19 %) samples had measured 25-OHD less than 10 μg/L, and 9 (12 %) had measured 25-OHD greater than 20 μg/L. For the IDS iSYS, the mean 25-OHD for these samples was 16.6 μg/L, no samples had measured 25-OHD less than 10 μg/L, but 17 (23 %) samples had measured 25-OHD greater than 20 μg/L. For the Advia Centaur, 52 sample results were available for this group; the mean concentration was 15.3 μg/L, no samples had measured 25-OHD less than 10 μg/L, but 4 (8 %) samples had measured 25-OHD greater than 20 μg/L.

For samples where the 25-OHD measured by TFC-LC-MS/MS was greater than 20 μg/L but less than 30 μg/L ('sub-optimal', N = 38), the immunoassays gave the following results. For the Diasorin Liaison, the mean 25-OHD for these samples was 25.2 μg/L, 8 (21 %) samples had measured 25-OHD less than 20 μg/L, and 8 (21 %) had measured 25-OHD greater than 30 μg/L. For the IDS iSYS, the mean 25-OHD for these samples was 27.1 μg/L, 9 (24 %) samples had measured 25-OHD less than 20 μg/L, and 12 (32 %) samples had measured 25-OHD greater than 30 μg/L. For the Advia Centaur, 29 sample results were available for this group; the mean concentration was 21.3 μg/L, 15 (52 %) samples had measured 25-OHD less than 20 μg/L, and 2 (7 %) samples had measured 25-OHD greater than 30 μg/L.

For samples where the 25-OHD measured by TFC-LC-MS/MS was greater than 30 µg/L ('optimum', N = 30), the immunoassays gave the following results. For the Diasorin Liaison, the mean 25-OHD for these samples was 35.8 µg/L, and 8 (27 %) samples had measured 25-OHD less than 30 µg/L. For the IDS iSYS, the mean 25-OHD for these samples was 38.4 µg/L, and 4 (13 %) samples had measured 25-OHD less than 30 µg/L. For the Advia Centaur, 20 sample results were available for this group; the mean concentration was 30.0 µg/L, and 10 (50 %) samples had measured 25-OHD less than 30 µg/L.

The correlation between methods was poorer when analysing only those results with 25-OHD concentrations measured by TFC-LC-MS/MS between 10-30 µg/L (N = 113 for Liaison and iSYS, N = 81 for Centaur). The Pearson correlation reduced from 0.77 to 0.52 for the Liaison comparison, from 0.76 to 0.52 for the iSYS comparison, and from 0.69 to 0.48 for the Centaur (Figure 2.9).

The Bland-Altman plots also demonstrated for each of the immunoassays that in some samples the concentration was greater than the TFC-LC-MS/MS method, and in other samples, the concentration was lower. Investigating this further by sub-grouping the data into concentration bands according to the TFC-LC-MS/MS concentration, it was found that the immunoassays produced higher results for those samples with TFC-LC-MS/MS concentrations below 10 µg/L (Figure 2.10).

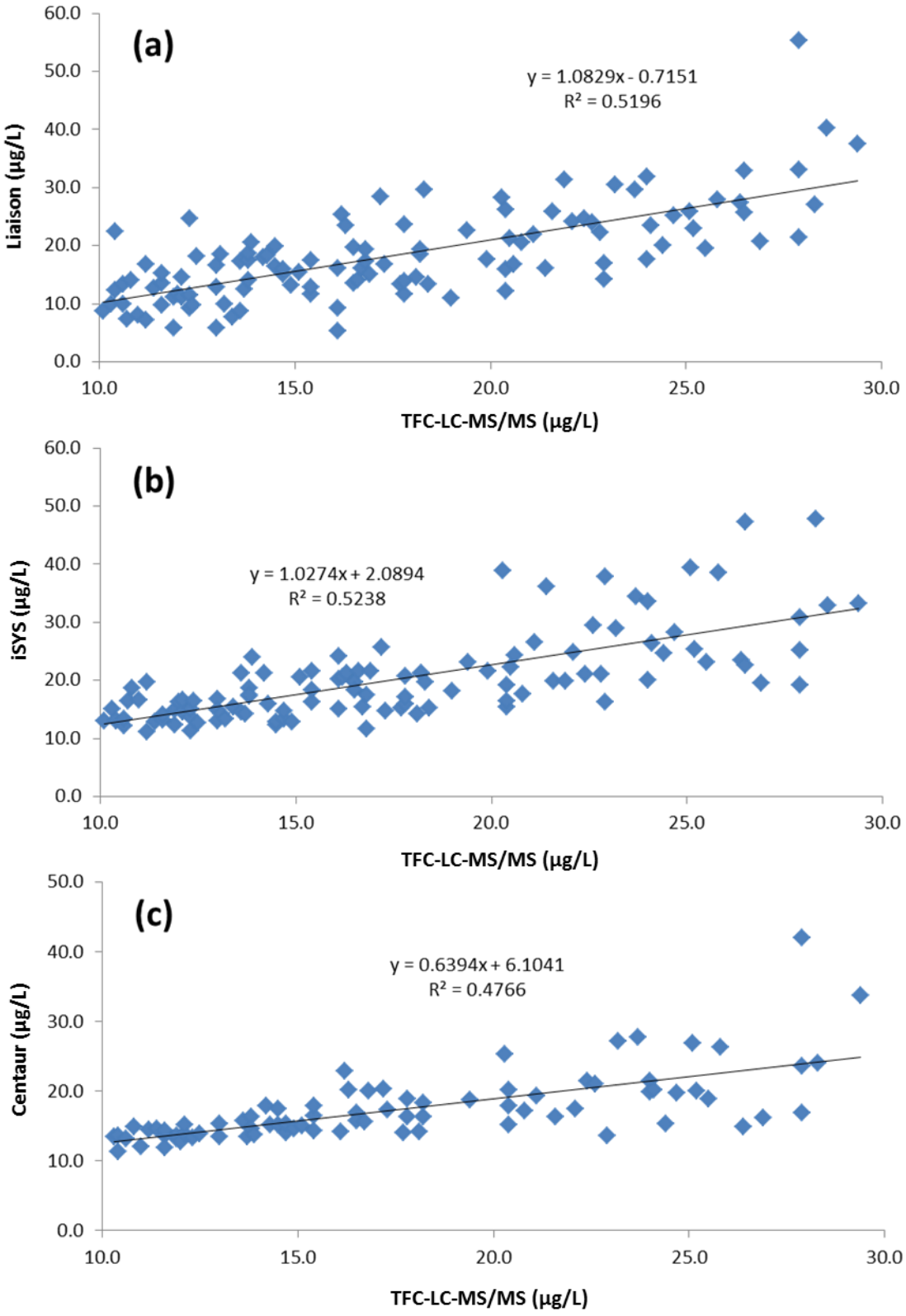

Figure 2.9. Correlation with TFC-LC-MS/MS results for 25-OHD concentrations from 10-30 µg/L. Shown are (a) Liaison, (b) iSYS and (c) Centaur comparisons.

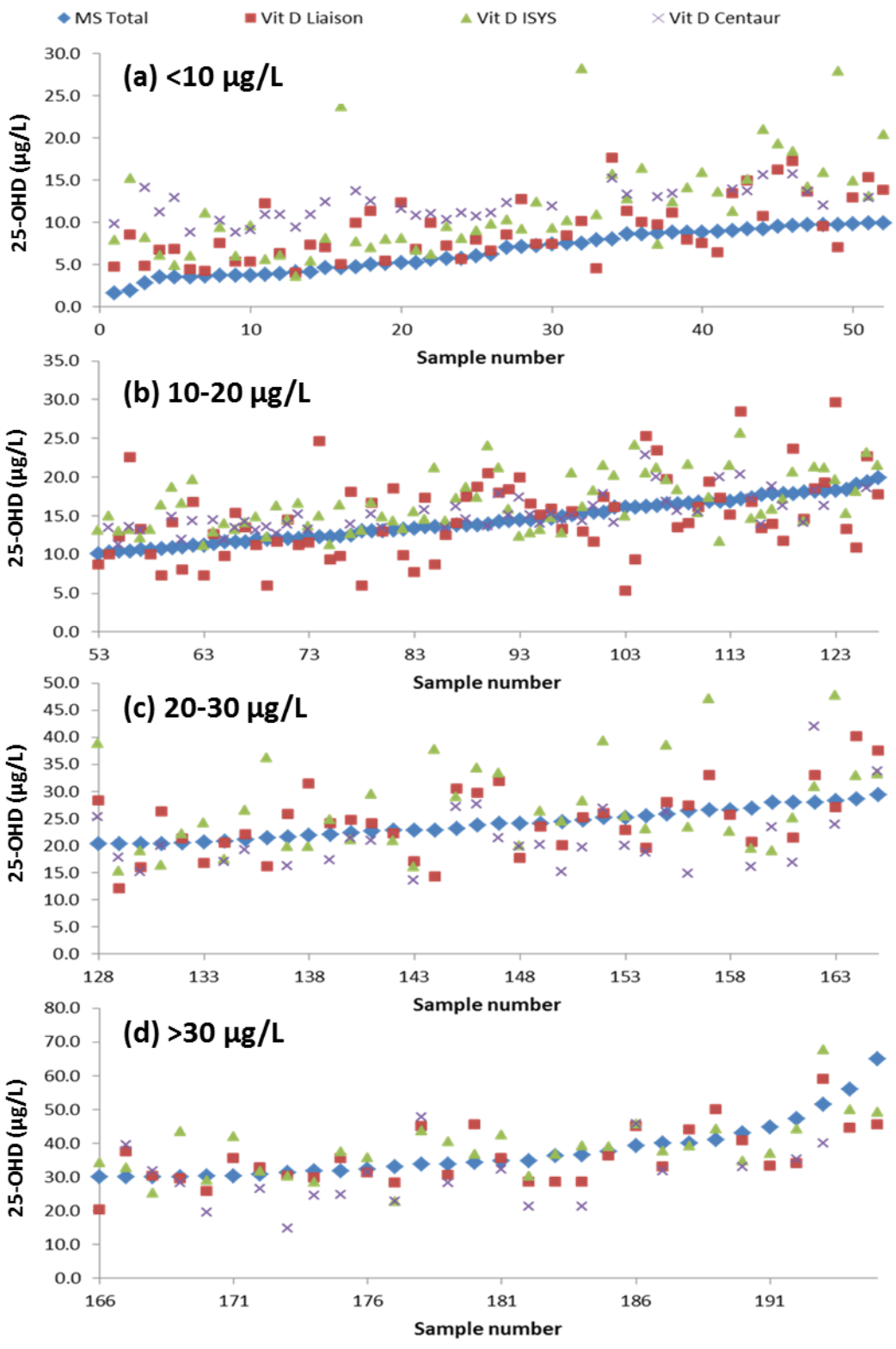

Figure 2.10. 25-OHD results for all samples (N = 195) summarised in order of increasing 25-OHD concentration as measured by TFC-LC-MS/MS, and grouped by 25-OHD concentration.

Excluding the data for the Advia Centaur for which there were fewer results available, discrepancy between individual sample results can be presented as a series of Venn diagrams for each vitamin D status group, as shown in Figure 2.11. This figure shows discrepancies between each of the assays for individual samples at each concentration group. The proportion of samples with status classification agreement between all three assays was generally low: for 25-OHD concentrations less than 10 µg/L, 22 (33 %) samples were in agreement, for 25-OHD concentrations between 10-20 µg/L, 43 (37 %) samples were in agreement, for 25-OHD concentrations between 20-30 µg/L, 13 (18 %) samples were in agreement, and for 25-OHD concentrations greater than 30 µg/L, 21 (47 %) samples were in agreement between the methods.

2.4.2.5. Samples containing 25-OHD2

From the samples studied, 7 samples were available from patients who appeared to be supplemented with D2, and with concentrations of 25-OHD2 greater than 10 µg/L as measured by TFC-LC-MS/MS. All three of the automated immunoassay platforms used claimed 100 % cross-reactivity of both species as follows: for the Siemens Advia Centaur method; "..equimolar total measurement of 25-OHD2 and 25-OHD3..", for the Diasorin Liaison TOTAL method; "…antibodies that are co-specific for 25-OHD2 and 25-OHD3…", and for the IDS iSYS method; "...co-specificity of 25-OHD3 and 25-OHD2…". The results for these samples are summarised in Table 2.5. Each immunoassay showed cross-reactivity with 25-OHD2. 25-OHD2 was detected (>0.7 µg/L) in 33 samples in total. The mean (range) proportion of the total 25-OHD which was from 25-OHD2 in these samples was 29.7 (3.1 – 88.8) %. No correlation was observed between the difference in results (immunoassay – TFC-LC-MS/MS, µg/L) and the proportion of 25-OHD2 in those samples where 25-OHD2 was detected by TFC-LC-MS/MS (Figure 2.12).

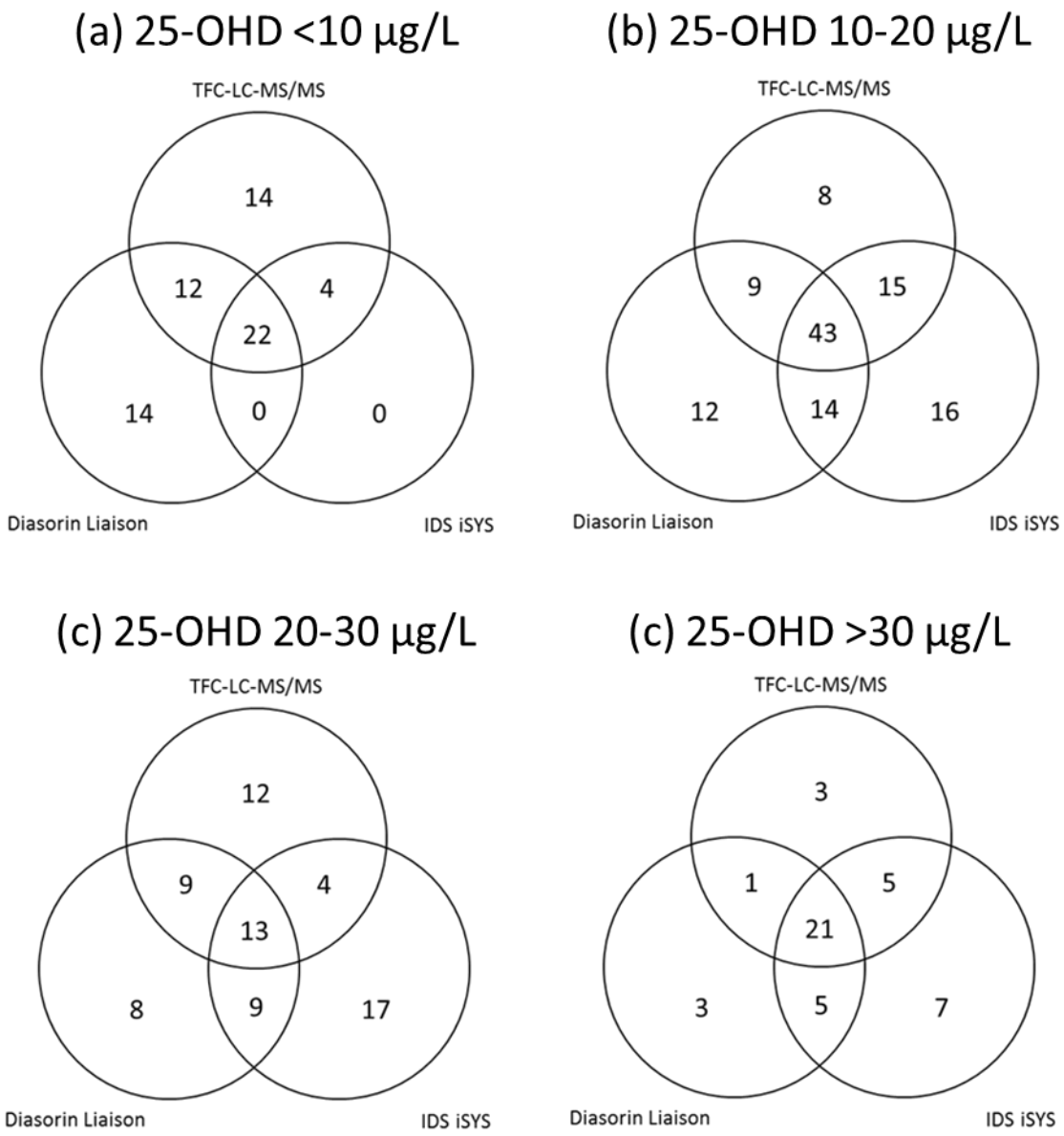

Figure 2.11. Numbers of vitamin D status classification discrepancies based on results produced using TFC-LC-MS/MS, Diasorin Liaison and IDS iSYS immunoassays.

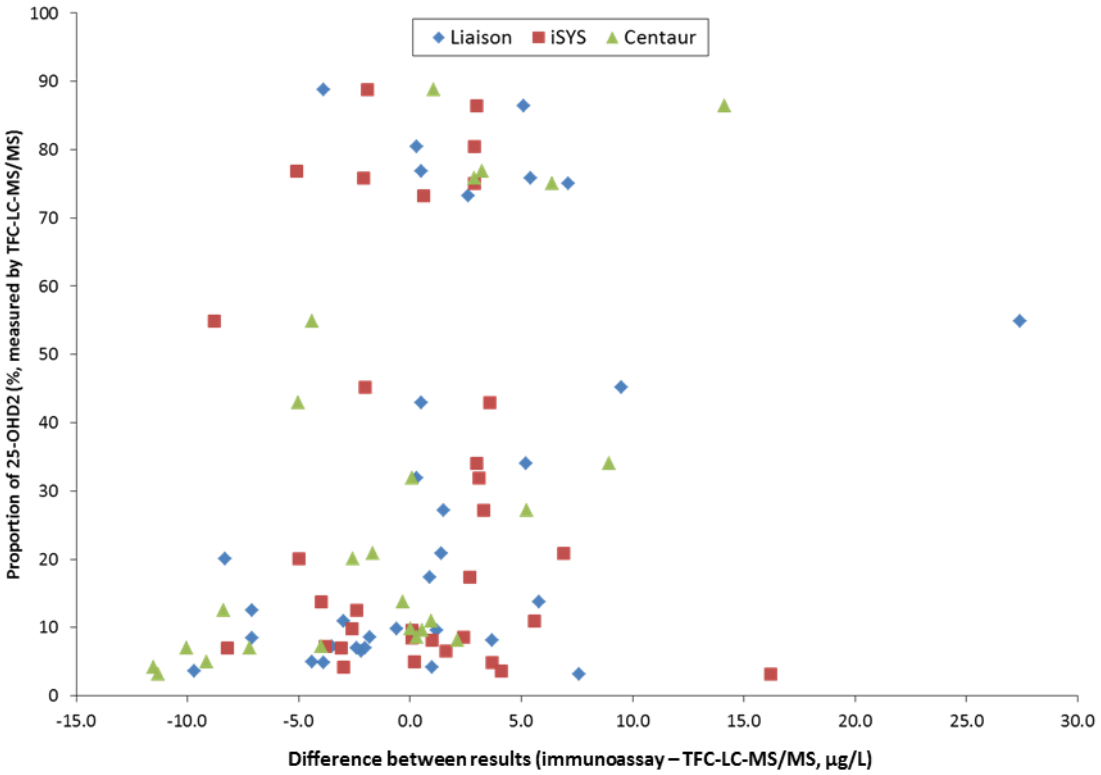

Figure 2.12. Scatter plot of the difference between each of the three immunoassays and the TFC-LC-MS/MS method versus the proportion to total 25-OHD which was 25-OHD2 (as measured by TFC-LC-MS/MS).

Sample	Diasorin Liaison (µg/L)	IDS iSYS (µg/L)	Advia Centaur (µg/L)	TFC-LC-MS/MS (25-OHD3, 25-OHD2 [total], µg/L)
1	25.2	28.3	19.7	14.1, 10.6 [24.7]
2	19.9	12.4	17.4	3.5, 11.0 [14.5]
3	19.4	17.4	*(Insufficient)*	4.5, 12.3 [16.8]
4	17.3	11.7	20.0	3.9, 12.9 [16.8]
5	55.3	19.1	23.5	12.6, 15.3 [27.9]
6	13.9	15.9	18.9	2.0, 15.8 [17.8]
7	33.0	30.9	42.0	3.8, 24.1 [27.9]

Table 2.5. Summary data for samples containing 25-OHD2 greater than 10 µg/L.

2.4.3. Automated 25-OHD analysis

The automated method using 96-well filter plates showed good intra-plate and inter-plate precision and accuracy for the two levels of Chromsystems IQC solutions (Table 2.6). The automated method was used in conjunction with the newly available 6PLUS1™ 25-OHD calibrator kit manufactured by Chromsystems, which demonstrated linear calibration curves (typical R^2> 0.99, *1/x* weighting applied, calibration not forced through the origin) for both analytes across the calibration range (Figure 2.13).

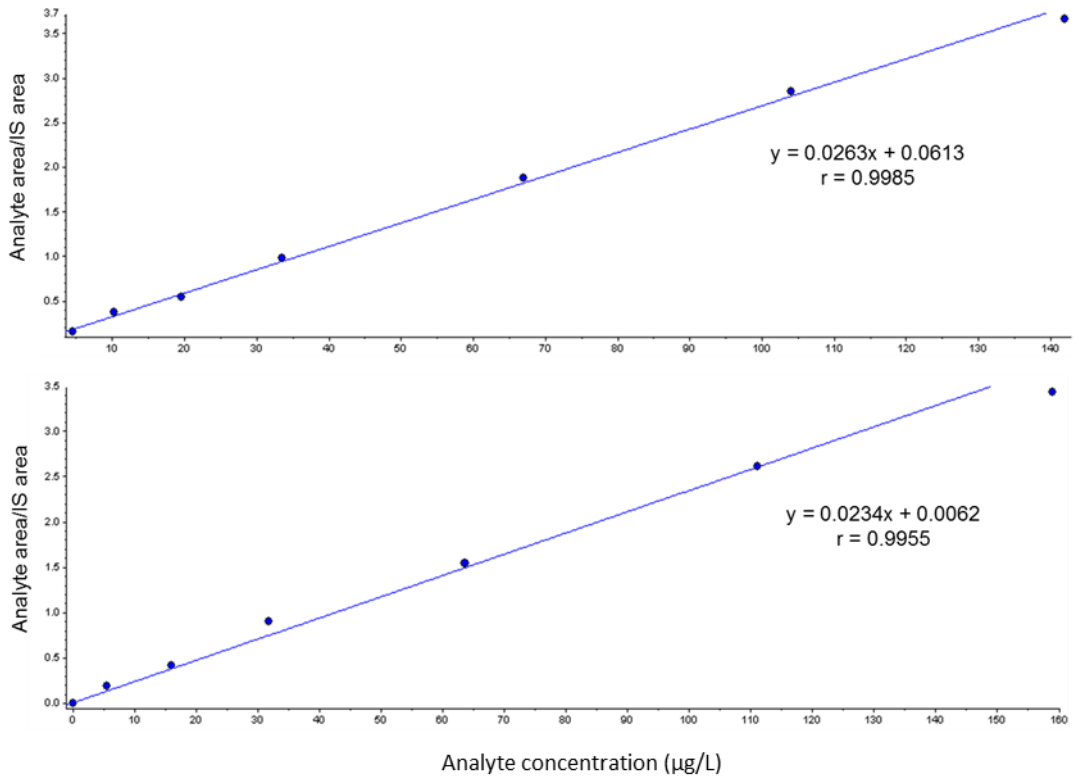

Figure 2.13. Example 6PLUS1™ MassChrom 25-OHD calibration curves produces using the 96-well filter plate automated LC-MS/MS method. Shown are calibration curves for 25-OHD3 (top), and 25-OHD2 (bottom). Both calibration curved were constructed using the peak area ratio with that of 25-OHD3-D_6.

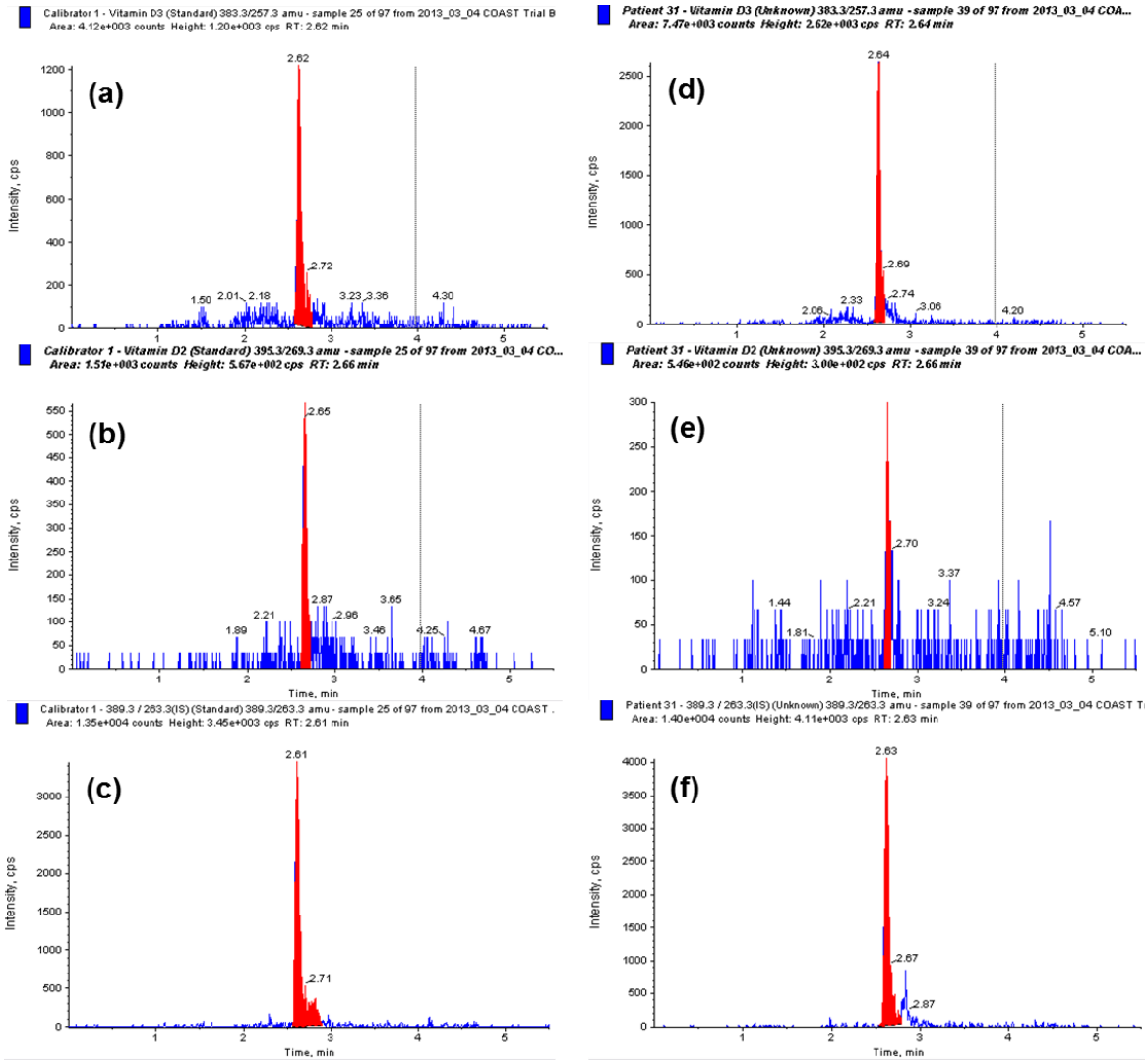

Figure 2.14. Example LC-MS/MS chromatograms following automated 96-well extraction. The extracted chromatograms on the left show (a) 25-OHD3, (b) 25-OHD3-D6, and (c) 25-OHD2 from a Chromsystems 6PLUS1™ Level 2 Calibrator, and the chromatograms on the right (d, e, and f) the equivalent chromatograms in a clinical sample.

	25-OHD2		25-OHD3	
	Level 1 (17.2 µg/L)	Level 2 (37.8 µg/L)	Level 1 (16.7 µg/L)	Level 2 (37.7 µg/L)
Intra-plate				
Mean (N = 4)	16.4	37.8	17.9	38.8
SD	0.39	2.65	0.66	3.37
CV (%)	2.41	7.01	3.71	8.71
Accuracy (%)	95.2	100.0	107.1	102.8
Inter-plate				
Mean (N = 4 in each of 8 batches)	16.9	38.0	16.5	37.0
SD	0.82	1.00	0.62	1.90
CV (%)	4.82	2.64	3.76	5.14
Accuracy (%)	98.5	100.4	98.8	98.1

Table 2.6. Summary intra-plate and inter-plate accuracy and precision data for the automated 96-well filter plate method.

2.3.3.1. Total sample preparation time

To manually prepare a batch of 96 tubes using a standard protein precipitation protocol such as that used for the TFC-LC-MS/MS method took approximately 1.5-2 hours, and included 96 individual pipetting steps for each of the samples/calibrators and IQCs, a further 96 pipetting steps for the addition of the internal standard solution, and 96 further transfer steps to take the supernatant to autosampler vials. Using the Chromsystems approach, since the precipitation reagent and internal standard solution are added separately, a further 96 pipetting steps would be required. With the automated approach using a 96-channel pipetting head, providing the samples/calibrators/IQCs were in a 96-well format, the time taken to pipette the samples, and add the internal standard and precipitation reagent was 4 minutes. Following mixing (10 min), supernatants were collected by centrifugation (2 min) with

no manual transfer of liquids. The total analysis time from samples being pipetted in to the wells of the filter plate to having a sealed plate for LC-MS/MS analysis was 20 minutes. No manual pipetting steps were used, and all that was required was the manual loading/disposal of pipette tip racks. Even if the samples were not presented in a 96-well format, they could be manually pipetted from primary tubes into the filter-plate (approximately 30 minutes), and the addition of internal standard and precipitation reagent carried out using the 96-channel pipetting robot, followed by centrifugation to filter supernatants into the collection plate, dramatically reducing the time taken for these steps if following a fully-manual process.

2.4.4. Chromatographic methods for resolution of 25OHD3 and 3-*epi*-25OHD

The TFC-LC-MS/MS and automated methods were carried out using reversed-phase chromatographic systems. As a result, neither method was capable of chromatographic resolution of 25-OHD3 and 3-*epi*-25-OHD3. By changing the analytical column in the TFC-LC-MS/MS method from the initial Hypersil GOLD™ C18 column to a 100 x 2.1 mm Accucore™ PFP column and, following the transfer step through the tee-piece to elute the retained analytes from the TurboFlow column, using an isocratic elution (65 + 35, *v/v* methanol and deionised water with 0.1 % *v/v* formic acid, 40 °C), chromatographic resolution of the epimeric forms was realised. The total analysis time, including TurboFlow extraction, was 13 minutes as shown in Figure 2.13. A 5-minute data window was used when multiplexing was required. This method was used for the analysis of samples to assess the prevalence of 3-*epi*-25-OHD3 (see below).

When the column length was reduced to 50 mm, the flow-rate was doubled to 0.8 mL/min, and the column temperature increased to 50 °C, whilst maintaining the same isocratic LC conditions, the analysis time was reduced to less than 5 min (Figures 2.15 and 2.16). The increase in flow-rate was made possible through (i) a shorter LC column length and (ii) the use of fused-core particles to reduce back-pressure.

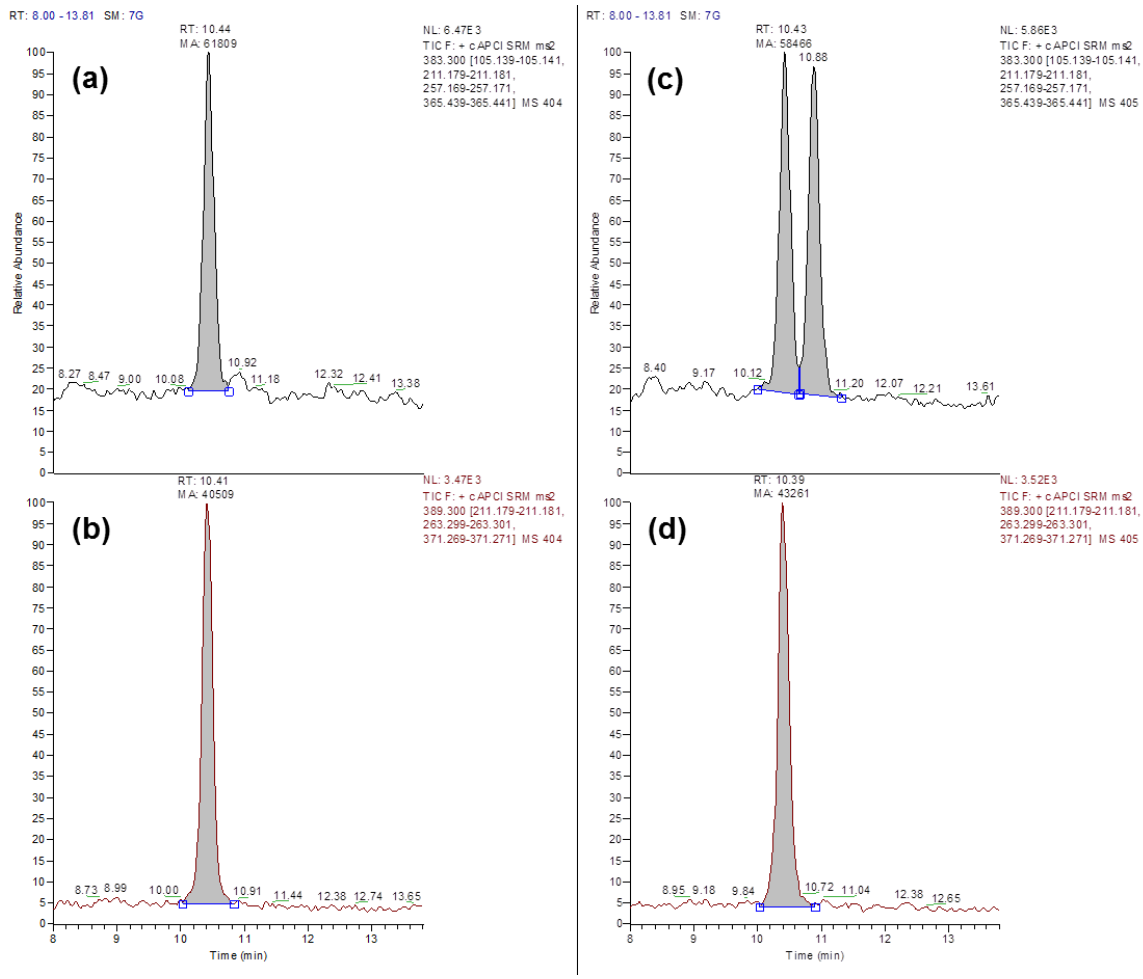

Figure 2.15. Example chromatogram showing the initial 13 minute TFC-LC-MS/MS PFP chromatographic resolution of 25-OHD3 and 3-*epi*-25-OHD3. Sample 404 (chromatograms a and b) and sample 405 (chromatograms c and d) were both provided by DEQAS – Sample 405 was the same sample matrix as Sample 404, but was fortified with 3-*epi*-25-OHD3. Chromatograms (a) and (c) show the 25-OHD3 SRM transitions, and chromatograms (b) and (d) show the 25-OHD3-D_6 SRM transitions.

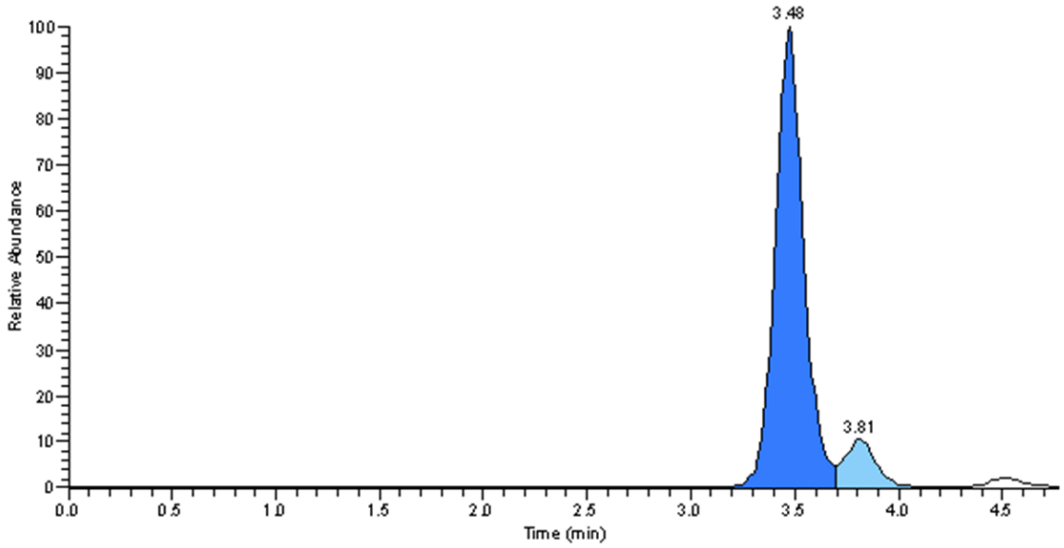

Figure 2.16. Chromatographic resolution of 25-OHD3 and 3-*epi*-25-OHD3 using a 50 x 2.1 mm Accucore™ PFP column (2.7 µm total particle size). The flow rate was 0.8 mL/min, with an isocratic elution using 65:35 methanol:deionised water eluent (constant 0.1 % *v/v* formic acid). Total analysis time was 4.8 min.

2.3.4.1. Prevalence of 3-epi-25-OHD3

Using the TFC-LC-MS/MS method, 3-*epi*-25-OHD3 was not directly quantified, as the epimer was not present at known concentrations in the Chromsystems calibrators or IQCs. An estimation of relative concentrations was made, assuming equivalent ionisation and matrix effects, by integrating chromatographic peaks at the retention time of the 3-*epi*-25-OHD3 standard, and by comparing the peak area response to that of 25-OHD3. Of the 74 samples analysed, the mean (10^{th}, 90^{th} percentile) 25-OHD3 concentration was 17.4 (7.3, 29.5) µg/L and the mean (10^{th}, 90^{th} percentile) proportion of 3-*epi*-25OHD3 was 2.37 (1.05, 3.81) %. There were two samples where the proportion of 3-*epi*-25-OHD3 exceeded 5 % of the 25-OHD3 peak area (6.7 % in a sample with 14.6 µg/L 25-OHD3 and 6.8 % in a sample with 15.1 µg/L 25-OHD3). There was an overall correlation between the 25-OHD3 and 3-*epi*-25-OHD3 peak areas (R^2 = 0.62, Figure 2.17).

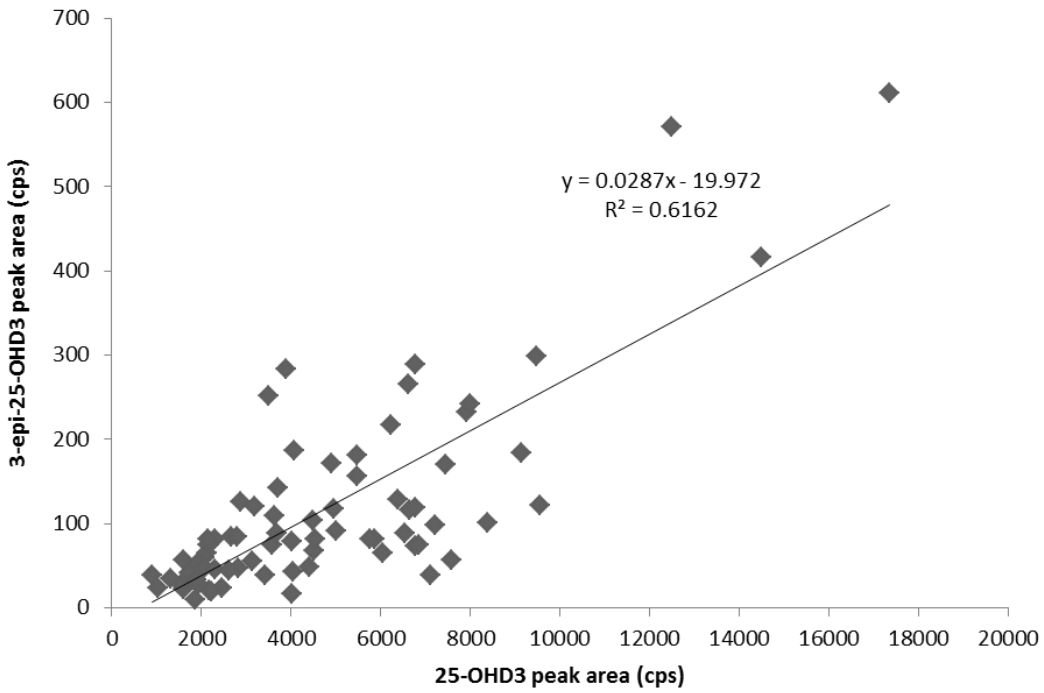

Figure 2.17. Correlation between the TFC-LC-MS/MS peak area for 3-*epi*-25-OHD3 (y-axis) and 25-OHD3 (x-axis) in 74 samples sent for routine 25-OHD3 analysis.

2.4.5. Investigating rapid resolution of 3-epi-25-OHD3

Separation of the mix of 25-OHD3-D_3 and 3-*epi*-25-OHD3 was investigated using 5 mm and 10 mm total column lengths (Figure 2.18), in both cases using 2.7 µm fused-core particles, and with a 2.1 mm internal diameter. The mix was analysed at different flow-rates (from 200-1,600 µL/min, pressure limitations permitting), and using different isocratic eluent compositions (from 60-70 % methanol). Excellent chromatographic peak shape was achieved (Figure 2.19). Baseline resolution of the two compounds was not achieved at the concentration tested (~100 µg/L, non-extracted and without matrix) for any combination of column length, flow-rate or eluent composition, though it was clear that resolution was improved by increased column length (Figure 2.20), and that efficiency at both 5 and 10 mm column lengths was greater at lower flow-rates (Figure 2.21).

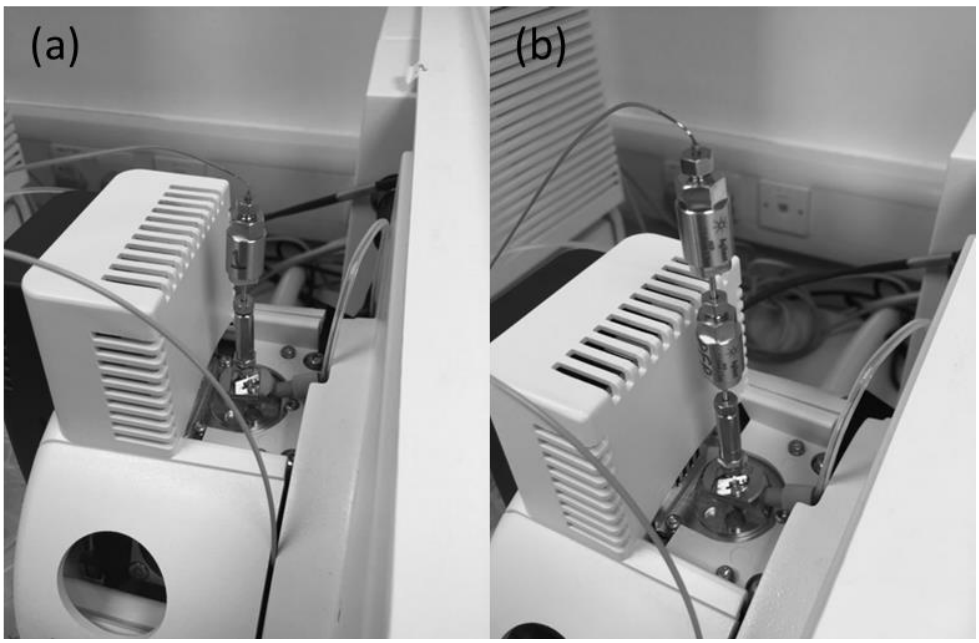

Figure 2.18. Direct ion source column connections for the investigation of 3-*epi*-25-OHD3 separation. Shown are the configurations for (a) 5 mm column length, and (b) two columns connected in series to give a total column length of 10 mm.

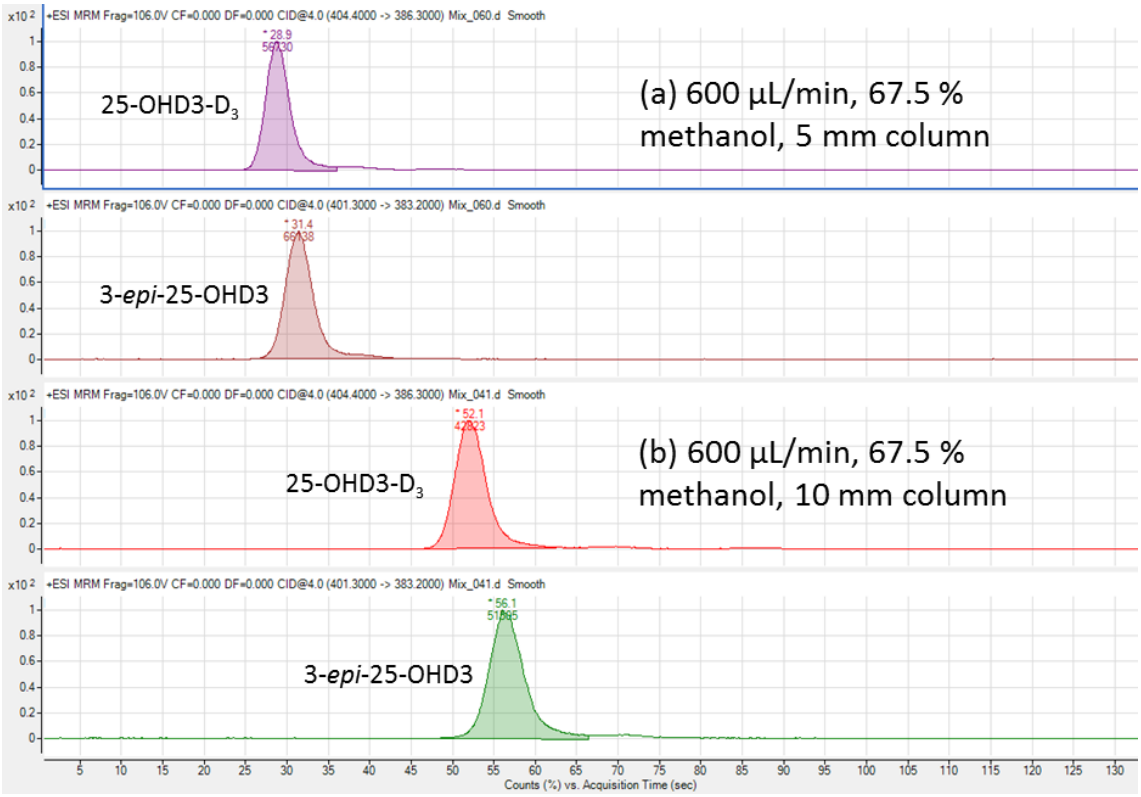

Figure 2.19. Example chromatograms of the 25-OHD3-D_3 and 3-*epi*-25-OHD3 mixture, analysed using short PFP Poroshell column(s). Shown are (a) a single guard column, with a column length of 5 mm, analysed using 67.5 % methanolic eluent, at 600 µL/min, compared to (b) the same eluent and flow conditions, but using two 5 mm columns in series.

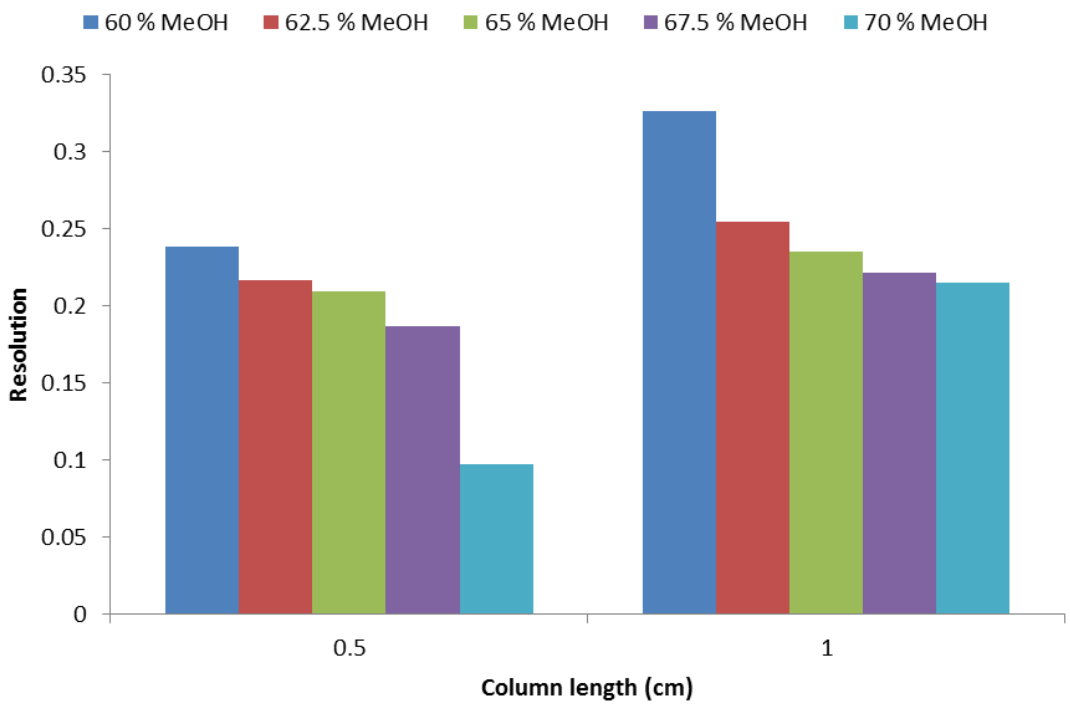

Figure 2.20. Resolution of 25-OHD3-D_3 and 3-*epi*-25-OHD3 at different isocratic eluent compositions. Plotted are the mean resolutions calculated for each eluent composition at for both 5 mm and 10 mm column lengths, taken from duplicate injections at all flow-rates tested for each eluent composition.

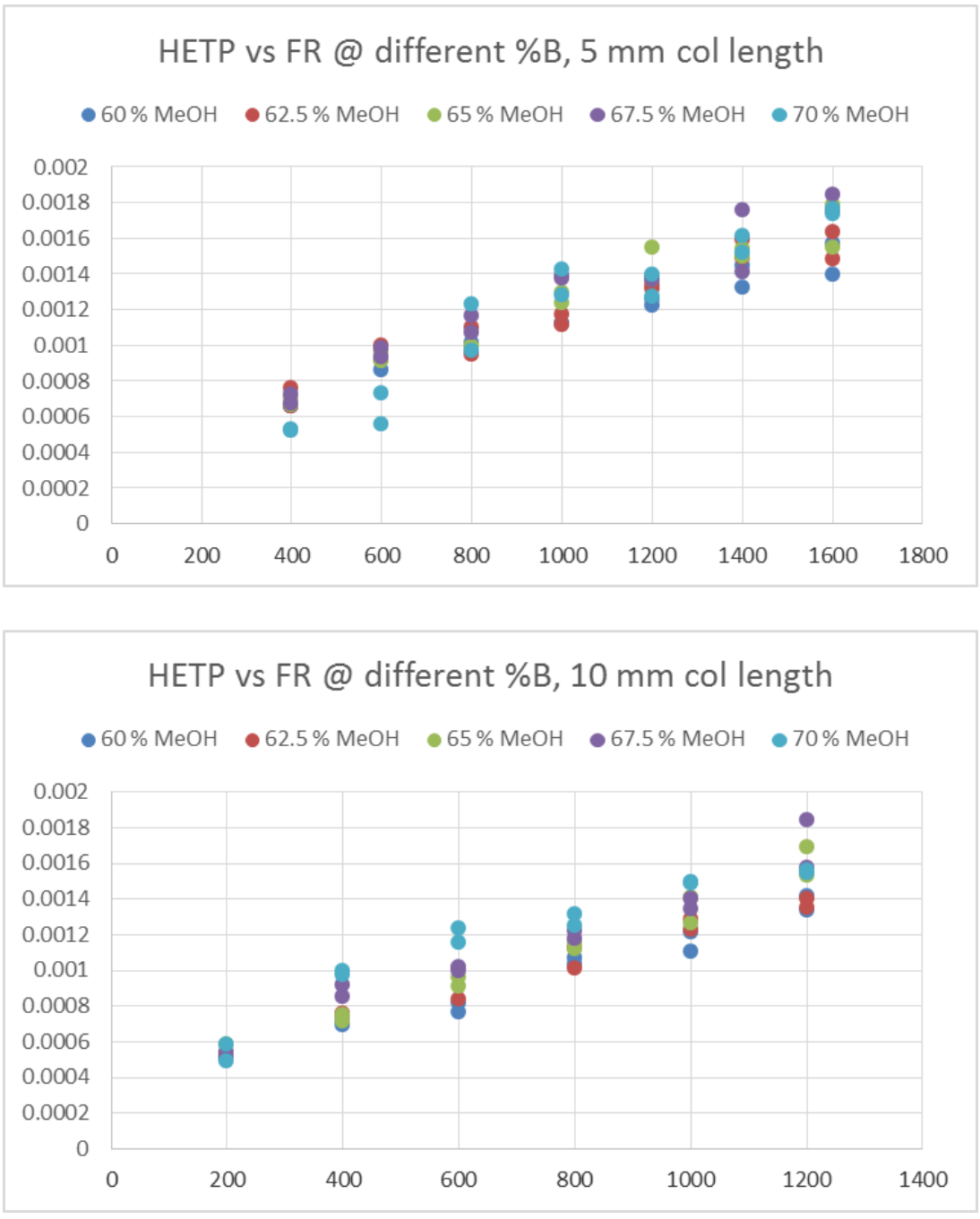

Figure 2.21. Efficiency (HETP, calculated using the 25-OHD3-D_3 peak parameters) versus eluent flow-rate (µL/min) for different isocratic eluent compositions at (top) 5 mm column length and (bottom) 10 mm column length.

2.4. Discussion

2.4.1. TFC-LC-MS/MS for 25-OHD and other applications

TFC offers a simple, automated process which can be incorporated into LC-MS/MS methods and potentially offers improved sample 'clean-up' via removal of matrix components when compared to analysis of supernatents from protein precipitation steps alone (Du & White, 2008; Couchman, 2012).

The large particles of the TFC columns themselves infer very poor chromatographic efficiency (i.e. low plate number, poor peak shape) when compared to analytical LC columns. The first TFC methods reported tended to be one-dimensional separations, i.e. the TFC column was used without a secondary analytical column, and without a tee-piece valve to allow analyte focussing (Ayrton *et al*., 1997). The simple valve set-up for this arrangement is now referred to as Quick Elute Mode. In Quick Elute Mode, the only chromatographic separation of retained compounds is that carried out as compounds are eluted from the TFC column, which is especially limited if shallow, low-flow-rate elution gradients are used. In these methods, analysis time is typically very short (< 1 min), since to overcome the poor efficiency of the TFC columns, very steep, or even step-gradients are used. Often there is little chromatographic resolution between target analytes.

With Focus Mode methods such as that described for 25-OHD, the poor efficiency of the TFC column is overcome by focussing analytes onto the head of a traditional small-particle LC column. Once the retained analytes are transferred and the two pumping systems separated via a switch of the tee-piece valve, efficient chromatographic analysis of the retained analytes occurs. One benefit of this approach is that the high flow rates used to generate turbulent flow within the TFC columns (typically 1.5-2.0 mL/min) means that the injection solvent is significantly diluted pre-column.To ensure thorough mixing of the injection solvent and the starting eluent conditions for the 25-OHD assay described, a mixing tube (50 x 2.1 mm tube filled with stainless steel beads) was placed in-line immediately after the injection port. With the Focus-mode arrangement, injection solvents with high proportions of organic solvent can be injected onto reversed-phase chromatographic systems with no effect on the

chromatographic peak shape in the second dimension, since the proportion of organic solvent as the analytes reach the head of the analytical column is determined simply to be the ratio of the flows through the tee-piece and the contents of the elution loop (Couchman, 2012). It has also been demonstrated that the TFC column can be used to 'stack' multiple injections prior to transferring all the retained analytes of interest from each injection onto the analytical column in order to detect low-abundance analytes (Herman, 2005).

The low back-pressure and large interstitial spaces between particles allows the direct injection of biological fluids onto TFC columns. In theory, this offers a number of advantages to workflows in clinical laboratories, since sample preparation is minimised. In reality, direct injection of biological fluids is not suitable for two main reasons. The first step of a quantitative LC-MS/MS analysis should be the addition of an internal standard to the sample. For many analytes, including 25-OHD, the internal standards used are only soluble and stable in organic solvents. Therefore, this initial step of the sample preparation process will result in some precipitation of the proteins, which will necessitate a mixing and centrifugation step prior to LC-MS/MS analysis (Herman, 2004). If this is so, it is worthwhile adding a larger volume of solvent to remove a greater proportion of the total protein in the sample prior to analysis. This also means the TFC and analytical column lifetimes will increase, and there will be a reduced likelihood of blockage elsewhere in the system, such as the autosampler needle and tubing (Wu *et al*., 2004).

More important clinically, and relevant especially to endogenous analytes such as 25-OHD, is the need to disrupt the binding of small molecule analytes to specific binding proteins for the measurement of total serum concentrations. The same concept would apply to highly protein-bound drugs. The concept of using TFC for the measurement of 'free' or 'bioavailable' analyte concentrations has been previously reported (Wright *et al*., 2011). In this work, carried out using serum testosterone as a model analyte, the total serum testosterone was measured by TFC-LC-MS/MS following precipitation of proteins. The same samples were then measured without pre-treatment (i.e. with direct injection) with the hypothesis that the protein-bound fraction would be excluded from the TFC column, and only the 'free' fraction would be retained. The

concentrations of 'free' testosterone were higher than anticipated, based on literature data using equilibrium dialysis and ammonium sulphate precipitation, suggesting that some disruption of protein binding occurred even with direct injection of serum samples, either through pre-column dilution in the injection process, or by the physical disruption of protein binding under the turbulent flow conditions. Further, direct injection of serum without wishing to disrupt protein binding would not allow the addition of an internal standard for accurate quantitation. Further work is required in this area.

2.4.2. Comparison of TFC-LC-MS/MS and immunoassay for 25-OHD

The comparison between TFC-LC-MS/MS and the three immunoassays in this study for 25-OHD showed an overall correlation between all of the methods. Furthermore, the mean bias between each method was close to zero. However, there were significant differences between methods for individual samples, which were only demonstrated through Bland-Altman difference plots. The use of simple, whole-population summary statistics such as correlation coefficients and linear regression equations can disguise significant sample-to-sample variability between two methods (Carter, 2012). For the comparison of the TFC-LC-MS/MS method against each of the immunoassay methods, the 95 % limits of agreement (TFC-LC-MS/MS – immunoassay, µg/L) were: -11.5 to 9.9 µg/L for the Liaison, -13.9 to 7.8 µg/L for the iSYS, and -11.9 to 10.8 µg/L for the Centaur. Differences of 10 µg/L or so are clinically relevant when one considers the vitamin D status classifications commonly used (Table 2.4), and subsequent decisions to treat or not to treat patients. Samples outside the 95 % limits of agreement showed even greater discrepancy – the largest difference between two measurements of a single sample was 27.4 µg/L in a sample with a 25-OHD concentration of 27.9 µg/L when measured using TFC-LC-MS/MS, and a concentration of 55.3 µg/L when measured by the Liaison method (iSYS 19.1 µg/L; Centaur 23.5 µg/L). However, there were smaller but more clinically relevant differences observed – three samples with 25-OHD concentrations below 10 µg/L when measured by TFC-LC-MS/MS had concentrations greater than 20 µg/L when measured by the iSYS method.

Those samples with concentrations greater than 30 µg/L, i.e. those samples with concentrations associated with 'optimal' vitamin D status, were in greater agreement between each of the methods (Figure 2.9), and so increased the overall correlation between methods in the summary statistics. For comparison between 25-OHD methods, results should be sub-divided to reveal true methodological differences at clinician decision points. In this study, at concentrations less than 10 µg/L, all three immunoassays appeared to overestimate 25-OHD when compared to the TFC-LC-MS/MS method.

A number of other methodological comparison studies for 25-OHD have previously been reported in the literature. Lai *et al*. (2012) carried out a comparison between two laboratories using the Liaison immunoassay, and a third laboratory using LC-MS/MS on a large sample set of 813 samples. They concluded that the rate of different vitamin D status classification was as high as 1-in-3 samples due to methodological differences alone. Overall, the results from this study showed the LC-MS/MS method to produce higher results than the Liaison method. Within-assay reproducibility was also assessed for a small sub-set of samples by both methods via blinded duplicate sample analysis of portions of the same sample, and revealed surprisingly high differences between duplicates in both methods. Holmes *et al*. (2013) compared three automated direct immunoassay methods with extraction-based RIA and LC-MS/MS methods as reference methods in 163 samples. Their study highlighted random errors and bias between the direct methods and the extraction-based methods, which also resulted in large numbers of samples being differently classified in terms of vitamin D status. A number of other studies demonstrate that LC-MS/MS methods produce lower 25-OHD results than comparator immunoassays (Roth *et al*., 2008; Costelloe *et al*., 2009; Ong et al., 2012). However, this is in contrast to the study by Lai *et al*. (2012), and other comparison studies (Chen *et al*., 2008; Snellman *et al*., 2010; De Koning *et al*., 2013) in which the LC-MS/MS methods tended to produce higher values than the comparator immunoassays. It should be noted that these findings may be explained in part by the different sample populations used for the comparison. In the samples described in this Chapter the prevalence of measurable 25-OHD2 was very low. This was similar to the study populations of Ong *et al*. (2012), Roth *et al.* (2008), and Costelloe *et al*. (2009).

The small number of samples that were analysed which contained measurable concentrations of 25-OHD2 suggested that the manufacturers' claims of equivalent cross-reactivity with both 25-OHD2 and 25-OHD3 was correct to some extent. However, studies from countries where vitamin D2 supplementation is preferred suggest that there may be under-recovery of 25-OHD2 by some immunoassays, which leads to the observed concentrations of total 25-OHD being lower by immunoassay than by LC-MS/MS (De Koning *et al*., 2013). A study by Freeman *et al*. (2015) evaluated the performance of a range of immunoassays and LC-MS/MS in clinical samples which contained 25-OHD2 (post-supplementation). The authors concluded that all the immunoassays tested showed 'acceptable' performance, although each showed a negative mean bias versus the LC-MS/MS reference method (range from -7 % to -16 %).

Each of the comparison studies mentioned recognised that the LC-MS/MS method should be used as the reference method against which each of the automated immunoassays should be compared. LC-MS/MS is not subject to the inherent problems of antibody cross-reactivity. Interference from other 25-OHD metabolites can largely be ruled out by either chromatographic resolution, or by virtue of different *m/z* values. 25-OHD2 and 25-OHD3 can be independently quantified. Other matrix interferences can be exluded in either the sample extraction or chromatographic steps. Most importantly, an internal standard is added to every sample. This is typically an isotopically-labelled analogue of the target analyte, and is used to account for sample-to-sample matrix differences. Immunoassays cannot be internally-standardised in the same way. For automated immunoassay platforms, the instrument output is simply a concentration. There is no additional information with which to identify potential matrix interferences in individual samples. Whilst immunoassays can be highly precise, the non-specificity of antibodies and the lack of internal reference standard(s) results in inaccuracy. Re-calibration of immunoassays and alignment with LC-MS/MS values for large sample populations goes some way to improving assay accuracy, but does not address the underlying analytical limitations. With LC-MS/MS, there are a number of additional assay outputs which can be used as 'diagnostic' tools indicate whether there is a potential interferent in a particular clinical sample within a batch, including (i) the

peak area of the internal standard, (ii) the retention times for both analyte and internal standard, and (iii) the product ion ratio in experiments where more than one *m/z* transition is used.

2.4.3. Automation

Compared to fully-automated immunoassay systems which have been used for many years, and which are integrated into total automation laboratories, LC-MS/MS for the analysis of 25-OHD is typically a largely manual process (Zhang & Rockwood, 2015). This is especially so in smaller clinical laboratories with limited experience with the technology. As a consequence, it is not just the capital expense of purchasing LC-MS/MS instrumentation, but also the ongoing operational costs of manual sample preparation which are hindering the widespread implementation of LC-MS/MS in clinical chemistry. In general, 'automation' of LC-MS/MS in clinical laboratories is limited to on-line sample preparation and automated multi-channel liquid handling (Vogeser & Kirchhoff, 2011). There is still some significant progress to be made before reaching the same level of automation that immunoassay-users have become accustomed to. That said, it must be remembered that manual immunoassays took some decades to become as automated as they are currently. Partial automation of some of the manual processes used in LC-MS/MS can offer a number of benefits in terms of the operational implementation of such methods, but more importantly, allows realisation of the benefits of this technology over immunoassay-based methods.

As well as the use of protein precipitation filtration plates and 96-channel pipetting robotics mentioned in this Chapter a range of alternative, or additional, sample preparation methods have been used for the anlaysis of 25-OHD, each of which offer advantages over manual processes, and some of which are designed specifically for use with LC-MS/MS assays. A good example is the use of extraction phases, commonly in 96-well plate format, for the removal of phospholipids. These compounds are abundant in serum samples, and are a known source of matrix effects (typically ion suppression) in LC-MS/MS assays (Janusch *et al*., 2013). There is evidence that some phospholipids can remain in the chromatographic system or MS ion source for a

number of injections, i.e. can cause suppression in successive injections (Little *et al.*, 2006). As they are often highly hydrophobic, they could be considered especially problematic for hydrophobic analytes such as 25-hydroxyvitamins D if not fully accounted for with isotope-labelled internal standards, or removed during sample preparation. A number of these phases are available through a range of commercial vendors, and are reported to improve robustness and accuracy of 25-hydroxyvitamin D assays when compared to assays without the phospholipid depletion step (Aurand *et al*., 2012; Lodder *et al*., 2015). A more recent approach is the use of adsorptive chemistry-based extraction plates, available commercially through Tecan (Mannedorf, Switzerland) and designed to allow fully-automated analysis on robotic liquid handling platforms. The wells of these plates are coated in a proprietary adsorptive coating (Tecan Immobilised Coating Extraction, TICE^{TM}) designed to extract small molecules of interest from matrix components. This approach allows control of pH and solvent/salt concentrations in each well to disrupt protein binding, and thus allows the extraction of 25-OHD metabolites with good recovery from serum without precipitation of proteins, and with no vortex mixing, filtration, or centrifugation steps (Baecher *et al*., 2014; Couchman *et al*., 2016).

2.4.4. 3-*Epi*-25-hydroxyvitamin D3

One limitation of the comparison study reported in this study is that the TFC-LC-MS/MS method did not resolve 3-*epi*-25OHD3 from 25-OHD3 (nor 3-*epi*-25OHD2 from 25-OHD2). There are conflicting reports in the literature regarding the prevalence of the 3-epi-25OHD metabolites, and whether it is a requirement to resolve them when measuring 25-OHD by LC-MS/MS. Some groups have demonstrated that in adult populations the prevalence of detectable 3-epi-25OHD is so low, that there is no significant bias between methods which do and do not resolve the epimeric forms (Wright *et al*., 2012). An early candidate reference method did not involve the separation of the epimeric 25-OHD metabolites (Vogeser *et al*., 2004). Even in paediatric populations, the bias which results from measuring total 25-OHD2 or 25-OHD3 (i.e. including measurement of the epimer) is small (Yang *et al*., 2016; Cooke *et al*., 2016). Other groups suggest that the 3-epimeric forms of 25-OHD can be detected

at appreciable concentrations even in adult populations (Stepman *et al*., 2011; Shah *et al*., 2011). Certainly, 3-*epi*-25-OHD3 could be detected in some samples analysed in this study (Figure 2.16), though peak areas were generally very low, and the relative proportions to the peak areas for 25-OHD3 itself were also low. That said, it should be made explicit on reports from clinical laboratories using LC-MS/MS for the analysis of 25-OHD in which the 3-epimeric metabolites are not resolved that the reported concentrations are in fact a 'total 25-OHD3' or 'total 25-OHD2', and that this may be relevant especially in samples from paediatric patients.

The suggestion that chromatographic separation of the 3-epimeric metabolites of 25-OHD takes considerably longer than methods which do not resolve the epimer, and so are not suited to high-throughput laboratories, is no longer valid. With traditional LC column technology and pumping capabilities, this was a justified argument. Indeed, the earliest commercial LC-MS/MS method for the separation of the 3-epimers from Chromsystems had an analysis time greater than 20 minutes per sample. However, with the use of fused core LC columns to allow higher flow-rates and improved efficiency without the significant pressure limitations of UHPLC, and with the introduction of PFP and cyano phases for these particles, analysis times including resolution of the 3-epimer were less than 5 minutes per sample in this study. For some targeted analyses, analysis times of less than 1 minute can be achieved. However, attempting to reduce the analysis time of 25-OHD and 3-*epi*-25OHD by dramatically shortening the column length as demonstrated in this study resulted in insufficient chromatographic plates to achieve baseline separation of the two compounds. Further work involving the analysis of 25-OHD3 and 3-*epi*-25-OHD3 on custom-made columns (e.g. 25 mm length) may result in analysis times less than 5 minutes.

2.4.5. Additional considerations

It has been demonstrated that some of the variability in vitamin D testing can be traced to pre-analytical factors (Carter *et al.*, 2007). Things which should be considered include firstly the effect of compounds leaching from tubing/plasticware into samples, but also the difference between endogenous and 'spiked' vitamin D, an effect thought

to be due to an influence of VDBP. These factors are important considerations, especially when preparing calibration standards and quality control material. It is fortunate that 25-OHD appears very stable in serum samples, i.e. in the presence of vitamin D binding protein, even at ambient temperature for extended periods (Wielders & Wijnberg, 2009).

2.5. Conclusions

The fact that the 'gold standard' reference measurement procedures (RMPs) for 25-OHD analysis are carried out using LC-MS/MS suggests that this technique has analytical advantages over immunoassay-based methods (Tai *et al*., 2010; Stepman *et al*., 2011a; Mineva *et al*., 2015). Inherent benefits are (i) the ability to internally standardise for accurate quantification in different sample matrices, and (ii) the ability to impart specificity through sample preparation and chromatographic separation steps. The TFC-LC-MS/MS method described is partially-automated to cope with the high-throughput workloads of clinical laboratories, and can be adapted to include rapid chromatographic separation of 3-*epi*-25-OHD.

A number of 25-OHD immunoassay developers, including the latest versions of the Advia Centaur assay, the IDS iSYS assay and the Diasorin Liaison assay kits, have commercially available methods which are 'certified procedures', an accreditation awarded by the CDC Vitamin D Standardization-Certification Program (VSDCP). These methods pass the performance criterion of ±5 % mean bias to the CDC and University of Ghent RMP (Mineva *et al.*, 2015), and an overall imprecision of <10 % over the concentration range 22-275 nmol/L (8.8-110 µg/L) for total 25-OHD. However, this certification does not account for the lack of internal standards in immunoassay-based methods, and hence sample-to-sample matrix variability. It is primarily this reason that gives rise to so many method comparison reports which demonstrate discrepant results between immunoassays and LC-MS/MS methods, resulting in misclassification of vitamin D status.

There is a danger in using summary statistics for large data-sets to conclude that methods show 'acceptable performance' when compared to LC-MS/MS methods (Carter, 2012). Differences between individual method results should be inspected using Bland-Altman plots.

There is also danger in assuming that LC-MS/MS guarantees a result to be accurate. Routine LC-MS/MS methods in high-throughput clinical laboratories will rarely, if ever, be validated and operated to the same rigours as the 'gold standard' RMPs, since such methods would be prohibitively time-consuming and expensive. Resolution of the 3-

epimeric 25-OHD metabolites is just one example which demonstrated the pitfalls of LC-MS/MS for this analysis. However, as demonstrated in this study, the flexibility of LC-MS/MS is another significant benefit - modifying the chromatographic system alone, without any change in sample preparation or MS/MS settings allows one to overcome this interference. With modern HPLC columns and pumping systems, and MS/MS ionisation sources capable of withstanding higher LC flow-rates, these chromatographic modifications can be implemented without increasing analysis time. In the future, prospective studies may reveal that independent quantitation of 3-*epi*-25-OHD is clinically relevant (e.g. in assessing vitamin D status in paediatric populations). Currently, most antibodies will not detect this analyte.

One major advantage of fully-automated and integrated immunoassay analysers over LC-MS/MS is the random-access analysis of samples for multiple assays on a single platform. LC-MS/MS has tended to be a batch-process driven technology, with sample received in the laboratory and stored until the next batch analysis is ready. Samples are analysed bracketed by calibration standards, and with quality control samples regularly interspersed throughout the batch. A number of groups are actively investigating moving away from batch-processing for LC-MS/MS analyses, either by considering less-frequent analysis of calibration standards (e.g. not with every batch of samples, or using single-point calibration – Peters & Maurer, 2007) or by using novel alternatives such as 'surrogate' calibration with isotopically labelled internal standards such that a calibrator is added to each sample (Olson *et al*., 2013; Cooper *et al*., 2013; Crawford *et al*., 2013; Couchman *et al*., 2015). The latter is an attractive approach which cannot be replicated in immunoassay-based analyses.

Chapter Three

Investigating method variability in the analysis of 25-hydroxyvitamin D using LC-MS/MS

3.1. Introduction

As already discussed, the measurement of totalserum 25-OHD is universally considered a reliable androbustmarker of vitamin D status and for monitoring supplementationin vitamin D deficient subjects, since this concentration reflectsboth dietary and/or supplementary intake and dermal production (Seamans & Cashman, 2009). It is known that severe deficiency (total serum 25-OHD below 10 µg/L) leads to rickets in children and osteomalacia in adults. The concentrations of total 25OHD that relate to adequacy and sufficiency are less well defined, and are a subject of ongoing debate, although current opinion is that the optimum concentration of 25-OHD should be greater than 30 µg/L (Holick, 2009; Vogeser, 2010). Vitamin D status has been the focus of much recent literature attention and has now been linked to a range of pathologies, including heart disease, hypertension, diabetes, cancer and autoimmune diseases (El-Khoury *et al*., 2011). As a consequence, there has been a dramatic increase in the number of requests for the measurement of serum 25-OHD (Carter, 2011).

In order to meet demands, many laboratories considered high-throughput, automated immunoassays to replace more laborious solvent extraction methods, such as the initial CPB assay reported by Haddad and Chyu (Haddad & Chyu, 1971). However, method differences between laboratories soon became apparent (Mayer & Schmidt-Gayk, 1984; Carter *et al*., 2004; Carter *et al*., 2004a; Binkley *et al*., 2004; Hollis, 2004), as was shown by the results of DEQAS, which was established in 1989. Immunoassays for 25-OHD have an inherent problem of inability to differentiate between a myriad of polar metabolites and vitamin D-like seco-steroids which contribute to the total 25-OHD assay. In addition, analytical methodology details, including assay calibration, are not always disclosed because of commercial sensitivities.

There has also been a move in the last decade towards clinical laboratories using liquid chromatography–tandem mass spectrometry (LC–MS/MS) for a number of analyses which were previously performed using immunometric techniques (Dooley, 2003). As has been demonstrated in the previous chapter, LC–MS/MS can distinguish and independently quantify 25-OHD2 and 25-OHD3 by *m/z* alone. Since the first reported use of LC–MS/MS for the analysis of 25-OHD by Watson *et al*. (1991), improvements in

the automation of sample preparation, the speed of chromatographic steps, and the sensitivity of MS instrumentation have meant that LC–MS/MS assays with higher sample throughput are increasingly being adopted, and the technique now accounts for over 10 % of all DEQAS returns. LC–MS/MS is considered by many the 'gold standard' for analysis of 25-OHD (Roth *et al*., 2008; Zerwekh, 2008; Carter, 2009; De la Hunty *et al*., 2010).

However, LC–MS/MS for the analysis of serum 25-OHD is not straightforward. As demonstrated in Chapter Two, the analysis of 25-OHD is complicated when using LC-MS/MS by the presence of the C3-epimeric forms of 25-OHD2 and 25-OHD3 (Figure 3.1). Since these epimers are isobaric with the target analyte, MS/MS alone cannot distinguish them. In 2006, Singh *et al*. reported the presence of 3-*epi*-25-OHD with especial reference to relatively high concentrations in neonates.

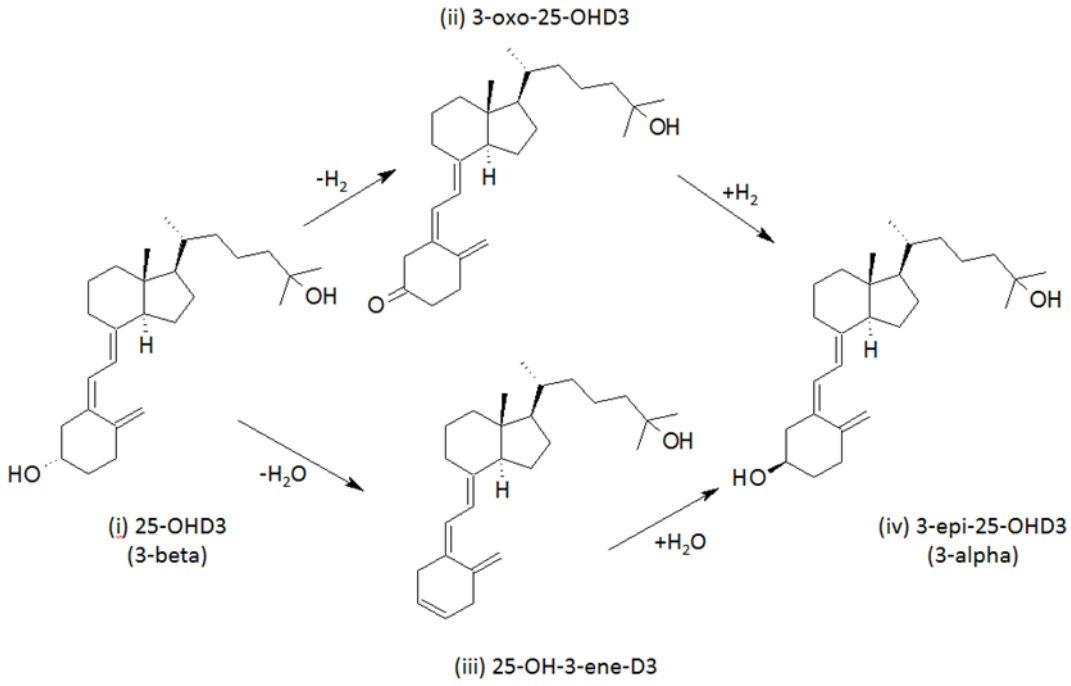

Figure 3.1. Proposed mechanisms for the interconversion of 25-OHD3 to 3-*epi*-25-OHD3 (adapted from Molnar *et al*., 2011). The 3-*oxo*-25-OHD3 intermediate is thought to be the major mechanism for the interconversion.

In the early days of LC-MS/MS for 25-OHD analysis, inter-laboratory (% CV) agreement between LC–MS/MS users was relatively poor, and certainly no better than any of the available immunoassays (IAs). Some of the variation could be explainedby the use of 'in-house' calibration standards, the preparation of which varied between laboratories. Indeed, in a DEQAS study reported by Carter and Jones (Carter & Jones, 2009), it was found that use of a common standard improved the mean inter-laboratory imprecision for total 25-OHD from 16.4 % to 10.4 %. Better insight into the importance of assay standardisation and other factors affecting LC–MS/MS methods, such as the tubes used for sample collection and preparation (Carter, 2007; Chen *et al*., 2008; Carter, 2011) and interference from other vitamin D metabolites has further improved inter-laboratory agreement, but variability between laboratories does still exist and requires investigation. Importantly, LC–MS/MS is not a single, 'off-the-shelf' technique. Variability in sample preparation, chromatographic separation and finally ionisation/fragmentation should each be considered. That said, the flexibility of LC–MS/MS systems may be beneficial, since there is the opportunity to adapt, individualise and standardise methods.

3.2. Aims

The work in this Chapter describes the retrospective interrogation of questionnaire results from DEQAS participants, submitting LC-MS/MS results for two distributions of DEQAS samples. In particular, method variables which may give rise to inter-laboratory variability were considered, including the specific ions and transitions used for MS/MS analysis of 25-OHD metabolites, the ionisation method used, and the type of MS instrument used.

3.3. Materials and methods

The results from a survey of LC–MS/MS users organised by the international Vitamin D External Quality Assessment Scheme were analysed to determine the influence of such variables on the reported results for two DEQAS distributions (10 samples, July and October 2010).

Questionnaires designed and organised by DEQAS were distributed in September 2010 to all DEQAS participants reporting results using LC-MS/MS (Table 3.1). Laboratories were asked to voluntarily complete the questions, and identify themselves by DEQAS laboratory number when returning results.

DEQAS Questionnaire
• Which LC–MS/MS instrument manufacturer/model do you use?
• Which LC system/column(s) do you use?
• Which method of sample preparation do you use?
• Do you use a commercially available assay kit?
• Do you use commercially available standards to calibrate your assay? If so, is this standard used as the primary standard in each batch analysis?
• Which internal standard(s) do you use?
• Which ionisation method do you use?
• Which *m/z* transition(s) do you use for 25-OHD2/25-OHD3 and internal standards?
• Are chromatograms/results visually inspected prior to reporting?
• Does your method resolve 3-*epi*-25-OHD3 from 25-OHD3?

Table 3.1. Questions posed to LC-MS/MS users for the analysis of 25-OHD.

3.3.1. Statistical analysis

Responses were collated, along with individual laboratory returns for two DEQAS distributions (10 samples, July and October, 2010). For statistical analysis, individual results for each of the 10 samples were divided by the corresponding LC-MS/MS method mean concentration for that sample. It was assumed that no changes were made to analytical methods used between the time of completing the questionnaires and analysis of the two sample distributions (i.e. the answers submitted for each question were applied to all 10 reported results for further analysis). Statistical analysis and production of box and whisker plots was carried out using GraphPad Prism for Windows (version 5.04). All calculations were carried out using reported results for total 25-OHD. All box and whisker plots are presented showing the median, interquartile range, and 5^{th} and 95^{th} percentile data with individually plotted outliers.

3.4. Results

3.4.1. LC-MS versus all methods

For the 10 samples used in this study, the number of laboratories reporting results using LC-MS/MS accounted for, on average, 11% of all reported results. Mean results for all samples using LC-MS/MS were generally higher than the all-laboratory trimmed mean (ALTM) results. In only two cases (Samples 377 and 379) were the ALTM results greater than the LC-MS/MS method mean result (Table 3.2). Precision was significantly greater (lower % CV) for the LC-MS/MS method sub-group compared to the ALTM (paired *t*-test, $P < 0.01$).

Sample number [total no. of reports from all methods (no. of reports by LC-MS)]	All methods			LC-MS		
	ALTM [nmol/L, (µg/L)]	SD [nmol/L, (µg/L)]	CV (%)	ALTM [nmol/L, (µg/L)]	SD [nmol/L, (µg/L)]	CV (%)
376 [815 (64)]	47.0 (18.8)	8.1 (3.2)	17.2	58.8 (23.5)	7.6 (3.1)	13.0
377 [795 (91)]	19.3 (7.7)	5.0 (2.0)	26.1	17.9 (7.2)	2.6 (1.1)	14.8
378 [815 (94)]	68.8 (27.5)	12.9 (5.2)	18.7	82.2 (32.9)	9.2 (3.7)	11.2
379 [812 (93)]	45.1 (18.0)	5.8 (2.3)	13.0	44.6 (17.8)	4.4 (1.7)	9.8
380 [814 (94)]	60.6 (24.3)	8.2 (3.3)	13.5	64.5 (25.8)	6.8 (2.7)	10.6
381 [875 (98)]	85.2 (34.1)	13.0 (5.2)	15.2	100.8 (40.3)	12.7 (5.1)	12.6
382 [875 (98)]	37.8 (15.1)	5.5 (2.2)	14.6	40.2 (16.1)	5.3 (2.1)	13.1
383 [874 (98)]	73.1 (29.2)	10.4 (4.2)	14.2	84.3 (33.7)	9.0 (3.6)	10.7
384 [873 (98)]	28.7 (11.5)	4.1 (1.6)	14.3	29.6 (11.8)	3.9 (1.5)	13.0
385 [874 (97)]	56.3 (22.5)	8.0 (3.2)	14.2	66.1 (26.4)	7.4 (3.0)	11.2

Table 3.2. Summary results for DEQAS samples 376-385.

3.4.2. LC-MS/MS method variables

Of the 605 results available from the returned questionnaires, 346 (57 %) were returned from laboratories using electrospray ionisation (ESI), and 259 (43 %) were from laboratories using atmospheric pressure chemical ionisation (APCI). No reports were returned from laboratories using alternative ionisation methods, such as atmospheric pressure photoionisation (APPI), though these have been reported (Guo *et al*., 2006; Hermann *et al*., 2010). Summary comparative results are shown in Figure 3.2. Although there was no significant difference in the mean ratio (reported result divided by LC–MS method mean result) between ESI and APCI (unpaired *t*-test, *P*=0.5828), the variances differed significantly (F test, *P* <0.0001) between the two groups. Variations (% CV) were 14.2 % and 11.3 % for ESI and APCI, respectively. Where information was supplied, all laboratories except one were using triple quadrupole instruments, or instruments with triple quadrupole functionality (i.e. ABSciex Q-Trap™ instruments, which may be operated in triple quadrupole mode). The only laboratory not using a triple quadrupole instrument was using a 3D ion-trap, and was performing derivatisation with 4-phenyl-1,2,4-triazoline-3,5-dione (PTAD) prior to analysis. The two other laboratories performing PTAD derivatisation used triple quadrupole instruments for quantification. All ionisation, regardless of ionisation source, was carried out in positive mode. For 25-OHD3 without PTAD derivatisation, all of the laboratories using ESI (N=36 where information available) monitored a nominal precursor in the first quadrupole (Q1) of *m/z* 401, corresponding to the intact protonated $[M+H]^+$ molecular ion. In comparison, only 5 laboratories reporting results using APCI used this Q1 *m/z*. The majority of APCI users (N=16, 76 %) instead monitored a Q1 nominal *m/z* of 383, corresponding to loss of a water moiety from the protonated molecular ion ($[M+H-H_2O]^+$) in-source. The same was true for the analysis of 25-OHD2, except for in three laboratories using APCI, where for 25-OHD3 the intact $[M+H]^+$ was monitored in Q1, but for 25-OHD2 the water loss ion was monitored ($[M+H-H_2O]^+$, *m/z* 395) instead. Analysis of the DEQAS reported results ratio as a function of monitored Q1 *m/z* (Figure 3.3) therefore mirrored the previous results for ESI versus APCI. There was no difference in the mean reported ratio (unpaired *t*-test, *P*=0.7542), but the variances were significantly different (F test, *P* <0.05). Variation (% CV) reduced from 14.1 % to 12.2 % when monitoring a Q1 *m/z* of 383.

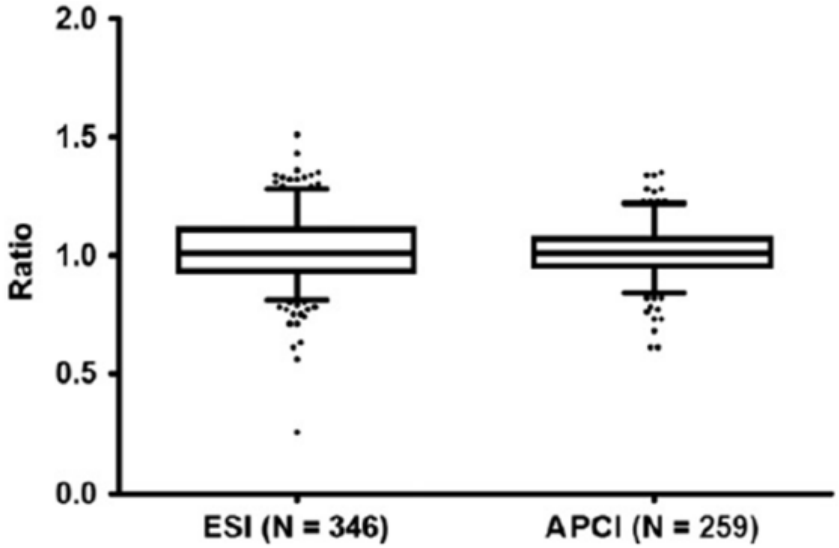

Figure 3.2. Distribution of results ratios (reported result divided by DEQAS LC-MS/MS method mean) for laboratories using ESI and APCI.

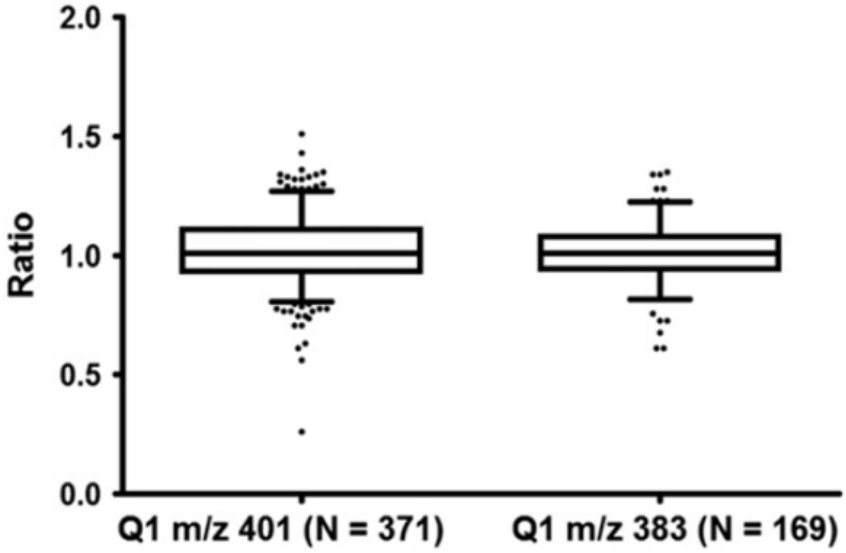

Figure 3.3. Distribution of results ratios (reported result divided by DEQAS LC-MS/MS method mean) for laboratories monitoring Q1 *m/z* values of 401 (mainly ESI users) and 383 (mainly APCI users).

For 25-OHD3, excluding those laboratories performing PTAD derivatisation, data from 57 laboratories were available regarding the transition(s) monitored (selected/multiple reaction monitoring, SRM/MRM). In total, 26 (46 %) laboratories monitored a water loss fragmentation. The remaining 31 laboratories (54 %) monitored alternative fragmentation reactions. There was no significant difference (unpaired *t*-test, *P*=0.7589) in the mean results ratio reported between these two groups, although the variation was significantly greater (F test, *P* <0.05) in those laboratories monitoring water-loss transitions (Figure 3.4). The variations (% CV) were 14.6 % and 12.6 % for the groups monitoring water-loss transitions and alternative product ions, respectively. Relating these data to ionisation method, a greater proportion of those laboratories using ESI used water loss MS/MS transitions than those using APCI (55 % and 29 % of laboratories used water loss transitions following ESI and APCI, respectively). Data were supplied by 23 laboratories regarding the use of qualifier ion transitions. In the data presented above on Q1 *m/z* values and MS/MS fragmentation, only quantifier ion Q1 *m/z* values and transitions were used. Only two laboratories (both using APCI) used different Q1 *m/z* values for quantifier and qualifier ions for 25-OHD3. In both cases, quantification of 25-OHD3 was carried out using a water loss MS/MS transition (*m/z* 401 to 383). One laboratory then used a second water loss transition for qualification (*m/z* 383 to 365), and the other used two alternative fragmentation reactions for qualification (*m/z* 383 to both 229 and 211). There was a small but significant difference in the mean results ratio (unpaired *t*-test, *P* <0.001) between those laboratories using qualifier ion transitions and those using single transitions. The mean ratio was greater in those laboratories using qualifier ions (Figure 3.5). No significant difference in variance was observed between the two groups (F test, *P*=0.6913). Variation (% CV) was similar between the two groups (13.2 % and 13.4 % for those laboratories using qualifier ions and those using single transitions, respectively). No data were available from this questionnaire regarding the use of product ion ratio(s) for analyte identification/confirmation.

All laboratories reported the use of at least one isotopically labelled 25-OHD internal standard. For both 25-OHD3, and for those laboratories which used a separate internal standard to quantify 25-OHD2, hexa-deuterated analogues were used (25-OHD2-

D_6/25-OHD3-D_6). All laboratories used MS/MS fragmentation for their internal standard(s) comparable to the respective analytes (i.e. those laboratories using a water-loss MS/MS transition to monitor 25-OHD3 did so too for 25-OHD3-D_6). A common standard was not used for this study. This would almost certainly explain some of the observed variation between methods, as has been previously shown (Carter & Jones, 2009). All laboratories carried out visual inspection of results prior to reporting.

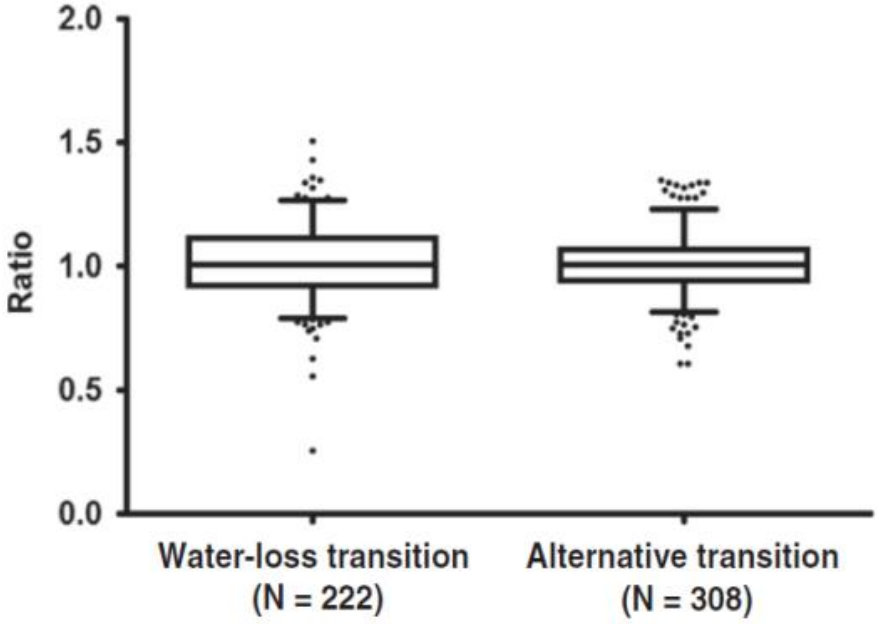

Figure 3.4. Distribution of results ratios (reported result divided by DEQAS LC-MS/MS method mean) for laboratories monitoring water-loss transitions and alternative, non-water-loss fragmentation reactions.

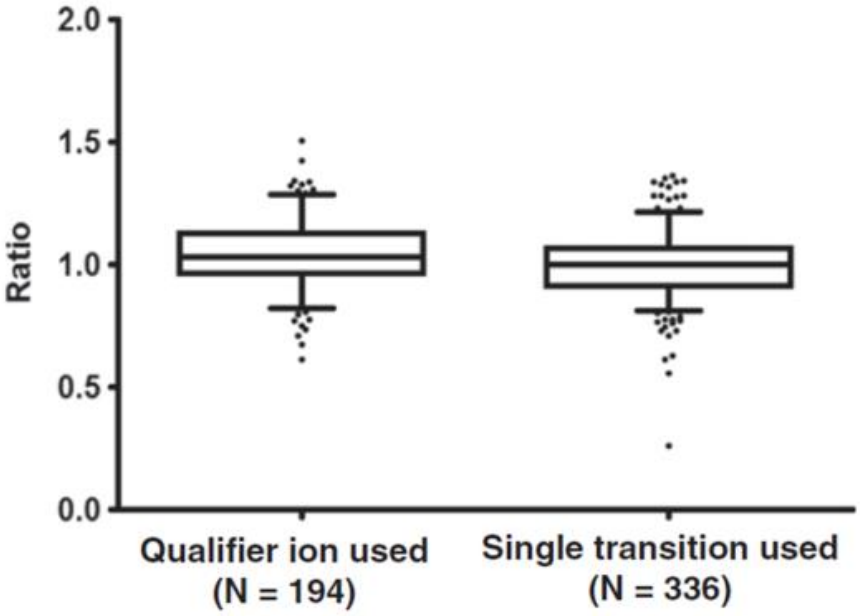

Figure 3.5. Distribution of results ratios (reported result divided by DEQAS LC-MS/MS method mean) for laboratories using qualifier ion transitions versus single fragmentation reactions.

3.4.3. 3-*Epi*-25-hydroxyvitamin D3

Of the 65 laboratories reporting LC–MS/MS results, only 3 (5 %) claimed that their method was capable of chromatographically resolving the isobaric 3-epimer metabolite from 25-OHD3. Of these laboratories, one was using a pentafluorophenyl (PFP) analytical column (column details not supplied), one was using a Phenomenex Luna™ C8 column, and one using another reversed-phase column (column details not supplied). No data were available on the analysis time in each case. 41 (63 %) laboratories stated that their method was unable to distinguish these compounds, and 21 (32 %) did not know whether their method could resolve the 3-epimer. In a qualitative study, DEQAS samples were sent out in October 2011 (Samples 404 and 405) to further investigate the influence of 3-*epi*-25-OHD3 on HPLC and LC-MS/MS methods. Both samples were from the same serum pool, but to Sample 405 3-*epi*-25-OHD3 was added (~51 nmol/L in ethanol). Analyte-free ethanol was added to Sample 404 to give the same final concentration of ethanol (0.2 %, *v/v*). In agreement with

results of the current LC–MS/MS survey, only 6 (5%) LC–MS users (total N=115) and 3 (11%) HPLC users (total N=27) use methods which resolve the 3-*epi*-25-OHD3. Those assays which did not resolve the epimer overestimated the 25-OHD3 concentration in Sample 405 (Figures 3.6 and 3.7, DEQAS report, October 2011).

Sample	Method	n	Method Mean	SD	CV
404	(all methods)	1066	46.0 (18.4)	6.2 (2.5)	13.4
404	Abbott Architect	22	44.7 (17.9)	3.1 (1.3)	7.0
404	Automated IDS EIA	122	45.1 (18.0)	4.1 (1.6)	9.1
404	Chromatographic Ligand Binding Assay	1	43.2 (17.3)	0.0 (0.0)	0.0
404	DIAsource	1	99.0 (39.6)	0.0 (0.0)	0.0
404	DiaSorin Liaison Total	408	43.4 (17.4)	4.4 (1.8)	10.2
404	DiaSorin RIA	29	47.7 (19.1)	6.8 (2.7)	14.2
404	HPLC	27	47.8 (19.1)	10.5 (4.2)	22.0
404	IDS EIA	153	44.4 (17.7)	4.3 (1.7)	9.6
404	IDS RIA	13	57.0 (22.8)	7.6 (3.0)	13.3
404	IDS-iSYS	119	52.6 (21.1)	5.1 (2.0)	9.7
404	LC-MS	115	51.2 (20.5)	5.5 (2.2)	10.8
404	Roche 25OHD3	4	37.9 (15.2)	8.9 (3.5)	23.4
404	Roche Total 25OHD	32	46.7 (18.7)	4.2 (1.7)	9.0
404	Siemens ADVIA Centaur	16	39.5 (15.8)	7.8 (3.1)	19.7
404	Unknown	4	56.6 (22.6)	5.8 (2.3)	10.3

Sample	Method	n	Method Mean	SD	CV
405	(all methods)	1065	51.9 (20.8)	16.0 (6.4)	30.8
405	Abbott Architect	22	44.9 (18.0)	2.9 (1.2)	6.4
405	Automated IDS EIA	121	45.7 (18.3)	4.1 (1.6)	8.9
405	Chromatographic Ligand Binding Assay	1	74.0 (29.6)	0.0 (0.0)	0.0
405	DIAsource	1	128.0 (51.2)	0.0 (0.0)	0.0
405	DiaSorin Liaison Total	408	43.5 (17.4)	4.4 (1.8)	10.1
405	DiaSorin RIA	29	48.9 (19.5)	5.4 (2.2)	11.0
405	HPLC	27	91.7 (36.7)	27.6 (11.1)	30.1
405	IDS EIA	153	44.7 (17.9)	4.5 (1.8)	10.0
405	IDS RIA	13	57.2 (22.9)	5.8 (2.3)	10.1
405	IDS-iSYS	119	52.7 (21.1)	5.4 (2.2)	10.3
405	LC-MS	115	109.2 (43.7)	25.6 (10.2)	23.5
405	Roche 25OHD3	4	57.1 (22.8)	22.1 (8.8)	38.6
405	Roche Total 25OHD	32	76.0 (30.4)	3.7 (1.5)	4.9
405	Siemens ADVIA Centaur	16	40.5 (16.2)	11.8 (4.7)	29.1
405	Unknown	4	69.7 (27.9)	14.2 (5.7)	20.4

Figure 3.6. DEQAS report from October 2011. Sample 404 and 405 are the same sample, but sample 405 was fortified with 3-*epi*-25-OHD3.

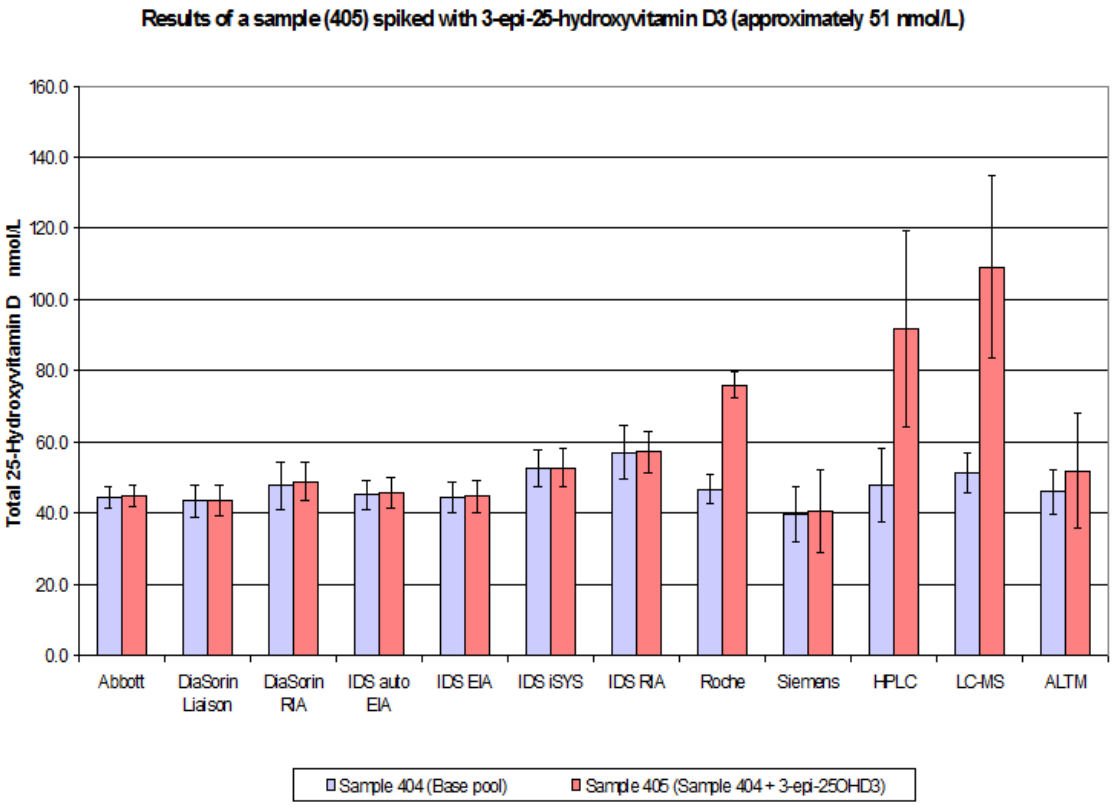

Figure 3.7. Summary DEQAS data from October 2011, samples 404 and 405. Shown are the method mean result (coloured bars, nmol/L), with the error bars representing the standard deviation either side of the mean (nmol/L).

3.5. Discussion

Analysis of these reported DEQAS results suggests that there is greater inter-laboratory variability when (i) using ESI rather than APCI, and (ii) when monitoring water-loss rather than alternative MS/MS transitions to quantify analytes.

3.5.1. Choice of ionisation method

With regards the choice of ionisation method, matrix effects are recognised as one of the major potential sources of error in LC-MS/MS analyses (Annesley, 2003). Analytical approaches to assess the degree of matrix effectsare widely used when developing and validating LC-MS/MS methods (Bonfiglio *et al*., 1999; Matuzewski *et al*., 2003), but these methods are less straightforward for endogenous compounds where truly representative blank matrices are unavailable, and synthetic or modified matrices do not always reflect real clinical samples. In the field of toxicology, it is documented that for the analysis of drugs in biological matrices, ESI is more susceptible to matrix effects than is APCI (Dams *et al*., 2003; Matuzewski, 2006). For some compounds, ESI offers greater sensitivity compared with APCI, although for the analysis of relatively non-polar compounds (i.e. those lacking easily ionisable groups), such as certain steroids which are structurally related to vitamin D, APCI is often advocated.

Derivatisation may be used to improve ionisation efficiency for ESI analyses (Iwasaki *et al*., 2011), typically via the introduction of a proton-accepting group to promote positive ionisation in the ESI source. In vitamin D analyses where derivatisation is employed to increase assay sensitivity (e.g. for low-volume samples, for the analysis of low concentration metabolites such as 1,25-OHD, or for the analysis of 25-OHD on less-sensitive MS instruments, PTAD is the most commonly used derivatisation reagent (as demonstrated by two of the laboratories in this study). However, for some metabolites, the Diels–Alder reaction involved (Figure 3.7) results in the production of two species (6*R* and 6*S*-isomers). When 25-OHD3 and 1,25-OHD3 were derivatised using PTAD and analysed using a short reversed phase LC column with gradient elution, the 25-OHD3-PTAD derivatives showed some chromatographic resolution of the two isomers (Figure 2.8). The 1,25-OHD3-PTAD derivatisation reaction yielded only

a single peak on the same chromatography column, suggesting either (i) the two isomeric forms of the 1,25-OHD3 derivative were not resolved, or (ii) the additional hydroxyl-group at the 1-position in 1,25-OHD3 sterically hinders the formation of one of the isomers. The latter theory is held up by the fact that derivatisation of 24,25-OHD yields two isomeric forms (Xue *et al*., 2009).

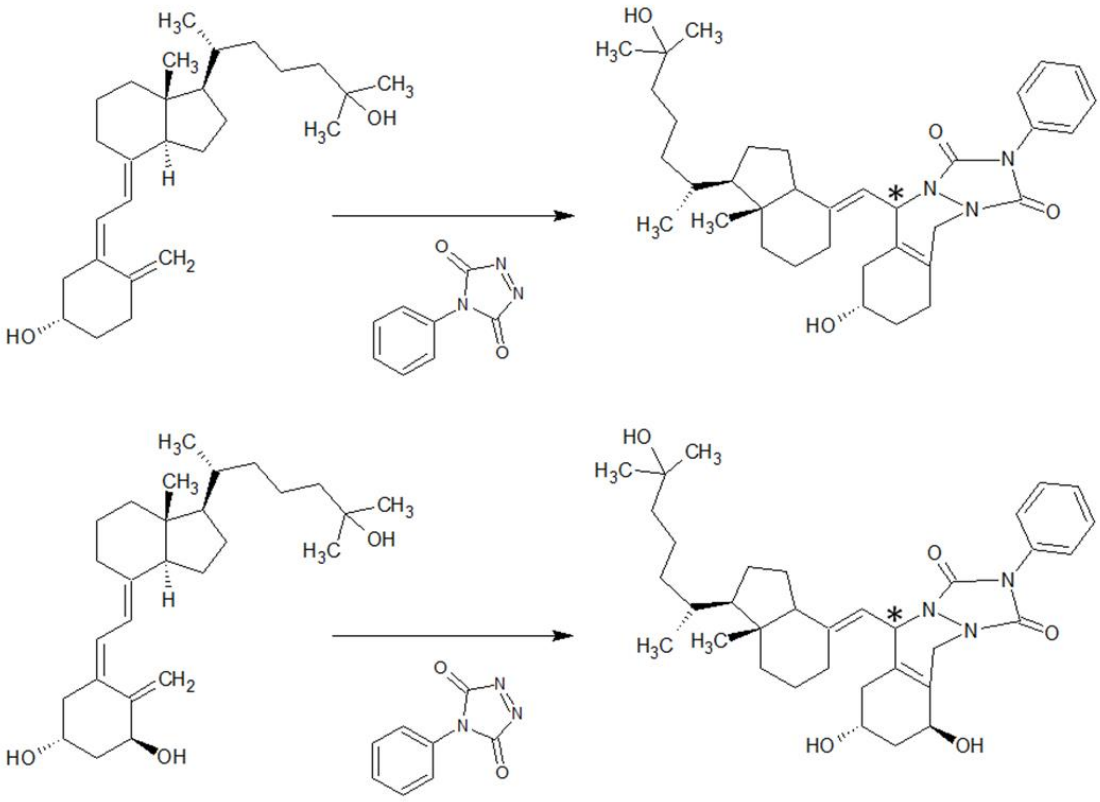

Figure 3.8. Derivatisation of 25-OHD3 (top) and 1,25-OHD3 (bottom) with 4-phenyl-1,2,4-triazoline-3,5-dione (PTAD). The planar PTAD structure reacts with both sides of the diene of the 25-OHD3 molecule to produce R and S isomers at the 6-position of the derivative structure (marked with an asterisk). For the 1,25-OHD3, upon LC-MS/MS analysis of the derivative, only a single compound is observed (Figure 3.9), suggesting the presence of the additional hydroxyl group in the 1-position hinders the formation of one of the PTAD-derivative isomers.

There are two additional considerations for PTAD-derivatisation of vitamin D metabolites. Firstly, the MS/MS product ion spectra of derivatised vitamin D metabolites are dominated by the product ion corresponding to the PTAD derivative moiety. Whilst this may yield good analytical sensitivity, it should also be remembered that any metabolite with a diene group will likely be derivatised, and so give rise to the same product ion. Selective analysis of derivatives therefore relies upon uniqueness of the precursor ion and LC retention time (which may be complicated by isomeric forms). Secondly, the PTAD derivatisation procedure produces the best yields in non-aqueous environments, and so this technique does not lend itself to high-throughput analysis. An exception to this was demonstrated by the work of Netzel *et al*., who employed the use of a homologous series of triazoline dione compounds to differentially derivatise multiple samples and allow for simultaneous analysis (Netzel *et al*., 2011).

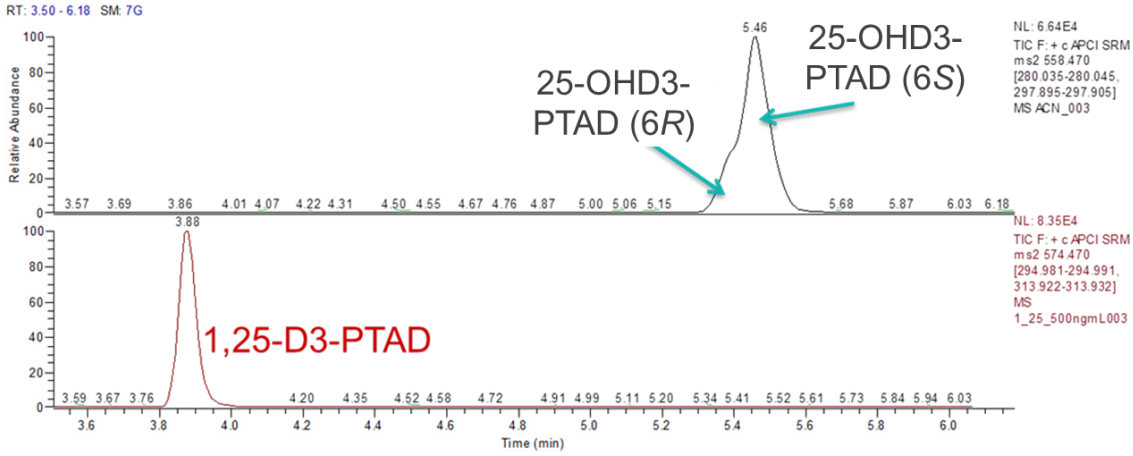

Figure 3.9. LC-MS/MS analysis of PTAD derivatives of 25-OHD3 (top) and 1,25-OHD3 (bottom). Shown are the summed SRM chromatograms of *m/z* 558 to 298 and 280 (for 25-OHD3) and *m/z* 574 to 294 and 314 (for 1,25-OHD3).

Though the data from this study suggest that there is greater inter-laboratory variability when using ESI than when using APCI, it should be noted that using ESI does not suggest inaccuracy in 25-OHD measurement, as evidenced by there being no significant difference in the mean results ratio.

3.5.2. Choice of product ion(s)

One of the major advantages of LC-MS/MS over immunoassays is considered to be improved specificity and selectivity. LC-MS/MS can easily distinguish 25-OHD2 from 25-OHD3, but other interfering compounds may be present in patient samples, such as structurally similar sterols and fatty acid derivatives, even after sample preparation procedures (Vogeser, 2010). Water-loss MS/MS transitions are very common to this group of compounds and so, although these transitions may provide the greatest signal intensity for 25-OHD analysis, they may also be subject to a greater risk of interference from co-eluting isobars/artefacts. That said, the NIST certified reference method (Tai *et al*., 2010) uses a water-loss transition as the quantifier ion. However, the NIST reference method is a low-throughput method, based upon (i) a thorough liquid-liquid extraction process and (ii) a long chromatographic analysis time (40 min). Both of these factors ensure that potential interferences and matrix effects are minimised when compared to, say, a non-selective protein precipitation followed by a short chromatographic analysis which would be more commonplace in a high-throughput clinical laboratory.

Although no difference in variation in results was observed in the results from this study, the use of product ion ratios to improve analyte identification has previously been reported for the analysis of drugs. For example, Nordgren *et al*. (2005) reported a significantly reduced false-positive rate when monitoring 23 analytes using two-transition SRM versus single-transition SRM analyses.

3.5.3. 3-*Epi*-25-hydroxyvitamin D

When this study was conducted, very few laboratories used methods which routinely resolve 3-*epi*-25-OHD3. It was of particular concern that some laboratories were unaware of the ability of their method to detect this metabolite. Of the three laboratories who reported that their methods were capable of resolving the 3-*epi*-25-OHD isomers, two were reportedly using reversed-phasde LC systems, which would not typically be able to resolve the two compounds. No further method details were available.For some time, it was thought that 3-*epi*-25-OHD3 was only present in samples from neonates (Singh *et al*, 2006), but recent literature also suggests presence of this compound in significant concentrations in some of the adult population (Stepman *et al*., 2011; Shah *et al*., 2011). This may become problematic for routine 25-OHD analysis, since resolution of 3-*epi*-25-OHD3 is thought to require a significantly longer chromatographic analysis. In the previous Chapter, this was shown not to be the case. Furthermore, the use of LC–MS/MS systems with column-switching LC systems is another approach to accommodate extra analysis time whilst meeting throughput demands. There are reportedly over 50 vitamin D metabolites (Zerwekh, 2008) and, although the concentrations of many of these are very low relative to 25-OHD and some have only been produced/measured in vitro, these must also be considered potential sources of assay interference. The analysis of serum 25-OHD using LC-MS/MS is not straightforward. That said, the flexibility of LC-MS/MS compared with immunoassay systems allows for methods to be easily modified (e.g. lengthened chromatographic analysis times or alternative column chemistries) in order to remove interferences from other vitamin D metabolites, such as 3-*epi*-25-OHD. Where possible/available, APCI should perhaps be used in preference to ESI, and MS/MS fragmentation reactions other than water-losses should be monitored to improve the precision of results, especially so for methods using non-specific sample preparation and/or with short chromatographic analysis times. Matrix effects should be evaluated thoroughly, although matrix effects arising from individual samples can never be fully eliminated. Assay standardisation has already been proven to have a significant impact on inter-laboratory agreement. Further work is needed to investigate inter-laboratory harmonisation with regards to sample preparation and chromatographic analysis to remove and/or resolve known interferences.

Chapter Four

Studies on the analysis of parathyroid hormone by LC-MS and LC-MS/MS

4.1. Background

Parathyroid hormone (PTH) is an 84-amino acid, single-chain peptide synthesised by the parathyroid glands and is the main hormone responsible for the regulation of plasma ionised calcium (Ca^{2+}). The intact active form of the hormone (PTH1-84), is produced by the sequential cleavage of the initially translated peptide, pre-pro-PTH (115 amino acids), via pro-PTH (90 amino acids, Figure 4.1). The analysis of PTH1-84 is not straightforward – there exists a surprisingly heterogeneous range of PTH-related peptides (Berson & Yalow, 1968) that give rise to assay interference. Both the exact composition and possible biological functions of these PTH fragments remain to be fully elucidated as does the variable influence of these fragments on currently available analytical methods for PTH testing (Garrett *et al*., 2013; Souberbielle *et al*., 2006). PTH1-84 can be proteolytically cleaved within the parathyroid gland prior to secretion, or cleavage can occur through the actions of endoproteases in hepatic Kuppfer cells (Bringhurst, 2003; Torres, 2006). Certain synthetic PTH fragments have been demonstrated to antagonise the biological activity of PTH1-84 both *in vitro* and *in vivo* (Zhang *et al*., 2006; D'Amour, 2006). The discovery of circulating PTH fragments in the late 1960s and 1970s was the main driver for the development of 2nd and 3rd generation immunoassay methods for PTH analysis.

It is perhaps ironic that it is in patients with renal failure, in whom the accurate analysis of PTH1-84 is clinically important for the prevention of mineral bone disorders and for guiding expensive drug treatments, that the accumulation of PTH fragments is the most pronounced. A review of circulating PTH isoforms based on immunoassay by D'Amour concluded that PTH1-84 accounts for just 20 % of the 'total' circulating PTH in normocalcaemic individuals, but can be as little as 5 % in patients with end stage renal failure, depending upon which assay is used for measurement (D'Amour, 2006).

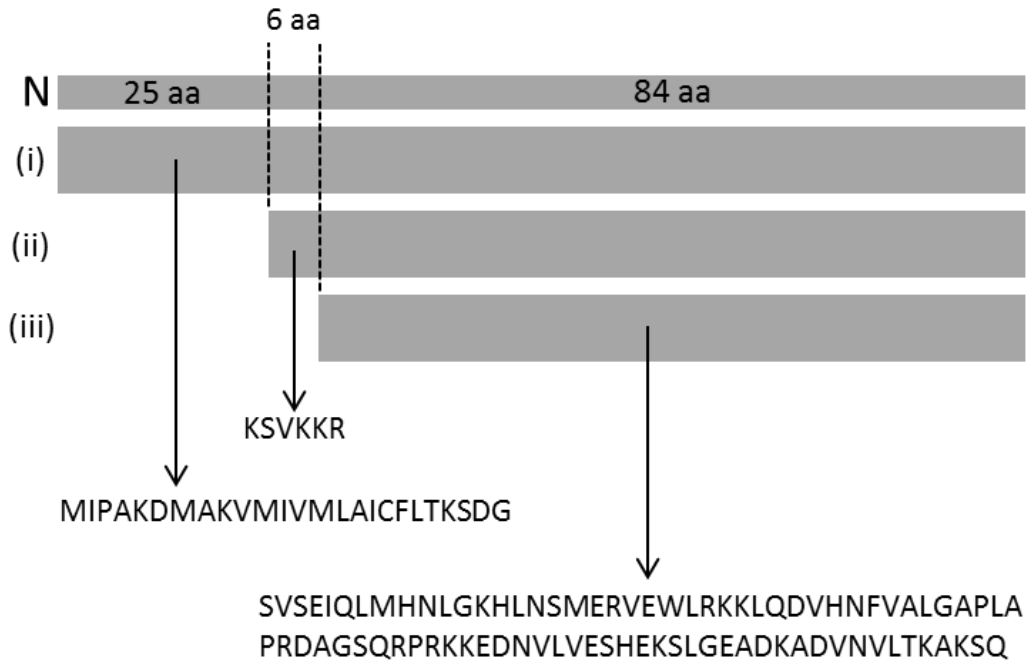

Figure 4.1. Amino acid sequences of (i) pre-pro-PTH (115 amino acids), (ii) pro-PTH (90 amino acids), and (iii) 'intact' PTH1-84 (84 amino acids).

Numerous publications have highlighted discrepancies between PTH1-84 concentrations measured in the same sample, but analysed using different assay platforms (Garrett *et al*., 2013; Souberbielle *et al*., 2006; Zimmerman *et al*., 2012). Indeed, it has been proposed that the difference between two different immunoassay-generated results (2nd versus 3rd generation immunoassays) could itself provide a useful index for the diagnosis and prognosis of parathyroid carcinomas (Caron *et al*., 2009; Cavalier *et al*., 2010; Caron *et al*., 2011).

There is an obvious clinical need for the harmonisation of PTH testing. The variability which exists in PTH testing should be considered a critical governance issue in patients with chronic kidney disease (Sturgeon *et al*., 2011). Given this variability in results produced using different methodologies, some clinicians question the relevance of measuring PTH at all in renal patients (Almond *et al*., 2012). Often, assay preference is governed more by reliance upon a method with which they have the most familiarity and clinical experience than by absolute analytical accuracy (Bringhurst, 2003). The establishment of an International Federation of Clinical Chemistry and Laboratory

Medicine (IFCC) working group for PTH (Sturgeon, 2014) should aid the development of reference methodologies, as well as harmonise the testing of PTH towards a traceable reference material (e.g. the World Health Organization Recombinant PTH1-84 International Standard 95/646, available through the National Institute for Biological Standards and Control, NIBSC – www.nibsc.org). Until such time as a reference method is developed and validated, which can be used to establish target values based on reference materials, the IFCC group are working towards the development of assay-specific target values (more information on the IFCC working group is available through http://www.ifcc.org/ifcc-scientific-division/sd-working-groups/parathyroid-hormone-wg-pth/).

2013 marked the 50th anniversary of the first competitive radioimmunoassay (RIA) developed for the analysis of PTH (Berson *et al*., 1963). During the intervening 50 years there can be no doubt that a significant number of developments and improvements have been made to assay specificity. This has been achieved both through an increased understanding of the biology of PTH (and its fragments) in different patient groups, as well as through improvements in the instrumentation and processes used for analysis. A timeline summarising the most important developments in PTH testing is outlined in Figure 4.2.

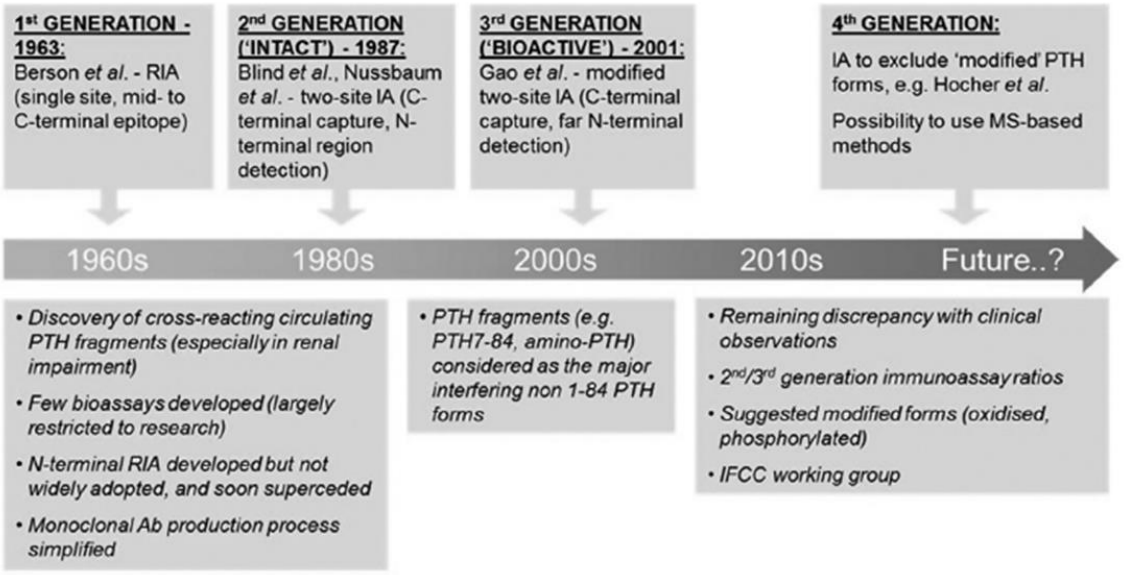

Figure 4.2.The historical development of PTH assays.

The development of the first radioimmunoassay for PTH by Berson and co-workers pre-dated the identification of truncated PTH forms (Berson *et al*., 1963). Needless to say, the lack of specificity of the single-site antibody used in these early RIAs (typically directed towards the mid-region of the PTH1-84 sequence – the region of greatest antigenicity) meant significant cross-reactivity from circulating PTH fragments, and thus overestimation of the true PTH1-84 concentrations. In some samples from patients with advanced renal disease, this overestimation could be several orders of magnitude when compared to individuals with normal renal and parathyroid function (Goodman, 2005). In the 1970s and early 1980s, a number of amino-terminal (N-terminal) RIAs were developed. As these were targeted more towards the biologically functioning regions of PTH1-84, they proved more useful than earlier more carboxy-terminal (C-terminal) RIAs for the diagnosis of renal bone disease. However, owing to important developments in the identification of PTH fragments and early work towards characterisation of their bioactivity, both these assays were quickly superseded by second-generation two-site immunometric assays and, later still, third-generation immunoassays.

4.2. Mass spectrometric immunoassay (MSIA)

In the last 10-15 years, LC-MS/MS has become a widely applied technique in clinical chemistry laboratories. It has largely been used for the quantitative analysis of small-molecules (i.e. <1,000 Da) such as steroids and related hormones (e.g. testosterone and vitamin D metabolites) and drugs and their metabolites. Modern instruments are highly sensitive, and coupled with appropriate sample preparation techniques, can often achieve limits of detection comparable with immunoassays (e.g. pmol/L for some analytes). However, it is the combination of chromatographic separation with a detection system based on mass-to-charge (*m/z*) ratio, which provides a specificity that is far superior to that of immunoassay-based detection (Vogeser & Seger, 2008; Rauh, 2009).

The analysis of more complex proteins and peptides using MS instrumentation was for a long time restricted to research laboratories and biomarker discovery/validation workflows. This work has typically been low-throughput, using micro-flow or nano-flow LC separations over hours rather than minutes. However, recent work has focused on the development of higher throughput, more robust, quantitative protein/peptide analyses suitable for the rigours of clinical chemistry work. The MS analysis of proteins and peptides can be done either directly using the intact analyte(s) in a top-down approach, or in a bottom-up approach following digestion with a suitable protease such as trypsin, and by monitoring specific (tryptic) peptides as surrogate markers.

The approach used depends on the target analyte; large proteins with *m/z* values exceeding the operating range of the MS instrument may require proteolytic digestion. Furthermore, some tryptic peptides offer superior ionisation efficiency or improved chromatographic peak shape than the intact species, and so the digestion step can be used to increase assay sensitivity. In the same manner as with quantitative small molecule MS analysis, isotopically-labelled internal reference standards can be synthesised, either for whole peptides/proteins or proteolytic peptides, and matrix-based calibration standards can be produced, ideally from reference standards, such as the PTH1-84 reference standard mentioned earlier.

For low abundance proteins/peptides such as PTH1-84 (and PTH fragments) in serum, the complexity of the sample matrix and the extremely large dynamic range of protein concentrations (Figure 4.3) necessitates thorough sample preparation prior to LC-MS analysis. For some small peptides of medium abundance, techniques traditionally used for small molecule analysis such as SPE may be useful, and have been successfully applied in a number of clinical assays, e.g. hepcidin (Li *et al*., 2009) and insulin (Chen *et al*., 2013).

For sensitivity (and specificity) when it comes to the analysis of less abundant proteins, it is necessary to somehow reduce the matrix complexity. A number of approaches have been reported, including the use of LC fractionation, depletion of the most abundant proteins (either by solvent precipitation, or using immunodepletion), enrichment by SPE, or by immunoaffinity for the target analyte(s). The latter of these techniques, immunoaffinity, has been reported using various techniques, including antibodies bound to nanoparticles or magnetic beads (Shi *et al*., 2012; Batalha *et al*., 2012; Thomas *et al*., 2012; Ackermann & Berna, 2007; Callesen *et al*., 2009).

An alternative immunoaffinity technique is that of mass spectrometric immunoassay (MSIA), a workflow now sold commercially through ThermoFisher Scientific. The workflow uses immobilised anti-target antibodies which are bound to monolithic micro-columns held in pipette tips (Figure 4.4). MSIA D.A.R.T.s (disposable automation research tips) are used with automated pipetting stations to enrich target analytes by simple aspirate-dispense cycling through the antibody-coated MSIA D.A.R.T.s (Nedelkov, 2006; Nedelkov, 2012; Kiernan *et al*., 2002; Becker & Hoofnagle, 2012).

MSIA D.A.R.T.s are prepared by baking soda lime glass beads in a stainless steel annealing mould to produce a solid, yet porous frit. The frits are then conditioned with acid prior to overnight treatment (>12 h) with 10 % (*v/v*) aminopropyl triethoxysilane solution to produce an amino-modified surface for binding ligands. The prepared frits are immobilised in wide-bore pipette tips and rinsed with physiological HBS-EP buffer solution (see Section 4.3.1 for details). Ligands are coupled to the amino-modified surfaces either via 1,1-carbonyldiimidazole or glutaraldehyde linkages (Kiernan *et al*., 2002). To allow greater ‘coverage’ of the functional surface, following the first reaction

with glutaraldehyde, polylysine and additional glutaraldehyde can be used to amplify the number of available amino-groups. Preparation of the MSIA D.A.R.T.s is typically carried out using the same automated pipetting stations as are used for the MSIA analysis.

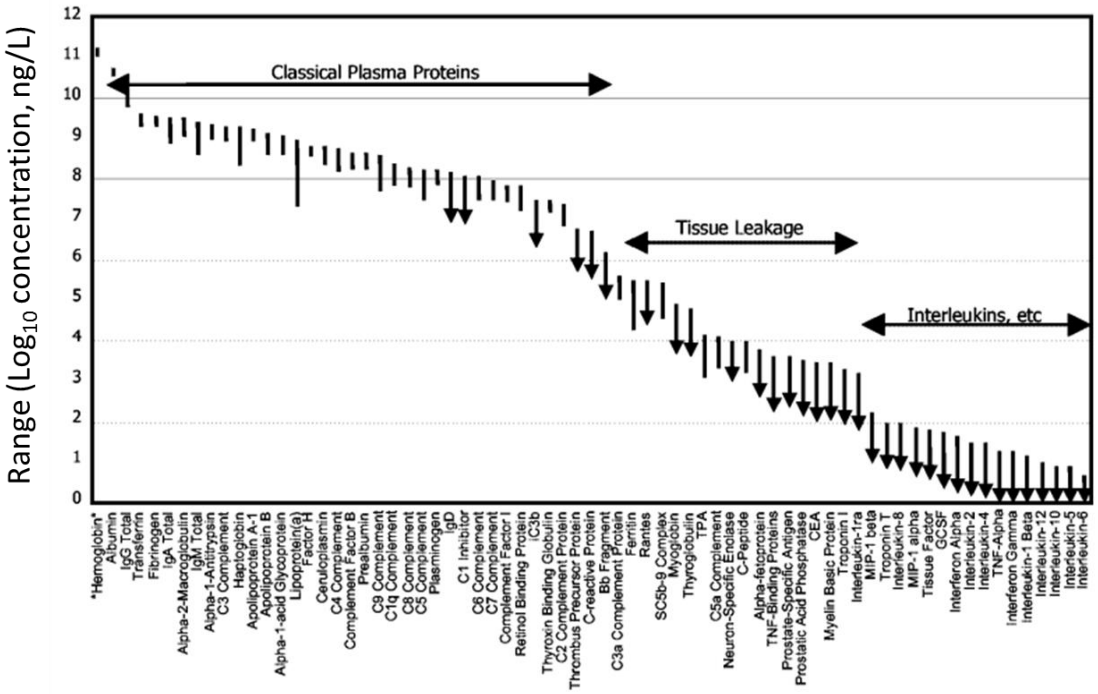

Figure 4.3. The normal range abundances of plasma proteins in humans. The use of immunoaffinity purification is relevant to low-abundance plasma proteins. Adapted from Anderson & Anderson, 2002.

The MSIA workflow was developed in the mid-1990s (Nelson *et al*., 1995), with early adoption of the technique primarily using matrix-assisted laser desorption ionisation coupled with time-of-flight MS (MALDI-TOF-MS) instruments for rapid population-wide protein analyses (Kiernan *et al*., 2002). MALDI-TOF MS has been widely used for peptide identification in proteomics studies. This technique has a wide *m/z* range, offers high-resolution MS, and a number of spectra deconvolution software packages

are available to aid spectral interpretation. Furthermore, although MALDI-TOF cannot be directly connected to chromatographic separation techniques as in LC-MS/MS experiments, these instruments can be used with immunoaffinity sample preparation and HPLC fraction collection methods to allow identification of low abundance proteins and peptides.

More recently, development of MSIA workflows has focussed on the use of LC-MS (and LC-MS/MS) rather than MALDI-TOF MS. With LC-MS as will be discussed, MSIA workflows can therefore include the use of protein digestion (Figure 4.4), and analysis using triple quadrupole or high-resolution instrumentation.

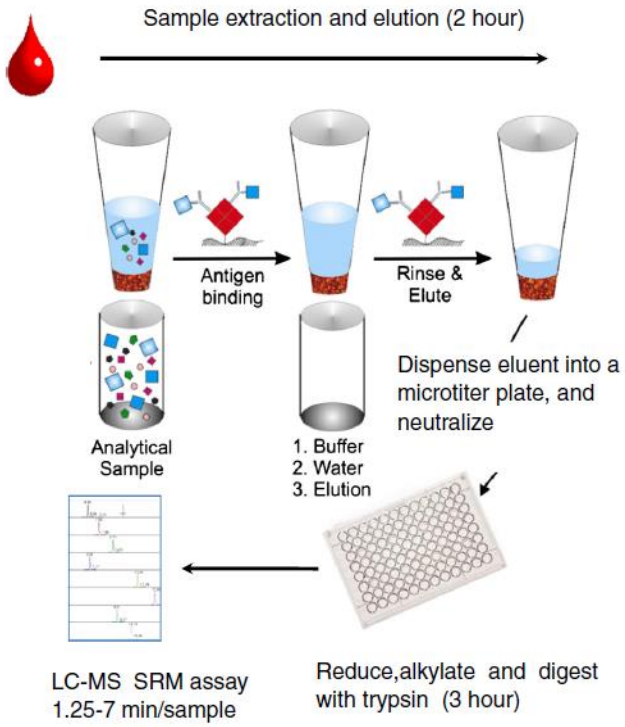

Figure 4.4. Schematic of a typical MSIA workflow. Samples are passed repeatedly through the MSIA D.A.R.T.s in the first step to allow antigen (analyte) binding. Following rinsing, captured analytes are then eluted from the D.A.R.T.s and can be analysed, either directly for analytes to be measured using a top-down approach, or following reduction, alkylation and digestion.

4.3. Aims

The work described in this chapter aimed to investigate the use of LC-MS and LC-MS/MS with MSIA for analyte enrichment for the analysis of PTH and identification of PTH variant forms. A MSIA method based on trypsin digestion and analysis of variant-specific tryptic peptides was evaluated and tested using samples sent for routine clinical PTH analysis. Results using the tryptic peptide MSIA-SRM method were compared to those produced using immunoassay, and correlated to other available biochemical measurements.

4.4. Materials and methods

4.4.1. Chemicals and reagents

Recombinant PTH1-84 reference material [WHO 1st International Standard reference material (95/646)] was purchased from NIBSC (www.nibsc.org). Additional recombinant PTH1-84 and glucagon were purchased from Bachem. Custom-made MSIA anti-PTH D.A.R.T.s were supplied by ThermoFisher Scientific (part number 991CUS02, 96 D.A.R.T.s). The D.A.R.T.s were supplied pre-bound with a goat polyclonal anti-human PTH antibody from Immutopics International (San Clemente, CA, USA). The antibody epitope was mapped using phage display technologies (by Differential Proteomics, Research Triangle, NC) to amino acids 72-79 of the PTH sequence (Krastins *et al*., 2013).

Iodoacetamide (IAA), dithiotreiol (DTT), urea, ammonium bicarbonate, tris(hydroxymethyl)aminomethane (tris), calcium chloride, nitrobenzoic acid (NBA), and ACS reagent grade formic acid were all from Sigma Aldrich (Poole, UK). Physiological HBS-EP buffer [working concentrations 0.01 mol/L 2-[4-(2-hydroxyethyl)piperazin-1-yl]ethane sulfonic acid (HEPES), 0.15 mol/L sodium chloride, 3 mmol/L ethylenediamine tetraacetic acid (EDTA) and 0.005 % (*v/v*) Surfactant P20] was purchased as a concentrate (10x, GE Healthcare, Little Chalfont, UK) and diluted with deionised water prior to use. Trypsin was MS sequencing grade and was from Pierce™ (ThermoFisher Scientific, Hemel Hempstead, UK). Solvents (acetonitrile, methanol and isopropanol) were all MS-grade and were from Fisher Scientific (Loughborough, UK). Water was deionised in-house (>12 milliohms, Purite, Thame, UK). Glucagon (~15 ug/mL) was added to the reconstitution buffer and was used as a 'scavenger' peptide to minimise analyte binding to plastic surfaces. Protein Lo-bind™ tubes (0.5 mL and 2.0 mL) were from Eppendorf (Stevenage, UK). Heavy-isotope labelled peptides were absolute quantitation (AQUA™) grade, and were custom-synthesised (Pierce™, ThermoFisher Scientific) to contain C-terminal lysine or arginine residues incorporating ^{13}C or ^{15}N ($\geq$98.5 % purity). Tryptic peptides were injected onto an Accucore™ aQ 100 x 2.1 mm LC column (2.7 um average particle size, superficiously-porous particles, ThermoFisher Scientific, Runcorn, UK). For the top-

down PTH analysis, a Proswift™ RP-4H 5 x 1.0 mm monolithic LC column was used (ThermoFisher Scientific, Runcorn, UK).

4.4.2. Instrumentation

SRM experiments were carried out using a TSQ Vantage triple quadrupole mass spectrometer. High resolution LC-MS experiments were carried out using a Q Exactive MS (ThermoFisher Scientific, San Jose, CA). For both instruments, the LC system was an Aria Transcend TLX-II instrument, each consisting of four Accela LC pumps (Accela 600 bar systems on the TSQ Vantage, and Accela 1250 bar systems on the Q Exactive instrument). For both LC columns, Eluent A was 0.2 % (*v/v*) formic acid in deionised water, and Eluent B was 0.2 % (*v/v*) formic acid in acetonitrile. Both MS instruments were fitted with heated electrospray ionisation (H-ESI) sources (HESI-II, Ion Max™ housing). All liquid handling was carried out using either a Versette™ 96-channel pipetting robot with six 96-well plate stages, or a Novus™ 12-channel automated pipette (both ThermoFisher Scientific).

4.4.3. Clinical samples

Excess, anonymysed clinical samples (N = 357) sent for routine PTH analysis were used to investigate the tryptic peptide SRM assay. For comparison of results, and for investigation of the correlation of any differences related to renal function, the samples also had PTH measured using a second generation PTH immunoassay (Advia Centaur, Siemens), and the estimated glomerular filtration rate (eGFR) calculated based on creatinine measurement (Advia Centaur, Siemens). Additional clinical details and biochemical measures were recorded where available. Kidney disease staging was carried out according to eGFR measurements as listed in Table 4.1.

Stage	eGFR (mL/min/1.73m^3)	Description
1	90+	Normal kidney function but urine findings or structural abnormalities or genetic trait point to kidney disease.
2	60-89	Mildly reduced kidney function, and other findings (as for stage 1) point to kidney disease.
3a	45-59	Moderately reduced kidney function.
3b	30-44	Moderately reduced kidney function.
4	15-29	Severely reduced kidney function.
5	<15	Very severe, or endstage kidney failure (sometimes call established renal failure).

Table 4.1. Classification of kidney function using eGFR, according to the the UK eCKD guide, available at www.renal.org/information-resources/the-uk-eckd-guide/ckd-stages, accessed 13th March, 2017.

4.4.4. Data processing

Protein sequences were taken from Uniprot (www.uniprot.org), and were digested *in silico* using Pinpoint™ software (ThermoFisher Scientific, version 1.3). Pinpoint software was also used to generate candidate SRM transitions for each proteotypic peptide based on fragmentation rules (Roepstorff & Fohlman, 1984), with custom peptide exclusion criteria (peptides fewer than 6 amino acids were excluded). To maximise sequence, no peptides were excluded based on amino acid composition. No missed cleavages were allowed for. Additional predicted tryptic peptides were added to the list for the detection and identification of variant PTH isoforms based on (i) literature searching and (ii) MALDI-TOF data (Lopez *et al*., 2010).

4.4.5. MSIA PTH sample preparation protocol

Prior to analysis, samples were thawed and thoroughly mixed to homogenise. Samples were centrifuged to remove particulates. Centrifuged samples (1 mL) were diluted with working HBS-EP buffer solution (750 µL) in 2 mL deep-well plates. MSIA D.A.R.T.s were conditioned with HBS-EP buffer (from 1 mL buffer in a separate well, 10 x 100 µL aspirate/dispense cycles). Analytes were captured (1,500 x 125 µL aspirate/dispense cycles). The D.A.R.T.s were then washed with separate portions of working HBS-EP buffer solution (2 x 15 aspirate/dispense cycles x 150 µL) and deionised water (15 aspirate/dispense cycles x 150 µL). Captured analytes were eluted from the D.A.R.T.s into either a 96-well, V-bottomed microplate, or 0.5 mL Lo-bind protein tubes containing 100 µL elution solvent [30 % (*v/v*) acetonitrile in 0.5 % (*v/v*) aqueous formic acid; 15 x 75 µL aspirate/dispense cycles].The tube/well contents were evaporated to dryness (nitrogen, 40 °C). Dried samples were reconstituted in a solution of 30 % (*v/v*) isopropanol in 100 mmol/L ammonium bicarbonate, pH 8.0, and briefly mixed (5 s). Freshly prepared trypsin solution (100 ng trypsin per tube/well, diluted in 25 mmol/L aqueous acetic acid, 100 µL) was added to each tube/well, and the samples were incubated (37 °C, > 4 h). Once digestion was complete, the tube/well contents were again evaporated to dryness (nitrogen, 40 °C), and reconstituted in 30 µL Eluent A containing (i) glucagon (~15 ug/mL) and (ii) heavy-isotope labelled tryptic peptides.

4.5. Results

4.5.1. Peptide selection/SRM optimisation

In silico (trypsin) digestion of PTH1-84 produced a list of candidate tryptic peptides (Table 4.2). Two tryptic peptides (VEWLR and AKSQ, amino acid sequence positions 21-25 and 81-84, respectively) were excluded from further analysis due to being fewer than 6 amino acids in length. Three of the mid-sequence tryptic peptides were not used since most literature suggests the presence of variant forms and/or isoforms of PTH is towards the N-terminus of the protein sequence (amino acids 1-34). The b- and y-ion series of either doubly- or triply-charged peptides were generated *in silico*, yielding a candidate list of 28 SRM transitions. Non-specific SRM transitions (e.g. those related to fragmentation of N-terminal lysine and arginine residues) were excluded. Through a series of iterative analyses of digested recombinant PTH1-84 (in the absence of any sample matrix), transitions were excluded based on (i) poor absolute signal intensity and (ii) 'noisy' extracted ion chromatograms (EICs). The final SRM transition list is summarised in Table 4.3, including the transitions for the heavy-labelled peptide internal reference standards. For the analysis of clinical samples, quantitation of the PTH1-13 tryptic peptide (SVSEIQLMHNLGK) was used as the surrogate for 'intact' PTH1-84 quantitation, given the MSIA antibody capture was at the far C-terminus (Lopez *et al*., 2010; Kumar *et al*., 2010).

4.5.2. PTH variant peptides

Theoretical transitions were generated representative of PTH variant forms. SRM transitions could not be optimised in the same way as for peptides relating to 'intact' PTH1-84 due to the lack of recombinant reference peptides, but theoretical transitions were based on those used for similar peptides from the intact sequence. Variant PTH peptide are summarised in Table 4.4. Quantitation for these pepeitdes was approximate, and was based on peptide peak area relative to known added concentrations of isotope-labelled peptides.

Peptide sequence	Sequence position
SVSEIQLMHNLGK	1-13
HLNSMER	14-20
LQDVHNFVALGAPLAPR	28-44
ADVNVLTK	73-80

Table 4.2. Tryptic peptides used for the analysis of 'intact' PTH1-84.

Peptide	Precursor Ion *m/z* (*z*)	Product Ion *m/z* (ion type)
SVSEIQLMHNLGK	485.296 (3)	527.297 (y9) 635.334 (y11)
SVSEIQLMHNLGK*	488.701 (3)	439.713 (y4) 639.456 (y11)
HLNSMER	443.714 (2)	435.202 (y3) 522.234 (y4) 636.276 (y5) 749.361 (y6)
HLNSMER*	448.718 (2)	445.210 (y3) 532.242 (y4) 646.285 (y5) 759.369 (y6)
LQDVHNFVALGAPLAPR	606.672 (3)	553.345 (y5) 681.404 (y7) 681.885 (y13) 865.525 (y9)
LQDVHNFVALGAPLAPR*	610.008 (3)	563.353 (y5) 686.890 (y13) 691.412 (y7) 875.533 (y9)
ADVNVLTK	430.248 (2)	361.244 (y3) 574.355 (y4) 673.424 (y5) 788.451 (y6)
ADVNVLTK*	434.255 (2)	369.258 (y3) 582.370 (y4) 681.438 (y5) 796.465 (y6)

Table 4.3. Summary of PTH tryptic peptide SRM transitions optimised through iterative analysis of digested recombinant PTH1-84.

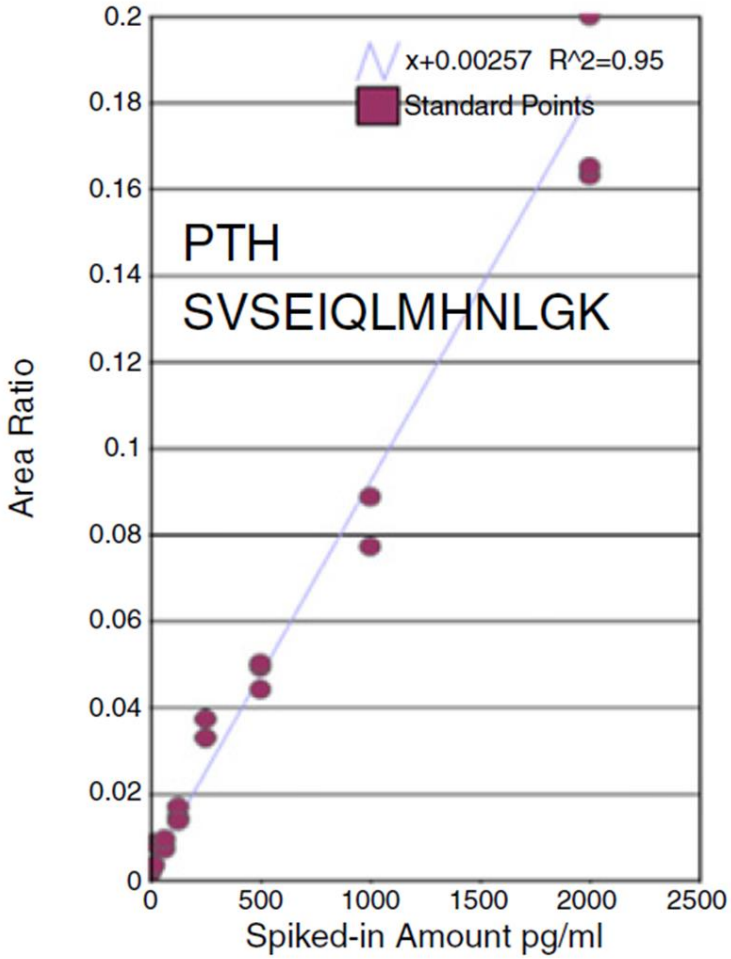

Figure 4.5. Example PTH1-13 tryptic peptide calibration curve.

Peptide	Sequence position	Source	Reference(s)
FVALGAPLAPR	34-44	PTH variant	
VALGAPLAPR	35-44	PTH variant	
LQDVHN	28-33	PTH variant	
LQDVHNF	28-34	PTH variant	
VSEIQLMHNLGK	2-13	?PTH variant	
SEIQLMHNLGK	3-13	?PTH variant	
EIQLMHNLGK	4-13	?PTH variant	
IQLMHNLGK	5-13	?PTH variant	
QLMHNLGK	6-13	?PTH variant	
LMHNLGK	7-13	PTH variant	D'Amour *et al*., 2003; 2007
HLNS(phospho)MER	14-20	?PTH variant	Rabbani *et al*., 1984

Table 4.4. PTH variant-specific tryptic peptides.

4.5.3. Analysis of clinical samples

Data from the clinical samples analysed was used to compare the performance of the SRM tryptic peptide assay with that of an established second generation immunoassay. Of the 357 samples, there were 174 samples (48.7 %) from female patients, and 183 samples (51.3 %) from male patients. For the females, the median (10^{th} and 90^{th} percentile) age at time of sampling was 59 (34-78 yrs), and for the males the median (10^{th} and 90^{th} percentile) age at time of sampling was 62 (40-79 yrs).

Of the 357 samples, 328 had eGFR measurements, allowing classification according to CKD stage. Of these, the majority (206, 62 %) were from patients with Stage 5 CKD. 14 (4 %) samples were from patients with Stage 4, 13 (4 %) samples were from patients with Stage 3b, 20 (6 %) samples were from patients with Stage 3a, 40 (12 %) samples were from patients with Stage 2, and 35 (11 %) samples were from patients with Stage 1 CKD.

4.5.3.1. SRM tryptic peptide data analysis

Since the PTH1-13 peptide was considered the surrogate for PTH1-84, the correlation between the PTH1-13 peptide concentration and the average of all observed tryptic peptide concentrations was investigated. 52 samples were excluded in which the PTH1-13 concentration was below 10 pg/mL. The corresponding median (range) average concentration of all tryptic peptides in these 52 samples was 63 (<10-1,556) pg/mL. In the remaining samples (N = 305), the average concentration of all peptides was consistently greater than the concentration of PTH1-13 alone (Figure 4.6). The median (10^{th} and 90^{th} percentile) concentrations were 101 (18-514) pg/mL and 623 (102-2854) pg/mL for PTH1-13 and the average of all tryptic peptides, respectively.

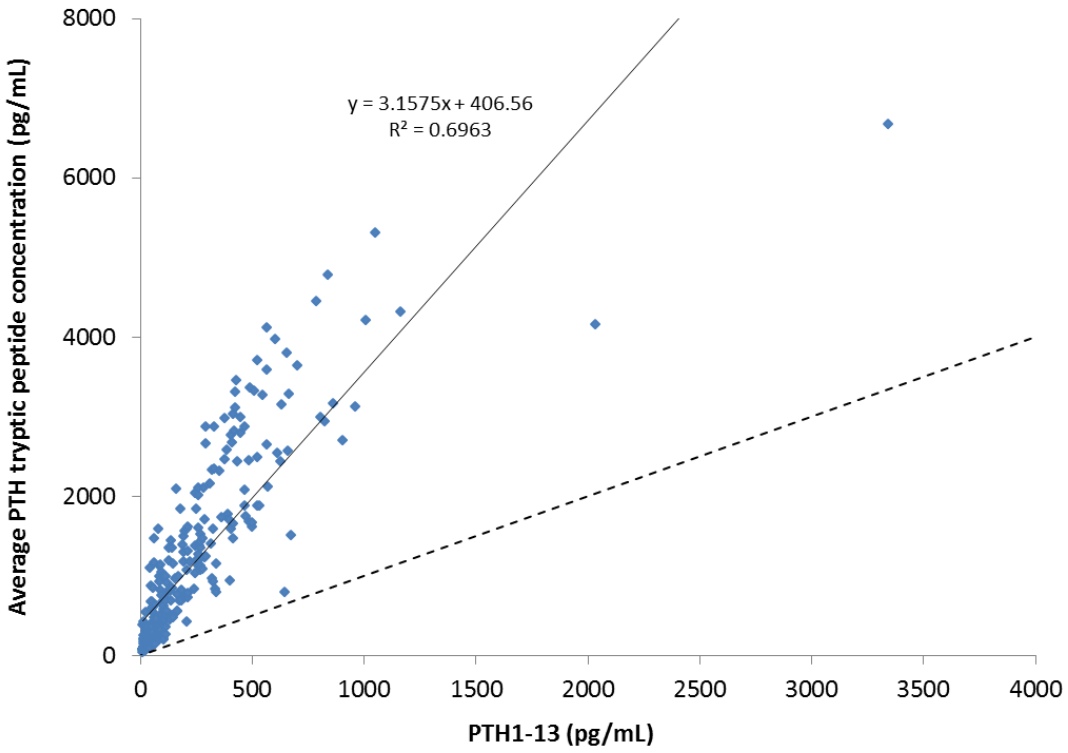

Figure 4.6. Correlation of PTH1-13 (SVSEIQLMHNLGK) concentration (pg/mL) with the average of all tryptic peptides, measured using the MSIA-SRM assay. The dashed line indicates the line of identity.

The PTH1-13 peptide concentrations showed correlation with the immunoassay results (R^2 = 0.7316), though there was a significant bias between the values, with the immunoassay results typically higher than the corresponding tryptic peptide value. The mean difference between the immunoassay results and the PTH1-13 concentrations was 119 pg/mL (Figures 4.7 and 4.8). One sample was excluded from the comparison due to the immunoassay measurement exceeding the maximum PTH concentration (>1,900 pg/mL). The corresponding PTH1-13 concentration in this sample was measured as 3,340 pg/mL. Additionally, 52 samples were excluded from correlation due to having PTH1-13 peptide concentrations below 10 pg/mL. Of these samples, the median (range) PTH immunoassay concentration was 28 (10-746) pg/mL.

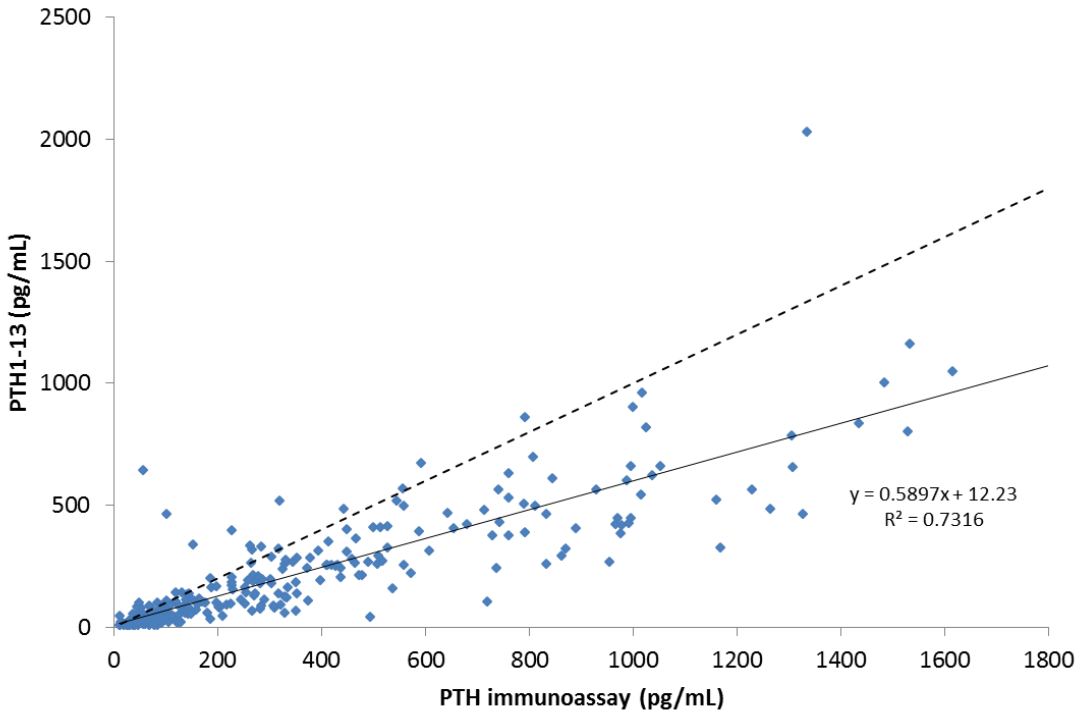

Figure 4.7. Overall correlation of PTH1-13 with the second generation PTH immunoassay (N = 304 samples). The dashed line indicates the line of identity.

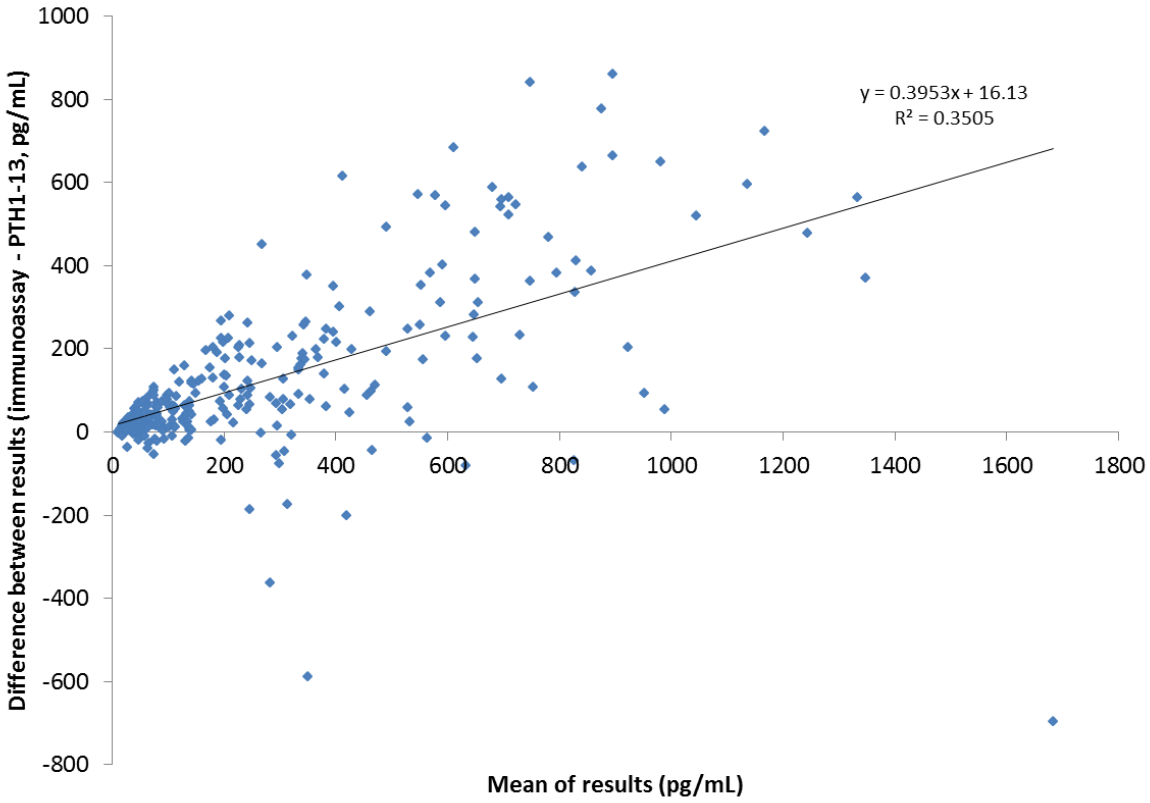

Figure 4.8. Bland-Altman plot of the mean concentration (PTH1-13 and PTH immunoassay, pg/mL) versus the difference between the results (PTH immunoassay – PTH1-13, pg/mL). The mean bias between the results was 119 pg/mL.

The PTH immunoassay and PTH1-13 concentration data were then classified according to CKD stage (Table 4.1) for the samples where eGFR results were available (N = 286). There were 26, 33, 14, 11, 13 and 189 samples classified as CKD Stage 1, 2, 3a, 3b, 4 and 5, respectively. For all CKD stages, the median, 10th and 90th percentile PTH concentration was lower when measured using the PTH1-13 surrogate tryptic peptide. Both the measured PTH concentration and the difference between the two assays were greatest for those patients at CKD stage 5 (Figures 4.9 and 4.10).

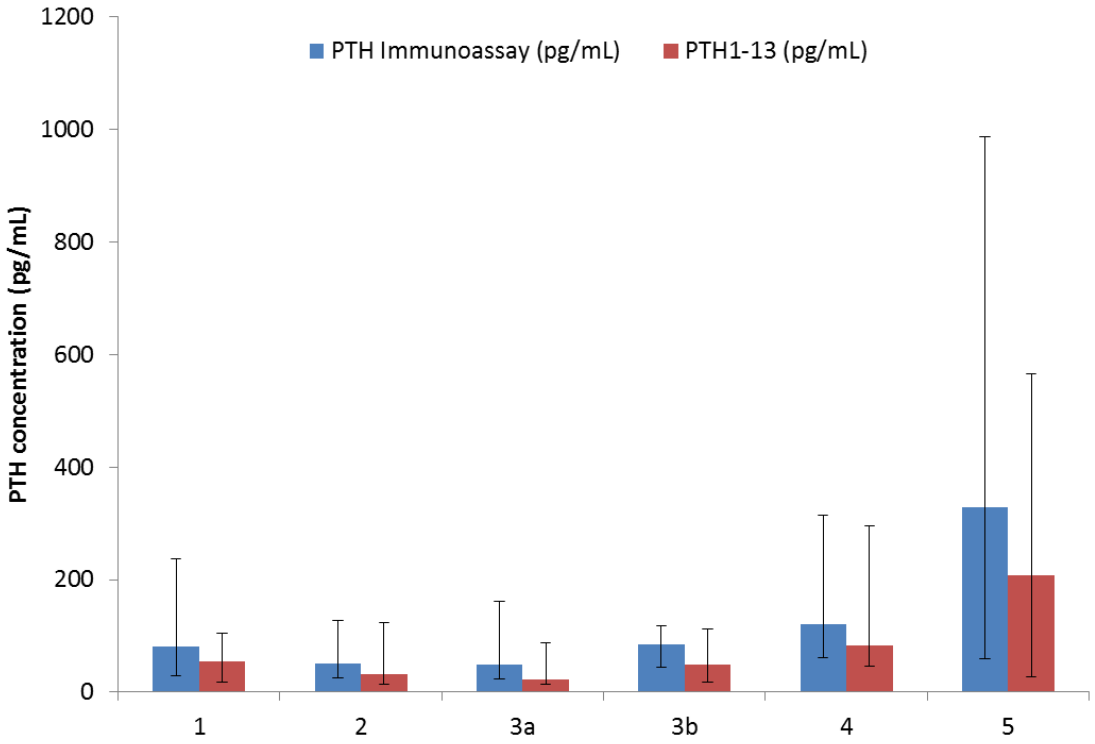

Figure 4.9. Median (10th and 90th percentiles shown as error bars) PTH concentrations as measured by the second generation PTH immunoassay (blue bars) and using the PTH1-13 tryptic peptide concentration (red bars) according to CKD stage.

The concentrations of the remaining tryptic peptides (i.e. non-PTH1-13) and the variant-specific tryptic peptides were analysed according to CKD stage. The proportions of the total PTH species of the four non-variant tryptic peptides are shown in Figure 4.11., and demonstrated slightly increased proportions of the mid- and C-terminal peptides in samples from patients at CKD stage 5. The results for the four tryptic peptides and the three detected variant-specific peptides (phosphorylated PTH14-20, PTH34-44 and PTH35-44) are summarised according to the median (10th and 90th percentile) concentrations in Figure 4.12 for those peptides which were detected. The series of theoretical peptides related to N-terminally truncated PTH isoforms (i.e. PTH2-13 through to PTH7-13) as well as the peptides corresponding to PTH28-33 and PTH28-44, were not detected in any of the samples tested (limit of detection taken as 10 pg/mL). Further analysis was carried out on the phosphorylated PTH14-20 peptide.

Of the 357 samples, 298 (83 %) had undetectable phosphorylated PTH14-20 (< 10 pg/mL). These samples had a median (range) corresponding non-phosphorylated PTH14-20 concentration of 57 (<10 – 720) pg/mL. There were 59 samples with phosphorylated PTH14-20 greater than 10 pg/mL. The majority (81 %, 48 samples) were from patients with stage 5 CKD. The median (range) proportion of phosphorylated to non-phosphorylated PTH14-20 was 8.8 (0.87-94.1) %. There was one sample from a patient with very high PTH14-20 and phosphorylated PTH14-20 (1,884 and 767 pg/mL, respectively, CKS stage 1, eGFR > 90 mL/min/1.73m^3). Excluding this sample from the data, there was no correlation (R^2 = 0.0095) observed between the concentrations of phosphorylated and non-phosphorylated PTH14-20.

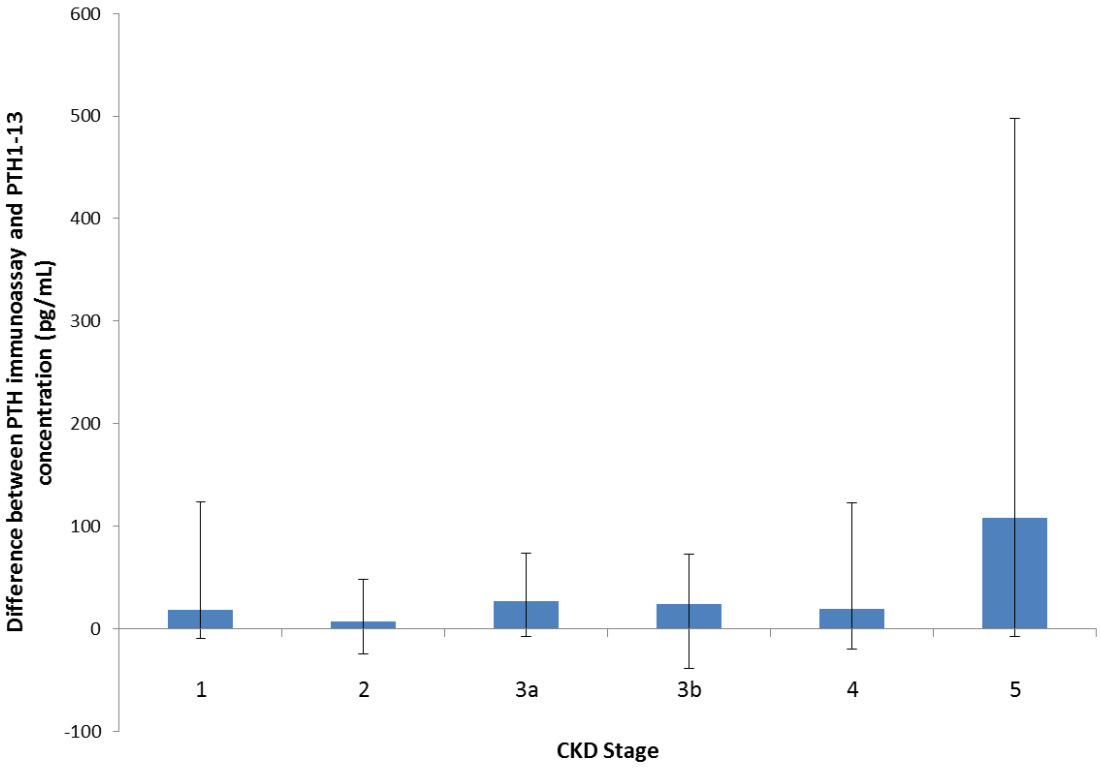

Figure 4.10. Differences between PTH concentrations measured using the second generation PTH immunoassay and the PTH1-13 tryptic peptide. Shown are the median difference (blue bars) and the 10th and 90th percentile differences (error bars).

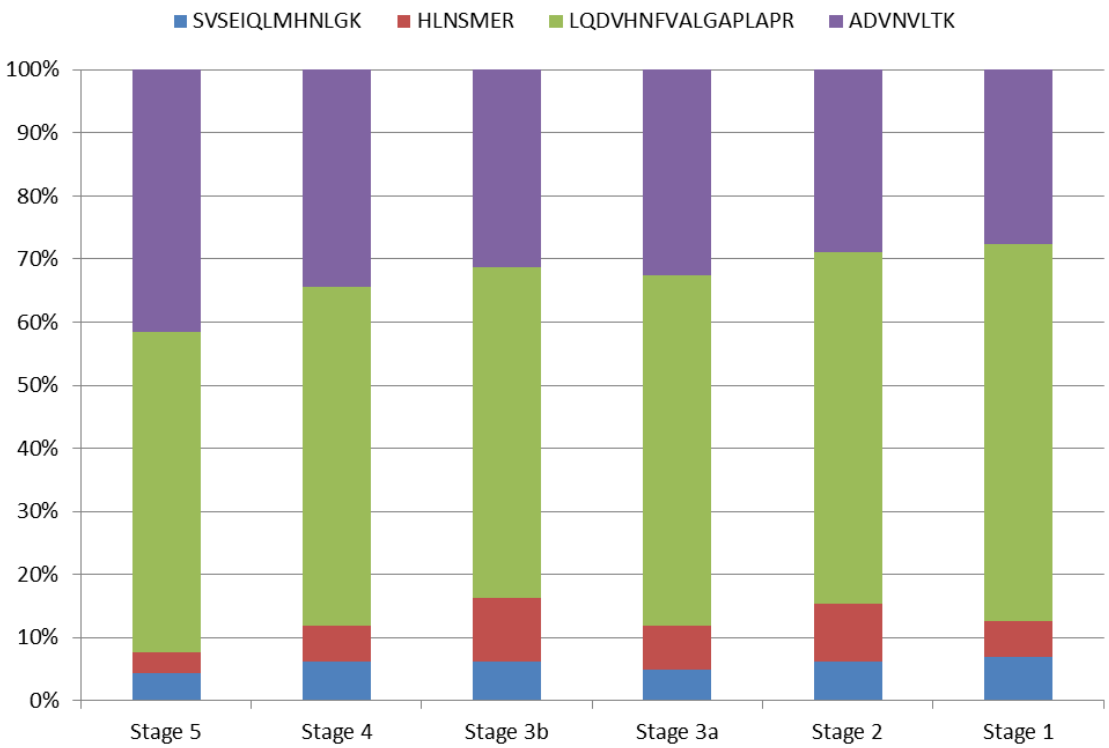

Figure 4.11. Mean relative proportions of the four tryptic PTH peptides (SVSEIQLMHNLGK, PTH1-13; HLNSMER, PTH14-20; LQDVHNFVALGAPLAPR, PTH28-44; ADVNVLTK, PTH73-80) according to CKD stage.

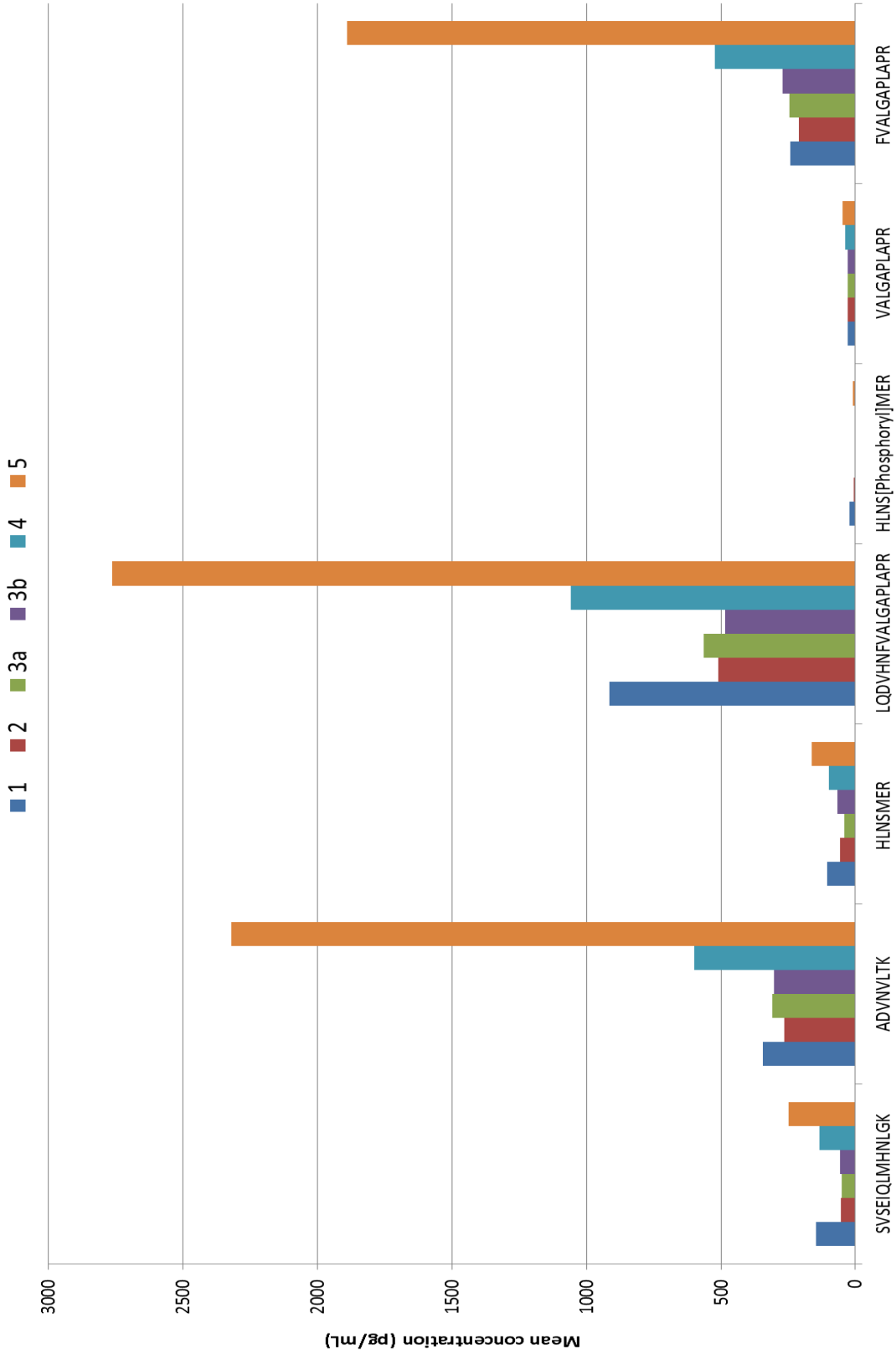

Figure 4.12. Mean concentrations (pg/mL) of PTH tryptic peptides and detected variant-specific tryptic peptides according to CKD stages.

Of the samples analysed, 91 samples had total serum 25-OHD results available. PTH concentrations as measured by (i) the second generation immunoassay and (ii) the PTH1-13 tryptic peptide were plotted against the total serum 25-OHD concentrations in these samples. The results are shown in Figure 4.13.

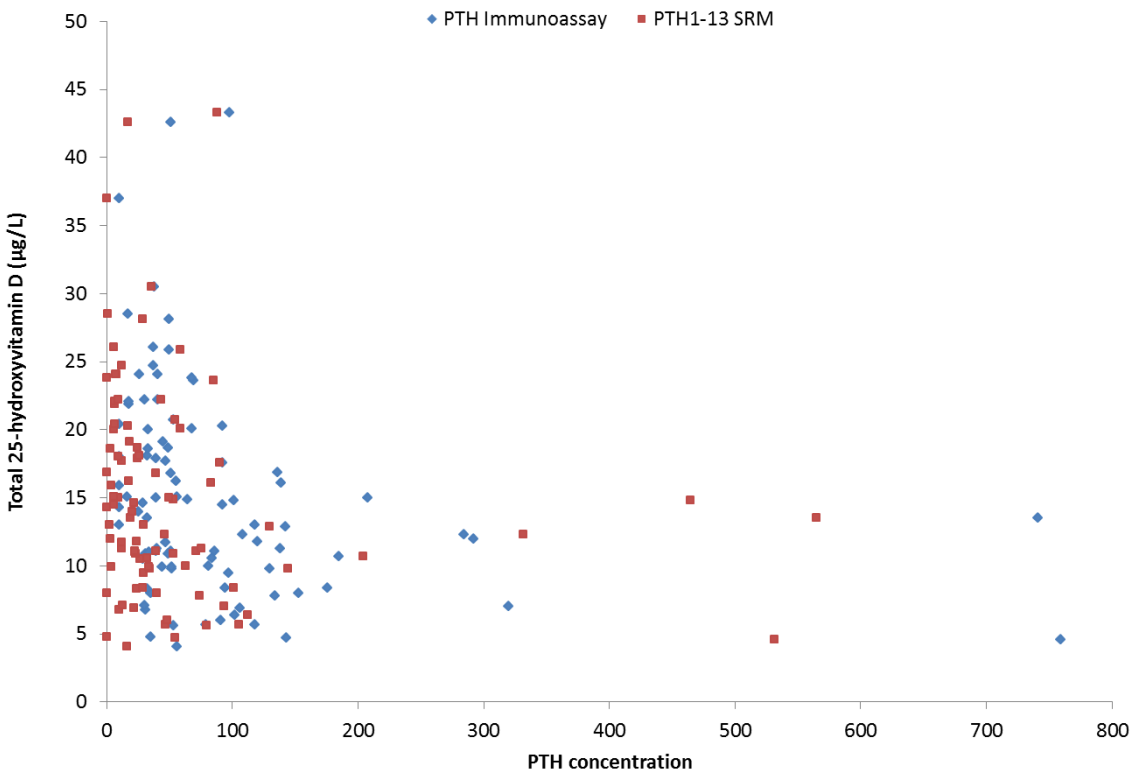

Figure 4.13. PTH concentrations using the second generation immunoassay (blue diamonds) and the PTH1-13 tryptic peptide assay (red squares) compared to total serum 25OHD concentration.

4.5.4. Top-down PTH1-84 analysis

Analysis of recombinant PTH1-84 without tryptic digestion produced a single, sharp chromatographic peak when analysed using a Dionex ProSwift™ RP-4H HPLC column (50 x 1 mm, 50 °C, Figure 4.14). However, interrogation of the mass spectra showed a wide charge state/isotopic distribution pattern, covering each possible charge state

between $[M+16H]^{16+}$ and $[M+7H]^{7+}$ (Figure 4.15). At physiological concentrations (10-100 pg/mL), the analyte signal was too 'diluted' across the charge states to allow detection. In an attempt to reduce the charge state spreading, recombinant PTH1-84 was injected onto the same HPLC column but with a 'supercharging' agent, nitrobenzoic acid (NBA), added to the elution buffers (0.1 %, *w/v*). There was no effect on the charge state distribution with the addition of NBA (Figure 4.16).

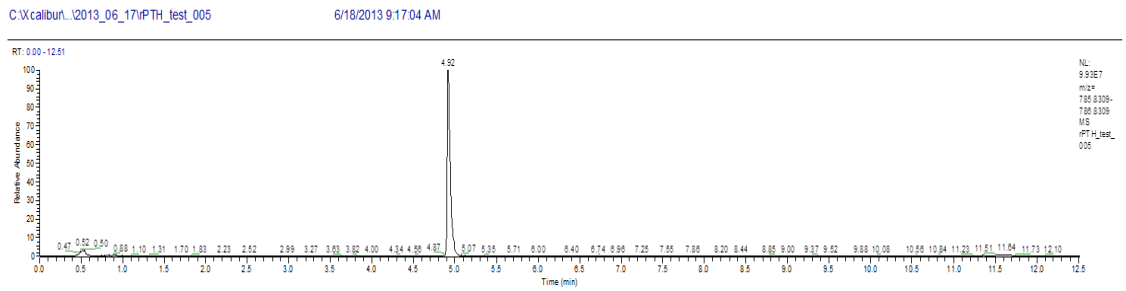

Figure 4.14. HPLC-MS chromatogram of recombinant PTH1-84.

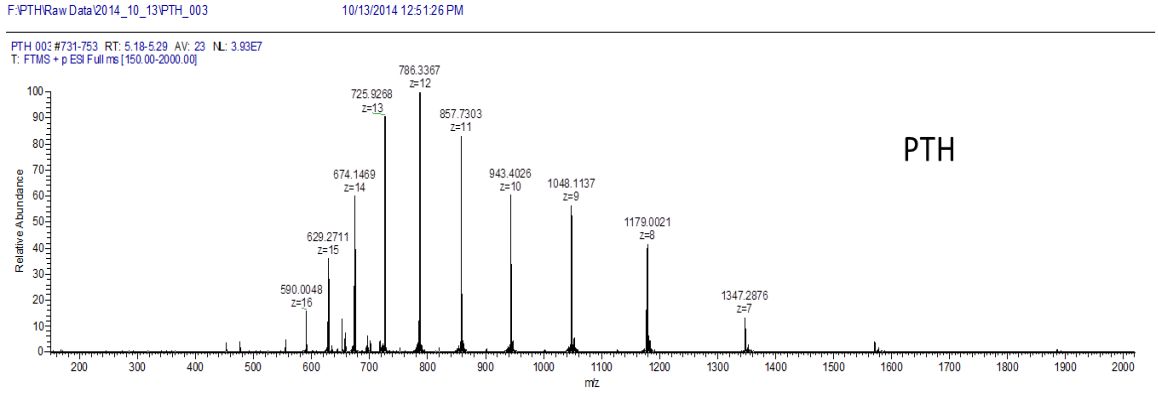

Figure 4.15. Charge state distribution of recombinant PTH1-84.

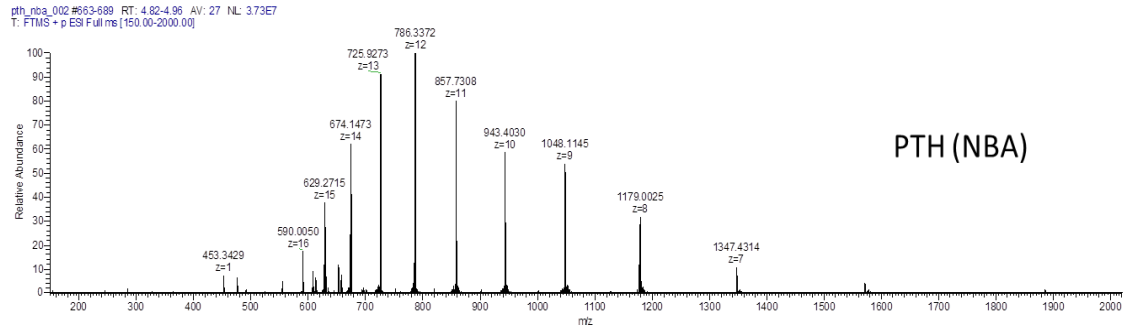

Figure 4.16. Charge state distribution of recombinant PTH1-84 in the presence of NBA.

4.6. Discussion

4.6.1. PTH fragments and variants – influences on assay development

Our understanding of the structure of circulating PTH fragments in normal individuals, and especially in patients with parathyroid pathology or renal impairment, has been aided by a number of developments in analytical technologies. These include (i) faster, simpler antibody production, (ii) more precise epitope mapping techniques, allowing for a more informed comparison of results between different immunoassays, (iii) the ability to synthesise custom recombinant peptides as controls or 'model' PTH fragments *in vitro*, (iv) peptide sequencing tools such as Edman degradation radio-sequencing (v) the improvement of chromatographic techniques and, more recently (vi) MS -based detection.

4.6.1.1. Second-generation immunoassays

It was the discovery of N-terminally truncated PTH fragments (e.g. PTH34-84) at high concentrations in patients with terminal renal failure, plus the knowledge that the biological activity of PTH1-84 resided within the N-terminal region, that led to the development and introduction of second-generation (or 'intact'), two-site immunoassays (Nussbaum *et al*., 1987; Blind *et al*., 1988). These intact PTH assays typically have a solid-phase capture antibody directed towards the C-terminal region of PTH (amino acids 39-84), and a detection antibody directed towards the N-terminus (Figure 4.17), usually towards amino acids 12-24, though a few second generation assays were developed with a detection antibody epitope directed towards the 26-32 region (D'Amour *et al*., 2003; D'Amour *et al*., 2005; D'Amour *et al*., 2005a). These assays were thought to be far more specific, since they avoided cross-reactivity with C-terminal PTH fragments. They were certainly an improvement upon the early single-antibody, mid-region, C-terminal RIAs as judged by correlation with clinical findings (Blind *et al*., 1988; Cohen-Salal *et al*., 1991). In this form, these assays were widely adopted by many clinical laboratories, reference ranges for different patient groups were developed, and indeed, they are still used by many to this day for routine PTH testing.

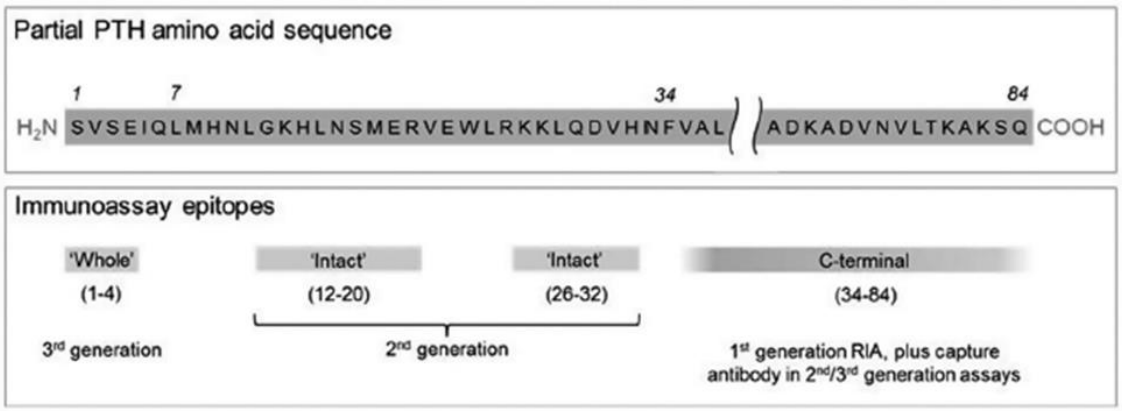

Figure 4.17. Antibody epitopes of first-generation RIAs, second generation ('intact') and third generation ('whole') PTH immunoassays.

4.6.1.2. Third-generation immunoassays

Based on findings from a parathyroid function study in 1993 (Brossard *et al*., 1993), Brossard *et al.* (1996) developed a chromatographic method to separate C-terminal PTH fragments from PTH1-84 prior to immunoassay analysis (second-generation). They reported that, in addition to the known C-terminal PTH fragments missing the entire N-terminus (e.g. PTH34-84), there existed a second group of larger C-terminal PTH fragments, with a partially-preserved N-terminus, which accumulated in renal failure. They later established that the fragmentation occurred somewhere within the first 19 amino acids of the PTH N-terminus, based on comparison of second-generation immunoassays with different detection antibody epitopes (D'Amour *et al*., 2005). These fragments were collectively described as 'non 1-84' PTH fragments, and were demonstrated to cross-react in second-generation immunoassays using recombinant PTH7-84, a commercially available peptide, as a surrogate for this group of peptides. In renal failure, the cross-reactivity of these non 1-84 fragments was shown to account for up to 60 % of total immunoreactive PTH, depending upon which immunoassay was used (Brossard *et al*., 1996; Lepage *et al*., 1998; D'Amour *et al*., 2003; D'Amour *et al*., 2005; D'Amour *et al*., 2005; D'Amour, 2006;). These observations supported clinical

findings that second-generation immunoassay results did not always correlate with other clinical and biochemical results (Quarles *et al*., 1992; Divieti *et al*., 2002).

This led to the development of third-generation ('whole PTH') assays (John *et al*., 1999; Gao *et al*., 2001), in which the detection antibody epitope was targeted further towards the N-terminus of PTH1-84, to amino acids 1-4, thus avoiding cross-reactivity with the newly observed large C-terminal PTH fragments (Figure 4.17). Despite the improved performance of these assays in some patient groups (Taniguchi *et al*., 2011), some anomalous results were still reported (Brossard *et al*., 2000; Lafferty *et al*., 2006; Hocher *et al*., 2012).

4.6.1.3. 'Amino' PTH

D'Amour and co-workers explored the exact structure of non 1-84 PTH fragments, using the array of second and third-generation immunoassays that were then available, plus Edman degradation radio-sequencing with PTH with ^{35}S-labelled methionine residues. Samples from healthy controls were compared with individual clinical samples and sample pools from patients with confirmed parathyroid pathology and/or renal failure. *Ex vivo* tissue samples from patients with confirmed primary and secondary hyperparathyroidism were also used to generate cell lines *in vitro.* Findings included first, that PTH7-84 was likely to be the most abundant form of the non 1-84 PTH cross-reacting in second-generation immunoassays; second, fragments corresponding to PTH4-84, PTH8-84, PTH10-84 and PTH15-84 were also present; and third, that another non 1-84 PTH fragment, over-expressed in severe hyperparathyroidism and parathyroid cancers, cross-reacted with third-generation but *not* second-generation immunoassays with a 12-20 epitope. It was suggested that this PTH variant (termed 'amino-PTH' in some references), which appears to have an intact N-terminus, may represent a modified variant form of PTH, with a modification in the 15-20 region. This would explain its lack of cross-reactivity with second generation immunoassays (D'Amour *et al*., 2005; Rubin *et al*., 2007).

The results of the MSIA-SRM method for the analysis of PTH tryptic peptides highlights the complexity of some clinical protein mass spectrometry assay when considering the use of tryptic peptides as surrogates for a mixture of circulating protein species. The first observation, that the average concentration of the four main tryptic peptides was significantly higher than the concentration of PTH1-13 (Figure 4.6), can be explained by considering the potential protein species from which each of the tryptic peptides can originate. For instance, if *all* the circulating PTH in a sample was PTH1-84, and assuming there were no variant forms or fragment peptides present, one would expect the concentrations of all four peptides to be equivalent. However, the presence of *any* truncated PTH variants or isoforms with an intact C-terminus would contribute to the measured concentration of the C-terminal tryptic peptides (i.e. the 'concentration' of the C-terminal peptide will be over-estimated in these samples). This was demonstrated by the higher measured concentrations of the PTH28-44 and PTH73-80 tryptic peptides (relative to the PTH1-13 and PTH14-20 peptides) in almost all samples, but especially in those samples from patients with the most severe renal impairment, in which the accumulation of PTH variants is likely to be greater.

The PTH1-13 tryptic peptide concentrations showed some correlation with the second generation PTH immunoassay results (R^2 = 0.7316, Figure 4.7), although there was significant sample-to-sample variability in the difference between the two assays. The PTH1-13 results were, on average, lower than the immunoassay results (slope of the scatter plot 0.5897, Figure 4.7). This suggested that the immunoassay was cross-reacting with at least some of the non-PTH1-84 variant forms present in these samples. For a few samples however, the immunoassay results were much lower than the PTH1-13 result. This could be explained by the presence of modified PTH species, which can be overestimated when using the PTH1-13 tryptic peptide method (see Section 4.5.3. below).

4.6.2. Truncated PTH isoforms

The SRM method used for this study was able to provide additional evidence for the presence and absence of some truncated PTH fragments. The PTH34-44 and PTH35-44 tryptic peptides were considered surrogate peptides for the presence of PTH34-84 and PTH35-84, respectively, and were detected in samples from this study, sometimes at high concentrations. These truncated forms have previously been observed in MALDI-TOF experiments (Zhang *et al*., 2006; Lopez *et al*., 2010).These tryptic peptides could, however, also arise from the presence of N- *and* C-terminally truncated peptides, such as PTH34-77 and PTH35-77, which were previously observed using MALDI-TOF experiments (Lopez *et al*., 2010). This small C-terminal truncation is difficult to detect using an SRM-based tryptic peptide approach, since the informative tryptic peptide for the presence/absence of this truncation (PTH73-77) would be only 5 amino acids in length.

The surrogate tryptic peptide for PTH7-84, the PTH7-13 peptide, was not detected in any of the samples analysed. This finding has since been replicated by other groups (Singh *et al*., 2015), and raises doubt over the existence of unmodified PTH7-84, which is widely cited in the literature as an interference in many PTH immunoassays. However, there are some limitations to the current SRM-based tryptic peptide method which must be considered, and could possibly provide some explanation to this observation (see Section 4.6.3 below).

4.6.3. Phosphorylated PTH

In vitro work using bovine and human PTH dating back to 1984 demonstrated that phosphorylation of serine residues in the PTH N-terminal region was possible (e.g. post-translational phosphorylation at serine 17), and indeed accounted for up to 20 % of the total PTH species present (Rabbani *et al*., 1984). Phosphorylated PTH14-20 was detected in a small percentage (17 %) of clinical samples in this study, and showed large variability with regards the relative proportion of the total PTH14-20. D'Amour *et al*. (2005) previously concluded that the phosphorylated PTH could be considered a potential interference in PTH immunoassays, but that further work was required to

demonstrate this. Given the phosphorylation site is that of the serine at position 17 in the PTH sequence (Figure 4.18), it could be possible that second generation immunoassays with a 12-20 amino acid epitope would not cross-react with phosphorylated PTH due to the presence of the phospho-group, but that third generation immunoassays with a more N-terminally directed epitope would be able to cross-react.Further work is still required to determine the biological activity, or the significance of circulating phosphorylated PTH variants. An immunoassay for the detection of phosphorylated PTH has also been developed (Zahradnik and Lavigne, 2011).

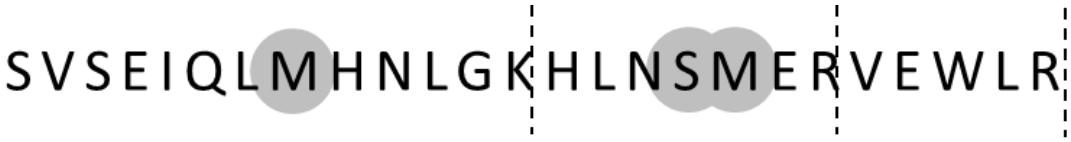

Figure 4.18. N-terminus of PTH (amino acids 1-25). Highlighted (grey circles) are the three amino acids which may be 'modified', either by phosphorylation (serine, position 17) or oxidation (methionine, positions 8 and 18). The dashed lines show the trypsin cleavage sites.

4.6.4. Study limitations and future work

4.6.4.1. Oxidised PTH

The discovery of the anabolic effects of PTH, and the subsequent use of recombinant PTH analogues as bio-therapeutic agents (e.g. teriparatide, recombinant PTH1-34) was an important development, and one which can be used to further our analytical ability to measure PTH variants in clinical samples. For these agents to be produced and licensed for use by regulatory authorities such as the US Food and Drug Administration (FDA), extensive purity and drug stability testing is required. Much research is carried out to investigate the use of solvents and other excipient formulations to stabilise protein-based drugs. A number of studies using MS on the stability of PTH1-34 formulations have therefore been carried out. In addition, analytical methods to identify and characterise degradation products, plus *in vitro* studies to assess their potential biological activity have also been developed. The N-terminus of PTH1-84 contains a number of residues prone to chemical degradation. Amongst other possible degradation products such as deamidation of asparagine (ASN, N) residues, methionine (MET, M) oxidation is likely to be the most prevalent. *In vitro* studies using high-resolution MS to identify oxidation products, following exposure of these compounds to peroxides, have demonstrated that the methionine residues at positions 8 and 18 of PTH1-34 and PTH1-84 can become oxidised (Hocher *et al*., 2012; Hocher *et al.*, 2013). Methionine 8 oxidises more slowly than methionine 18 (Chu *et al*., 2004), and both methionine residues can be singly or doubly oxidised (to sulfoxides and sulfones, respectively). It is also well-established that all oxidised PTH variants are less biologically active than non-oxidised PTH (Tashjian *et al*., 1964; Galceran *et al*., 1984; Horiuchi, 1988; Zull *et al*., 1990). With these findings considered in the context of clinical PTH measurement, Hocher *et al*. (2012; Hocher *et al.*, 2013) raised a monoclonal antibody against oxidised PTH, and immobilised this antibody in microcolumns. High-resolution MS was used to demonstrate the efficiency of the antibody prior to use. These affinity columns were then used to remove oxidised PTH in clinical samples from haemodialysis patients prior to analysis of non-oxidised PTH species using immunoassay (second-generation, Roche PTH assay). It was

demonstrated that a large, yet highly variable, proportion (> 90 % in some cases) of the total PTH in these samples was present in an oxidised form.

Whilst the assay performance data (e.g. precision and accuracy, calibration linearity) looked encouraging for PTH1-13 in this study, the assay may be subject to interferences in real clinical samples. As discussed, modified PTH1-84 and potentially modified PTH fragments have been observed in clinical samples, with phosphorylation at serine-17 and oxidation at methionine-8 and methionine-18. When using LC-MS/MS, and monitoring the PTH1-13 peptide as the surrogate for PTH1-84 using SRM, the concentration of PTH1-13 is actually a *total* of at least three species: PTH1-84, oxidised PTH1-84 (at methionine-18) and phosphorylated PTH1-84 (as serine-17), since the site of modification is after the tryptic cleavage site. There is thus no way in which to distinguish between these variants. In the same way, our failure to detect PTH7-84 in patient samples may be explained by modification by oxidation at methionine-8, so that it was 'missed' when using SRMs towards the non-oxidised PTH7-13 tryptic peptide. Further work is necessary to evaluate this.

Alternative proteases could be another option for the analysis of PTH in a bottom-up approach. In this study, trypsin was the only protease used. The issues relating to non-selectivity with trypsin digestion result primarily from fragmentation at the lysine residue at position 13. One possible protease which may be useful is Arg-C, which hydrolyses peptides at the C-terminal side of arginine residues and so, in theory, would produce a PTH1-20 peptide – this peptide would then include within the sequence both the sites of oxidation and phosphorylation. However, even sequencing grade Arg-C has been shown to possess some tryptic activity (i.e. hydrolysis at lysine residues), and so for absolute quantitation this still may not provide an ideal solution (Mitchell and Harrington, 1968).

4.6.4.2. Alternative peptide quantitation approaches

The MSIA-SRM assay described has some limitations, but also some potential benefits over alternative approaches for bottom-up peptide quantitation using immunoaffinity. In the described approach, isotopically-labelled peptides were used as internal

reference standards for the quantitation of each of the tryptic peptides. However, this may not be considered ideal, as the internal reference standards do not account for variability in (i) the MSIA enrichment or (ii) the trypsin digestion step of the workflow. For the PTH assay in particular, there are some features which may reduce these potential issues. Firstly, the digestion process takes place following the enrichment step, meaning the trypsin has only to digest the target protein and related variants, as opposed to adding trypsin to whole, or immunodepleted, serum. Secondly, PTH is a linear peptide, with little tertiary or quaternary structure likely to cause steric hindrance of the tryptic cleavage sites.

An alternative approach to overcoming these potential issues would be the use of isotope-labelled PTH1-84, as was described by Kumar *et al.* (2010). This standard was added to the samples prior to enrichment and digestion, and accounted for these steps to some extent. Aside from the additional time and expense of having a fully-labelled protein synthesised and purified, there are still some assumptions made when using this technique for quantitative protein analysis – firstly, that the isotope-labelled protein shows affinity for the enrichment antibody, and secondly that the digestion process is equivalent.

Another alternative approach which is widely used in the field of biomarker validation and verification is that of 'stable isotope standards and capture by anti-peptide antibodies', or SISCAPA (Anderson *et al*., 2004). This differs from the MSIA-SRM approach since the antibody capture takes place at the peptide level – proteins are digested with a protease (typically trypsin), and antibodies raised against target peptide(s) and corresponding isotope-labelled peptides added to each sample at a known concentration (i.e. for PTH1-13, an anti-SVSEIQLMHNLGK antibody would be used). Both approaches are automatable using modern liquid handling systems, though the SISCAPA approach requires one to raise anti-peptide antibodies. For this study, the MSIA approach was preferable as a number of tryptic peptides could be investigated using a single anti-PTH antibody, without the need for a large series of anti-peptide antibodies.

4.6.4.3. Sensitivity for top-down PTH analysis

The analysis of PTH without prior digestion is one solution to the described limitations of an SRM approach. Indeed, the acquisition of high-resolution, full-scan MS data may also be valuable since these data can be interrogated retrospectively for the presence of other fragments or modified PTH variants. The preliminary data from this Chapter, plus reports from other groups using a similar approach (Zhang *et al*., 2006), suggest that whilst PTH1-84 itself can be analysed 'intact', it accumulates multiple charges during the ionisation process in the MS source, with multiple isotopes at each charge state. Attempts to reduce the signal spreading have so far proved unsuccessful. With the sensitivity of currently available MS instrumentation, the only foreseeable way to overcome the sensitivity issues would be to either (i) use nano-flow LC separation and/or (ii) to concentrate analytes from much larger sample volumes prior to analysis – both approaches which are not ideally suited to routine clinical chemistry analysis, but may be useful for research purposes or, indeed, a reference method for the standardisation of existing PTH immunoassays.

4.6.5. Conclusions

Despite its clinical importance, it is clear that the analysis of PTH for clinical diagnostics and patient management is highly complex. Whilst the development of three generations of immunoassays have been key to our improved understanding of the biology of PTH and PTH fragments, there remains an obvious need for the harmonisation of PTH testing between laboratories. Further work is also required to better understand the exact structures of the PTH species that can be observed in different clinical settings. MS methods will be critical for the future development of this work – permitting unambiguous identification of PTH forms based on their mass-to-charge ratio and fragmentation characteristics, as opposed to inferring the structure of PTH fragments by differential antibody cross-reactivity.

A traceable reference methodology for PTH1-84 is still needed to harmonise PTH testing and reduce the variability which currently limits clinical application of this assay. Current PTH testing inadequacies are of grave concern for patients with renal

failure, with potential influences on patient misclassification, inappropriate treatment outcomes and patient management (Sturgeon *et al*., 2011). The establishment of the IFCC working group is an important step towards this goal, as are the analytical developments discussed in this chapter. Absolute quantitation of peptides and proteins by mass spectrometric techniques is still a relatively new field, and no consensus currently exists regarding the most reliable, robust approach for these types of analysis. The vast experience gained by using antibody-based capture and detection systems in the last fifty years will remain important, as immunoaffinity techniques used to capture, enrich and even remove interfering PTH fragments, coupled to mass spectrometric detection, could be the most useful tool in the future development of reference methods. It has been demonstrated that some PTH fragments show biological activity, and in fact that some C-terminal fragments show antagonistic calcaemic activity to PTH1-84 and PTH1-34 through a different receptor system. With this considered, future assay developments should not only aim to exclude these fragments as interferences in the measurement of true PTH1-84, but also include the independent quantitation of these fragments in different patient groups.

Chapter Five

Investigation of the use of turbulent flow chromatography for the analysis of tryptic digests

5.1. Background

In recent years, interest in the measurement of clinically-relevant proteins and peptides using liquid chromatography-mass spectrometry (LC-MS) has gained momentum. Proteomics is still largely restricted to the research environment, but the specificity and sensitivity provided by MS, and hence the ability to identify protein isoforms and variants, is an attractive prospect for translation to the clinical laboratory. The IFCC has convened a working group dedicated to clinical quantitative mass spectrometry proteomics (Lehmann *et al*., 2013). Furthermore, those more accustomed to LC-MS for targetted small-molecule workflows can now develop quantitative protein assays owing to the number of protein quantitation strategies possible, the availability of stable isotope-labelled proteins and peptides (Lange *et al.*, 2008; Picotti & Aebersold, 2012), and the accessibility of vast on-line protein/peptide databases/spectral libraries (Deutsch *et al.*, 2008).

Whilst analysis of 'intact' proteins/peptides is possible, and arguably preferable for some target proteins (e.g. insulin – Peterman *et al*., 2014), for many others a digestion step using a suitable protease (typically trypsin) is required prior to mass spectrometric analysis of surrogate proteotypic peptides (Lehmann *et al.*, 2013; Lange *et al*., 2008; Picotti & Aebersold, 2012). The digestion step in such workflows can be carried out either directly on the biological matrix itself, or following some form of sample clean-up (e.g. removal of high-abundance proteins or immunoenrichment) prior to digestion of remaining proteins/peptides.

Post-digestion sample 'clean-up' typically uses SPE techniques. This reduces the complexity of the digested matrix, as well as helping to remove residual denaturants and reduction/alkylation reagents prior to injection onto the analytical HPLC column. These procedures are often carried out 'off-line' using either 96-well plate-based SPE systems, or with modified pipette-tips containing silica beds (Rappsilber *et al*., 2007; van den Broek *et al*., 2010) and is primarily based on reversed-phase interactions with C18-modified phases. Some groups have also used mixed-mode cation exchange systems or two-dimensional SPE approaches for specific target peptides (Capelo *et al*., 2009).

5.2. Aims

TFC is a rapid, on-line sample clean-up technique that has been applied in the field of quantitative small-molecule analysis for many years (Couchman, 2012), and was used in Chapter Two for the analysis of 25-OHD. As discussed, this approach uses high eluent flow-rates, and narrow columns packed with large (>50 µm), irregularly-shaped particles to induce turbulent flow. This allows separation of large biomolecules from smaller analytes of interest by way of a 'pseudo-size-exclusion' mechanism, which results from the fact that larger molecules diffuse more slowly in solution than small molecules, and so do not have sufficient time within the turbulent flow column to enter the particle pores and interact with the stationary phase chemistry. In this study, the performance of TFC for the automated, on-line analysis of tryptic digests was investigated, using an aqueous solution of bovine serum albumin (BSA) as a model protein.

5.3. Materials and methods

Ammonium bicarbonate, urea, DTT (as solid), IAA, calcium chloride, tris(hydroxymethyl)aminomethane (*Trizma*®, 99.9 %), bovine serum albumin (BSA), TCPK-treated trypsin (from bovine pancreas) and LC-MS grade acetonitrile were all purchased from Sigma-Aldrich (Poole, UK). MS grade formic acid and trifluoroacetic acid (TFA) were from Fluka (Poole,UK). Ammonia solution (>25 %), isopropanol, acetone and glacial acetic acid were from VWR (all AnalaR grade, Lutterworth, UK). Water was de-ionised (>12 mΩ, Purite, Thame, UK). A 1 mol/L aqueous stock solution of DTT was prepared and stored in portions at -20 °C. Reducing solution (8 mol/L urea, 300 mmol/L tris, and 10 mmol/L DTT in 2.5 % (*v/v*) isopropanol in deionised water) was prepared immediately prior to digestion. IAA solution (200 mmol/L in 100 mmol/L aqueous ammonium bicarbonate) was prepared and stored in the dark in amber glass vials at 2-8 °C. Dilution buffer (50 mmol/L tris and 5 mmol/L calcium chloride, aqeuous) was prepared and stored at 2-8 °C. The required volume of trypsin solution (0.5 µg/µL in aqueous 25 mmol/L acetic acid) was prepared immediately prior to digestion. For this study, an aqueous solution was prepared containing 50 g/L BSA.

5.3.1. Instrumentation and conditions

An Aria Transcend™ TLX-II system (ThermoFisher Scientific, San Jose, USA) consisting of four Accela™ 1250 high pressure quaternary pumps, VIM, and CTC PAL autosampler was used with a Q Exactive™ high-resolution mass spectrometer (ThermoFisher Scientific, Bremen, Germany). The autosampler tray was maintained at 10 °C. Instrument control was performed using XCalibur™ software (version 2.2, ThermoFisher Scientific). System eluents were as follows: (Loading Pump Eluent A) 0.1 % (*v/v*) formic acid and 0.05 % (*v/v*) TFA in deionised water, (Eluting Pump Eluent A) 0.1 % (*v/v*) formic acid in deionised water, (Loading/Eluting Pump Eluents B) 0.1 % (*v/v*) formic acid in acetonitrile, (Loading Pump Eluent C) 1+2+2 (*v/v/v*) acetone, acetonitrile and isopropanol ('Magic Mix'), and (Loading Pump Eluent D) 2 % (*v/v*) ammonia solution in deionised water.

Prepared sample digests (50 µL) were injected onto the TurboFlow™ columns (Cyclone MCX-2 and C18-XL connected in series, each 50 x 0.5 mm i.d.) under turbulent flow (1.5 mL/min). Retained peptides were subsequently eluted from the TurboFlow column using elution solvent (100 µL, 2+3 (*v/v*) Loading Pump Eluent B:Loading Pump Eluent D, stored in a holding loop), and focussed through a tee-piece onto the analytical HPLC column (Figure 5.1). Peptides were separated using a Zorbax™ Eclipse XDB-C18 HPLC column (Agilent Technologies, 1.8 µm average particle size, 50 x 4.6 mm i.d.) maintained at 50 °C. During gradient elution (total flow-rate 300 µL/min) of the analytes from the analytical HPLC column, the TurboFlow column was washed with Loading Pump Eluent B, followed by Loading Pump Eluent C, and the elution solvent loop re-filled for the subsequent injection. The whole system was then re-equilibrated prior to the next injection. The gradient elution and valve-switching profile is summarised in Table 5.1. Total analysis time was 15 minutes. Eluent flow was diverted to waste for the first and final two minutes of each analysis, with MS/MS data only acquired for 12 minutes.

Detection was carried out in positive ionisation mode using heated electrospray (H-ESI) ionisation (spray voltage 4.5 kV; temperatures: vaporiser 200 ºC; capillary 320 ºC; auxiliary, sheath, and sweep gases 50, 5 and 0 (arbitrary units) respectively, S-lens voltage 100 V). Data were acquired in full-scan mode (70,000 resolution, range *m/z*

300–1,500, maximum injection time 200 ms, AGC target 3 x $10e^6$). For this study, no fragmentation (MS^2) data were acquired.

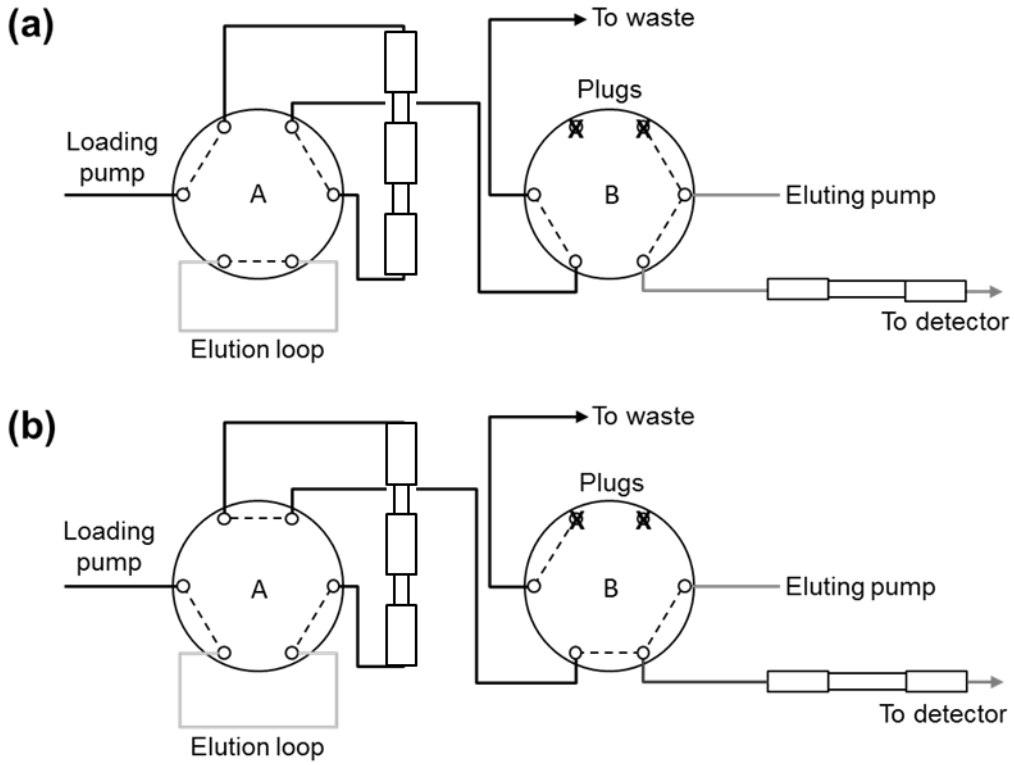

Figure 5.1. TurboFlow valve arrangement for the direct analysis of tryptic digests. Shown are (a) the valve positions during the loading and re-equilibration steps, during which the elution loop and tee-piece are both excluded from the flow path, and (b) the transfer/focussing step, during which both valves switch, and the elution loop is used to transfer retained peptides, via dilution through the tee-piece, onto the head of the analytical column.

5.3.2. Digestion procedure

Digestion was carried out in 2 mL Lo-Bind tubes (Eppendorf, Stevenage, UK). Freshly prepared reducing solution (60 µL) was added to BSA solution (50 g/L, 20 µL) and the tube then capped and incubated at 37 °C for 1 h. The tube was centrifuged briefly (10,000 rpm, 30 s) to remove condensation from the tube cap, and allowed to cool to room temperature. IAA solution (10 µL) was then added, the tube re-capped, and the mixture incubated at room temperature in the dark for 30 min. The mixture was diluted with dilution buffer (350 µL) and vortex mixed (5 s) to reduce the urea concentration prior to digestion. Freshly prepared trypsin solution was then added (trypsin:BSA ratio 1:12.5), and the tubes were re-capped and vortex mixed (5 s), and incubated (37 °C, 4 h). Digestion was quenched by the addition of formic acid (6 µL), and digests were diluted (1+3, *v/v*) with Loading Pump Eluent A in 2 mL glass autosampler vials prior to analysis.

5.3.3. Peptide targetting and data processing/analysis

Eighteen BSA tryptic peptides were identified following *in silico* digestion (trypsin, assuming no missed cleavages) of the amino acid sequence imported sequence from Uniprot (www.uniprot.org, entry [position] P02769 [25-607]), accessed 03/06/2015) using PinPoint^{TM} software (version 1.3, ThemoFisher Scientific). For this study, peptides containing cysteine residues, and those less than 7 amino acids in length were excluded (Table 5.2).

For all data processing and calculation of recovery, full scan data were filtered (± 5 ppm exclusion window) for the *m/z* values of interest for each tryptic peptide (cumulative peak are for the top 3 most intense isotopes for the most abundant charge state). No chromatographic smoothing was performed prior to peak integration. Recovery (%) for each peptide was calculated by comparison of the mean integrated peak areas (N = 10 injections of each) of direct laminar flow (LX) and turbulent flow (TX) injections of BSA digests.

		Loading pump (MCX2/C18 XL)							Eluting pump (XDB-C18)		
Step	**Time (sec)**	**Flow rate (mL/min)**	**%A**	**%B**	**%C**	**%D**	**Tee**	**Loop**	**Flow rate (mL/min)**	**%A**	**%B**
1	30	1.50	100	-	-	-	Out	Out	0.30	98	2
2	40	0.10	100	-	-	-	In	In	0.90	98	2
3	500	0.50	-	100	-	-	Out	In	0.30	40	60
4	1	0.50	-	-	100	-	Out	Out	0.30	-	100
5	60	0.50	-	-	100	-	Out	Out	0.40	-	100
6	1	0.50	-	-	100	-	Out	Out	0.40	98	2
7	60	1.00	-	40	-	60	Out	In	0.40	98	2
8	80	1.00	100	-	-	-	Out	Out	0.40	98	2
9	40	1.50	100	-	-	-	Out	Out	0.30	98	2

Table 5.1. Summary of the gradient elution and TurboFlow valve switching method.System eluents were as follows: (Loading Pump Eluent A) 0.1 % (*v/v*) formic acid and 0.05 % (*v/v*) TFA in deionised water, (Eluting Pump Eluent A) 0.1 % (*v/v*) formic acid in deionised water, (Loading/Eluting Pump Eluents B) 0.1 % (*v/v*) formic acid in acetonitrile, (Loading Pump Eluent C) 1+2+2 (*v/v/v*) acetone, acetonitrile and isopropanol ('Magic Mix'), and (Loading Pump Eluent D) 2 % (*v/v*) ammonia solution in deionised water.

	Peptide sequence	Predicted *m/z* (3 most intense isotopes from the most abundant charge state)	Krokhin hydrophobicity factor	Sequence location
1	ATEEQLK	409.7163, 410.2178, 410.7191	6.14	538-544
2	VLASSAR	352.2085, 352.7099, 353.2111	7.47	188-194
3	DDSPDLPK	443.7113, 444.2127, 444.7140	15.56	107-114
4	DLGEEHFK	487.7325, 488.2340, 488.7353	15.92	13-20
5	LVTDLTK	395.2395, 395.7409, 396.2422	17.82	233-239
6	AEFVEVTK	461.7477, 462.2491, 462.7505	22.22	225-232
7	HLVDEPQNLIK	653.3617, 653.8631, 654.3645	22.27	378-388
8	LVVSTQTALA	501.7951, 502.2966, 502.7979	25.47	574-583
9	YLYEIAR	464.2504, 464.7518, 465.2532	28.22	137-143
10	HPEYAVSVLLR	642.3589, 642.8604, 643.3618	29.97	337-347
11	VPQVSTPTLVEVSR	756.4250, 756.9265, 757.4278	30.00	414-427
12	LVNETEFAK	582.3190, 582.8204, 583.3218	31.99	42-51
13	QTALVELLK	507.8133, 508.3148, 508.8161	35.35	525-533
14	LGEYGFQNALIVR	740.4014, 740.9028, 741.4042	38.67	397-409
15	HPYFYAPELLYYANK	630.3138, 630.6481, 630.9824	40.20	145-159
16	DAIPENLPPLTADFAEDK	978.4835, 978.9849, 979.4863	43.27	295-312
17	TVMENFVAFVDK	700.3499, 700.8514, 701.3522	45.10	545-556
18	DAFLGSFLYEYSR	784.3750, 784.8765, 785.3779	50.58	323-335

Table 5.2. The 18 tryptic BSA peptides used for the evaluation of TurboFlow analysis, along with their calculated hydrophobicity factor. Peptides fewer than 7 amino acids on length, and those containing cysteine residues were excluded.

5.4. Results

Example total ion current (TIC) chromatograms and extracted ion chromatograms for representative peptides (LX and TX injections) are shown in Figure 5.2. There was excellent correlation (R^2 = 0.9686) between the observed peptide retention times on the analytical column with the Krokhin hydrophobicity factors (Krohkin & Spicer, 2009) calculated within Pinpoint software (Figure 5.3).

Repeat injection of prepared BSA digests (N = 10) showed excellent peak area reproducibility for both LX (% RSD for all peptides 1.4-6.9 %) and TX (1.0-5.9 %) injections (Table 5.3). The peptide VLASSAR was not observed in any chromatogram (LX or TX injections) following the 4 hour digestion protocol described.

Aside from the most hydrophilic peptide, ATEEQLK (hydrophobicity factor 6.14), TurboFlow recovery was greater than 30 % for all peptides, and was greater than 50 % for 12 of the 18 peptides studied (Table 5.3). There was a broad correlation (R^2 = 0.5254) between the hydrophobicity factor and the observed recovery (Figure 5.4).

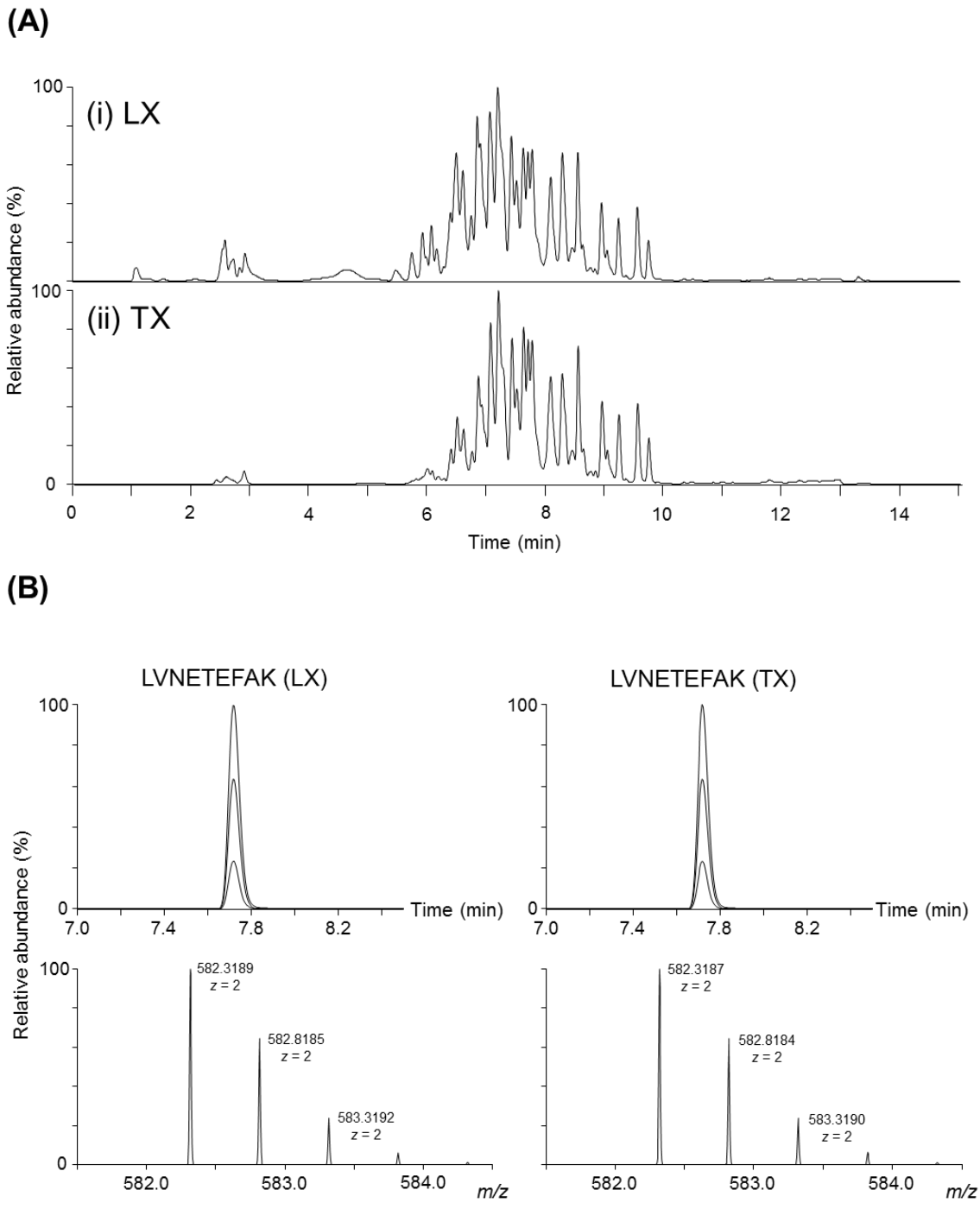

Figure 5.2. (A) Example total ion chromatograms for (i) LX and (ii) TX injections of BSA digests. (B) Extracted ion chromatograms (± 5 ppm) and averaged mass spectra for LX and TX injections of BSA digest showing the peptide LVNETEFAK. Shown separately are the three most abundant isotopes for the most abundant charge state (2+; 582.3189, 582.8204, 583.3218). Chromatograms are scaled relative to the largest peak (582.3189 *m/z*).

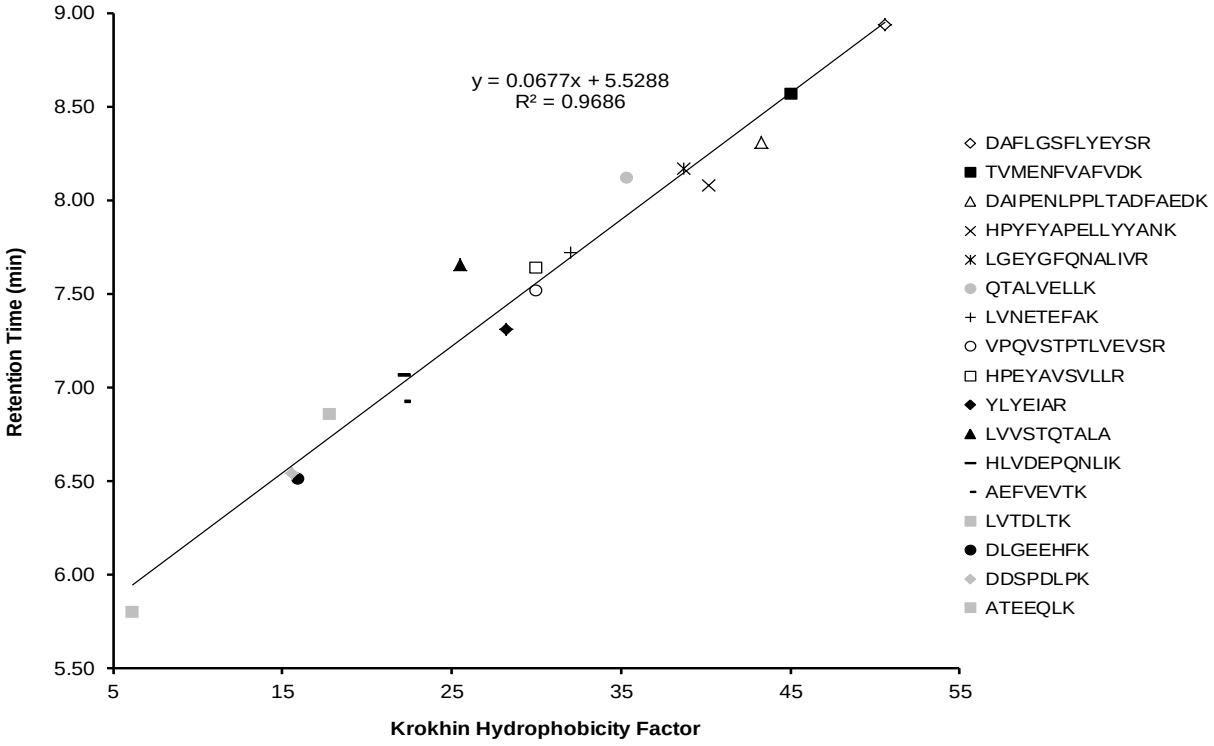

Figure 5.3. Observed chromatographic retention time (min) compared to the calculated hydrophobicity factor (from Pinpoint software) for the 17 BSA peptides.

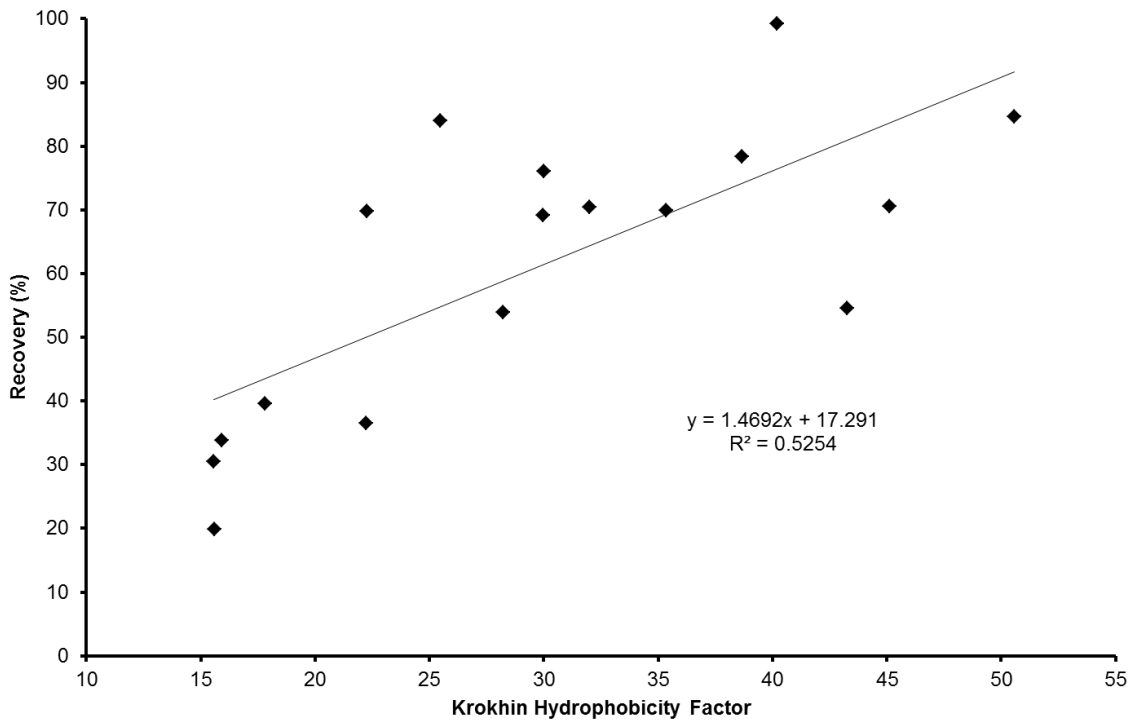

Figure 5.4. Correlation between the calculated hydrophobicity factor for the 17 BSA peptides and the TurboFlow recovery (% mean peak area, TX vs LX injections).

	Peptide sequence	Retention time (min)	Krokhin hydrophobicity factor	Precision (%RSD, N = 10), LX	Precision (%RSD, N = 10), TX	Recovery (%)
1	ATEEQLK	5.80	6.14	6.24	2.30	15.3
2	VLASSAR	-	(7.47)	-	-	-
3	DDSPDLPK	6.54	15.56	3.85	4.50	30.5
4	DLGEEHFK	6.51	15.92	1.63	4.99	27.7
5	LVTDLTK	6.86	17.82	3.11	2.77	39.5
6	AEFVEVTK	6.93	22.22	3.15	3.51	36.5
7	HLVDEPQNLIK	7.07	22.27	2.22	1.44	69.8
8	LVVSTQTALA	7.66	25.47	2.76	5.56	84.0
9	YLYEIAR	7.31	28.22	1.70	2.36	53.9
10	HPEYAVSVLLR	7.64	29.97	2.20	2.36	69.1
11	VPQVSTPTLVEVSR	7.52	30.00	2.25	1.03	76.0
12	LVNETEFAK	7.72	31.99	1.76	1.86	70.5
13	QTALVELLK	8.12	35.35	1.43	1.88	69.9
14	LGEYGFQNALIVR	8.17	38.67	1.56	2.81	78.3
15	HPYFYAPELLYYANK	8.08	40.20	6.85	5.51	99.2
16	DAIPENLPPLTADFAEDK	8.31	43.27	3.10	5.85	54.5
17	TVMENFVAFVDK	8.57	45.10	1.79	2.91	70.5
18	DAFLGSFLYEYSR	8.94	50.58	5.85	4.88	84.6

Table 5.3. Summary TurboFlow recovery data for selected BSA tryptic peptides.

5.5. Discussion

Although a preliminary study based on a single model protein, these data suggest that TFC may be useful for the on-line analysis of tryptic digests, and thus could be well-suited to high-throughput, targetted, peptide-based protein analyses. Compared to off-line SPE techniques, this approach is rapid and fully-automated with regards to the valve-switching set-up. Even when compared against methods where tryptic digests are analysed directly by LC-MS with no additional sample pre-treatment, since the TFC separation process occurs very rapidly (within 20-30 s) following injection, there is very little impact on the total analysis time. Furthermore, the physics of turbulent flow chromatography mean that non-digested, high molecular weight proteins and peptides, as well as excess trypsin and salts from the digestion protocol, are excluded from interaction with column particles. As such, these components do not reach the analytical HPLC column, serving to increase column lifetime, and reduce the frequency of MS ion-source maintenance – both important considerations in high-throughput laboratories. TFA is not favoured by some for MS analysis due to the risk of ion suppression effects (Annesley, 2003), despite the chromatographic benefits that can be gained for hydrophilic peptide analysis in particular. In the method described, TFA was used to maximise recovery on the TurboFlow columns, but was not transferred to the analytical HPLC column or to the MS source guarding against the possibility of ensuing ion suppression effects.

Using the focus-mode plumbing arrangement (Figure 5.1), the elution loop contents were diluted (1+9, *v/v*) prior to the analytical HPLC column, such that the retained peptides were focussed at the head of the analytical column prior to gradient elution. This focussing meant that no evaporation/reconstitution steps were employed, thus avoiding the risk of loss of some peptides during these steps.

In this study using a single protein and with the chosen combination of TurboFlow column chemistries, good recovery was observed for a number of the tryptic peptides (Table 5.3). Recovery for the more hydrophilic BSA peptides was greater using the two TurboFlow columns in series than for each of the columns individually, suggesting that both cation-exchange and hydrophobic/hydrophilic interactions were contributing to peptide recovery (similar to mixed-mode SPE methods). As one would predict, the

relative recovery of the more hydrophobic peptides was greater than for the hydrophilic peptides. Recovery of the most hydrophilic peptide, ATEEQLK, was relatively poor (15 %), but nonetheless showed good injection-to-injection peak area precision. One of the 18 peptides in this study (VLASSAR) was not observed. This was not considered to be due to poor recovery on the TurboFlow column, since this peptide was not observed in LX injections. It is more likely that this peptide was either not produced, or was unstable or modified during the digestion protocol.

In cases where a number of possible tryptic peptides can be used, the choice of which surrogate peptide(s) to use for quantitative protein analysis remains important (Holman *et al.*, 2012), and the use of stable isotope-labelled internal standards is always advocated where possible. Owing to the inevitable differences in peptide recovery (as observed in this study, but also equally likely with SPE-based methods), the use of isotope-labelled standards for *each* of the targetted tryptic peptides should be recommended, and recovery studies carried out during method validation to ensure similarity between the labelled and unlabelled peptides. However, as with SPE workflows, TurboFlow methods can be optimised to ensure maximal recovery of the target peptide for analyses which require a *specific* tryptic peptide to be quantified (e.g. in the quantitation of protein isoforms and variants). Examples could include manipulation of the Loading Eluent pH, variation in the TFA concentration, and optimisation of the elution loop contents.For instance, the recovery of more hydrophobic peptides may be increased by increasing the organic solvent content in the elution loop. It should be noted that this may affect the chromatographic peak shape of more hydrophilic peptides as there may be less analyte focussing during the transfer step, and so often a compromise must be reached in cases where multiple peptides with different retention characteristics are to be simultaneously analysed.

Overall, the data from this study suggest that turbulent flow chromatography offers a rapid, on-line alternative to SPE for the analysis of peptide digests by LC-MS. A wide range of TurboFlow column chemistries are available, and so the technique can be further customised for analyses which are targetted to specific peptides. As with turbulent flow chromatography for small-molecule workflows (Couchman, 2012), this

approach may be ideally suited to high-throughput protein-based applications, such as those which are emerging in clinical laboratories.

Chapter Six

Studies on the analysis of vitamin D binding proteins using LC-MS and LC-MS/MS

6.1. Background

The concept of measuring binding proteins as a useful adjunct to the measurement of total circulating hormone concentrations is not especially novel. The use of this approach in the analysis of testosterone, for example, is widely cited in the literature (Vermeulen, 2004). The underlying principle is that the majority of the testosterone circulates extensively bound to plasma proteins, and that only a small proportion (1-2 %) is 'free', and thus available to enter cells and/or interact with androgen receptors and have biological effect. In the case of testosterone, approximately one quarter to one half (25-50 %) of the total serum testosterone is bound to a specific plasma protein (sex hormone binding globulin, SHBG), and most of the remaining fraction is weakly bound to albumin (50-75 %). The total of the free testosterone and the final (non-specifically bound) fraction, which is weakly bound to albumin, is often referred to as the 'bioavailable' fraction. It therefore follows that, in cases where there are variations in either SHBG and/or albumin concentrations (e.g. due to obesity, dysthyreosis, and ageing), the measurement of total testosterone in isolation may not be the best biomarker for androgen status (Vermeulen, 2004).

Direct measurement of the free and/or bioavailable testosterone concentrations are cumbersome, and rely on equilibrium dialysis or ammonium sulphate precipitation methods, which are time-consuming, and not easily automated for high-throughput, routine applications. The free androgen index (FAI) is a useful alternative, and can be calculated using Equation 6.1. with simpler analytical measurements of the SHBG concentration and total serum testosterone (e.g. both by fully-automated immunoassay systems or, for total testosterone, by LC-MS/MS). There are some limitations to the use of the FAI, related to (i) method-dependent variability in the measurements of both the total testosterone and the SHBG and (ii) the fact that the FAI equation does not involve measurement of albumin. Nonetheless, the FAI remains a useful tool in the routine clinical evaluation of androgen status (Vermeulen, 2004).

Equation 6.1. Calculation of the free androgen index (FAI - Vermeulen, 2004).

$$FAI = 100\ x \frac{Total\ testosterone}{SHBG}$$

6.1.1. Vitamin D binding protein (VDBP) and VDBP isoforms

Vitamin D binding protein (VDBP; also referred to as vitamin D binding globulin, group specific component, or Gc globulin) is a multi-functional, three-domain protein which, along with alpha-fetoprotein, belongs to the albumin gene family (Cooke & David, 1985; Yang *et al*., 1985; Schoentgen *et al*., 1985; Schoentgen *et al*., 1986). It is coded for by the Gc gene, located on chromosome 4 (4q11-q13, HUGO Gene Nomenclature Committee, HGNC). Although over 80 variants of human VDBP have been identified, there are three major genetic isoforms of serum VDBP in humans: Gc-2, Gc-1f and Gc-1s (Svasti *et al*., 1979; Braun *et al*., 1992; Christiansen *et al*., 2007), which result from non-synonymous single-nucleotide polymorphisms (SNPs, reference SNP numbers rs7041 and rs4588) of the Gc gene. These two SNPs give rise to missense mutations (Figure 6.1) which according to the universal genetic code (Table 6.1) result in amino acid substitutions at positions 416 and 420 in the VDBP peptide sequence. For the rs7041 SNP, the rs7041-T allele (GAU codon) codes for an aspartic acid residue, and the rs7041-G allele (GAG codon) codes for a glutamic acid residue. For the rs4588 SNP, the rs4588-C allele (ACG codon) codes for a threonine residue, and the rs4588-A allele (AAG codon) codes for a lysine residue.

Wild-type mRNA	*5′*	**GCU**	**GAA**	**CGG**	**CAA**	**GAU**	**GGA**	**CCA**	*3′*
Wild-type peptide	*N*	Ala	Glu	Arg	Gln	Asp	Gly	Pro	*C*
Silent mutation	*5′*	**GCU**	**GA*G***	**CGG**	**CAA**	**GAU**	**GGA**	**CCA**	*3′*
	N	Ala	Glu	Arg	Gln	Asp	Gly	Pro	*C*
Missense mutation	*5′*	**GCU**	**GAA**	**CGG**	**CA*C***	**GAU**	**GGA**	**CCA**	*3′*
	N	Ala	Glu	Arg	*His*	Asp	Gly	Pro	*C*
Nonsense mutation	*5′*	**GCU**	**GAA**	**CGG**	***U*AA**				*3′*
	N	Ala	Glu	Arg	*STOP*				*C*

Figure 6.1. Example SNP mutations (substitutions). Substitutions relative to the wild-type mRNA and peptide sequences are underlined and italicised.

First base	Second base									Third base
	U			*C*		*A*		*G*		
U	**UUU**	Phe	**UCU**	Ser	**UAU**	Tyr	**UGU**	Cys	*U*	
	UUC	Phe	**UCC**	Ser	**UAC**	Tyr	**UGC**	Cys	*C*	
	UUA	Leu	**UCA**	Ser	**UAA**	STOP	**UGA**	STOP	*A*	
	UUG	Leu	**UGC**	Ser	**UAG**	STOP	**UGG**	Trp	*G*	
C	**CUU**	Leu	**CCU**	Pro	**CAU**	His	**CGU**	Arg	*U*	
	CUC	Leu	**CCC**	Pro	**CAC**	His	**CGC**	Arg	*C*	
	CUA	Leu	**CCA**	Pro	**CAA**	Gln	**CGA**	Arg	*A*	
	CUG	Leu	**CCG**	Pro	**CAG**	Gln	**CGG**	Arg	*G*	
A	**AUU**	Ile	**ACU**	Thr	**AAU**	Asn	**AGU**	Ser	*U*	
	AUC	Ile	**ACC**	Thr	**AAC**	Asn	**AGC**	Ser	*C*	
	AUA	Ile	**ACA**	Thr	**AAA**	Lys	**AGA**	Arg	*A*	
	AUG	Met/ START	**ACG**[b]	Thr	**AAG**[b]	Lys	**AGG**	Arg	*G*	
G	**GUU**	Val	**GCU**	Ala	**GAU**[a]	Asp	**GGU**	Gly	*U*	
	GUC	Val	**GCC**	Ala	**GAC**	Asp	**GGC**	Gly	*C*	
	GUA	Val	**GCA**	Ala	**GAA**	Glu	**GGA**	Gly	*A*	
	GUG	Val	**GCG**	Ala	**GAG**[a]	Glu	**GGG**	Gly	*G*	

[a]Codons for the rs7041 SNP; [b]codons for the rs4588 SNP

Table 6.1. The universal genetic code. Messenger RNA codons are shown in bold font, along with the corresponding amino acids for which they code. The codons which are altered in the SNPs relevant to VDBP isoforms are also indicated.

6.1.1.1. Protein variant forms

The two SNPs in the Gc gene give rise to missense mutations which code for different protein isoforms. A summary of the VDBP haplotypes and diplotypes is shown in Figure 6.2. Note that the rs7041-G/rs4588-A haplotype displays strong linkage disequilibrium (LD) and is therefore extremely rarely observed in humans (Malik *et al.*, 2013).

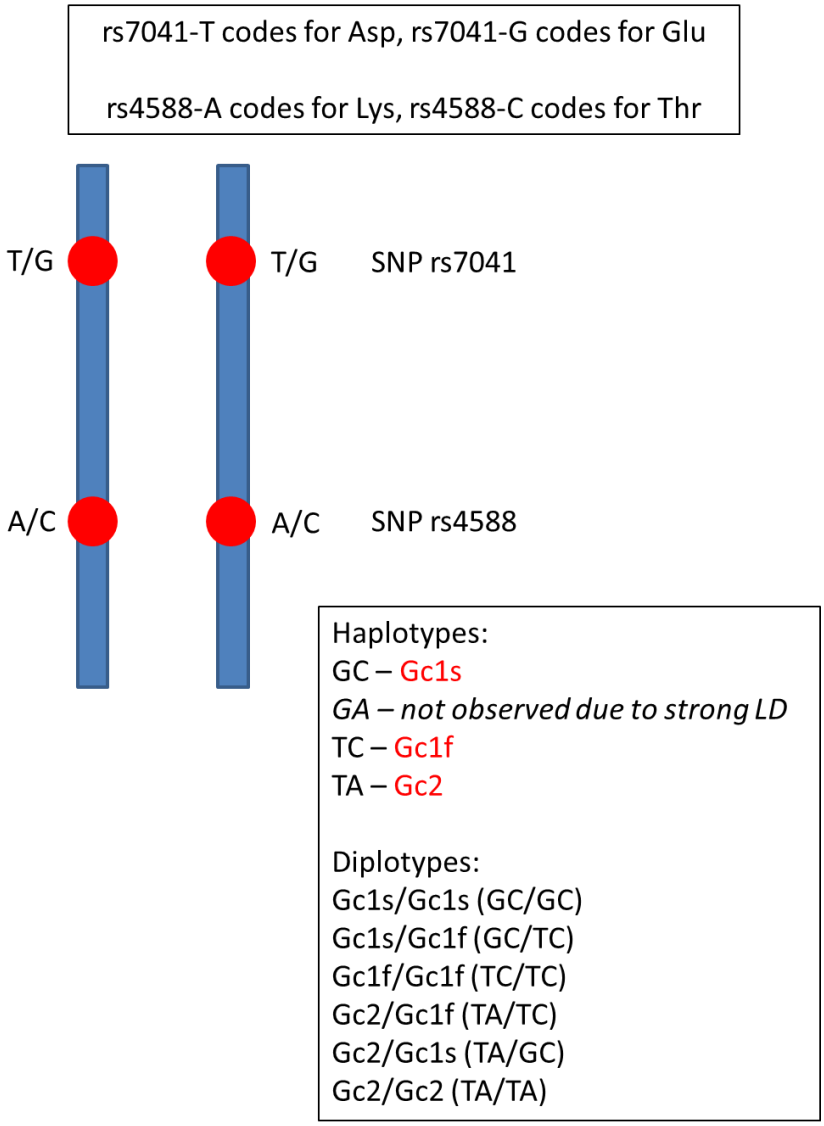

Figure 6.2. VDBP isoforms. Summary of haplotypes and diplotypes resulting from rs7041 and rs4588 SNPs.

Glycosylation (via an O-linked trisaccharide) of two of the three VDBP isoforms (Gc-1s and Gc-1f) has been reported (Ravnsborg *et al*., 2010). The glycosylation has been mapped to the threonine at amino acid position 420, and this is the reason the glycosylation cannot occur in the GC-2 isoform, since the rs4588 SNP codes for a lysine substitution in this isoform. However, the use of ion exchange chromatography and MS to characterise the VDBP isoforms has revealed that the majority of VDBP isoforms were non-glycosylated, and only a minor proportion of the VDBP molecules are in the glycosylated form (Christiansen *et al*., 2007).

The relevance of VDBP isoforms to vitamin D status has received much literature attention recently. It has been demonstrated that the configurational differences of the three major isoforms (and hence an individuals' VDBP diplotype) affect the VDBP substrate binding affinity (Chun *et al*., 2014; Braithwaite *et al*., 2015). It is suggested that the Gc-1f isoform shows the highest avidity for vitamin D metabolites, and the Gc-2 isoform the lowest (Arnaud *et al*., 1993; Bouillon *et al*., 1980). It has also been shown using immunometric techniques that the different VDBP isoforms also differ in abundance (Lauridsen *et al*., 2001). As with the data for substrate affinity, in this study it was demonstrated that serum Gc-2 concentrations are the lowest, and Gc-1f concentrations are the highest. However, it was noted by the authors that the assay used to quantify the total VDBP assumes equivalent antigenicity and affinity for the anti-VDBP antibodies used for of each of the VDBP isoforms.

The allele frequencies of the three major VDBP isoforms are also strongly linked to geographical distribution. The Gc-1f allele frequency is markedly lower in Caucasian populations than in black American and black African populations. Caucasians have a significantly higher Gc-2 allele frequency (Speeckaert *et al*., 2006).

In 2013, Powe and co-workers reported data from a large cohort of black and white community-dwelling American adults, in whom VDBP was measured and vitamin D status (as 'bioavailable vitamin D') was assessed by calculation (Powe *et al*., 2013). The key findings of this study were (i) that black Americans had lower 25-OHD than white

Americans, but (ii) that the black Americans also had lower concentrations of VDBP, thus giving rise to equivalent 'bioavailable vitamin D' concentrations. The authors attributed this latter finding to the fact that the black population had a significantly higher incidence of the Gc-1f isoform, which in the immunoassay used for VDBP (a monoclonal sandwich assay from R&D Systems, Minneapolis, MN) gave the lowest concentrations. It should be noted that this is contrary to the findings of the earlier study by Lauridsen *et al*. (2001), in which a polyclonal nephelometric immunoassay was used.

6.1.2. Analysis of VDBP

6.1.2.1. Quantitation of VDBP by immunoassay

The serum concentrations of VDBP are relatively high, and the majority of methods for VDBP measurement have been using immunochemical methods, ranging from radioimmunoassay, turbidimetry and nephelometry to more modern ELISA-based platforms. The available ELISA-based methods for total VDBP may be based on monoclonal or polyclonal antibodies (Speeckaert *et al.*, 2006). The discrepancy between the results of the Powe *et al*. study and the Lauridsen *et al*. study may be attributed to the choice of antibody which can have a seemingly large influence on the measured VDBP concentration in different ethnic populations, due to the different allele frequencies for the major isoforms. In a more recent study, Jemielita *et al*. (2016) carried out analysis of VDBP using two ELISA-based methods, one matching that of the Powe et al. study, and the other a polyclonal ELISA (ALPCO Diagnostics, Salem, NH). The results of the two assays were significantly different. Whilst use of the monoclonal ELISA allowed the authors to replicate the findings of the Powe *et al*. study (i.e. that black participants had much lower VDBP concentrations than white participants), the polyclonal ELISA showed that VDBP concentrations were actually significantly *higher* in black females, and with no significant difference in males. There was no correlation between the results of the two assays. In a reponse to this article, it has been suggested that differences between the two immunoassays with regards antibody cross-reactivity to different protein isoforms could, in part, explain the discrepant results (Hollis & Bickle, 2014).

6.1.2.2. Identification of VDBP phenotype

VDBP SNP genotyping may be carried out in a few different ways. Firstly, both the Gc gene SNPs have commercially available TaqMan™ assays (Life Technologies, ThermoFisher Scientific), and so analysis of samples through both of these assays will give the haplotype. Alternatively, since the different VDBP isoforms have different isoelectric points, they can be identified by isoelectric focussing (Lauridsen *et al*., 2001).

6.2. Aims

This Chapter aims to investigate the development of an LC-MS/MS assay for the measurement of 'total' VDBP, including the possibility of simultaneous identification of the three major VDBP isoforms and thus assigning VDBP diplotype in human serum. The method decribed will use in-solution tryptic digestion of whole serum samples. Following digestion to generate multiple proteotypic peptides, some of these peptides will be used for qualitative identification of isoforms and some for use as surrogate peptides for protein quantitation.

6.3. Materials and methods

Ammonium bicarbonate, urea, DTT (as solid), IAA, calcium chloride, tris(hydroxymethyl)aminomethane (*Trizma*®, 99.9 %), BSA, TCPK-treated trypsin (from bovine pancreas) and LC-MS grade acetonitrile were all purchased from Sigma-Aldrich (Poole, UK). MS grade formic acid and trifluoroacetic acid (TFA) were from Fluka (Poole, UK). Ammonia solution (>25 %), isopropanol, acetone and glacial acetic acid were from VWR (all AnalaR grade, Lutterworth, UK). Water was de-ionised (>12 mΩ, Purite, Thame, UK). For the traditional in-solution tryptic digest, a 1 mol/L aqueous stock solution of DTT was prepared and stored in portions at -20 °C. Reducing solution (8 mol/L urea, 300 mmol/L tris, and 10 mmol/L DTT in 2.5 % (*v/v*) isopropanol in deionised water) was prepared immediately prior to digestion. IAA solution (200 mmol/L in 100 mmol/L aqueous ammonium bicarbonate) was prepared and stored in the dark in amber glass vials at 2-8 °C. Dilution buffer (50 mmol/L tris and 5 mmol/L calcium chloride, aqeuous) was prepared and stored at 2-8 °C. The required volume of trypsin solution (0.5 µg/µL in aqueous 25 mmol/L acetic acid) was prepared immediately prior to digestion.

For the rapid in-solution tryptic digestion, SMARTDigest™ kits including immobilised, heat-treated trypsin pre-aliquoted into 200 µL PCR reaction tubes, and SMARTDigest buffer solution, were from ThermoFisher Scientific (Runcorn, UK). All isotope-labelled peptides were custom-synthesised (AQUA™ grade, ThermoFisher Scientific). Pooled human VDBP (as lyophilised powder, purified to ≥90 % by SDS-PAGE) was from Sigma Aldrich (Poole, UK).

6.3.1. Instrumentation and conditions

Aria Transcend™ TLX-II systems (ThermoFisher Scientific, San Jose, USA) consisting of Accela™ quaternary pumps, VIM, and CTC PAL autosampler were used with either a Q Exactive™ high-resolution mass spectrometer (ThermoFisher Scientific, Bremen, Germany), or a TSQ Vantage™ triple quadrupole mass spectrometer (ThermoFisher Scientific, San Jose, CA). Autosampler trays were maintained at 10 °C. Instrument control was performed using XCalibur™ software (version 2.2, ThermoFisher

Scientific). System eluents were as follows: (Loading Pump Eluent A) 0.1 % (*v/v*) formic acid and 0.05 % (*v/v*) TFA in deionised water, (Eluting Pump Eluent A) 0.1 % (*v/v*) formic acid in deionised water, (Loading/Eluting Pump Eluents B) 0.1 % (*v/v*) formic acid in acetonitrile, (Loading Pump Eluent C) 1+2+2 (*v/v/v*) acetone, acetonitrile and isopropanol ('Magic Mix'), and (Loading Pump Eluent D) 2 % (*v/v*) ammonia solution in deionised water.

For the standard in-solution digestion, prepared sample digests (50 µL) were injected onto the TurboFlow™ columns (Cyclone MCX-2 and C18-XL connected in series, each 50 x 0.5 mm i.d.) under turbulent flow (1.5 mL/min). Retained peptides were subsequently eluted from the TurboFlow column using elution solvent (100 µL, 2+3 (*v/v*) Loading Pump Eluent B:Loading Pump Eluent D, stored in a holding loop), and focussed through a tee-piece onto the analytical HPLC column. Peptides were separated using a Zorbax™ Eclipse XDB-C18 HPLC column (Agilent Technologies, 1.8 µm average particle size, 50 x 4.6 mm i.d.) maintained at 50 °C. During gradient elution (total flow-rate 300 µL/min) of the analytes from the analytical HPLC column, the TurboFlow column was washed with Loading Pump Eluent B, followed by Loading Pump Eluent C, and the elution solvent loop re-filled for the subsequent injection. The whole system was then re-equilibrated prior to the next injection. Total analysis time was 15 minutes. Eluent flow was diverted to waste for the first and final two minutes of each analysis, with MS data only acquired for 12 minutes.

For the SMARTDigest method, the TFC system was bypassed, and digests were directly injected on the Zorbax™ Eclipse XDB-C18 HPLC column (Agilent Technologies, 1.8 µm average particle size, 50 x 4.6 mm i.d.). Detection for both the Q Exactive and TSQ Vantage methods was carried out in positive ionisation mode using heated electrospray (H-ESI) ionisation (spray voltage 4.5 kV; temperatures: vaporiser 200 ºC; capillary 320 ºC; auxiliary, sheath, and sweep gases 50, 5 and 0 (arbitrary units) respectively, S-lens voltage 100 V).

6.3.2. Tryptic digestion procedure

Traditional tryptic digestion was carried out in 2 mL Lo-Bind tubes (Eppendorf, Stevenage, UK). Freshly prepared reducing solution (60 µL) was added to samples (20

µL) and the tubes were then capped and incubated at 37 °C for 1 h. The tube was centrifuged briefly (10,000 rpm, 30 s) to remove condensation from the tube cap, and allowed to cool to room temperature. IAA solution (10 µL) was then added, the tube re-capped, and the mixture incubated at room temperature in the dark for 30 min. The mixture was diluted with dilution buffer (350 µL) and vortex mixed (5 s) to reduce the urea concentration prior to digestion. Freshly prepared trypsin solution was then added (trypsin:BSA ratio 1:12.5), and the tubes were re-capped and vortex mixed (5 s), and incubated (37 °C, 4 h). Digestion was quenched by the addition of formic acid (6 µL), and digests were diluted (1+3, *v/v*) with Loading Pump Eluent A in 2 mL glass autosampler vials prior to analysis.

For the SMARTDigest method, samples (20 µL) were diluted with SMARTDigest buffer solution (180 µL) in Lo-Bind tubes, and vortex mixed (10 s). The diluted samples were transferred to SMARTDigest tubes containing the immobilised trypsin buffer, the tubes were capped and thoroughly mixed by inversion. Following incubation, the tubes were centrifuged (13,000 rpm, 5 min), and the supernatents were diluted with Eluent A in 2 mL glass autosampler vials prior to analysis.

6.3.3. Samples

Anonymised samples previously analysed for a range of bone biochemical markers including the analysis of VDBP and identification of VDBP genotype by Taqman assays were transferred from the University of Sheffield to King's College Hospital under a Materials Transfer Agreement.

6.4. Results

6.4.1. Identification of VDBP tryptic peptides

6.4.1.1. Isoform-specific VDBP peptides

The full amino acid sequences for each of the three VDBP isoforms were obtained from Uniprot (www.uniprot.org – Uniprot ID P02774, VTDB_HUMAN), and are shown in Figure 6.3. *In silico* tryptic digestion of the three protein sequences yielded three variant-specific tryptic peptides. For the Gc-2 isoform, the substitution of threonine for lysine at position 420 of the amino acid sequence (rs4588 SNP) introduced an additional trypsin cleavage site, and thus a shorter, 7-amino acid, Gc-2-specific tryptic peptide, LPDATPK. The two Gc-1 isoforms which both have a threonine at position 420 produce 11-amino acid peptides, which differ at position 416 due to the rs7041 SNP, thus giving rise to two further variant-specific peptides – LPDATPTELAK for the Gc-1f isoform, and LPEATPTELAK for the Gc-1s isoform. VDBP phenotyping based on the presence/absence of tryptic peptides can therefore be summarised as shown in Table 6.2. The isoform-specific peptides are not suitable for quantitation of the VDBP, especially since the Gc-1 isoforms are also subject to some degree of glycosylation (Christiansen *et al*., 2007; Ravnsborg *et al*., 2010), and so would not be observed using an SRM-based assay for the non-glycosylated form. Instead, SRM transitions for these three peptides were only used to identify VDBP diplotype.

Gc-2

LERGRDYEKNKVCKEFSHLGKEDFTSLSLVLYSRKFPSGTFEQVSQLVKEVVSLTEACCAEGADPDCYDTRTSAL
SAKSCESNSPFPVHPGTAECCTKEGLERKLCMAALKHQPQEFPTYVEPTNDEICEAFRKDPKEYANQFMWEYS
TNYGQAPLSLLVSYTKSYLSMVGSCCTSASPTVCFLKERLQLKHLSLLTTLSNRVCSQYAAYGEKKSRLSNLIKLA
QKVPTADLEDVLPLAEDITNILSKCCESASEDCMAKELPEHTVKLCDNLSTKNSKFEDCCQEKTAMDVFVCTYF
MPAAQLPELPDVELPTNKDVCDPGNTKVMDKYTFELSRRTHLPEVFLSKVLEPTLKSLGECCDVEDSTTCFNAK
GPLLKKELSSFIDKGQELCADYSENTFTEYKKKLAERLKAKLPDATPKELAKLVNKRSDFASNCCSINSPPLYCDSEI
DAELKNIL

Gc-1f

LERGRDYEKNKVCKEFSHLGKEDFTSLSLVLYSRKFPSGTFEQVSQLVKEVVSLTEACCAEGADPDCYDTRTSAL
SAKSCESNSPFPVHPGTAECCTKEGLERKLCMAALKHQPQEFPTYVEPTNDEICEAFRKDPKEYANQFMWEYS
TNYGQAPLSLLVSYTKSYLSMVGSCCTSASPTVCFLKERLQLKHLSLLTTLSNRVCSQYAAYGEKKSRLSNLIKLA
QKVPTADLEDVLPLAEDITNILSKCCESASEDCMAKELPEHTVKLCDNLSTKNSKFEDCCQEKTAMDVFVCTYF
MPAAQLPELPDVELPTNKDVCDPGNTKVMDKYTFELSRRTHLPEVFLSKVLEPTLKSLGECCDVEDSTTCFNAK
GPLLKKELSSFIDKGQELCADYSENTFTEYKKKLAERLKAKLPDATPTELAKLVNKRSDFASNCCSINSPPLYCDSEI
DAELKNIL

Gc-1s

LERGRDYEKNKVCKEFSHLGKEDFTSLSLVLYSRKFPSGTFEQVSQLVKEVVSLTEACCAEGADPDCYDTRTSAL
SAKSCESNSPFPVHPGTAECCTKEGLERKLCMAALKHQPQEFPTYVEPTNDEICEAFRKDPKEYANQFMWEYS
TNYGQAPLSLLVSYTKSYLSMVGSCCTSASPTVCFLKERLQLKHLSLLTTLSNRVCSQYAAYGEKKSRLSNLIKLA
QKVPTADLEDVLPLAEDITNILSKCCESASEDCMAKELPEHTVKLCDNLSTKNSKFEDCCQEKTAMDVFVCTYF
MPAAQLPELPDVELPTNKDVCDPGNTKVMDKYTFELSRRTHLPEVFLSKVLEPTLKSLGECCDVEDSTTCFNAK
GPLLKKELSSFIDKGQELCADYSENTFTEYKKKLAERLKAKLPEATPTELAKLVNKRSDFASNCCSINSPPLYCDSEI
DAELKNIL

Figure 6.3. Amino acid sequences for the Gc-2, Gc-1f and Gc-1s isoforms of VDBP. Highlighted are the three isoform-specific tryptic peptides. The Gc-2 isoform produces a 7-amino acid tryptic peptide due to the substitution of an additional lysine residue, whereas the two Gc-1 isoforms produce 11-amino acids peptides which differ in position 3 (or position 416 of the total protein sequence) by the substitution of an aspartic acid residue (Gc-1f) for a glutamic acid (Gc-1s).

SNP	Genotype	Haplotype	Isoform	Peptide
rs7041	T	TA	Gc-2	LPDATPK
	G	TC	GC-1f	LPDATPTELAK
rs4588	A	GA	N/A	-
	C	GC	Gc-1s	LPEATPTELAK

Diplotype	Peptide(s) present
Gc-2/Gc-2	LPDATPK
Gc-2/Gc-1s	LPDATPK, LPEATPTELAK
Gc-2/Gc-1f	LPDATPK, LPDATPTELAK
Gc-1f/Gc-1s	LPDATPTELAK, LPEATPTELAK
Gc-1s/Gc-1s	LPEATPTELAK
Gc-1f/Gc-1f	LPDATPTELAK

Table 6.2. Possible haplotype combinations of the two Gc gene SNPs (rs7041 and rs4588), the corresponding VDBP isoforms, and the resulting tryptic peptide(s) which are present in samples from homozygous and heterozygous individuals.

6.4.1.2. Non-specific VDBP peptides

The full list of candidate VDBP tryptic peptides, excluding those fewer than 6-amino acids or greater than 20-amino acids in length, and excluding the three isoform-specific peptides, is shown in Table 6.3. From this initial list of 20 candidate peptides, 9 were excluded due to them containing cysteine residues. There were no proteins found with common tryptic peptides following a BLAST search via Uniprot. Human serum albumin showed 24 % sequence similarity, but no common peptides. Following reduction, alkylation and overnight tryptic digestion as described above, the FPSGTFEQVSQLVK peptide showed no observable peak in full-scan MS following digestion of the pooled VDBP reference material and was also excluded. All other peptides gave acceptable signal in full-scan mode, and showed good mass accuracy against predicted *m/z* values. Also of note, at nominal mass resolution, the precursor ion *m/z* of the THLPEVFLSK peptide was isobaric with the LPEATPTELAK variant-specific peptide. The peptides YTFELSR and VLEPTLK were chosen as representative non-variant-specific peptides. Extracted ion chromatograms (from full-scan MS data on the Q Exactive) and MS^2 product ion spectra are shown for these two peptides and their isotope-labelled analogues in Figure 6.4. The transitions used for SRM analysis of the five peptides are summarised in Table 6.4.

Candidate peptides	
EFSHLGK	ELPEHTVK
EDFTSLSLVLYSR	*LCDNLSTK*
FPSGTFEQVSQLVK	*FEDCCQEK*
TSALSAK	*DVCDPGNTK*
SCESNSPFPVHPGTAECCTK	YTFELSR
LCMAALK	THLPEVFLSK
HLSLLTTLSNR	VLEPTLK
VCSQYAAYGEK	*SLGECCDVEDSTTCFNAK*
LSNLIKLAQK	ELSSFIDK
CCESASEDCMAK	*GQELCADYSENTFTEYK*

Table 6.3. Candidate tryptic VDBP peptides following *in silico* digestion, and exclusion of peptides with fewer than 6 amino acids or greater than 20 amino acids. Those peptides containing cysteine residues (shown in italics) were subsequently excluded.

Peptide	Precursor Ion *m/z* $[M+2H]^{2+}$	Product Ion *m/z*
LPDATPK	371	527.297 635.334
LPDATPTELAK	578	439.713 639.456
LPEATPTELAK	585	435.202 522.234
VLEPTLK	400	445.210 532.242
VLEPTLK*	404	553.345 681.404
YTFELSR	458	563.353 686.890
YTFELSR*	463	361.244 574.355

Table 6.4. Summary SRM transitions for variant-specific and non-variant-specific VDBP peptides. Asterisks indicate isotope-labelled residues.

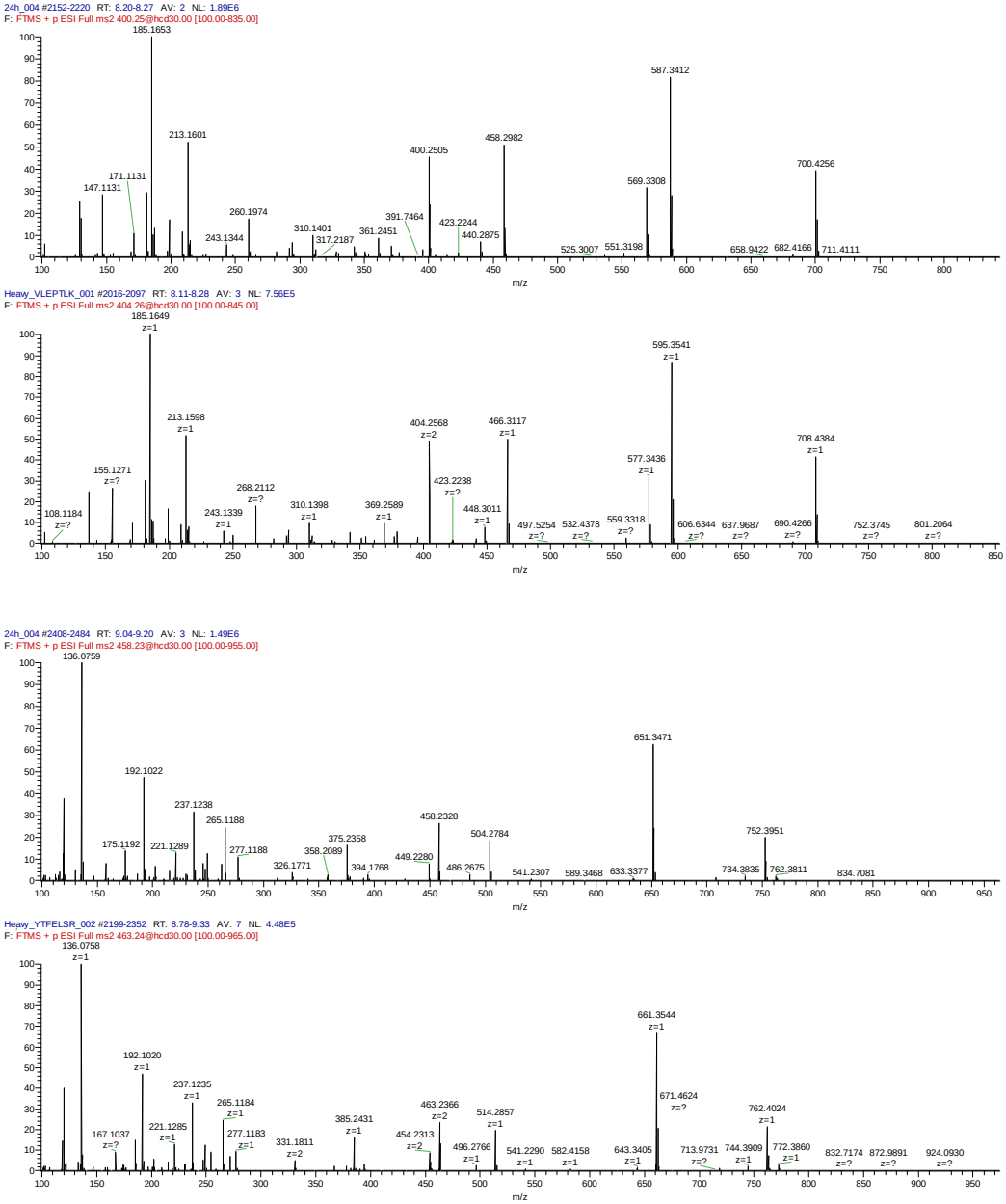

Figure 6.4. Data-dependent MS^2 product ion scans (NCE = 35) of VLEPTLK, YTFELSR and their corresponding isotope-labelled peptides. Spectra shown are the averaged spectra taken across chromatographic peaks for each peptide. For both target peptides, the isotope-labelled peptides co-eluted.

6.4.2. Tryptic digestion

6.4.2.1. Traditional in-solution digest

For the five chosen peptides, the trypsin digestion time-course was investigated using standard in-solution digestion of a VDBP calibrator (500 mg/L) as described. Mean (duplicate analysis of two digestion reactions) extracted peak areas (from full-scan MS data using the Q Exactive) were taken (i) in the absence of trypsin, (ii) immediately following addition of the trypsin, and (iii) with the digestion reactions quenched at 1, 2, 4, 22, and 24 hours. For all five peptides, no peak was detected in the absence of trypsin, and each of the peptides were detectable immediately after trypsin digestion (0 hours). The digestion time profiles are shown in Figure 6.5.

It has previously been reported for the qualitative analysis of variant-specific tryptic peptides for haemoglobin variants that trypsin digestion can be carried out without prior reduction and alkylation in cases where the peptides of interest do not require alkylation (Daniel *et al*., 2005), and where the quaternary protein structure allows the trypsin access to the cleavage sites. Direct addition of trypsin to the pooled VDBP revealed that this was not possible for the digestion of these proteins (Figure 6.6).

6.4.2.2. SMARTDigest

A similar experiment was carried out for the digestion of the VDBP calibrator using the SMARTDigest protocol. The quenching of the SMARTDigest method occurs after centrifugation and dilution of the buffer. Reactions were stopped, and relative peak areas for each of the five peptides assessed at 5, 15, 30, 45, 60, 90, 120 and 240 minutes. The SMARTDigest time profiles are shown in Figure 6.7. Comparative chromatograms highlighting the remaining non-digested protein content from SMARTDigest reactions quenched at 5 and 240 minutes, respectively, are shown in Figure 6.8.

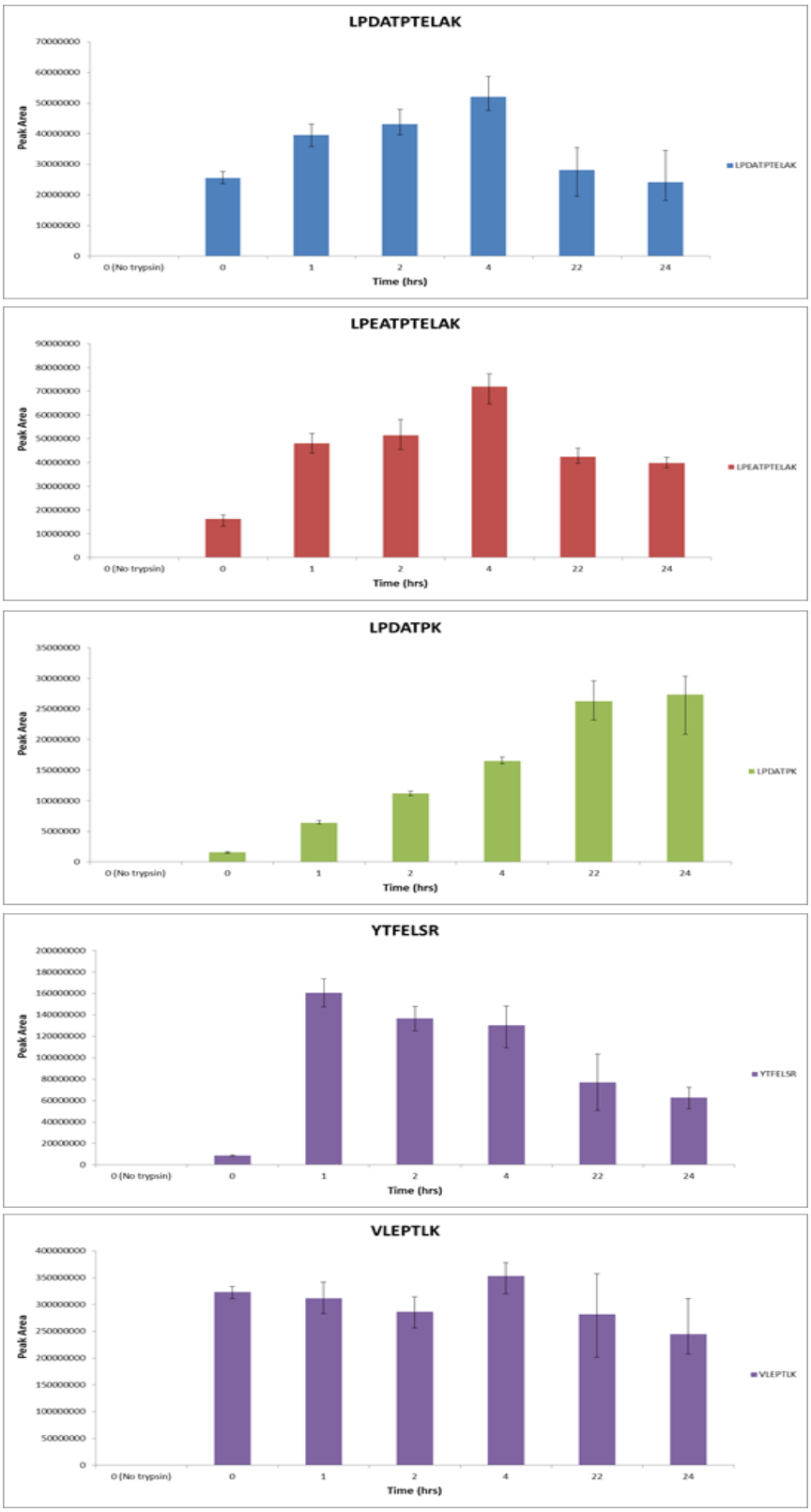

Figure 6.5. Trypsin digestion time profiles for the five VDBP peptides. Shown (top to bottom) are the variant-specific peptides LPDATPTELAK, LPEATPTELAK, LPDATPK, and the non-specific peptides YTFELSR and VLEPTLK.

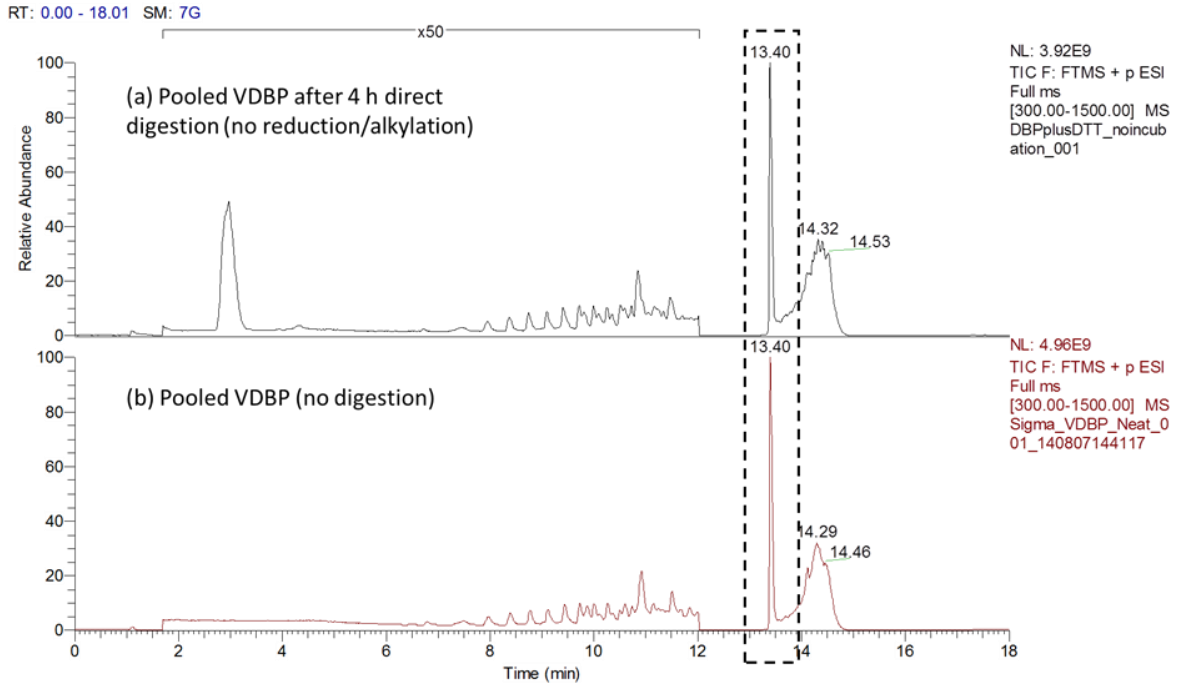

Figure 6.6. Total ion chromatograms (TICs) of pooled VDBP analysed following trypsin digestion *without* prior reduction and alkylation (a), compared to (b) pooled VDBP analysed directly without any digestion.

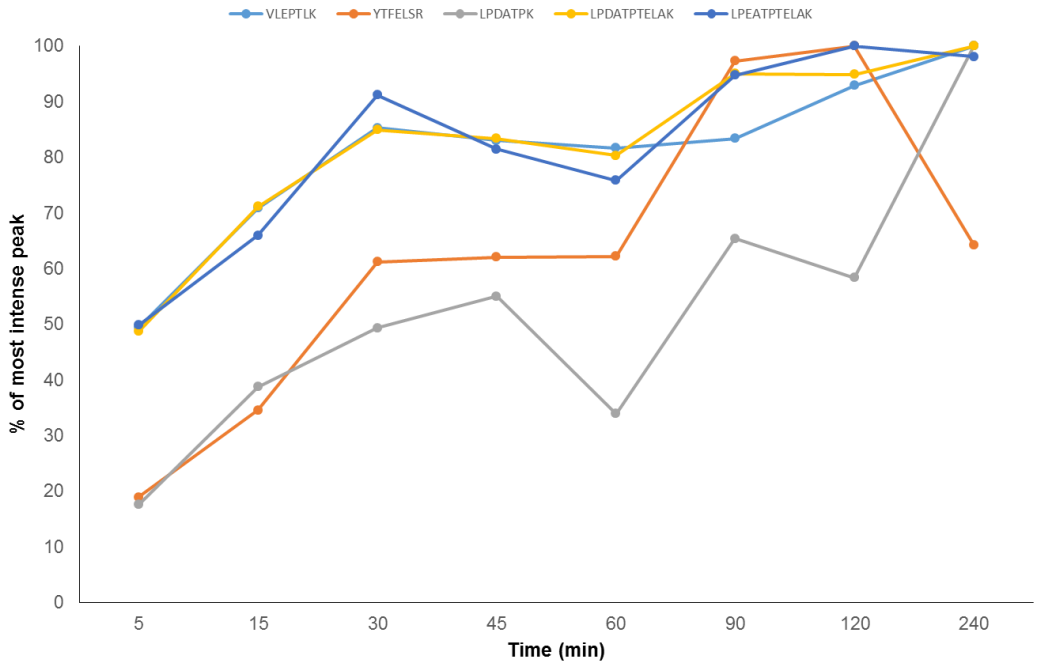

Figure 6.7. Trypsin digestion time profiles for the five VDBP peptides using SMARTDigest at 70 °C. Each analysis was carried out in singlicate.

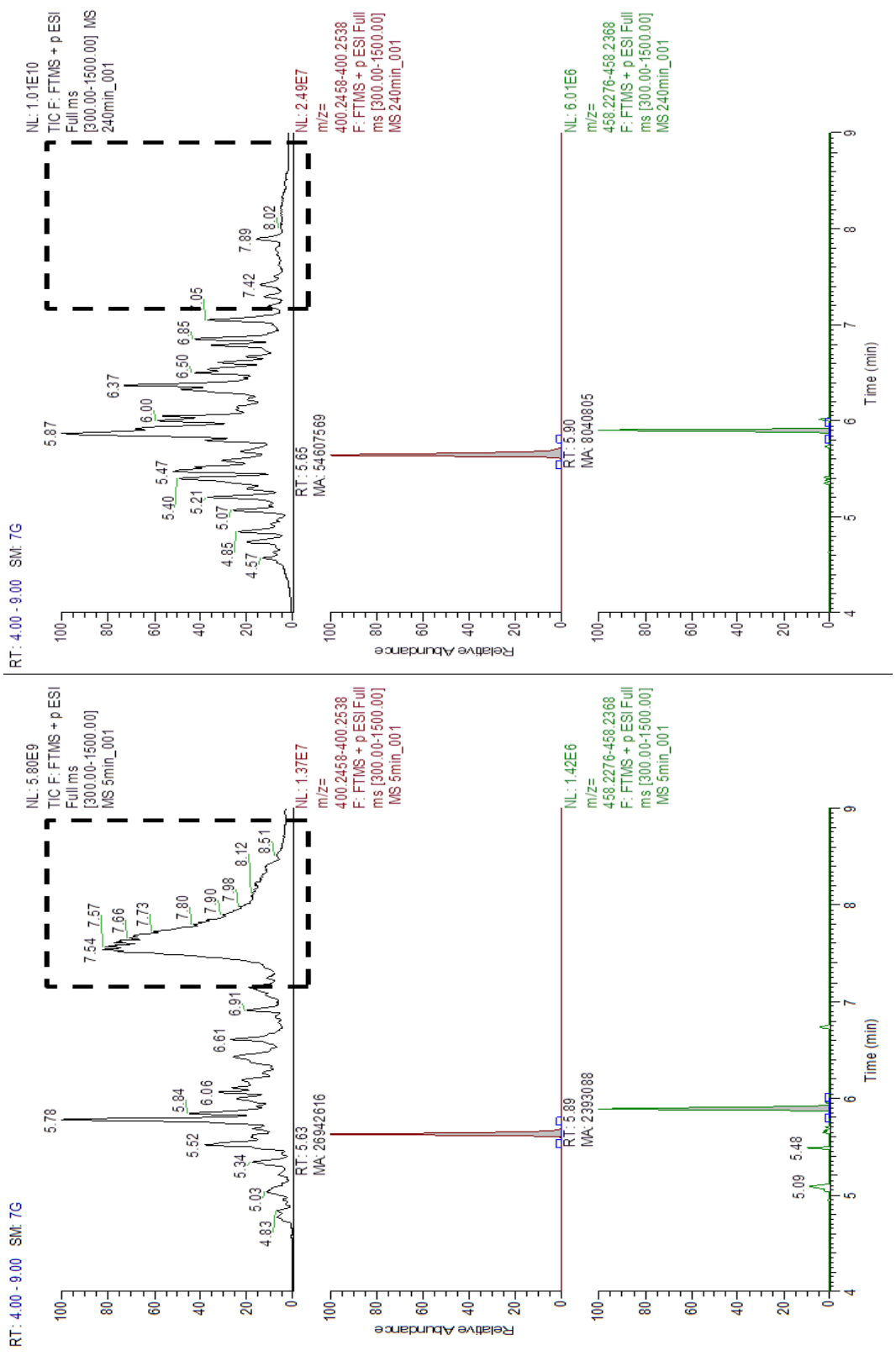

Figure 6.8. Remaining undigested protein after SMARTDigest™ at 5 minutes (left) and 240 minutes (right).

6.4.3. VDBP diplotype

Each of the 6 VDBP diplotypes were observed in the samples analysed. Extracted MS/MS (SRM) chromatograms for representative samples from each diplotype are shown in Figure 6.9. There was complete agreement in assigned diplotype between the 20 samples analysed by LC-MS/MS and the combined Taqman assays.

6.4.4. Quantitative analysis

Analysis of the digest calibration standards prepared from the pooled VDBP (diluted in BSA) gave linear calibration curve (Figure 6.10). Analysis of the 20 samples mentioned above showed similar concentrations of VDBP for all samples, based on the concentration of the VLEPTLK peptide. The YTFELSR/VLEPTLK peak area ratios were relatively consistent across all samples (Table 6.5).

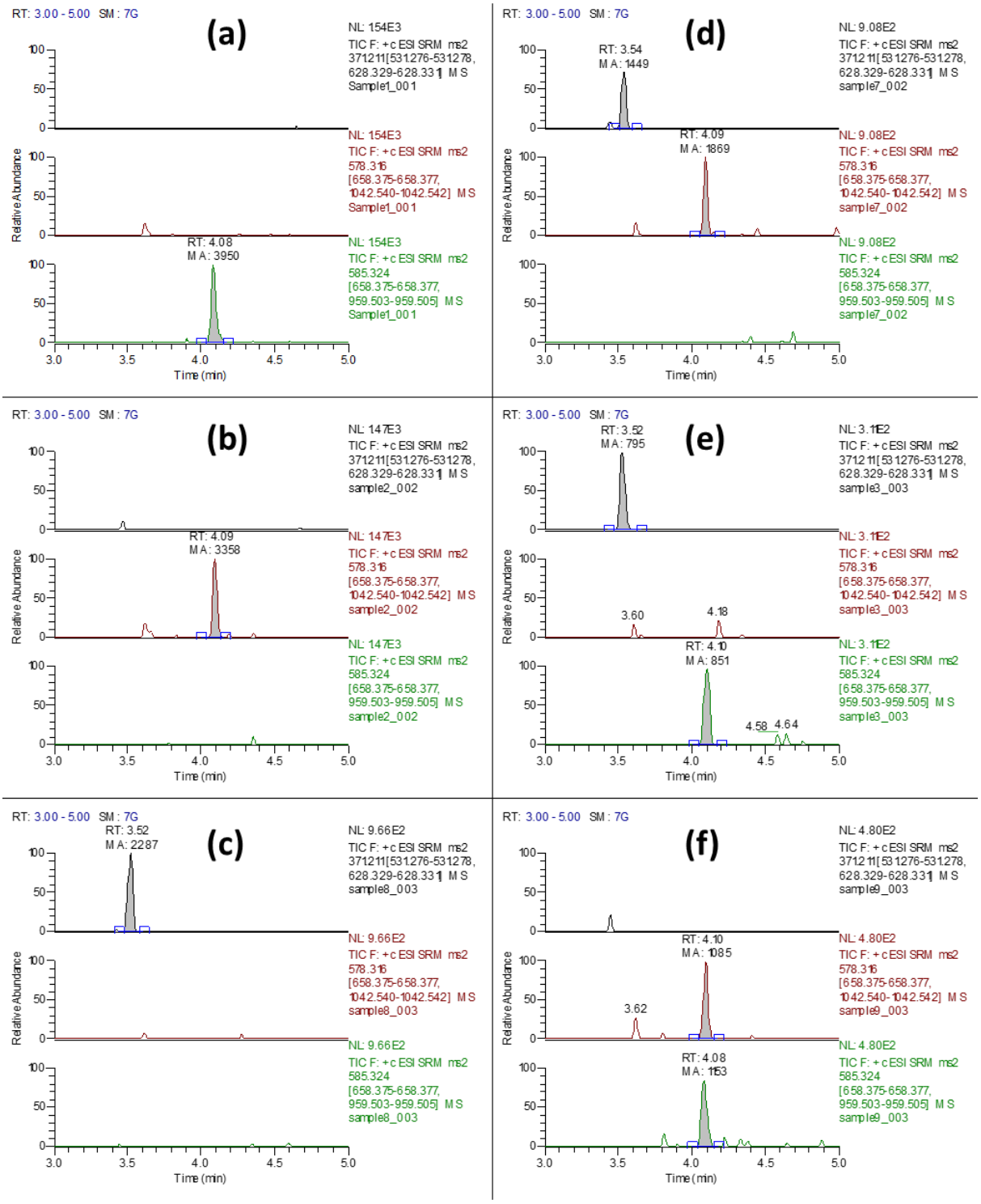

Figure 6.9. Example extracted ion chromatograms for the three variant-specific tryptic peptides of VDBP, and for each of the 6 possible VDBP diplotypes. Shown are samples from (a) a Gc-1s homozygous subject, (b) a Gc-1f homozygous subject, (c) a Gc-2 homozygous subject, (d) a Gc-2/Gc-1f heterozygous subject, (e) a Gc-2/Gc-1s heterozygous subject, and (f) a Gc-1f/Gc-1s heterozygous subject. All diplotypes were confirmed by Taqman assays.

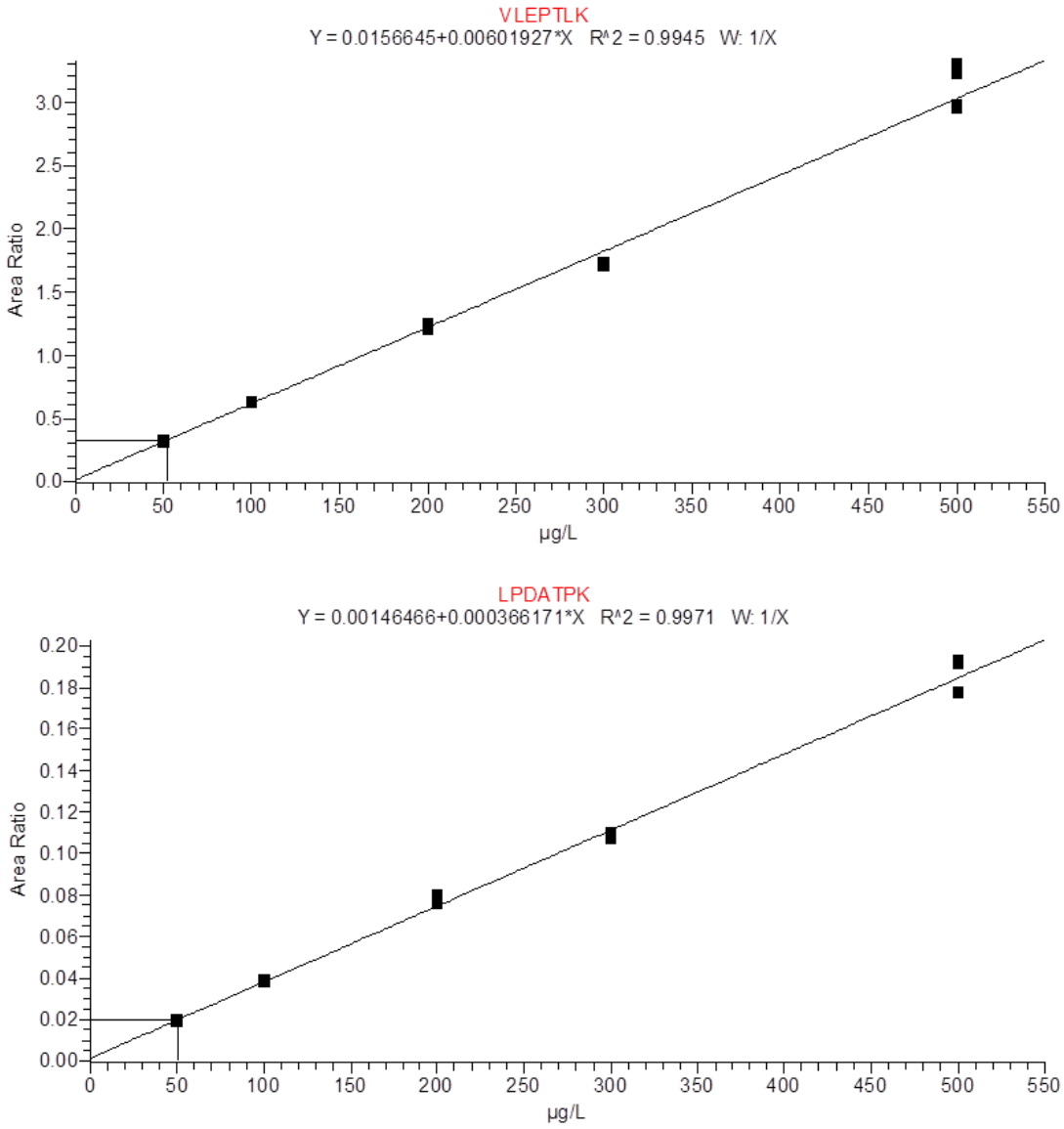

Figure 6.10. Example VDBP tryptic peptide calibration curves for VLEPTLK (non-variant-specific) and LPDATPK (variant-specific), produced using pooled human VDBP reference material.

Sample Number	Diplotype	VDBP (mg/L, by VLEPTLK)	VLEPTLK/YTFELSR peak area ratio
1	Gc-1s/Gc-1s	146	0.42
2	Gc-1f/Gc-1f	147	0.56
3	Gc-2/Gc-1s	116	0.42
4	Gc-1s/Gc-1s	127	0.51
5	Gc-2/Gc-1s	116	0.43
6	Gc-2/Gc-1s	124	0.47
7	Gc-2/Gc-1f	144	0.47
8	Gc-2/Gc-2	123	0.47
9	Gc-1s/Gc-1f	100	0.49
10	Gc-1s/Gc-1s	128	0.49
11	Gc-2/Gc-2	108	0.51
12	Gc-2/Gc-2	108	0.43
13	Gc-2/Gc-1s	112	0.52
14	Gc-2/Gc-1s	130	0.46
15	Gc-2/Gc-1s	133	0.55
16	Gc-1s/Gc-1f	115	0.48
17	Gc-1s/Gc-1s	132	0.57
18	Gc-2/Gc-1s	95	0.57
19	Gc-2/Gc-1s	110	0.58
20	Gc-2/Gc-2	109	0.57

Table 6.5. VDBP diplotype, VDBP concentration (measured by surrogate quantitation of VLEPTLK peptide), and the VLEPTLK/YTFELSR peak area ratio for 20 samples.

6.5. Discussion

6.5.1. Trypsin digestion

The data presented in this Chapter suggest that bottom-up VDBP analysis via surrogate peptide identification and quantitation may be beneficial when compared to (i) immunoassays for the analysis of VDBP and (ii) Taqman assays for VDBP genotyping. Traditional in-solution digestion following denaturing, reduction and alkylation yields the target peptides, but involves multiple steps and incubation periods. It was an interesting observation that all of the target peptides were present immediately following addition of the trypsin solution. For VLEPTLK in particular, the mean peak intensity at t = 0 was similar to that at each time point, and was greater than the mean peak area following 24 hour incubation at 37 °C (Figure 6.5). Previous applications of trypsin digestion for haemoglobin variant analysis have been reported in which trypsin was added directly to whole blood samples, without prior denaturing, reduction and alkylation (Daniel *et al*., 2007). Since none of the target peptides contained cysteine residues, this was investigated for VDBP, but it was shown that none of the peptides were liberated from VDBP without these steps, presumably since the target peptides were mid-sequence and the quaternary structure of the protein prevented the typsin accessing cleavage sites. Therefore, even with evidence that a short trypsin digestion incubation period would be suitable for routine quantation of the five tryptic VDBP pepitdes, the denaturing, reduction and alklyation steps would still be required, and these steps may not be suited to high-throughput laboratories, especially if the reagents for each of these steps were to be prepared fresh for each batch analysis.

With the SMARTDigest approach described, the sample and buffer were added directly to the immobilised trypsin. The 70 °C temperature served to denature the proteins and allow liberation of the target peptides to begin immediately, with all target peptides detectable after 5 minutes. That said, there remained a large amount of undigested protein in the sample taken from the reaction mixture at 5 minutes (Figure 6.8).

Further, compared to the traditional trypsin digestion method, the trypsin in the SMARTDigest method was immobilised and so could be removed by centrifugation

prior to analysis, this approach could be suitable for laboratories without access to TFC instrumentation. With overnight incubation, a further risk is that of peptide degradation. There was some suggestion of this in the 24 hour incubation study for the five peptides monitored in this work (Figure 6.5), despite the use of low-binding tubes. One could argue that with the more rapid SMARTDigest approach, unless there are temperature-related stability considerations, the risk of peptide degradation as a function of time in solution is less.

6.5.2. LC-MS for VDBP diplotype identification

Trypsin digestion of VDBP isoforms yields three variant-specific peptides. It is advantageous that all three peptides show good chromatographic performance, yield characteristic product ions, and are not sequences observed in any other human proteins by BLAST searching. Analysis of the variant-specific peptides alone by either LC-HR-MS, or by the LC-MS/MS method described showed complete agreement with the combined rs7041 and rs4588 Taqman assays for assigning VDBP diplotype. This novel method provides a simple and cheap alternative to the Taqman approach, especially so when the traditional in-solution trypsin digestion is followed.

6.5.3. LC-MS/MS for VDBP quantitation

The use of non-variant-specific peptides permits quantitative analysis of total VDBP in all samples, irrespective of VDBP diplotype. The quantitative work described in this study demonstrated that linear calibration curves could be achieved for the peptides VLEPTLK and YTFELSR. As the work in this study was being carried out, a very similar method was published by a group at the University of Washington (Henderson *et al*. 2016; Denburg *et al*., 2016). This group also identified the three variant-specific peptides, and the opportunity to quantify total VDBP using non-variant-specific peptides. Indeed, one of the non-specific peptides used for quantitation was the VLEPTLK peptide used in this study. For the second quantitative peptide they used ELPEHTVK, and for quality control they used the THLPEVFLSK peptide. This method was applied to a large cohort of samples from individuals covering all six possible VDBP

diplotypes, and results were compared to two immunoassay-based methods, one the monoclonal antibody-based ELISA (R&D Systems), and the other using the polyclonal ELISA (ALPCO).

The method reported in the first of these publications (Henderson *et al*., 2016) demonstrated some very useful approaches to bottom-up protein quantitation, and discussed some of the possible limitations of the study. Calibration of the quantitative peptides was achieved by peak area ratios to isotopically-labelled versions of the target peptides in an approach similar to that used in this study for VDBP quantitation. This approach is not always considered ideal since the isotope-labelled peptides, although added prior to trypsin digestion, do not undergo any tryptic cleavage prior to detection by LC-MS/MS (Scott *et al*., 2015). Alternative approaches to internal standardisation in bottom-up protein quantitation assays are discussed in more detail in the following Chapter.

In this study, lyophilised VDBP pooled from multiple donors was used to prepare calibrators and construct calibration curves. The lyophilised proteins were purified by SDS Page, and only had a purity of 95 %. In the Henderson *et al*. study (2016), recombinant Gc-1f VDBP was used for assay calibration, and quantitative amino acid analysis was carried out to assign the concentration of each amino acid in a hydrolysed sample of the stock calibrator solution. A valid concern noted by the authors regarding the quantitation of VDBP based on surrogate calibration using tryptic peptides was the possibility that the three VDBP isoforms could have different different digestion efficiencies, or different digestion kinetics. Without reference proteins for each of the three isoforms, the authors suggested the use of peptide peak area ratios as a check of the digestion process. The ratio between these peptides showed no statistical difference for each of the 6 diplotypes, suggesting these peptides were liberated from the proteins equally in all combinations of the isoforms. The use of peptide ratios is also a good tool for identification of missed cleavage sites during the digestion process.

Not presented in this Chapter are the early data generated using immunoaffinity LC-MS/MS for the analysis of VDBP (Couchman *et al*., 2013). This work was quickly superceded by the use of whole serum digestion and LC-MS/MS, as the immunoaffinity

was not required to reach the required assay sensitivity, as VDBP is an abundant protein. Furthermore, the use of antibody affinity during the sample preparation step introduces the possibility of non-equivalent isoform enrichment. This could not be proven without the availability of individual reference materials for each of the isoforms. A possible additional benefit of using whole serum digestion (i.e. without prior antibody enrichment or protein selection) is that other high-abundance proteins can be measured simultaneously. For instance, tryptic peptides for albumin could be used to simultaneously quantify albumin and VDBP in a single assay. This will be discussed in more detail in the next Chapter.

6.5.3.1. Quantitative protein analysis by LC-MS/MS – standardisation

Whilst the use of LC-MS/MS for VDBP genotype identification has been proven comparable to the Taqman assays, and is arguably preferable due to cost and simplicity (both SNPs can be identified in a single digestion), the quantitation of VDBP by LC-MS/MS is still in its infancy. As with the analysis of 25-OHD discussed in Chapters Two and Three, the availability of reference standards is required prior to any attempt of assay harmonisation.

6.5.3. LC-MS/MS compared to immunoassay for total VDBP measurement

There are a few recent studies reporting comparison between VDBP assays. In 2015, Aloia and co-workers planned a study similar to that of Powe *et al*. (2013) in a population of black and white post-menopausal women, but with the aim of measuring free 25-OHD using a newly available direct ELISA for free 25-OHD, and measuring VDBP concentrations by two immunoassays (one monoclonal and one polyclonal). In the population studies, the results of the two VDBP immunoassays were discordant. With the monoclonal assay, the black subjects had significantly lower VDBP than the white subjects. With the polyclonal assay, the VDBP concentrations were higher, and in fact the white subjects had higher VDBP concentrations (Aloia *et al*., 2015). More recently, three studies have compared both immunoassays and LC-MS/MS methods for VDBP (Henderson *et al.*, 2016; Denburg *et al*., 2016; Nielson *et al*.,

2016). The Nielsen *et al*. study also included a radial immunodiffusion assay which used polyclonal antibodies (Bouillon *et al*., 1977). All three concluded that the monoclonal immunoassay is subject to isoform specific difference in cross-reactivity. This was clearly demonstrated by comparison of LC-MS/MS and monoclonal immunoassay results by diplotype (Figure 6.11).

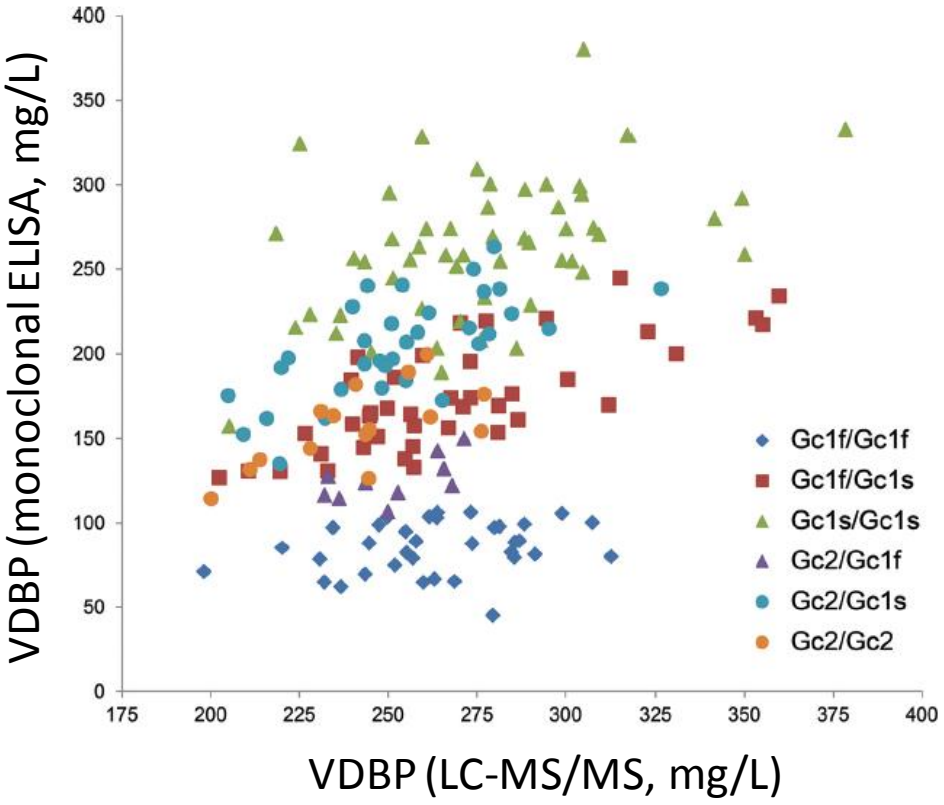

Figure 6.11. Correlation of VDBP concentrations measured by monoclonal ELISA (R&D Systems) and by LC-MS/MS, with results separated based on VDBP diplotype. Figure shown is adapted from Henderson *et al.,* 2016.

6.6. Conclusions and future work

The analysis of VDBP may be useful in assessment of vitamin D status. However, analysis of VDBP should include not only quantitative analysis of the total concentration, but also qualitative analysis of the six possible VDBP diplotypes. With regards analytical considerations for these measurements, it is clear that for the quantitation of total VDBP, monoclonal immunoassays give misleading results as a result of genotype-specific cross-reactivity differences. Owing to the ethnicity-related allele frequencies in the Gc gene, this analytical artefact has resulted in studies concluding that African populations have lower VDBP concentrations than Caucasian populations.

Polyclonal immunoassays are preferable to monoclonal assay, as the results show no genotype-related bias. By LC-MS/MS, VDBP concentrations have been shown not to be significantly different in black and white subjects. Therefore, contrary to the Powe *et al*. study, the calculated 'free' and 'bioavailable' vitamin D concentrations, as well as the concentrations of total 25-OHD were lower in black subjects. However, the absolute VDBP concentrations as measured by polyclonal ELISA and by LC-MS/MS do not agree. In the study by Denburg *et al.* (2016), the polyclonal ELISA gave consistently and considerably higher concentrations than the LC-MS/MS method. In the small number of samples measured in this study using different reference material, the VDBP concentrations were lower than the other LC-MS/MS methods.

These findings suggest that the 'vitamin D paradox' still remains in black subjects, with apparently low 25-OHD, yet clinically good bone health (Aloia *et al*., 2015). However, VDBP analysis is in its infancy, and the role of VDBP analysis in assessing vitamin D status as it relates to bone health requires further work. Certainly, there is some evidence that the three isoforms of VDBP show different binding affinity for 25-OHD metabolites (Chun *et al*., 2014; Braithwaite *et al*., 2015; Herrmann *et al*., 2016). In individuals with identical VDBP concentrations but different VDBP diplotypes, it follows that there may be a difference in the transport and/or bioavailability of 25-OHD. Indeed, studies already exist which show a relationship between serum 25-OHD and VDBP genotype alone, rather than VDBP concentration, or calculated bioavailable vitamin D (Lauridsen *et al*., 2005; Herrmann *et al*., 2016). The role of VDBP genotype

on 25-OHD analysis (especially by immunoassay) has yet to be shown. A round of DEQAS specimens for circulation late 2016 are due to be analysed using the VDBP method described in this Chapter to assign VDBP diplotype to further investigate this possibility.

Wherever possible, studies in which hypothesised differences in vitamin D status between individuals are carried out involving analysis of VDBP, populations should be grouped according to VDBP genotype rather than ethnicity. Ethnicity has been used to group populations in a number of studies, and is arguably an acceptable surrogate for VDBP genotype due to the allele frequencies in different ethinc groups. However, with simple methods such as the LC-MS/MS method described in this Chapter, there should be no requirement to use a surrogate for VDBP genotype.

As with 25-OHD, the accuracy of quantitative VDBP assays remains an issue. Polyclonal VDBP assays and LC-MS/MS assays can begin to address this issue since they do not suffer genotype-related bias, but already these two approaches show discrepant concentrations. Reference materials are required for further harmonisation, and ideally individual reference materials for each of the three isoforms will be required.

Chapter Seven

Investigating the use of non-human sera for internal standardisation of human protein quantitation

7.1. Introduction – peptide quantitation approaches

For quantitative assays which require a bottom-up approach following proteolytic digestion, assay calibration is complex and can be approached in a number of ways. Stable isotope-labelled peptides can be custom-synthesized and used as internal standards, but these do not always account for variability during the digestion process (Bronsema *et al*., 2012). Novel approaches such as 'winged peptides' (Figure 7.1) or concatenated labelled peptides (quantitative concatenation, 'QconCAT') that incorporate cleavage sites go some way to overcoming this problem (Pratt *et al*., 2006). However, digestion time profiles of the shorter peptides do not always account fully for the digestion of the native protein in clinical samples, and can be affected by the choice of 'flanking' amino acids (Bronsema *et al*., 2012; Scott *et al*., 2015). Fully-labelled proteins are therefore preferable, but are expensive, especially for large proteins with many variant forms. Moreover, the labelled proteins should ideally incorporate tertiary and quaternary structure of the native protein, which is not always a straightforward synthetic process. Analogues for target proteins from other species (Czerwenka *et al*., 2007), or monoclonal antibodies derived from other species (Dubois *et al*., 2008), have been used with some success for protein quantitation, but rely upon production or commercial availability of the analogue protein.

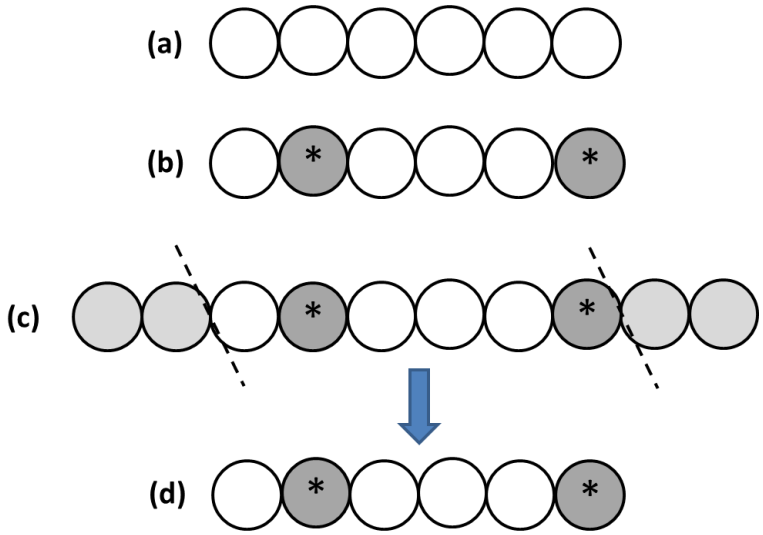

Figure 7.1. 'Winged' tryptic peptides sometimes used for protein quantitation. Shown are (a) a 6-amino acid target peptide, (b) the more commonly used isotope-labelled version of the target peptide, (c) a 'winged' labelled peptide with 2 additional residues added to both the N- and C-termini of the target peptide, thus including two tryptic cleavage sites, and (d) the liberated isotope-labelled target peptide.

7.2. Aims

In this Chapter, bovine serum was investigated as a single, readily available, internal standard for the simultaneous quantitation of human proteins. The development of a Microsoft Excel-based spreadsheet was also carried out, with the aim of inputting human and non-human protein sequences to suggest candidate non-human peptides based on peptide similarity. VDBP and albumin were used as exemplar proteins.

7.3. Materials and methods

7.3.1. Development of candidate peptide generating software

Development of software to generate candidate tryptic peptide pairs was carried out using Microsoft Excel in collaboration with a colleague with experience in Visual Basic programming language, Serkan Osman. All imported protein sequences were from Uniprot (www.uniprot.org).

7.3.2. Analysis of human VDBP and albumin using bovine serum internal standard

Newborn calf serum, human serum albumin, pooled human VDBP, formic acid (MS grade), and acetonitrile (MS grade) were from Sigma Aldrich (Poole, UK). Pooled human plasma (dipotassium EDTA) was from Sera Laboratories (West Sussex, UK). Water was deionised (>12 mΩ, Purite, Thame, UK). SMARTDigest™ kits, comprising (i) digestion vials containing immobilized trypsin and (ii) SMARTDigest buffer, were from ThermoScientific (Hemel Hempstead, UK). Lo-Bind™ protein (0.5 mL) tubes were from Eppendorf (Stevenage, UK). Glass autosampler vials (2 mL) and snap-caps were from Kinesis (St Neots, UK).

Eluent A was 0.2 % (*v/v*) formic acid in deionised water and Eluent B was 0.2 % (*v/v*) formic acid in acetonitrile. The elution gradient was from 2 % B ramped to 100 % B over 5 minutes (Aria Transcend™ TLX-II with Accela™ 600 HPLC pumps, Thermo Scientific). The total flow-rate was 0.5 mL/min, and eluent was diverted to waste for (i) the first 120 s and (ii) the last 60 s of each injection. Total analysis time was 7 min. The LC column [50 x 4.6 mm i.d. (1.8 µm average particle size) Zorbax™ XDB-C18 (Agilent Technologies, Santa Clara, CA)] was maintained at 50 °C (Hot Pocket™, Thermo Scientific). Analytes were detected using a TSQ Vantage™ MS/MS instrument (Thermo Scientific, San Jose, CA), operated in selected reaction monitoring (SRM) mode (0.7 FHWM resolution on both quadrupoles, 2 transitions per peptide), and using heated electrospray ionisation.

Stock solutions of human albumin (100 g/L) and human VDBP (1.00 g/L) were prepared in Eluent A. Combined calibrators were prepared by appropriate dilution of the human

protein stock solutions with Eluent A, at concentrations of 10, 20, 40, 60, 80 and 100 mg/L for VDBP and of 5, 10, 20, 30, 40, and 50 g/L for albumin. Prepared calibrators were stored at -20 °C in approximately 200 µL portions in Lo-Bind tubes prior to use. Calibrators (25 µL) were diluted with bovine serum (25 µL) and SMARTDigest buffer (450 µL) in Lo-Bind tubes, and the mixtures vortex mixed (10 s). After mixing, 200 µL portions were transferred to SMARTDigest trypsin tubes, and the tubes were capped. The contents of the tubes were vortex mixed (30 s), and incubated (70 °C, 60 min). After cooling and centrifugation (13,000 rpm, 5 min), the supernatant from each tube was diluted (1+19, *v/v*) with Eluent A in 2 mL autosampler vials for analysis. The six calibrators, a pooled human serum sample (without bovine serum), a bovine serum sample (without human serum or calibrator solution) and a 'blank' sample (SMARTDigest buffer only), were each digested in duplicate, and digests analysed in triplicate. A sample containing a mixture of the pooled human serum and bovine serum was also analysed, and results compared to the pooled human serum sample analysed without bovine serum to check for any differences in response caused by either matrix effects of the bovine tryptic peptides or influence of the additional matrix on the digestion process.

7.4. Results

7.4.1. Candidate peptide generating software

For the initial development of the candidate peptide generating software, visual basic programming was used to digest protein sequences *in silico* using standard trypsin digestion rules (cleavage after the C-terminus of lysine and arginine residues, except when either residue was followed by a C-terminal proline residue). The software interface was designed to allow user input for the minimum and maximum number of residues for candidate peptides to refine the peptide list. There was also the opportunity to exclude specific residues (e.g. cysteine, methionine, histidine, etc.). No input was designed to allow for missed cleavage sites. As the software was designed just to identify potential human and non-human peptide pairs, there was no user input designed to account for post-translational modifications.

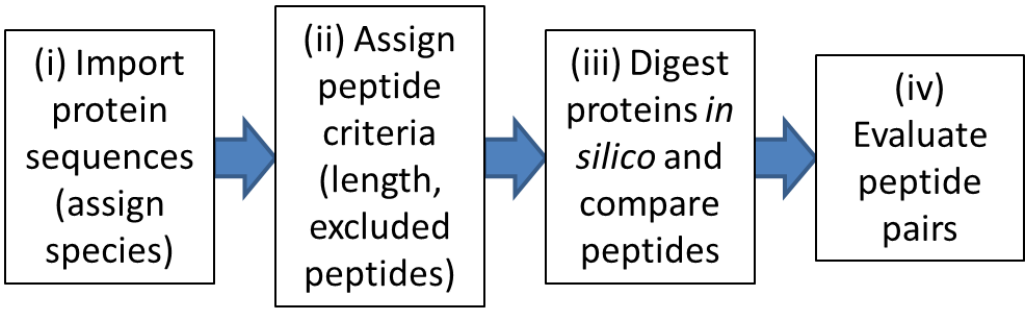

Figure 7.2. Summary workflow for the developed candidate peptide pair software.

Tryptic peptides within the assigned peptide length limits were then compared using Levenschtein Distances (LD) to calculate similarity scores (Levenschtein, 1966). Similarity scores were transformed to give LD scores such that an LD score of 1 indicated an identical peptide sequence, and that the closer the LD score to 1, the more similar the peptide sequences. The process is summarised in Figure 7.2. For human and bovine albumin, there were 79 and 78 tryptic peptides on *in silico* tryptic digestion, respectively. When filtered for peptides between 6 and 15 amino acids in length (not excluding any amino acids), there remained 33 human and 42 bovine candidate tryptic peptides. All peptides were compared to one another, and those with

calculated LD scores of <0.7 and those with LD scores of 1 were also excluded. There were 34 resulting peptide pair comparisons made for human vs bovine albumin. As well as the LD score, the peptide hydrophobicity was also considered, since a high LD score resulting from only one amino acid substitution may result in two markedly different peptides with regards chromatographic behaviour. The overall hydrophobicity for the initial software development was calculated using the simple model described by Kyte & Doolittle (1982), and 'spark charts' were added to visualise major hydrophobicity differences between candidate peptides. Peptide hydrophobicity values were also generated using Pinpoint^{TM} software (version 1.3, ThermoFisher Scientific) using the Krohkin hydrophobicity index (Krohkin & Spicer, 2009). Calculated hydrophobicity was not included in calculation of the LD score. A screenshot of the software output is shown in Figure 7.3.

The selected peptide pairs for human vs bovine albumin and human vs bovine VDBP were as follows. The Uniprot references for the protein sequences used were P02774 (VTDB_HUMAN), Q3MHN5 (VTDB_BOVIN), P02768 (ALBU_HUMAN) and P02769 (ALBU_BOVIN). Similarity analysis of the human and bovine protein sequences (UniProt Align Tool) revealed 80 % sequence identity (380 identical positions, 71 similar positions) for VDBP and 76.3 % sequence identity (465 identical positions, 105 similar positions) for albumin. For albumin, the peptide pairs generated by the software were: LVNEVTEFAK (human) and LVNELTEFAK (bovine), and QTALVELVK (human) and QTALVELLK (bovine). For VDBP, as well as the peptide exclusion criteria mentioned, variant form-specific peptides (Henderson *et al*., 2016) were also excluded. The chosen peptide pairs were: TSALSAK (human) and TSALSDK (bovine), and VLEPTLK (human) and ILESTLK (bovine). The YTFELSR peptide used in the previous chapter was not used, since the lysine-to-glutamine substitution in the corresponding bovine peptide (VLDQYIFELSR) resulted in a longer tryptic peptide, and hence a low LD similarity score of 0.72. The summary output from the software is shown in Table 7.1.

Peptide	Protein	Human/ bovine	LD score	Hydrophobicity index
LVNEVTEFAK	Albumin	Human	0.95	-0.09
LVNELTEFAK		Bovine		-0.24
QTALVELVK		Human	0.94	4.27
QTALVELLK		Bovine		4.16
TSALSAK	VDBP	Human	0.93	2.36
TSALSDK		Bovine		0.24
VLEPTLK		Human	0.86	-0.38
ILESTLK		Bovine		0.16

Table 7.1. Calculated similarity output, given as the LD score, for the chosen human and bovine peptide pairs for albumin and VDBP.

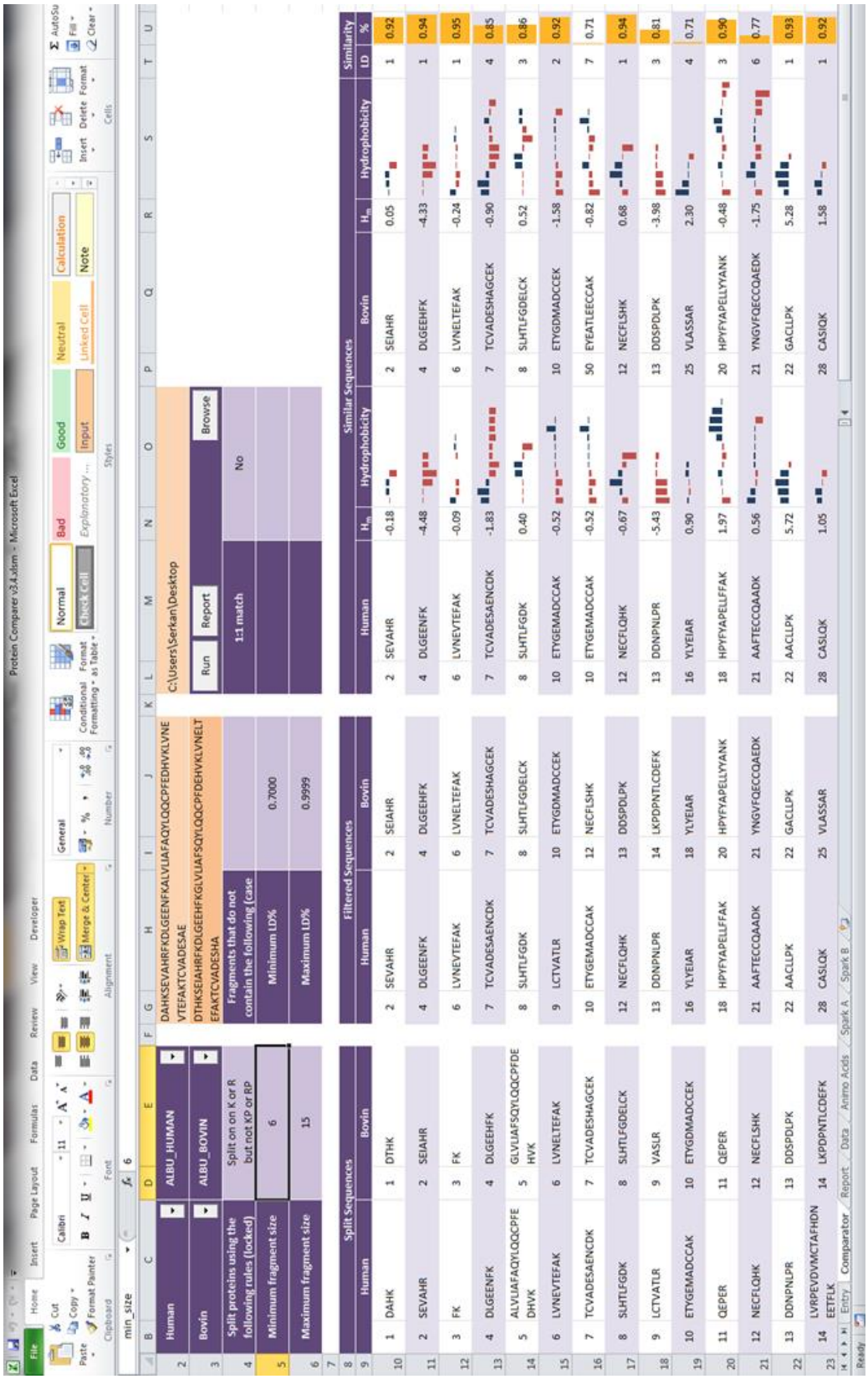

Figure 7.3. Example output of the candidate peptide pair generator software for the comparison of human and bovine albumin.

7.4.2. Analysis of human VDBP and albumin

Summary MS/MS characteristics for the chosen peptides are shown in Table 7.2. Example chromatograms are shown in Figures 7.4, 7.5, 7.6, 7.7 and 7.8. The calibration curves produced by plotting the mean peak area ratios (N = 6, human to bovine peptide SRM peak areas) against analyte concentration were linear for all four peptides (R^2>0.99, Figure 7.5). None of the human peptides of interest were detected in the samples containing bovine serum only, and none of the bovine peptides of interest were detected in the samples containing human serum only. No signal was observed for the peptides of interest in the 'blank' samples.

Retention times for the 8 peptides were as follows: TSALSAK/TSALSDK 3.15 and 3.98 minutes, VLEPTLK/ILESTLK 3.98 and 3.83 minutes, LVNEVTEFAK/LVNELTEFAK 4.55 and 4.91 minutes, and QTALVELVK/QTALVELLK 4.27 and 4.58 minutes. The mean peak areas were lower for all four human peptides in the samples containing a mixture of both matrices compared to the samples containing just human serum (mean % difference 59.6, 40.3, 68.4 and 41.3 % for QTALVELVK, LVNEVTEFAK, VLEPTLK and TSALSAK, respectively).

Peptide[a]	Precursor ion (*m/z*), all $[M+2H]^{2+}$	CE	Q3 [*m/z*(ion type)]	Krohkin Hydro-phobicity factor	Sequence position
TSALSAK	339.195	13	489.303 (y5); 576.335 (y6)	6.11	88-94
TSALSDK	361.190	13	533.292 (y5); 620.324 (y6)	6.43	88-94
VLEPTLK	400.252	17	587.339 (y5); 700.423 (y6)	18.49	364-370
ILESTLK	402.249	17	448.276 (y4); 690.403 (y6)	17.64	363-369
LVNEVTEFAK	575.311	32	595.308 (y5); 694.376 (y6)	27.50	66-75
LVNELTEFAK	582.321	32	708.392 (y6); 837.435 (y7)	32.00	66-75
QTALVELVK	500.805	28	700.460 (y6); 771.497 (y7)	29.90	550-558
QTALVELLK	507.815	28	714.476 (y6); 785.513 (y7)	35.35	549-557

Table 7.2. Peptide *m/z* values used for LC-MS/MS analysis.

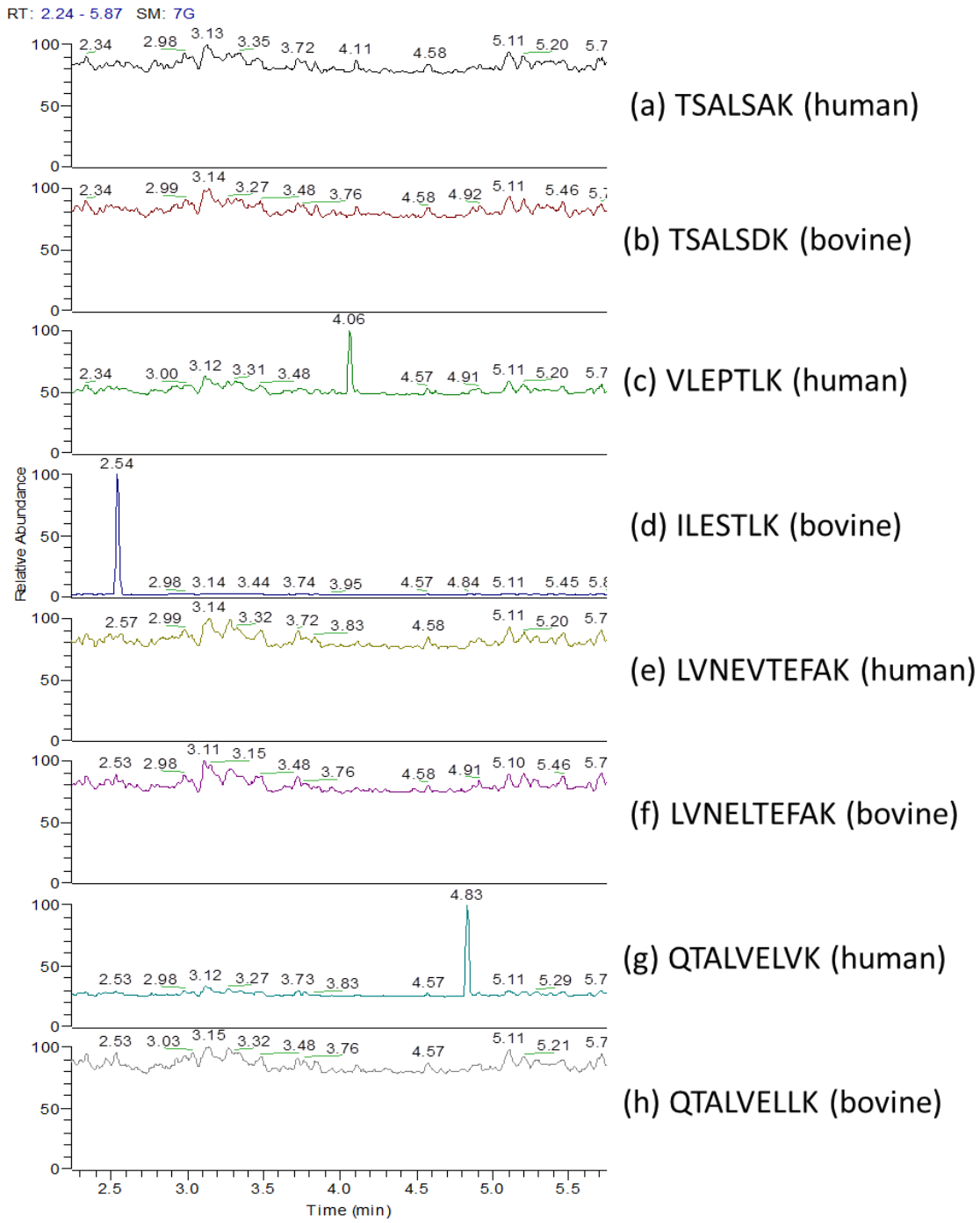

Figure 7.4. Extracted ion chromatograms for tryptic peptides from deionised water ('blank') processed using the SMARTDigest method.

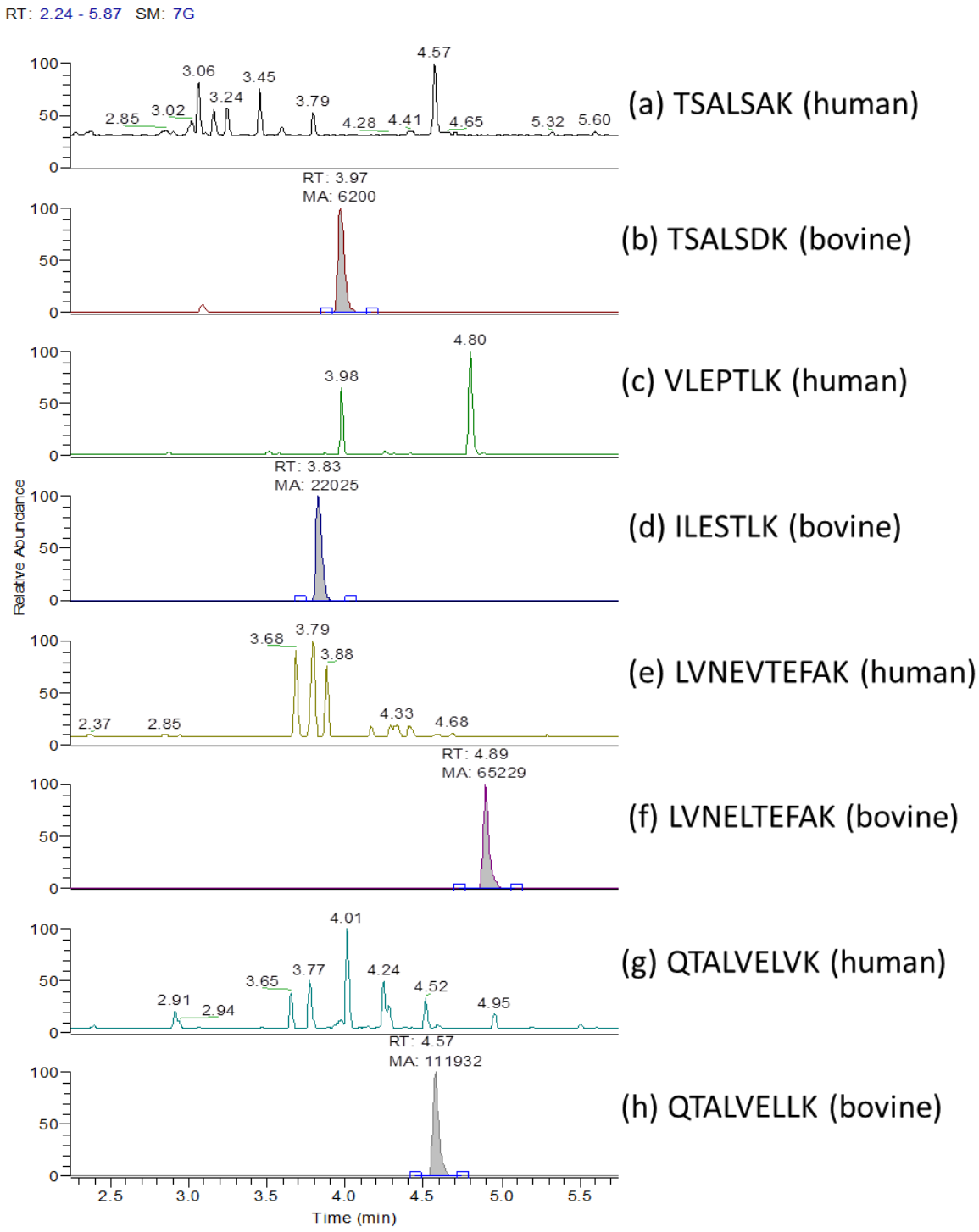

Figure 7.5. Extracted ion chromatograms for tryptic peptides from calf serum only (no human serum) digested using the SMARTDigest method.

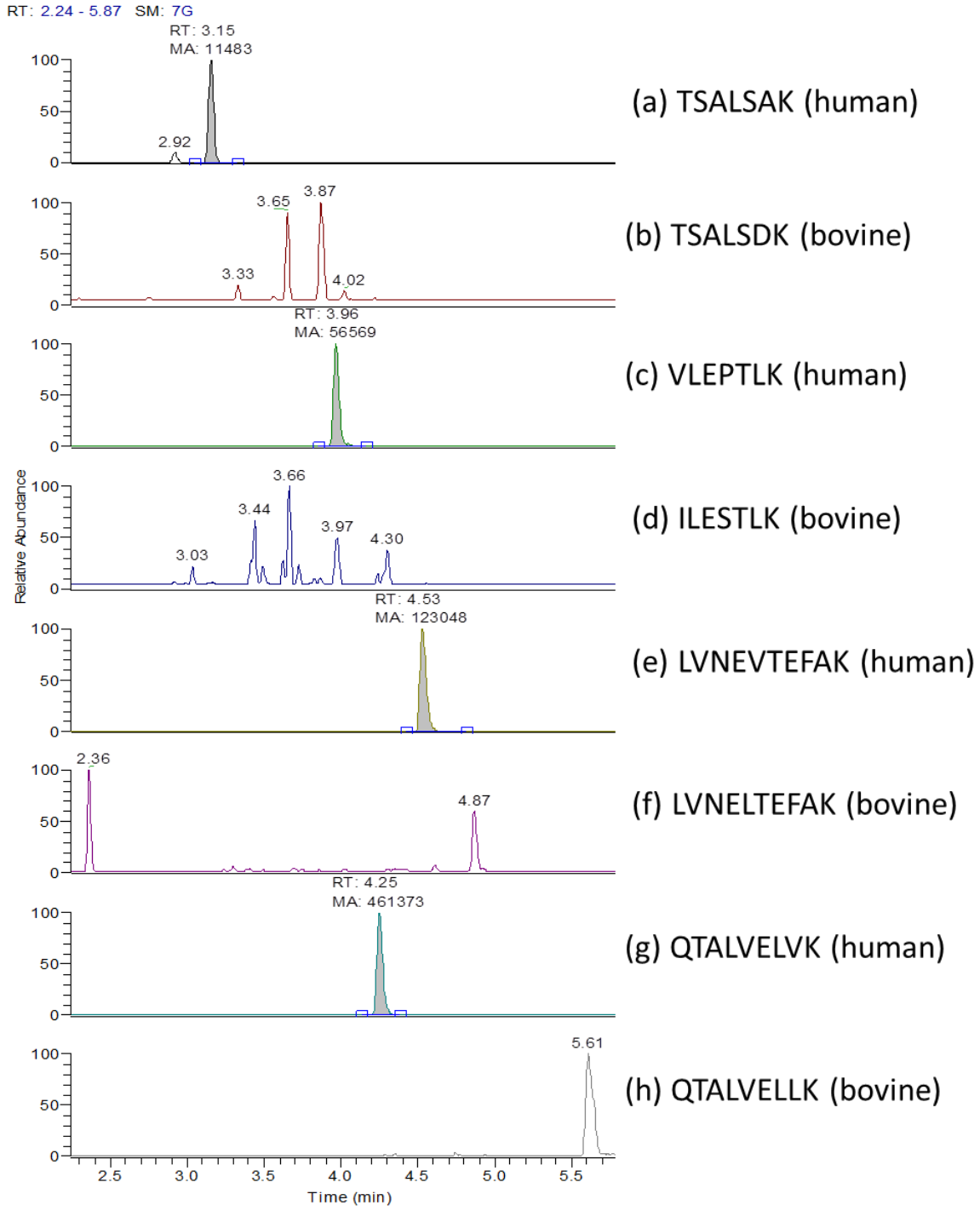

Figure 7.6. Extracted ion chromatograms for tryptic peptides from human serum only (no calf serum) digested using the SMARTDigest method.

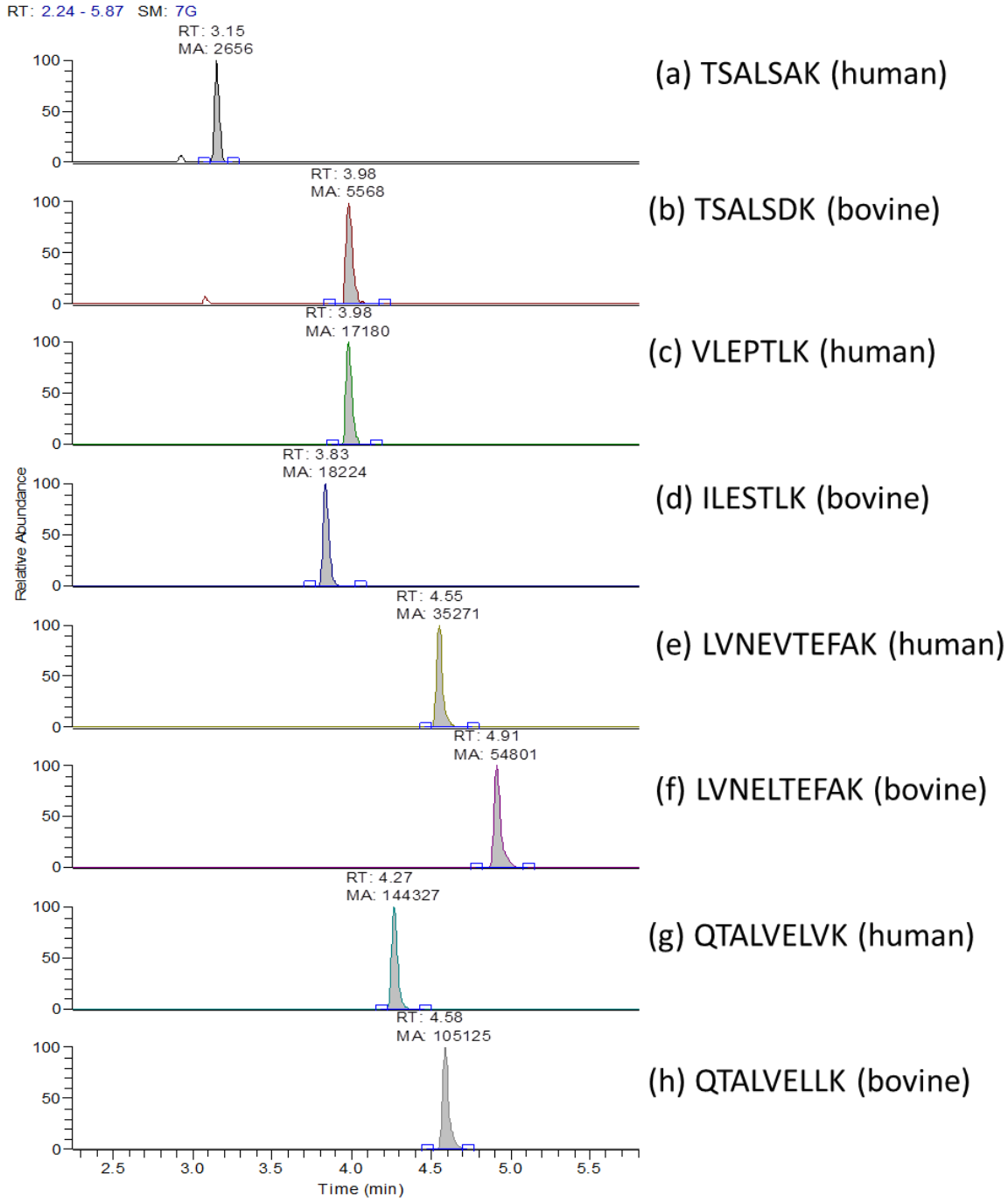

Figure 7.7. Extracted ion chromatograms for tryptic peptides from a human protein calibration standard (40 mg/L VDBP, 20 g/L albumin) with added whole calf serum internal standard, digested using the SMARTDigest method.

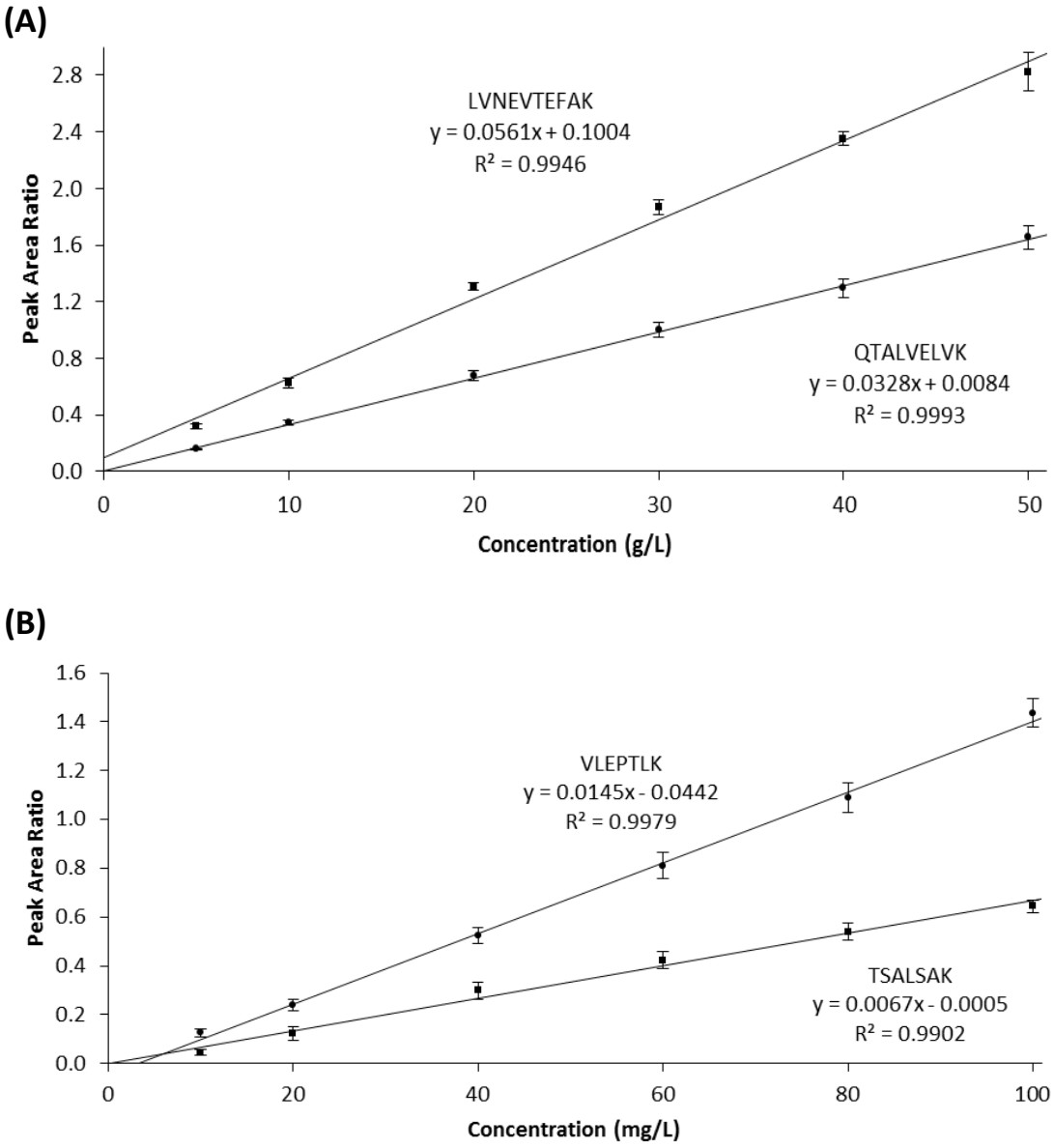

Figure 7.8. Calibration curves for (A) albumin and (B) VDBP peptides. Plotted are the mean (± SD, N = 6 for each calibrator) peak area ratios (human:bovine peptide) against analyte concentration.

7.5. Discussion and further work

Despite seeming counter-intuitive to add a second highly-complex matrix to human samples, the small study described here shows the potential of using non-human peptides/proteins from an undiluted matrix as an extremely cost-efficient internal standard for simultaneous quantitation of multiple human proteins and peptides. Rather than using multiple analogue internal standards for each target analyte, use of the entire non-human matrix means that this approach could provide a single, almost 'universal' internal standard for a wide array of proteins, provided that unique, species-specific peptides are produced during the digestion step. The availability of multi-species protein sequence databases such as UniProt, *in silico* digestion softwares, and the ability to run vast sequence similarity searches is invaluable in choosing an appropriate internal standard matrix for any target protein using this approach. The described peptide-pair generating spreadsheet provides a tool for rapidly screening protein sequences for the best likely tryptic peptides for such applications, and can be used for any available protein sequence. For the analysis of some proteins, non-human matrices other than bovine serum (e.g. porcine, murine) may be useful and/or necessary, providing that protein sequences are available. In the example application described, selected tryptic peptides derived from bovine serum were used to standardise the digestion and LC-MS/MS analysis of corresponding human peptides from a mixture of the two matrices. The chosen peptides for both species were (i) of similar length, (ii) had similar predicted chromatographic properties, and (iii) were from corresponding positions within the entire protein sequences. For both the model proteins chosen there was a high degree of sequence similarity. The absolute amount of bovine VDBP and albumin in this study was not known, although the peak area ratios in the calibrators for all peptides were close to 1.0, suggesting similar concentrations of both proteins in both matrices. This may not always be the case for other species and other target proteins, and so this approach may require dilution of one of the matrices to get similar instrument response for accurate quantitation. Unless there are expected to be significant differences in the concentration of the target proteins between species, such that the amount of non-human protein against which samples are calibrated is too great or too little relative to the target protein assay calibration range, the absolute amount of the non-human

protein itself is not essential to know. All that is required is that the amount added to each sample and to the calibrators is kept constant.

It is worth noting that the two proteins analysed in this work are very high-abundance proteins. However, it may be possible to analyse less abundant proteins by combining this approach with other commonly-used techniques. For instance, it may be possible to mix the sera of two species, and then either immuno-deplete (providing the antibodies show affinity for the abundant proteins of both species) or partially precipitate the high-abundance proteins from both species prior to digestion. Demonstration of this requires further investigation.

In summary, the approach described for human protein quantitation using non-human sera is highly cost-efficient. For assays in which many proteins are to be analysed simultaneously, and where isotope-labelled proteins or peptides are either unavailable, or are prohibitively expensive, this method offers a simple solution, providing suitable candidate proteotypic peptides can be identified. It is important to remember that, as with small molecule applications of LC-MS/MS, internal standards provide a means for robust calibration against a reference standard. The absolute accuracy of the quantitation is dependent upon standardised reference materials for the preparation of calibrators, and it is these that are currently lacking for human proteins.

Chapter Eight

Final discussion

'Vitamin D status' is used to define whether an individual is vitamin D deficient, sufficient, or intoxicated (Holick, 2009). Despite recent advances in the analysis of other vitamin D-related biomarkers that may contribute towards this measure, including those that have been discussed in this thesis, the most widely used and clinically accepted biochemical marker for assessing vitamin D status will continue to be the total serum 25-hydroxyvitamin D (25-OHD) concentration (Holick, 2007).

Current clinical guidelines suggest that optimal vitamin D status should be defined by a total serum 25-OHD concentration greater than 30 µg/L (75 nmol/L), and that the concentrations associated with deficiency are from 10-20 µg/L (25-50 nmol/L) (Heaney, 2013). There are other suggestions that higher concentrations of 25-OHD may be required in some individuals (Pludowski *et al*.,2012). In some situations, there is no doubt that analysis of 25-OHD is useful to confirm clinical observations, for instance in severe vitamin D deficiency related to very low 25-OHD concentrations. However, as has been demonstrated, the analysis of 25-OHD is complex, and is not harmonised despite dating back over 40 years. In situations where the clinical evidence for hyper- or hypo-vitaminosis D is less clear, it should be remembered that the vitamin D metabolic pathway is a highly complex and dynamic system involving a number of structurally-similar compounds (Zerwekh, 2008). The roles of these compounds in assessing true vitamin D status, and then assigning 'reference ranges' for physiology and pathophysiology (potentially with separate reference ranges in different populations) should ideally be considered alongside interactions with other calcitropic hormones such as parathyroid hormone (PTH) and calcitonin, as well as plasma transporter proteins such as the vitamin D binding proteins. Crucially, these decisions should be based on accurate analytical data.

From the results of this thesis, there are two main considerations which clinicians requesting the 'assessment of vitamin D status' in their patients should be aware of. The first regards variability in the analytical approaches to the measurement of 25-OHD, and the ongoing work towards harmonisation of 25-OHD testing (Sempos *et al*. 2012). The second regards the possible value of measuring additional biomarkers to give a more complete picture of vitamin D status.

Chapters Two and Three explored the limitations of 25-OHD assays. *Every* analytical platform used for 25-OHD analysis in clinical laboratories has both advantages and disadvantages that give rise to inter-assay variability. Ultimately, the cause of inaccuracy and variation in 25-OHD assay results is due to variability in the composition of individual sample matrices. In trying to increase throughput and simplify assay processes (for example use of homogneous immunoassays), these matrix-related differences risk being exacerbated. Further, these differences are almost impossible to account for in every sample when using automated immunoassay-based instrumentation, since the instrument output is simply a numeric value. Immunoassay-based techniques are inherently sensitive, often requiring low sample volumes when compared to chromatographic methods, but as was demonstrated, lack accuracy when compared to LC-MS/MS methods such as the TFC-LC-MS/MS method developed in this work. Misclassification of vitamin D status, purely as a consequence of using different analytical platforms is a significant clinical problem, and one that has been replicated by a number of groups around the world (Lai *et al*., 2012; Holmes *et al*., 2013).

A major attraction to high-throughput clinical chemistry laboratories is that immunoassays are easily integrated into fully-automated, random-access laboratory track systems, thus allowing rapid analysis times. However, with methods such as the TFC-LC-MS/MS method described in Chapter Two, LC-MS/MS is becoming more amenable to high-throughput workloads, and should no longer be confined to use in large reference laboratories. Potential issues such as the isobaric 3-*epi*-25-OHD metabolites can be resolved by the flexibility of LC-MS/MS as a technique, and using modern chromatographic approaches require little or no additional analysis time.

Complete 'primary sample-to-result' LC-MS/MS platforms are not yet available, and LC-MS/MS workflows are not yet automated to the extent of immunoassays. However, until such instruments are available there are a number of options for partial automation, including those discussed such as automated liquid handling and parallel processing in 96-well formats. There has been substantial progress towards the automation of LC-MS/MS technology in the past few years (Vogeser & Kirchhoff, 2011). That said, the complexity of LC-MS/MS instrumentation, and the fact that

methods are not 'locked down' as with immunoassay kits, means there are number of LC and MS instrumentation parameters and calibration approaches that will vary between laboratories, and can potentially cause inter-laboratory variability, as was discussed in Chapter Three.

Harmonisation of 25-OHD testing has been a challenge for many years. The Vitamin D External Quality Assessment Scheme (DEQAS) was established in 1989 in response to concerns over the poor performance and large variability between 25-OHD assays (Carter *et al*. 2004; Binkley *et al*. 2004), and has dramatically reduced the variability between participating laboratories since its inception. More recently, efforts to harmonise 25-OHD analysis have been significantly aided by the availability of SRMs and by the development of LC-MS/MS-based RMPs. The most recent SRM (SRM 972a) from the National Institute of Standards and Technology (NIST), produced in collaboration with the National Institutes of Health (NIH) Office of Dietary Supplements (ODS) contains four human serum-based solutions containing different concentrations levels of vitamin D metabolites, including 25-OHD2, 25-OHD3, 3-*epi*-25-OHD3 and 24*R*,25-OHD3. These SRMs are commercially available, and should be used by clinical laboratories for method validation. Each level SRM is supplied with certified reference values assigned using the NIST RMP (Tai *et al*. 2010; Tai *et al*. 2015). Subsequent methods by the University of Ghent (Stepman *et al*. 2011) and the Center for Diseases Control (CDC) (Mineva *et al*. 2015) have since been validated and accredited to ISO 15193 and JCTLM guidelines. DEQAS subscribers now have access to results produced using the NIST RMP, and these values should also be used during method validation where possible.

Analysis of other vitamin D metabolites was not discussed in this thesis. However, many of the analytical techniques discussed are applicable to the development of new methods for these analytes, and these may be considered important for assessing vitamin D status in certain patient groups. 24R,25-OHD (24,25-OHD) is the most abundant product of catabolism by 25-hydroxyvitamin D-24-hydroxylase (CYP24A1) of 25-OHD, with circulating concentrations in the low µg/L region, and a half-life of approximately one week (Leeuwenkamp *et al*. 1993). Studies have suggested that when 24,25-OHD is detectable, there is good correlation between serum 24,25-OHD

and 25-OHD concentrations (Kaufmann *et al*. 2014). At low 25-OHD concentrations, 24,25-OHD is often below analytical limits of detection. Elevation in the ratio of serum 25-OHD to 24,25-OHD (25-OHD/24,25-OHD) is clinically useful to diagnose hypercalcaemia due to loss-of-function CYP24A1 mutations (Kaufmann *et al*. 2014; Ketha *et al*. 2016), and may also itself be useful to assess vitamin D deficiency. Studies have also an association between the 25-OHD to 24,25-OHD ratio and the response of 25-OHD concentrations following supplementation (Wagner *et al*. 2011; Cashman *et al*. 2015). Serum 24,25-OHD concentrations have also been shown to be reduced in chronic kidney disease (Bosworth *et al*. 2012).

Rare clinical circumstances which may warrant 1,25-OHD analysis are (i) in the differential diagnosis of patients with vitamin D hydroxylation-deficient rickets Type 1A, caused by a mutation in the 1a-hydroxylase (CYP27B1) gene, (ii) in the differential diagnosis of patients with vitamin D hydroxylation-deficient rickets Type 2A, caused by a mutation in the vitamin D receptor gene, (iii) to confirm unregulated 1,25-OHD production, e.g. in sarcoidosis or granulomatous diseases, in conjunction with high calcium and suppressed PTH, and perhaps (iv) in patients with end-stage renal disease, since the 1-alpha-hydroxylase enzyme is produced in the kidneys. Furthermore, measurement of total serum 1,25-OHD is analytically challenging since concentrations are much lower than those of 25-OHD.

Analysis of calcium and PTH are useful adjuncts to the measurement of 25-OHD. Whilst 25-OHD measurement in isolation is commonly used to clinically define vitamin D deficiency/sufficiency, serum PTH concentrations are inversely correlated with 25-OHD concentrations, and it is this PTH-to-25-OHD relationship which forms the basis of many suggested cut-off concentrations to make these clinical decisions. Generally, serum PTH is raised in vitamin D deficiency, and interrogation of the 25-OHD concentration at which serum PTH levels plateau is used to define vitamin D sufficiency. However, this is not always the case, since not all patients with hypovitaminosis D will develop secondary hyperparathyroidism (Sahota *et al*. 2004).

Whilst measurement of calcium is relatively straightforward, as demonstrated in Chapter Four, the analysis of PTH is complex, especially so in patients with kidney

disease in whom PTH fragments can accumulate and cause assay interference (Garrett *et al*. 2012). As with 25-OHD, there is a clinical need for the harmonisation of PTH testing (Sturgeon *et al*. 2012). Immunoassays are inherently sensitive techniques, but multiple iterations of two-site immunoassay methods have yet to provide a robust analytical approach to measuring PTH1-84 without interference from modified or truncated PTH isoforms. Despite claims that LC-MS/MS may offer an alternative for much needed harmonisation of PTH analysis (Sturgeon *et al.*, 2012), there remain two key problems with this approach. Firstly, as was discussed in Chapter Four, the approach referred to in the review by Sturgeon *et al*. (2012) used tryptic digestion of PTH following immunoaffinity sample preparation. This approach can not differentiate oxidised and phosphorylated PTH isoforms. This can be overcome by the analysis of intact PTH1-84, but ionisation of PTH1-84 results in significant signal dilution due to multiple charge states. For the development of reference methods for PTH, more sensitive triple quadrupole MS instruments and/or low-flow LC approaches will be required to reach the required limits of measurement from reasonable sample volumes. As with reference methods for 25-OHD, these approaches will not be suited to high-throughput clinical laboratories.

Finally, the relevance of VDBP isoforms to vitamin D status has received much literature attention recently. It has been demonstrated that the configurational differences of the three major isoforms affect the VDBP substrate binding affinity (Chun *et al*. 2014; Braithwaite *et al*. 2015). The Gc-1f isoform has the highest avidity for vitamin D metabolites, and the Gc-2 isoform the lowest (Arnaud *et al*. 1993; Bouillon *et al*. 1980). In 2013, Powe and co-workers reported data from a large cohort of black and white community-dwelling American adults, in whom VDBP was measured by immunoassay and vitamin D status (as 'bioavailable vitamin D') was assessed by calculation (Powe *et al*. 2013). The key findings of this study were (i) that black Americans had lower 25OHD than white Americans, but (ii) that since the black Americans also had lower concentrations of VDBP, the calculated bioavailable vitamin D was a better marker of vitamin D status than 25OHD. More recently however, it has been demonstrated that monoclonal immunoassays, such as that used in the Powe *et al.* study, are subject to isoform-specific differences in cross-reactivity. As studied in

Chapter Six, LC-MS/MS offers a useful alternative to immunoassays for VDBP, and is advantageous since (i) the approach does not appear influenced by VDBP genotype and (ii) the availability of isoform-specific tryptic peptides allows simultaneous genotype identification. When measured by LC-MS/MS, VDBP concentrations do not vary by race (Henderson *et al*. 2016; Denburg *et al*. 2016). Further studies are required to understand the importance of different VDBP isoforms, perhaps including the role of VDBP glycosylation.

An analytical consideration is the possible combined analysis of 25-OHD and VDBP. This has not previously been reported, but could be achieved as shown in Figure 8.1. Whole serum digests may be diluted with the supernatent from a whole serum protein precipitation or the organic extract from liquid-liquid extraction, and the combined sample analysed in a single LC-MS/MS analysis. There are some considerations to be made for this development. Firstly, the 25-OHD analysis would ideally be carried out using a PFP analytical column to resolve 3-*epi*-25-OHD metabolites. Tryptic digests are typically carried out using reversed-phase LC columns, which are unlikely to resolve the epimers. It would be required to assess the chromatographic performance of tyrptic peptides on a PFP phase, or to consider two-dimensional LC. In theory, the peptide mixture (and certainly the peptides of interest) would elute prior to the 25-OHD metabolites. An additional chromatographic consideration would be the possible effect of organic content in the injection solvent on the peptide peak shape (particularly the LPDATPK peptide). In this regard, liquid-liquid extraction with an evaporation step may be preferable. Secondly, the matrix effects which would result from the addition of a highly-complex tryptic peptide mixture would need to be assessed. Likewise, ionisation effects related to the serum extract on the tryptic peptides might be problematic.

As with 25-OHD, accurate absolute quantitation of VDBP requires further work. Reference materials are required, and this is more complex than for 25-OHD and other vitamin D metabolites. To be sure of accurate quantitation across all VDBP genotypes, individual reference compounds for each genotype will be required. This work is currently being carried out as part of the ongoing efforts of the VDSP. To include accurate representation of tertiary and quaternary protein structure, this is not a

trivial task. To additionally include and account for glycosylated protein forms is even more complex.

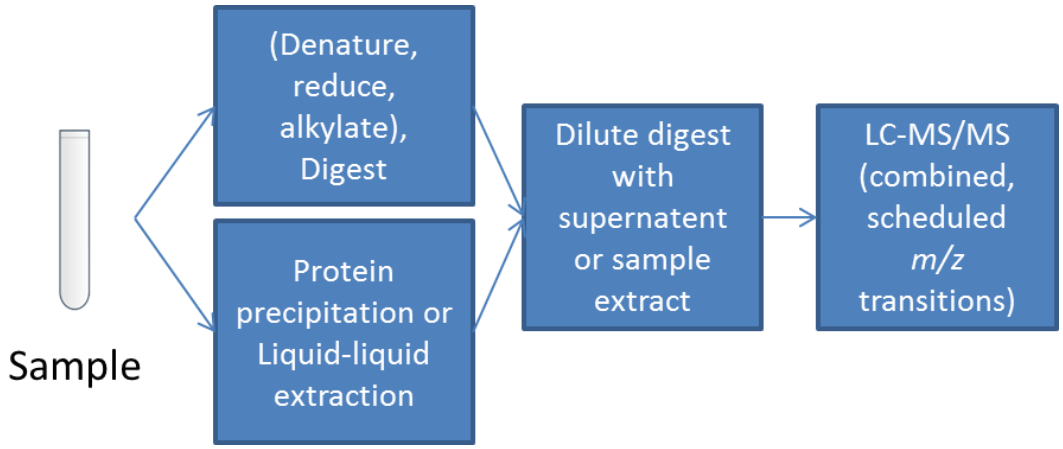

Figure 8.1. Proposed method combining VDBP and 25-OHD analysis in a single LC-MS/MS injection.

Compared to small molecule quantitation using readily available and affordable isotope-labelled analogues, methods for assay calibration for proteins using a bottom-up approach are many and varied. In Chapter 7, a novel approach was described which has potential for wide application in proteomic research. Using the developed software for searching peptide similarity and existing multi-species protein libraries, researchers can use non-human sera to access a range of intact-protein internal reference standards for quantitation of the corresponding human proteins. This software will be further developed to include non-trypsin digestion protocols, and to allow further refinement of candidate peptide lists. Formal comparison of this approach with other approaches such as labelled peptides, winged labelled peptides, and fully-labelled proteins would also be useful to validate this novel method.

To conclude, assessing vitamin D status is clinically important and directly impacts clinical decisions to treat or not treat patients. It remains the case that, either in isolation, or in combination with other well-established biomarkers such as calcium

and PTH, serum 25-OHD is the most useful biomarker available. However, it is clear that the analysis of 25-OHD is challenging, and harmonisation of testing between laboratories is still problematic. Clinicians should be aware of these pitfalls and if the information is not readily available, should ask their local laboratory for reassurance that the assay used is traceable. Participation in an EQA scheme such as DEQAS should be highly recommended. The 'gold-standard' 25-OHD analyses use LC-MS/MS, but these RMPs are often very different from those carried out in routine, high-throughput laboratories. These latter methods are designed to increase throughput, and in larger laboratories are now at least semi-automated. Again, these methods should be fully traceable to a higher order reference standard.

Analysis of additional biomarkers are useful in some rare clinical circumstances (e.g. 24,25-OHD in CYP24A1 mutations, 1,25-OHD in sarcoidosis), and tests are available in a few specialist centres for this purpose. More recent developments regarding the analysis of VDBP isoforms, the performance of monoclonal immunoassays when compared to polyclonal assays and the significant potential for LC-MS/MS for VDBP measurements require some further work, but are already providing useful insights into population-wide (or genotype-specific) differences in vitamin D status. Future developments in VDBP analysis, especially the development of reference methods, should be based on LC-MS/MS analysis individually calibrated for each VDBP isoform. Modern analytical tools and techniques such as rapid tryptic digestion, TFC, and novel approaches to protein quantitation will aid these endeavours.

References

Ackermann, B.L. & Berna, M.J., 2007. Coupling immunoaffinity techniques with MS for quantitative analysis of low-abundance protein biomarkers. *Expert Reviews in Proteomics*. **4**, 175-186.

Alam, U., Najam, D., Al-Himdani, S., Benoliel, S., Jinadev, P., Berry, J.L., Kew, M., Asqhar, O., Petropoulos, I.N., Malik, R.A., 2012. Marked vitamin D deficiency in patients with diabetes in the UK: ethnic and seasonal differences and an association with dyslipidaemia. *Diabetic Medicine*. **29**, 1343-1345.

Allan, G.M., Cranston, L., Lindblad, A., McCormack, J., Kolber, M.R., Garrison, S., Korownyck, C., 2016. Vitamin D: a narrative review examining the evidence for ten beliefs. *Journal of General and Internal Medicine.***31**, 780-791.

Almond, A., Ellis, A.R., Walker, S.W., 2012. Current parathyroid hormone immunoassays do not adequately meet the needs of patients with chronic kidney disease. *Annals of Clinical Biochemistry.* **49**,63-67.

Aloia, J., Mikhail, M., Dhaliwal, R., Shieh, R., Usera, G., Stolberg, A., Ragiola, L., Islam, S., 2015. Free 25(OH)D and the vitamin D paradox in African Americans. *Journal of Clinical Endocrinology and Metabolism*. **100**, 3356-3363.

Anderson, N.L. & Anderson, N.G., 2002. The human plasma proteome: history, character and diagnostic prospects. *Molecular and Cellular Proteomics*. **1**, 845-867.

Anderson, N.L., Anderson, N.G., Haines, L.R., Hardie, D.B., Olafson, R.W., Pearson, T.W., 2004. Mass spectrometric quantitation of peptides and proteins using stable isotope standards and capture by anti-peptide antibodies (SISCAPA). *Journal of Proteome Research*. **3**, 235-244.

Annesley, T.M., 2003. Ion suppression in mass spectrometry. *Clinical Chemistry*. **49**, 1041-1044.

Arnaud, J. & Constans, J., 1993. Affinity differences for vitamin D metabolites associated with the genetic isoforms of the human serum carrier protein (DBP). *Human Genetics*. **92**, 183-188.

Aspray, T.J., Bowring, C., Fraser, W., Gittoes, N., Javaid, M.K., Macdonald, K., Patel, S., Selby, P., Tanna, N., Francis, R., 2014. National Osteoporosis Society vitamin D guideline summary. *Age and Ageing.* **43**, 592-595.

Aurand, C.R., Bell, D.S., Wright, M., 2012. Highly selective isolation and separation of 25-hydroxyvitamin D and 3-epi-25-hydroxyvitamin D metabolites from serum. *Bioanalysis*. **4**, 2681-2691.

Aurbach, G.D., Marx, S.J., Spiegel, A.M., 1992. Parathyroid hormone, calcitonin, and the calciferols. In: Wilson JD, Foster DW, eds. Williams textbook of endocrinology. Philadelphia: WB Saunders, 1397–1517.

Ayrton, J., Dear, G.J., Leavens, W.J., Mallett, D.N., Plumb, R.S., 1997. The use of turbulent flow chromatography/mass spectrometry for the rapid, direct analysis of a novel pharmaceutical compound in plasma. *Rapid Communications in Mass Spectrometry.* **11**, 1953-1958.

Baecher, S., Geyer, R., Lehmann, C., Vogeser, M., 2014. Absorptive chemistry based extraction for LC-MS/MS analysis of small molecule analytes from biological fluids – an application for 25-hydroxyvitamin D. *Clinical Chemistry and Laboratory Medicine*. **52**, 363-371.

Barrueto, F Jr., Wang-Flores, H.H., Howland, M.A., Hoffman, R.S., Nelson, L.S., 2005. Acute vitamin D intoxication in a child. *Pediatrics*. **116**, e453-456.

Batalha, I.L., Lowe, C.R., Roque, A.C. 2012. Platforms for enrichment of phosphorylated proteins and peptides in proteomics. *Trends in Biotechnology*. **30**, 100-110.

Becker, J.O. & Hoofnagle, A.N. 2012. Replacing immunoassays with trypticdigestion-peptide immunoaffinity enrichment and LC–MS/MS. *Bioanalysis*. **4**, 281-290.

Bedner, M. & Phinney, K.W., 2012. Development and comparison of three liquid chromatography-atmospheric pressure chemical ionization/mass spectrometry

methods for determining vitamin D metabolites in human serum. *Journal of Chromatography A*. **1240**, 132-139.

Bell, D.A., Crooke, M.J., Hay, N., Glendenning, P., 2013. Prolonged vitamin D Intoxication: presentation, pathogenesis and progress. *Internal Medicine Journal*. **43**, 1148-1150.

Berna, M.J., Ackermann, B.L., Murphy, A.T., 2004. High-throughput chromatographic approaches to liquid chromatographic/tandem mass spectrometric bioanalysis to support drug discovery and development. *Analytica Chimica Acta*. **509**, 1-9.

Berson, S.A. & Yalow, R.S., 1968. Immunochemical heterogeneity of parathyroid hormone in plasma. *The Journal of Clinical Endocrinology and Metabolism*. **28**, 1037-1047.

Berson, S.A., Yalow, R.S., Aurbach, G.D., Potts, J.T., 1963. Immunoassay of Bovine and Human Parathyroid Hormone. *Proceedings of the National Academy of Sciences of the United States of America.* **49,** 613-617.

Binkley, N., Krueger, D., Cowgill, C.S., Plum, L., Lake, E., Hansen, K.E., DeLuca, H.F., Drezner, M.K., 2004. Assay variation confounds the diagnosis of hypovitaminosis D: a call for standardization. *Journal of Clinical Endocrinology & Metabolism.* **89**,3152-3157.

Binkley, N., Sempos, C.T., Vitamin D Standardization Program, 2014. Standardizing vitamin D assays: the way forward. *Journal of Bone & Mineral Research*. **29**, 1709-1714.

Bischoff-Ferrari, H.A., Giovannucci, E., Willett, W.C., Deitrich, T., Dawson-Hughes, B., 2006. Estimation of optimal serum concentrations of 25-hydroxyvitamin D for multiple health outcomes. *American Journal of Clinical Nutrition*. **84**, 18-28.

Bjelakovic, G., Gluud, L.L., Nikolova, D., Whitfield, K., Krstic, G., Wetterslev, J., Gluud, C., 2014. Vitamin D supplementation for prevention of cancer in adults. *The Cochrrane database of systematic reviews*. **6**, CD007469, doi: 10.1002/14651858.CD007469.pub2.

Bjelakovic, G., Gluud, L.L., Nikolova, D., Whitfield, K., Wetterslev, J., Simonetti, R.G., Bjelakovic, M., Gluud, C., 2014a. Vitamin D supplementation for prevention of

mortality in adults. *The Cochrrane database of systematic reviews*. **7**, CD007470, doi: 10.1002/14651858.CD007470.pub2.

Blind, E., Schmidtgayk, H., Scharla, S., Flentje, D., Fischer, S., Gohring, U., Hitzler, W., 1988. 2-Site Assay of Intact Parathyroid-Hormone in the Investigation of Primary Hyperparathyroidism and Other Disorders of Calcium-Metabolism Compared with a Midregion Assay. *Journal of Clinical Endocrinology & Metabolism.* **67,** 353-360.

Bonfiglio, R., King, R.C., Olah, T.V., Merkle, K., 1999. The effects of sample preparation methods on the variability of electrospray ionization response for model drug compounds. *Rapid Communications in Mass Spectrometry*. **13**, 1175-1185.

Bosworth, C.R., Levin, G., Robinson-Cohen, C., Hoofnagle, A.N., Ruzinski, J., Young, B., Schwartz, S.M., Himmelfarb, J., Kestenbaum, B., de Boer, I.H., 2012. The serum 24,25-dihydroxyvitamin D concentration, a marker of vitamin D catabolism, is reduced in chronic kidney disease. *Kidney International*. **82,** 693-700.

Bouillon, R., van Baelen, H., de Moor, P., 1977. The measurement of vitamin D-binding protein in human serum. *Journal of Clinical Endocrinology and Metabolism*. **45**, 225-231.

Bouillon, R., van Baelen, H., de Moor, P., 1980. Comparative study of the affinity of the serum vitamin D binding protein. *Journal of Steroid Biochemistry*. **13**, 1029-1034.

Braithwaite, V.S., Jones, K.S., Schoenmakers, I., Silver, M., Prentice, A., Hennig, B.J., 2015. Vitamin D binding protein genotype is associated with plasma 25OHD concentration in West African children. *Bone*. **74**, 166-170.

Braun, A., Bichlmaier, R., Cleve, H., 1992. Molecular analysis of the gene for human vitamin D binding protein (group-specific component): allelic differences of the common genetic GC types. *Human Genetics*. **89**, 401-406.

Bringhurst, F.R., 2003. Circulating forms of parathyroid hormone: Peeling back the onion. *Clinical Chemistry.* **49,** 1973-1975.

Bronsema, K.J., Bischoff, R., van de Merbel, N.C., 2012. Internal standards in the quantitative determination of protein biopharmaceuticals using liquid chromatography coupled to mass spectrometry. *Journal of Chromatography B*. **893-894**, 1-14.

Brossard, J.H., Whittom, S., Lepage, R., D'Amour, P., 1993. Carboxyl-terminal fragments of parathyroid hormone are not secreted preferentially in primary hyperparathyroidism as they are in other hypercalcemic conditions. *Journal of Clinical Endocrinology & Metabolism*. **77**, 413-419.

Brossard, J.H., Cloutier, M., Roy, L., Lepage, R., Gascon-Barre, N., D'Amour, P., 1996. Accumulation of a non-(1-84) molecular form of parathyroid hormone (PTH) detected by intact PTH assay in renal failure: importance in the interpretation of PTH values. *Journal of Clinical Endocrinology & Metabolism*. **81**, 3923-3929.

Brossard, J.H., Lepage, R., Cardinal, H., Roy, L., Rousseau, L., Dorais, C., D'Amour, P. 2000. Influence of glomerular filtration rate on non-(1-84) parathyroid hormone (PTH) detected by intact PTH assays. *Clinical Chemistry*. **46**, 697-703.

Bunch, D.R., Miller, A.Y., Wang, S., 2009. Development and validation of a liquid chromatography-tandem mass spectrometry assay for serum 25-hydroxyvitamin D2/D3 using turbulent flow online extraction technology. *Clinical Chemistry and Laboratory Medicine*. **47**, 1565-1572.

Callesen, A.K., Madsen, J.S., Vach, W., Kruse, T.A., Mogensen, O., Jensen, O.N. 2009. Serum protein profiling by solid phase extraction and mass spectrometry: a future diagnostics tool? *Proteomics.***9,** 1428-1441.

Capelo, J.L., Carreira, R., Diniz, M., Fernandes, L., Galesio, M., Lodeiro, C., Santos, H.M., Vale, G., 2009. Overview on modern approaches to speed up protein identification workflows relying on enzymatic cleavage and mass spectrometry based techniques. *Anaytica Chimica Acta.***650**, 151-159.

Caron, P., Maiza, J.C., Renaud, C., Cormier, C., Barres, B.H., Souberbielle, J.C., 2009. High third generation/second generation PTH ratio in a patient with parathyroid carcinoma: clinical utility of third generation/second generation PTH ratio in patients with primary hyperparathyroidism. *Clinical Endocrinology.* **70,** 533-538.

Caron, P., Simonds, W.F., Maiza, J., Rubin, M., Cantor, T., Rousseau, L., Bilezikian, J.P., Souberbielle, J., D'Amour, P., 2011. Nontruncated amino-terminal parathyroid hormone overproduction in two patients with parathyroid carcinoma: a possible link to HRPT2 gene inactivation. *Clinical Endocrinology.* **74,** 694-698.

Carter, G.D., Carter, C.R., Gunter, E., Jones, J., Jones, G., Makin, H.L.J., Sufi, S., 2004. Measurement of vitamin D metabolites: an international perspective on methodology and clinical interpretation. *Journal of Steroid Biochemistry and Molecular Biology*. **89-90**, 467-471.

Carter, G.D., Carter, R., Jones, J., Berry, J., 2004a. How accurate are assays for 25-hydroxyvitamin D? Data from the international vitamin D external quality assessment scheme. *Clinical Chemistry*. **50**, 2195-2197.

Carter, G.D., Jones, J.C., Berry, J.L., 2007. The anomalous behaviour of exogenous 25-hydroxyvitamin D in competitive binding assays. *Journal of Steroid Biochemistry and Molecular Biology.* **103**, 480-482.

Carter, G.D., 2009. 25-Hydroxyvitamin D assays: the quest for accuracy. *Clinical Chemistry*. **55**, 1300-1302.

Carter, G.D. & Jones, J., 2009. Use of a common standard improves the performance of liquid chromatography-tandem mass spectrometry methods for serum 25-hydroxyvitamin D. *Annals of clinical biochemistry*. **46**, 79-81.

Carter, G.D., Berry, J.L., Gunter, E., Jones, G., Jones, J.C., Makin, H.L.J., Sufi, S., Wheeler, M.J., 2010. Proficiency testing of 25-hydroxyvitamin D (25-OHD) assays. *Journal of Steroid Biochemistry and Molecular Biology*. **121**, 176-179.

Carter, G.D., 2011. Accuracy of 25-hydroxyvitamin D assays: confronting the issues. *Current Drug Targets*. **12**, 19-28.

Carter, G.D., 2012. 25-Hydroxyvitamin D: a difficult analyte. *Clinical Chemistry*. **58**, 486-488.

Carter, G.D., & Phinney, K.W., 2014. Assessing vitamin D status: time for a rethink? *Clinical Chemistry*. **60**, 809-811.

Carter, G.D., Jones, J.C., Shannon, J., Williams, E.L., Jones, G., Kaufmann, M., 2015. 25-Hydroxyvitamin D assays: potential interference from other circulating vitamin D metabolites. *Journal of Steroid Biochemistry and Molecular Biology.* doi: 10.1016/j.jsbmb.2015.12.018 [EPub ahead of print].

Cashman, K.D., Hayes, A., Galvin, K., Merkel, J., Jones, G., Kaufmann, M., Hoofnagel, A.N., Carter, G.D., Durazo-Arvizu, R.A., Sempos, C.T., 2015. Significance of serum 24,25-dihydroxyvitamin D in the assessment of vitamin D status: a double-edged sword? *Clinical Chemistry*. **61**, 636-645.

Cavalier, E., Daly, A.F., Betea, D., Pruteanu-Apetrii, P.N., Delanaye, P., Stubbs, P., Bradwell, A.R., Chapelle, J., Beckers, A., 2010. The Ratio of Parathyroid Hormone as Measured by Third- and Second-Generation Assays as a Marker for Parathyroid Carcinoma. *Journal of Clinical Endocrinology & Metabolism.* **95,** 3745-3749.

Chassaing, C., Stafford, H., Luckwell, J., Wright, A., Edgington, A., 2005. A parallel micro turbulent flow chromatography-tandem mass spectrometry method for the analysis of a pharmaceutical compound in plasma. *Chromatographia*. **62**, 17-24.

Chen, H., McCoy, L.F., Schleicher, R.L., Pfeiffer, C.M., 2008. Measurement of 25-hydroxyvitamin D3 (25OHD3) and 25-hydroxyvitamin D2 (25OHD2) in human serum using liquid chromatography-tandem mass spectrometry and its comparison to a radioimmunoassay method. *Clinica Chimica Acta*. **391**, 6-12.

Chen, Z., Caulfield, M., McPhaul, M.J., Reitz, R.E., Taylor, S.W., Clarke, N.J. 2013. Quantitative insulin analysis using liquid chromatography-tandem mass spectrometry in a high-throughput clinical laboratory. *Clinical Chemistry*. **59**, 1349-1356.

Cheng, J.B., Levine, M.A., Bell, N.H., Mangelsdorf, D.J., Russell, D.W., 2004. Genetic evidence that the human CYP2R1 enzyme is a key vitamin D 25-hydroxylase. *Proceedings of the National Academy of Sciences of the United States of America.* **101**, 7711-7715.

Chick, H., Palzell, E.J., Hume, E.M., 1923. Study of rickets in Vienna 1919-1922. *Medical Research Council*. Special Report No. 77.

Chick, H., 1924. Discussion on nutritional diseases in animals. *Proceedings of the Royal Society of Medicine*. **17**, 25-27.

Christiansen, M., Joergensen, C.S., Laursen, I., Hirschberg, D., Hoejrup, P., Houen, G., 2007. Protein chemical characterisation of GC globulin (vitamin D binding protein) isoforms; Gc-1f, Gc-1s, and Gc-2. *Biochimica et Biophysica Acta – Proteins and Proteomics*. **1774**, 481-492.

Chu, J-W., Yin, J., Brooks, B.R., Wang, D.I., Ricci, M.S., Brems, D.N., Trout, B.L., 2004. A comprehensive picture of non-site specific oxidation of methionine residues by peroxides in protein pharmaceuticals. *Journal of Pharmaceutical Science*. **93**, 3096-3102.

Chun, R.F., Peercy, B.E., Orwoll, E.S., Nielson, C.M., Adams, J.S., Hewison, M., 2014. Vitamin D and DBP: the free hormone hypothesis revisited. *Journal of Steroid Biochemistry and Molecular Biology*. **144**, 132-137.

Cohen-Salal, M.E., Sebert, J.L., Boudailliez, B., Marie, A., Moriniere, P., Gueris, J., Bouillon, R., Fournier, A., 1991. Comparison of intact, midregion and carboxy-terminal assays of parathyroid hormone for the diagnosis of bone disease in hemodialyzed patients. *Journal of Clinical Endocrinology and Metabolism*. **73**, 516-524.

Coldwell, R.D., Trafford, D.J., Varley, M.J., Makin, H.L., Kirk, D.N., 1989. The measurement of vitamin D2 and D3 and seven major metabolites in a single sample of human plasma using gas chromatography/mass spectrometry. *Biomedical & Environmental Mass Spectrometry*. **16**, 81-85.

Cooke, D.J., Cooke, B.R., Bell, D.A., Vasikaran, S., Glendenning, P., 2016. 25-Hydroxyvitamin D C3-epimer is universally present in neonatal Western Australian samples but is unlikely to contribute to diagnostic misclassification. *Annals of Clinical Biochemistry*. **53**, 593-298.

Cooke, N.E. & David, E.V., 1985. Serum vitamin D binding protein is a 3rd member of the albumin and alpha-fetoprotein gene family. *Journal of Clinical Investigation*. **76**, 2420-2424.

Cooper, D.P., Eastwood, M.P., Roberts, M., 2013. Internal calibration: toward random access LC-MS analysis. Presented at MSACL 2013, abstract available at http://https://www.msacl.org/2013_Long_Abstracts/201212010515_27984.pdf, accessed 9th August 2016.

Costelloe, S.J., Woolman, E., Rainbow, S., Stratiotis, L., O'Garro, G., Whiting, S., Thomas, M., 2009. Is high-throughput measurement of 25-hydroxyvitamin D3 without 25-hydroxyvitamin D2 appropriate for routine clinical use? *Annals of Clinical Biochemistry.* **46**, 86-87.

Couchman, L., 2012. Turbulent flow chromatography in bioanalysis: a review. *Biomedical Chromatography.* **26**, 892-905.

Couchman, L., Benton, C.M., Moniz, C.F., 2012. Variability in the analysis of 25-hydroxyvitamin D by liquid chromatography-tandem mass spectrometry: the devil is in the detail. *Clinica Chimica Acta*. **413**, 1239-1243.

Couchman, L., Taylor, D.R., Krastins, B., Lopez, M.F., Prakash, A., Sarracino, D.A., Garces, A., Vogelsang, M., Peterman, S., Vadali, G., Robinson, S., Moniz, C.F., 2013. Mass spectrometric immunoassay for intact parathyroid hormone: correlation with immunoassay and application to clinical samples. *Endocrine Abstracts*. **31**, 41.

Couchman, L., Taylor, D.R., Krastins, B., Lopez, M.F., Moniz, C., 2014. LC-MS candidate reference methods for the harmonisation of parathyroid hormone (PTH) measurement: a review of recent developments and future considerations. *Clinical Chemistry and Laboratory Medicine.* **52**, 1251-1263.

Couchman, L., Belsey, S.L., Handley, S.A., Flanagan, R.J., 2015. A novel approach to quantitative LC-MS/MS: therapeutic drug monitoring of clozapine and norclozapine using isotopic internal calibration. *Analytical and Bioanalytical Chemistry*. **405**, 9455-9466.

Couchman, L., Subramaniam, K., Fisher, D.S., Belsey, S.L., Handley, S.A., Flanagan R.J., 2016. Automated analysis of clozapine and norclozapine in human plasma using novel extraction plate technology and flow-injection tandem mass spectrometry. *Therapeutic Drug Monitoring*. **38**, 42-49.

Crawford, M., Rappold, B., Grant, R.P., 2013. Clinical calibration: moving away from the line. Presented at MSACL 2013, abstract available at: http://https://www.msacl.org/2013_Long_Abstracts/crawfm1labcorp_201210101341_6878583.pdf, accessed 9th August 2016.

Cundy, T., Grey, A., Reid, I.R., 2008. Calcium, phosphate and magnesium. In *Clinical Biochemistry: Molecular and Clinical Aspects*, Marshall, W.J., Bangert, S.K. (eds.), 2nd Ed. Elsevier Saunders, London.

Czerwenka, C., Maier, I., Potocnik, N., Pittner, F., Lindner, W., 2007. Absolute quantitation of beta-lactoglobulin by protein liquid chromatography-mass spectrometry and its application to different milk products. *Analytical Chemistry.***79**, 5165-5172.

D'Amour, P., Brossard, J.H., Rousseau, L., Roy, L., Gao, P., Cantor, T., 2003. Amino-terminal form of parathyroid hormone (PTH) with immunologic similarities to hPTH(1-84) is overproduced in primary and secondary hyperparathyroidism. *Clinical Chemistry.* **49,** 2037-2044.

D'Amour, P., Brossard, J.H., Rakel, A., Rousseau, L., Albert, C., Cantor, T., 2005. Evidence that the amino-terminal composition of non-(1-84) parathyroid hormone fragments starts before position 19. *Clinical Chemistry.* **51,** 169-176.

D'Amour, P., Brossard, J.H., Rousseau, L., Nguyen-Yamamoto, L., Nassif, E., Lazure, C., Gauthier, D., Lavigne, J.R., Zahradnik, R.J., 2005a. Structure of non-(1-84) PTH fragments secreted by parathyroid glands in primary and secondary hyperparathyroidism. *Kidney International.* **68,** 998-1007.

D'Amour, P., 2006. Circulating PTH molecular forms: What we know and what we don't. *Kidney International.* **70,** S29-S33.

Daniel, Y.A., Turner, C., Haynes, R.M., Hunt, B.J., Dalton, R.N., 2005. Rapid and specific detection of clinically significant haemoglobinopathies using electrospray mass spectrometry-mass spectrometry. *British Journal of Haematology*. **130**, 635-643.

Dams, R., Huestis, M.A., Lambert, W.A., Murphy, C.M., 2003. Matrix effect in bioanalysis of illicit drugs with LC-MS/MS: influence of ionization type, sample preparation, and biofluid. *Journal of the American Society of Mass Spectrometry*. **14**, 1290-1294.

De Koning, L., Al-Turkmani, M.R., Berg, A.H., Shkreta, A., Law, T., Kellogg, M.D., 2013. Variation in clinical vitamin D status by DiaSorin Liaison and LC-MS/MS in the presence of elevated 25-OH vitamin D2. *Clinica Chimica Acta*. **415**, 54-58.

De la Hunty, A., Wallace, A.M., Gibson, S., Viljakainen, H., Lamberg-Allardt, C., Ashwell, M., 2010. UK Food Standards Agency workshop consensus report: the choice of method for measuring 25-hydroxyvitamin D to estimate vitamin D status for the UK National Diet and Nutrition Surveys. *British Journal of Nutrition*. **104**, 612-619.

De Leenheer, A.P. & Cruyl, A.A., 1978. Vitamin D3 in plasma: quantitation by mass fragmentography. *Analytical Biochemistry*. **91**, 293-303.

Demetriou, E.T.W., Travison, T.G., Holick, M.F., 2012. Treatment with 50,000 IU vitamin D2 every other week and effect on serum 25-hydroxyvitamin D2, 25-hydroxyvitamin D3, and total 25-hydroxyvitamin D in a clinical setting. *Endocrine Practice*. **18**, 399-402.

Denburg, M.R., Hoofnagle, A.N., Sayed, S., Gupta, J., de Boer, I.H., Appel, L.J., Durazo-Arvizu, R., Whitehead, K., Feldman, H.I., Leonard, M.B., Chronic renal insufficiency cohort study investigators, 2016. Comparison of two ELISA methods and mass spectrometry for measurement of vitamin D-binding protein: implications for the assessment of bioavailable vitamin D concentrations across genotypes. *Journal of Bone & Mineral Research*. **31**, 1128-1136.

Deutsch, E.W., Lam, H., Aebersold, R., 2008. PeptideAtlas: a resource for target selection for emerging targeted proteomics workflows. *EMBO Reports.***9**, 429-34.

Dinis-Oliviera, R.J., 2014. Heterogeneous and homogeneous immunoassays for drug analysis. *Bioanalysis*. **6**, 2877-2896.

Divieti, P., John, M.R., Juppner, H., Bringhurst, F.R. 2002. Human PTH-(7-84) inhibits bone resorption in vitro via actions independent of the type 1 PTH/PTHrP receptor. *Endocrinology*. **143**, 171-176.

Dooley, K.C., 2003. Tandem mass spectrometry in the clinical chemistry laboratory. *Clinical Biochemistry*. **36**, 471-481.

Dole, M., Mack., L., Hines, R., Mobley, R., Ferguson, L., Alice, M., 1968. Molecular beams of macroions. *Journal of Chemical Physics*. **49**, 2240-2249.

Du, L.H. & White, R.L., 2008. Reducing glycerophosphocholine lipid matrix interference effects in biological fluid assays by high-turbulence liquid chromatography. *Rapid Communications in Mass Spectrometry*. **22**, 3362-3370.

Dubois, M., Fenaille, F., Clement, G., Lechmann, M., Tabet, J.C., Ezan, E., Becher, F., 2008. Immunopurification and mass spectrometric quantification of the active form of a chimeric therapeutic antibody in human serum. *Analytical Chemistry.* **80**, 1737-1745.

Edge, T., 2003. Turbulent flow chromatography in bioanalysis. In *Handbook of Analytical Separations*, Wilson, I.D. (ed.), Vol. 4. Elsevier Science, Oxford.

El-Khoury, J.M., Reineks, E.Z., Wang, S., 2011. Progress of liquid chromatgraphy-mass spectrometry in the measurement of vitamin D metabolites and analogues. *Clinical Biochemistry.* **44**, 66-76.

Fenn, J.B., Mann, M., Meng, C.K., Wong, S.F., Whitehouse, C.M., 1989. Electrospray ionization for mass-spectrometry of large biomolecules. *Science*. **246**, 64-71.

Flanagan, R.J., Taylor, A., Watson, I.D., Whelpton, R., 2007. Fundamentals of Analytical Toxicology. John Wiley & Sons, Chichester, UK.

Fraser, D., Kooh, S.W., Kind, H.P., Holick, M.F., Tanaka, Y., DeLuca, H.F., 1973. Pathogenesis of hereditary vitamin-D-dependent rickets – inborn error of vitamin-D metabolism involving defective conversion of 25-hydroxyvitamin-D to 1-alpha-25-dihydroxyvitamin-D. *New England Journal of Medicine*. **289**, 817-822.

Freeman, J., Wilson, K., Spears, R., Shalhoub, V., Sibley, P., 2015. Performance evaluation of four 25-hydroxyvitamin D assays to measure 25-hydroxyvitamin D2. *Clinical Biochemistry*. **48**, 1097-1104.

Friedman, P.A., 2009. Molecular biology of parathyroid hormone. In *Textbook of Nephro-endocrinology,* Singh, A., Williams, G. (eds.), Elsevier Saunders, St Louis.

Funk, C., 1911. The chemical nature of the substance that cures polyneuritis in birds produced by a diet of polished rice. *Journal of Physiology*. **43**, 395-402.

Galceran, T., Lewis-Finch, J., Martin, K.J., Slatopolsky, E., 1984. Absence of biological effects of oxidized parathyroid hormone-(1-34) in dogs and rats. *Endocrinology*. **115**, 2375-2378.

Gao, P., Scheibel, S., D'Amour, P., John, M.R., Rao, S.D., Schmidt-Gayk, H., Cantor, T.L., 2001. Development of a novel immunoradiometric assay exclusively for biologically active whole parathyroid hormone 1-84: implications for improvement of accurate assessment of parathyroid function. *Journal of Bone and Mineral Research*. **16**,605-614.

Garrett, G., Sardiwal, S., Lamb, E.J., Goldsmith, D.J.A., 2013. PTH-A Particularly Tricky Hormone: Why Measure It at All in Kidney Patients? *Clinical Journal of the American Society of Nephrology.* **8,** 299-312.

Goodman, W.G., 2005. The evolution of assays for parathyroid hormone. *Seminars in Dialysis.* **18,** 296-301.

Guo, T., Taylor, R.L., Singh, R.J., Soldin, S.J., 2006. Simultaneous determination of 12 steroids by isotope dilution liquid chromatography-photospray ionization tandem mass spectrometry. *Clinica Chimica Acta.***372**, 76-82.

Haddad, J.C. & Chyu, K.J., 1971. Competitive protein-binding radioassay for 25-hydroxycholecalciferol. *Journal of Clinical Endocrinology and Metabolism*. **33**, 992-995.

Hardman, M. & Makarov, A.A., 2003. Interfacing the orbitrap mass analyzer to an electrospray ion source. *Analytical Chemistry*. **75**, 1699-1705.

Heaney, R.P., 2013. Health is better at serum 25(OH)D above 30 µg/L. *Journal of Steroid Biochemistry and Molecular Biology.***136**, 224-228.

Heijboer, A.C., Blankenstein, M.A., Kema, I.P., Buijs, M.M., 2012. Accuracy of 6 routine 25-hydroxyvitamin D assays: influence of vitamin D binding protein concentration. *Clinical Chemistry*. **58**, 543-548.

Henderson, C.M., Lutsley, P.L., Misialek, J.R., Laha, T.J., Selvin, E., Eckfeldt, J.H., Hoofnagle, A.N., 2016. Measurement by a novel LC-MS/MS methodology reveals similar serum concentrations of vitamin D binding protein in blacks and whites. *Clinical Chemistry.***62**, 179-187.

Herman, J.L., 2004. Generic approach to high throughput ADME screening for lead candidate optimization. *International Journal of Mass Spectrometry*. **238**, 107-117.

Herman, J.L., 2005. The use of turbulent flow chromatography and the isocratic focussing effect to achieve on-line cleanup and concentration of neat biological samples for low-level metabolite analysis. *Rapid Communications in Mass Spectrometry*. **19**, 696-700.

Herman J.L. & Edge, T., 2012. Theoretical concepts and applications of turbulent flow chromatography. *LCGC North America*. **3**, 200-214.

Hermann, M., Harwood, T., Gaston-Parry, O., Kouzios, D., Wong, T., Lih, A., Jimenez, M., Janu, M., Seibel, M.J., 2010. A new quantitative LC tandem mass spectrometry assay for serum 25-hydroxyvitamin D. *Steroids*. **75**, 1106-1112.

Hess, A.F. & Unger, A.L., 1921. The cure of infantile rickets by sunlight. *Journal of the American Medical Association*. **77**, 39-41.

Hess, A.F., Unger, L.J., Pappenheimer, A.M., 1921. Experimental rickets in rats: VII. The prevention of rickets by sunlight, by the rays of the mercury lamp, and by the carbon arc lamp. *The Journal of Experimental Medicine*. **36**, 427-476.

Hess, A. & Weinstock, M., 1924. Antirachitic properties imparted to lettuce and to growing wheat by ultraviolet irradiation. *Proceedings of the Society of Experimental Biological Medicine*. **22**, 5-6.

Hocher, B., Armbruster, F.P., Stoeva, S., Reichetzeder, C., Gron, H.J., Lieker, I., Khadzhynov, D., Slowinski, T., Roth, H.J., 2012. Measuring parathyroid hormone (PTH) in patients with oxidative stress – do we need a fourth generation parathyroid hormone assay? *PLoS One*. **7**, e40242 (doi: 10.1371/journal.pone.0040242).

Hocher, B., Oberthur, D., Slowinski, T., Querfeld, U., Schaefer, F., Doyon, A., Tepel, M., Roth, H.J., Gron, H.J., Reichetzeder, C., Betzel, C., Armbruster, F.P., 2013. Modeling of oxidized PTH (oxPTH) and non-oxidized PTH (n-oxPTH) receptor binding and relationship of oxidized to non-oxidized PTH in children with chronic renal failure, adult patients on hemodialysis and kidney transplant recipients. *Kidney and Blood Pressure Research*. **37**, 240-251.

Holick, M.F., Maclaughlin, J.A., Clark, M.B., Holick, S.A., Potts, J.T., Anderson, R.R., Blank, I.H., Parrish, J.A., 1980. Photosynthesis of previtamin-D3 in human skin and the physiologic consequences. *Science*. **210**, 203-205.

Holick, M.F., 1987. Photosynthesis of vitamin-D in the skin – effect of environmental and life-style variable. *Federation Proceedings*. **46**, 1876-1882.

Holick, M.F., 2006. High prevalence of vitamin D inadequacy and implications for health. *Mayo Clinic Proceedings*. **81**, 353-373.

Holick, M.F., 2007. Vitamin D deficiency. *New England Journal of Medicine*. **357**, 266-281.

Holick, M.F., 2008. Deficiency of sunlight and vitamin D. *British Medical Journal*. 336, 1318-1319.

Holick, M.F., 2009. Vitamin D status: measurement, interpretation and clinical application. *Annals of Epidemiology*. **19**, 73-78.

Holick, M.F., Binkley, N.C., Bischoff-Ferrari, H.A., Gordon, C.M., Hanley, D.A., Heaney, R.P., Murad, M.H., Weaver, C.M., 2011. Evaluation, treatment, and prevention of vitamin D deficiency: an Endocrine Society clinical practice guideline. *Journal of Clinical Endocrinology and Metabolism*. **96**, 1911-1930.

Hollis, B.W. & Napoli, J.L., 1985. Improved radioimmunoassay for vitamin D and its use in assessing vitamin D status. *Clinical Chemistry*. **31**, 1815-1819.

Hollis, B.W., 2004. The determination of circulating 25-hydroxyvitamin D: no easy task. *Journal of Clinical Endocrinology & Metabolism.***89**, 3149-3151.

Hollis, B.W., Marshall, D.T., Savage, S.J., Garrett-Mayer, E., Kindy, M.S., Gattoni-Celli, S., 2013. Vitamin D3 supplementation, low-risk prostate cancer, and health disparities. Journal of Steroid Biochemistry & Molecular Biology. **136**, 233-237.

Hollis, B.W. & Bickle, D.D., 2014. Vitamin D-binding protein and vitamin D in blacks and whites. *New England Journal of Medicine.* **370**, 879-880.

Holman, S.W., Sims, P.F., Eyers, C.E., 2012. The use of selected reaction monitoring in quantitative proteomics. *Bioanalysis*. **4**, 1763-1786.

Holmes, E.W., Garbincius, J., McKenna, K.M., 2013. Analytical variability among methods for the measurement of 25-hydroxyvitamin D: still adding to the noise. *American Journal of Clinical Pathology*. **140**, 550-560.

Hoofnagle, A.N. & Wener, M.H., 2009. The fundamental flaws of immunoassays and potential solutions using tandem mass spectrometry. *Journal of Immunological Methods.* **347**, 3-11.

Hopkins, F.G., 1912. Feeding experiments illustrating the importance of accessory factors in normal dietaries. *The Journal of Physiology*. **44**, 425-460.

Horiuchi, N., 1988. Effects of oxidation of human parathyroid hormone on its biological activity in continuously infused, thyroparathyroidectomized rats. *Journal of Bone and Mineral Research*. **3**, 353-358.

Hossein-Nezhad, A. & Holick, M.F., 2013. Vitamin D for health: a global perspective. *Mayo Clinic Proceedings*. **88**, 720-755.

Hu, Q., Noll, R.J., Li, H., Makarov, A.A., Hardman, M., Cooks, R.G., 2005. The orbitrap: a new mass spectrometer. *Journal of Mass Spectrometry*. **40**, 430-443.

Hulshinsky, K., 1919. Heilung von rachitis durch künstlich hohen-sonne. *Deutsche Medizinische Wochenschrift.* **45**, 712–713.

Hume, E.M. &Smith, H.H., 1924. The effect of irradiation of the environment with ultra-violet light upon the growth and calcification of rats, fed on a diet deficient in fat-soluble vitamins. The part played by irradiated sawdust. *The Biochemical Journal*. **18**, 1334-1348.

Hummer, L., Nilas, L., Tjellesen, L., Christiansen, C., 1984. A selective and simplified radioimmunoassay of 25-hydroxyvitamin D3. *Scandinavian Journal of Clinical Laboratory Investigation*. **44**, 163-167.

Ikekawa, N. & Koizumi, N., 1976. Separation of vitamin D metabolites and their analogues by high-pressure liquid chromatography. *Journal of Chromatography*. **119**, 227-232.

Institute of Medicine (US) Committee to Review Dietary Reference Intakes for Vitamin D and Calcium; Ross AC, Taylor CL, Yaktine A.L., Del Valle, H.B., editors. Dietary Reference Intakes for Calcium and Vitamin D. Washington (DC): National Academies Press (US); 2011. Available from: http://www.ncbi.nlm.nih.gov/books/NBK56070, accessed 7th July 2015.

Iwasaki, Y., Nakano, Y., Mochizuki, K., Nomoto, M., Takahashi, Y., Ito, R., Saito, K., Nakazawa, H., 2011. A new strategy for ionization enhancement by derivatization for mass spectrometry. *Journal of Chromatography B*. **879**, 1159-1165.

Janusch, F., Kalthoff, L., Hamscher, G., Mohring, S.A.I., 2013. Evaluation and subsequent minimization of matrix effects caused by phospholipids in LC-MS analysis of biological samples. *Bioanlaysis*. **5**, 2101-2114.

Jemielita, T.O., Leonard, M.B., Baker, J., Sayed, S., Zemel, B.S., Shults, J., Herskovitz, R., Denburg, M.R., 2016. Association of 25-hydroxyvitamin D with areal and volumetric measures of bone density and parathyroid hormone: impact of vitamin D binding protein and its assays. *Osteoporosis International*. **27**, 617-626.

John, M.R., Coolman, W.G., Gao, P., Cantor, T., Salusky, I.B., Juppner, H. 1999. A novel immunoradiometric assay detects full-length human PTH but not amino-terminally truncated fragments: implications for PTH measurements in renal failure. *Journal of Clinical Endocrinology & Metabolism.* **84**,4287-4290.

Jones, G. & De Luca, H.F., 1975. High pressure liquid chromatography: separation of the metabolites of vitamin D2 and D3 on small-particle silica columns. *Journal of Lipid Research*. **16**, 448-453.

Jones, G., 1978. Assay of vitamins D2 and D3, and 25-hydroxyvitamins D2 and D3 in human plasma by high-performance liquid chromatography. *Clinical Chemistry*. **24**, 287-298.

Jones, G., 2012. Metabolism and biomarkers of vitamin D. *Scandinavian Journal of Clinical & Laboratory Investigation*. **72** (S243), 7-13.

Jones, G., Prosser, D.E., Kaufmann, M., 2012. 25-hydroxyvitamin D-24-hydroxylase (CYP24A1): its important role in the degradation of vitamin D. *Archives of Biochemistry and Biophysics*. **523**, 9-18.

Kaufmann, M., Gallagher, J.C., Peacock, M., Schlingmann, K.P., Konrad, M., DeLuca, H.F., Siqueiro, R., Lopez, B., Mourino, A., Maestro, M., St. Arnaud, R., Finkelstein, J.S., Cooper, D.P., Jones, G., 2014. Clinical utility of simultaneous quantitation of 25-hydroxyvitamin D and 24,25-dihydroxyvitamin D by LC-MS/MS involving derivatization with DMEQ-TAD. *Journal of Clinical Endocrinology and Metabolism.* **99**, 2567-2574.

Ketha, H., Kumar, R., Singh, R.J., 2016. LC-MS/MS for identifying patients with CYP24A1 mutations. *Clinical Chemistry.* **62**, 236-242.

Kiernan, U., Tubbs, K.A., Gruber, K., Nedelkov, D., Niederkofler, E.E., Williams, P., Nelson, R.W. 2002. High-throughput protein characterization using mass spectrometric immunoassay. *Analytical Biochemistry*. **301**, 49-56.

Konerman, L., Ahadi, E., Rodriguez, A.D., Vahidi, S., 2013. Unraveling the mechanism of electrospray ionization. *Analytical Chemistry*. **85**, 2-9.

Krastins, B., Prakash, A., Sarracino, D.A., Nedelkov, D., Neiderkofler, E.E., Kiernan, U.A., Nelson, R.W., Vogelsang, M.A., Vadali, G., Garces, A., Sutton, J.N., Peterman, S., Byram, G., Darbouret, B., Perusse, J., Seidah, N.G., Coulombe, B., Goborn, J., Portelius, E., Pannee, J., Blennow, K., Kulasingam, V., Couchman, L., Moniz, C., Lopez, M.F. 2013. Rapid development of sensitive, high-throughput, quantitative and highly selective mass spectrometric targeted immunoassays for clinically important proteins in human plasma and serum. *Clinical Biochemistry*. **46**, 399-410.

Krokhin, O.V. & Spicer, V., 2009. Peptide retention standards and hydrophobicity indexes in reversed-phase high-performance liquid chromatography of peptides. *Analytical Chemistry.***81**, 9522-9530.

Kumar, V., Barnidge, D.R., Chen, L-S., Twentyman, J.M., Cradic, K.W., Grebe, S., Singh, R.J. 2010. Quantification of serum 1-84 parathyroid hormone in patients with hyperparathyroidism by immunocapture in situ digestion liquid chromatography-tandem mass spectrometry. *Clinical Chemistry*. **56**, 306-313.

Kyte, J. & Doolittle, R.F., 1982. A simple method for displaying the hydropathic character of a protein. *Journal of Molecular Biology*. **157**, 105-132.

Lafferty, F.W., Hamlin, C.R., Corrado, K.R., Arnold, A., Shuck, J.M. 2006. Primary hyperparathyroidism with a low-normal, atypical serum parathyroid hormone as shown by discordant immunoassay curves. *Journal of Clinical Endocrinology and Metabolism*. **91**, 3826-3829.

Lai, J.K., Lucas, R.M., Banks, E., Ponsonby, A.L., Ausimmune Investigator Group, 2012. Variability in vitamin D assays imparis clinical assessment of vitamin D status. *International Medicine Journal*. **42**, 43-50.

Lange, V., Picotti, P., Domon, B., Aebersold, R., 2008. Selected reaction monitoring for quantitative proteomics: a tutorial. *Molecular Systems Biology.***4**, 222.

Lauridsen, A.L., Vestergaard, P., Nexo, E., 2001. Mean serum concentration of vitamin D binding protein (Gc globulin) is related to Gc phenotype in women. *Clinical Chemistry*. **47**, 753-756.

Lauridsen, A.L., Vestergaard, P., Hermann, A.P., Brot, C., Heickendorff, L., Mosekilde, L., Nexo, E., 2005. Plasma concentrations of 25-hydroxyvitamin D and 1,25-dihydroxyvitamin D are related to the phenotype of Gc (vitamin D-binding protein): a cross-sectional study on 595 early postmenopausal women. *Calcified Tissue International*. **77**, 15-22.

Leeuwenkamp, O., van der Weil, H., Lips, P., van der Vijgh, W.J., Barto, R., Greuter, H., Netelenbos, J.C., 1993. Human pharmacokinetics of orally administered (24R)-hydroxycalcidiol. *European Journal of Clinical Chemistry and Clinical Biochemistry.* **31**, 419-426.

Lehmann, S., Hoofnagle, A., Hochstrasser, D., Brede, C., Glueckmann, M., Cocho, J.A., Ceglarek, U., Lenz, C., Vialaret, J., Scherl, A., Hirtz, C., IFCC working group on clinical quantitative mass spectrometry proteomics, 2013. Quantitative Clinical Chemistry Proteomics (qCCP) using mass spectrometry: general characteristics and application. *Clinical Chemistry and Laboratory Medicine*. **51**, 919-935.

Lepage, R., Roy, L., Brossard, J.H., Rousseau, L., Dorais, C., Lazure, C., D'Amour, P. 1998. A non-(1-84) circulating parathyroid hormone (PTH) fragment interferes significantly with intact PTH commercial assay measurements in uremic patients. *Clinical Chemistry*. **44**, 805-809.

Levenschtein, V.I., 1966. Binary codes capable of correcting deletions, insertions and reversals. *Soviet Physics-Doklady*. **10**, 707-710.

Li, H., Rose, M.J., Tran, L., Zhang, J., Miranda, L.P., James, C.A., Sasu, B.J. 2009. Development of a method for the sensitive and quantitative determination of hepcidin in human serum using LC-MS/MS. *Journal of Pharmacological and Toxicological Methods*. **59**, 171-180.

Liesener, A. & Karst, U., 2005. Turbulent flow chromatography for the reduction of matrix effects in electrospray ionization mass spectrometry-based enzyme assays. *Journal of Separation Science*. **28**, 1658-1665.

Little, J.L., Wempe, M.F., Buchanan, C.M., 2006. Liquid chromatography-mass spectrometry/mass spectrometry method development for drug metabolism studies:

examining lipid matrix ionization effects in plasma. *Journal of Chromatography B.* **833**, 219-230.

Lodder, H., Challenger, K., Edgington, A., Williams, L., Jones, R., Teehan, K-J., Senior, A., Davies, G., Jordan, S., Desbrow, C., Roberts, P., Vandell, V., Gairloch, E., 2015. Comparison of 25-hydrovitamin D extraction using supported liquid extraction and phospholipid depletion plate technology using manual and automated sample preparation prior to LC-MS analysis. Presented at MSACL 2015, abstract available at: https://www.msacl.org/2015_US_Long_Abstracts/201502111009_22497.pdf, accessed 9th August 2016.

Lopez, M.F., Rezai, T., Sarracino, D.A., Prakash, A., Krastins, B., Athanas, M., Singh, R.J., Barnidge, D.R., Oran, P., Borges, C., Nelson, R.W. 2010. Selected reaction monitoring-mass spectrometric immunoassay responsive to parathyroid hormone and related variants. *Clinical Chemistry*. **56**, 281-290.

Makarov, A., 2000. Electrostatic axially harmonic orbital trapping: a high-performance technique of mass analysis. *Analytical Chemistry*. **72**, 1156-1162.

Malik, S., Fu, L., Juras, D.J., Karmali, M., Wong, B.Y.L., Gozdzik, A., Cole, D.E., 2013. Common variants of the vitamin D binding protein gene and adverse health outcomes. *Critical Reviews in Clinical Laboratory Sciences*. **50**, 1-22.

Martin, A.J.P., & Synge, R.L.M., 1941. A new form of chromatogram employing two liquid phases. *Biochemical Journal*. **35**, 1358-1368.

Masuda, S., Okano, T., Kamao, M., Kanedai, Y., Kobayashi, T., 1997. A novel high-performance liquid chromatography assay for vitamin D metabolites using a coulometric electrochemical detector. *Journal of Pharmaceutical and Biomedical Analysis*. **15**, 1497-1502.

Matuzewski, B.K., Constanzer, M.L., Chavez-Eng, C.M., 2003. Strategies for the assessment of matrix effect in quantitative bioanalytical methods based on HPLC-MS/MS. *Analytical Chemistry*. **75**, 3019-3030.

Matuzewski, B.K., 2006. Standard line slopes as a measure of relative matrix effects in quantitative HPLC-MS bioanalysis. *Journal of Chromatography B*. **830**, 293-300.

Mayer, E. & Schmidt-Gayk, H., 1984. Interlaboratory comparison of 25-hydroxyvitamin D determination. *Clinical Chemistry*. **30**, 1199-1204.

McCollum, E.V. & Davis, M., 1913. The necessity of certain lipins in the diet during growth. *Journal of Biological Chemistry*. **25**, 167-175.

McCollum, E.V., 1914. Butter-fat in infant feeding. *Journal of the American Medical Association*. **63**, 420.

McCollum, E.V., 1918. Influence of heat on growth-promoting properties of food. *American Journal of Public Health*. **8**, 191-194.

Mellanby, E., 1920. Discussion on the importance of accessory food factors (vitamines) in the feeding of infants. *Proceedings of the Royal Society of Medicine*. **13**, 57-77.

Mellanby, E., 1924. A British Medical Association lecture on deficiency diseases, with special reference to rickets. *British Medical Journal.***1**, 895-900.

Michopoulos, F., Edge, A.M., Theodoridis, G., Wilson, I.D., 2010. Application of turbulent flow chromatography to the metabonomic analysis of human plasma: comparison with protein precipitation. *Journal of Separation Science*. **33**, 1472-1479.

Mineva, E.M., Schlecher, R.L., Chaudhary-Webb, M., Maw, K.L., Botelho, J.C., Vesper, H.W., Pfeiffer, C.M., 2015. A candidate reference measurement procedure for quantifying serum concentrations of 25-hydroxyvitamin D3 and 25-hydroxyvitamin D2 using isotope-dilution liquid chromatography-tandem mass spectrometry. *Analytical and Bioanalytical Chemistry*. **407**, 5615-5624.

Mitchell, W.M. & Harrington, W.F. 1968. Purification and properties of Clostridiopeptidase B (Clostripain). *The Journal of Biological Chemistry*. **243**, 4683-4692.

Mitri, J., Muraru, M.D., Pittas, A.G., 2011. Vitamin D and type 2 diabetes: a systematic review. *European Journal of Clinical Nutrition*. **65**, 1005-1015.

Molnar, F., Siqueiro, R., Sato, Y., Araujo, C., Schuster, I., Antony, P., Peluso, J., Muller, C., Mourino, A., Moras, D., Rochel, N., 2011. 1-alpha,25(OH)2-3-epi-vitamin D3, a natural physiological metabolite of vitamin D3: its synthesis, biological activity and crystal structure with its receptor. *PloS One*. **6**, e18124 (doi: 10.1371/journal.pone.0018124).

Morgan, P.E., Couchman, L., Robinson, S., McDonnell, S., Flanagan, R.J., 2010. Analysis of clozapine and norclozapine in plasma using on-line sample preparation and LC-MS/MS. *The Column*. **6**, 10-16.

Mosekilde, L., Torring, O., Rejnmark, L., 2011. Emerging anabolic treatments in osteoporosis. *Current Drug Safety*. **6**, 62-74.

Mundy, G.R. & Guise, T.A., 1999. Hormonal control of calcium homeostasis. *Clinical Chemistry*. **45**, 1347-1352.

Nedelkov, D. 2006. Mass spectrometry-based immunoassays for the next phase of clinical applications. *Expert Reviews in Proteomics*. **3**, 631-640.

Nedelkov, D. 2012. Mass spectrometry-based protein assays for in vitro diagnostic testing. *Expert Reviews in Molecular Diagnostics*. **12**, 235-239.

Nelson, R.W., Krone, J.R., Bieber, A.L., Williams, P., 1995. Mass spectrometric immunoassay. *Analytical Chemistry*. **67**, 1153-1158.

Netzel, B.C., Cradic, K.W., Bro, E.T., Girtman, A.B., Cyr, R.C., Singh, R.J., Grebe, S.K., 2011. Increasing liquid chromatography-tandem mass spectrometry throughput by mass-tagging: a sample-multiplexed high-throughput assay for 25-hydroxyvitamin D-2 and D-3. *Clinical Chemistry*. **57**, 431-440.

Nielson, C.M., Jones, K.S., Chun, R.F., Jacobs, J.M, Wang, Y., Hewison, M., Adams, J.S., Swanson, C.M., Lee, C.G., Vanderschueren, D., Pauwels, S., Prentice, A., Smith, R.D., Shi, T., Gao, Y., Schepmoes, A.A., Zmuda, J.M., Lapidus, J., Cauley, J.A., Bouillon, R., Schoenmakers, I., Orwoll, E.S., Osteoporotic fractures in men (MrOS) research group, 2016. Free 25-hydroxyvitamin D: impact of vitamin D binding protein assays on racial-

genotype associations. *Journal of Clinical Endocrinology and Metabolism.* **101**, 2226-2234.

Ng, L.L., Sandhu, J.K., Squire, I.B., Davies, J.E., Jones, D.J., 2013. Vitamin D and prognosis in acute myocardial infarction. *International Journal of Cardiology*. **168**, 2341-2346.

Nordgren, H.K., Holmgren, P., Liljeberg, P., Eriksson, N., Beck, O., 2005. Application of direct urine LC-MS/MS analysis for screening of novel substances in drug abusers. *Journal of Analytical Toxicology*. **29**, 234-239.

Nurmi, T., Tuomainen, T.P., Virtanen, J., Mursu, J., Voutilainen, S., 2013. High-performance liquid chromatography and coulometric electrode array detector in serum 25-hydroxyvitamin D3 and 25-hydroxyvitamin D2 analyses. *Analytical Biochemistry*. **435**, 1-9.

Nussbaum, S.R., Zahradnik, R.J., Lavigne, J.R., Brennan, G.L., Nozawaung, K., Kim, L.Y., Keutmann, H.T., Wang, C.A., Potts, J.T., Segre, G.V., 1987. Highly Sensitive 2-Site Immunoradiometric Assay of Parathyrin, and its Clinical Utility in Evaluating Patients with Hypercalcemia. *Clinical Chemistry.* **33,** 1364-1367.

Olson, M.T., Breaud, A., Harlan, R., Emezienna, N., Schools, S., Yergey, A.L., Clarke, W., 2013. Alternative calibration strategies for the clinical laboratory: application to nortriptyline therapeutic drug monitoring. *Clinical Chemistry*. **59**, 920-927.

Ong, L., Saw, S., Sahabdeen, N.B., Tey, K.T., Ho, C.S., Sethi, S.K., 2012. Current 25-hydroxyvitamin D assays: do they pass the test? *Clinica Chimica Acta*. **413**, 1127-1134.

Pasco, J.A., Henry, M.J., Kotowicz, M.A., Sanders, K.M., Seeman, E., Pasco, J.R., Schneider, H.G., Nicholson, G.C., 2004. Seasonal periodicity of serum vitamin D and parathyroid hormone, bone resorption, and fractures: the Geelong osteoporosis study. *Journal of Bone and Mineral Research*. **19**, 752-758.

Peterman, S., Neiderkofler, E.E., Phillips, D.A., Krastins, B., Kiernan, U.A., Tubbs, K.A., Nedelkov, D., Prakash, A., Vogelsang, M.A., Schoeder, T., Couchman, L., Taylor, D.R., Moniz, C.F., Vadali, G., Byram, G., Lopez, M.F., 2014. An automated, high-throughput

method for targeted quantitation of intact insulin and its therapeutic analogs in human serum or plasma coupling mass spectrometric immunoassay with high resolution and accurate mass detection (MSIA-HR/AM). *Proteomics.***14**, 1445-1456.

Peters, F.T. & Maurer, H.H., 2007. Systematic comparison of bias and precision data obtained with multiple-point and one-point calibration in six validated multianalyte assays for quantification of drugs in human plasma. *Analytical Chemistry*. **79**, 4967-4976.

Picotti, P. & Aebersold, R., 2012.Selected reaction monitoring-based proteomics: workflows, potential, pitfalls and future directions. *Nature Methods.***9**, 555-566.

Pliener-Duxneuner, J., Zwettler, E., Paschalis, E., Roschger, P., Nell-Duxneuner, V., Klaushofer, K., 2009. Treatment of osteoporosis with parathyroid hormone and teriparatide. *Calcified Tissue International*. **84**, 159-170.

Pludowski, P., Karczmarewicz, E., Bayer, M., Carter, G., Chlebna-Sokol, D., Debski, R., Desci, T., Dobrzanska, A., Franek, E., Gluszko, P., Grant, W.B., Holick, M.F., Yankovskaya, L., Konstantynowicz, J., Ksiazyk, J.B., Ksiezopolska-Orlowska, K., Lewinski, A., Litwin, M., Lohner, S., Lorenc, R.S., Lukaszkiewicz, L., Marcinowska-Suchowierska, E., Milewicz, A., Misiorowski, W., Nowicki, M., Povoroznyuk, V., Rozentryt, P., Rudenska, E., Schoenfeld, Y., Socha, P., Solnica, B., Szalecki, M., Talalaj, M., Varbiro, S., Zmijewski, M.A., 2013. Practical guidelines for the supplementation of vitamin D and the treatment of deficits in central Europe – recommended vitamin D intakes in the general population and groups at risk of vitamin D deficiency. *Endokrynologia Polska.***64**, 319-327.

Powe, C.E., Evans, M.K., Wenger, J., Zonderman, A.B., Berg, A.H., Nalls, M., Tamez, H., Zhang, D., Bhan, I., Karumanchi, S.A., Powe, N.R., Thadani, R., 2013. Vitamin D binding protein and vitamin D status of black Americans and white Americans. *New England Journal of Medicine*. **369**, 1991-2000.

Pramyothin, P. &Holick, M.F., 2012. Vitamin D supplementation: guidelines and evidence for subclinical deficiency. *Current Opinion in Gastroenterology*. **28**, 139-150.

Pratt, J.M., Simpson, D.M., Doherty, M.K., Rivers, J., Gaskell, S.J., Beynon, R.J., 2006. Multiplexed absolute quantitation for proteomics using concatenated signature peptides encoded by QconCAT genes. *Nature Protocols*. **1**, 1029-1043.

Pretorius, V. & Smuts, T.W., 1966. Turbulent flow chromatography: a new approach to faster analysis. *Analytical Chemistry*. **38**, 274-281.

Quarles, L.D., Lobaugh, B., Murphy, G. 1992. Intact parathyroid hormone overestimates the presence and severity of parathyroid-mediated osseous abnormalities in uremia. *Journal of Clinical Endocrinology and Metabolism*. **75**, 145-150.

Quinn, H.M. & Takarewski, J.J., 1999. High performance liquid chromatography and apparatus. US Patent No 5,919,368, filed December 1997.

Rabbani, S.A., Kremer, R., Bennett, H.P.J., Goltzman, D. 1984. Phosphorylation of parathyroid hormone by human and bovine parathyroid glands. *Journal of Biological Chemistry*. **259**, 2949-2955.

Rajakumar, K., Reis, E.C., Holick, M.F., 2013. Dosing error with over-the-counter vitamin D supplement: a risk for vitamin D toxicity in infants. *Clinical Pediatrics*. **52**, 82-85.

Rappsilber, J., Mann, M., Ishihama, Y., 2007. Protocol for micro-purification, enrichment, pre-fractionation and storage of peptides for proteomics using StageTips. *Nature Protocols.* **2**, 1896-1906.

Rasheed, K., Sethi, P., Bixby, E., 2014. Severe vitamin D deficiency induced myopathy associated with rhabdomyolysis. *North American Journal of Medical Sciences*. **5**, 334-336.

Rauh, M. 2009. Steroid measurement with LC-MS/MS in pediatric endocrinology. *Molecular and Cellular Endocrinology*. **301**, 272-281.

Ray, R., Banks, M., Abuzahra, H., Eddy, V.J., Persons, K.S., Lucia, M.S., Lambert, J.R., Holick, M.F., 2012. Effect of dietary vitamin D and calcium on the growth of androgen-

insensitive human prostate tumor in a murine model. *Anticancer Research*. **32**, 727-731.

Ravnsborg, T., Olsen, D.T., Thysen, A.H., Christiansen, M., Houen, G., Heojrup, P., 2010. The glycosylation and characterisation of the candidate Gc macrophage activating factor. *Biochimica et Biophysica Acta*. **1804**, 909-917.

Roepstorff, P. & Fohlman, J. 1984. Proposal for a common nomenclature for sequence ions in mass spectra of peptides. *Biomedical Mass Spectrometry*. **11**, 601.

Roth, H.J., Schmidt-Gayk, H., Weber, H., Niederau, C., 2008. Accuracy and clinical implications of seven 25-hydroxyvitamin D methods compared with liquid chromatography–tandem mass spectrometry as a reference. *Annals of Clinical Biochemistry*.**45**, 153-159.

Rosen, C.J., Abrams, S.A., Aloia, J.F., Brannon, P.M, Clinton, S.K., Duraro-Arvizu, R.A., Gallagher, J.C., Gallo, R.L., Jones, G., Kovacs, C.S., Manson, J.E., Mayne, S.T., Ross, A.C., Shapses, S.A., Taylor, C.L., 2012. IOM Committee members respond to Endocrine Society vitamin D guideline. *Journal of Clinical Endocrinology and Metabolism*. **97**, 1146-1152.

Ross, A.C., Manson, J.E., Abrams, S.A., Aloia, J.F., Brannon, P.M., Clinton, S.K., Durazo-Arvizu, R.A., Gallagher, J.C., Gallo, R.L., Jones, G., Kovacs, C.S., Mayne, S.T., Rosen, C.J., Shapses, S.A., 2011. The 2011 report on dietary reference intakes for calcium and vitamin D from the Institute of Medicine: what clinicians need to know. *Journal of Clinical Endocrinology & Metabolism*. **96**, 53-58.

Roth, H.J., Schmidt-Gayk, H., Weber, H., Niederau, C., 2008. Accuracy and clinical implications of seven 25-hydroxyvitamin D methods compared with liquid chromatography-tandem mass spectrometry. *Annals of Clinical Biochemistry*. **45**, 153-159.

Rubin, M.R., Silverberg, S.J., D'Amour, P., Brossard, J.H., Rousseau, L., Sliney, J. Jr, *et al*. 2007. An N-terminal molecular form of parathyroid hormone (PTH) distinct from hPTH(1-84) is overproduced in parathyroid carcinoma. *Clinical Chemistry*. **53**, 1470-1476.

Sahota, O., Mundey, M.K., San, P., Godber, I.M., Lawson, N., Hosking, D.J., 2004. The relationship between vitamin D and parathyroid hormone: calcium homeostatis, bone turnover, and bone mineral density in postmenopausal women with established osteoporosis. *Bone.* **35**, 312-319.

Salameh, W.A., Redor-Goldman, M.M., Clarke, N.J., Reitz, R.E., Caulfield, M.P., 2010. Validation of a total testosterone assay using high-turbulence liquid chromatography tandem mass spectrometry: total and free testosterone reference ranges. *Steroids*. **75**, 169-175.

Schellen, A., Ooms, B., van de Lagemaat, D., Vreeken, R., van Dongen, W.D., 2003. Generic solid phase extraction-liquid chromatography–tandem mass spectrometry method for fast determination of drugs in biological fluids. *Journal of Chromatography B*. **788**, 251–259.

Schlingmann, K.P., Kaufmann, M., Weber, S., Irwin, A., Goos, C., John, U., Misselwitz, J., Klaus, G., Kuwertz-Broking, E., Fehrenbach, H., et al., 2011. Mutations in CYP24A1 and idiopathic infantile hypercalcemia. *New England Journal of Medicine*. **365**, 410-421.

Schoentgen, F., Metz-Boutigue, M.H., Jolles, J., Constans, J., Jolles, P., 1985. Homology between the human vitamin D binding protein (group-specific component), alpha-fetoprotein and serum albumin. *FEBS Letters*. **185**, 47-50.

Schoentgen, F., Metz-Boutique, M.H., Jolles, J., Constans, J., Jolles, P., 1986. Complete amino acid sequence of human vitamin D-binding protein (group-specific component): evidence of a three-fold internal homology as in serum albumin and alpha-fetoprotein. *Biochimica et Biophysica Acta.* **871**, 189-198.

Scott, K.B., Turko, I.V., Phinney, K.W., 2015. Quantitative performance of internal standard platforms for absolute protein quantification using multiple reaction monitoring-mass spectrometry. *Analytical Chemistry*. **87**, 4429-4435.

Seamans, K.M. & Cashman, K.D., 2009. Existing and potentially novel functional markers of vitamin D status: a systematic review. *Americal Journal of Clinical Nutrition*. **89**, 1997-2008.

Sempos, C.T., Vesper, H.W., Phinney, K.W., Theinpont, L.M., Coates, P.M., Vitamin D standardization program, 2012. Vitamin D status as an international issue: national surveys and the problem of standardization. *Scandinavian Journal of Clinical and Laboratory Investigation. Supplementum.* **242**, 32-40.

Shah, I., James, R., Barker, J., Petroczi, A., Naughton, D.P., 2011. Misleading measures in vitamin D analysis: a novel LC-MS/MS assay to account for epimers and isobars. *Nutrition Journal*. **10**, 46-55.

Shi, T., Su, D., Liu, T., Tang, K., Camp II, D.G., Qian, W.J., *et al*. 2012. Advancing the sensitivity of selected reaction monitoring-based targeted quantitative proteomics. *Proteomics*. **12**, 1074–1092.

Shi, Y., Chang, J.S., Esposito, C.L., Lafontaine, C., Berube, M.J., Fink, J.A., Espourteille, F.A., 2012. Rapid screening for pesticides using automated online sample preparation with a high-resolution benchtop Orbitrap mass spectrometer. *Food Additives and Contaminants Part A – Chemistry Analysis Control Exposure & Risk Assessment*. **28**, 1383-1392.

Singh, R.J., Taylor, R.J., Satyanarayana, R., Grebe, S.K.G., 2006. C-3 epimers can account for a significant proportion of total circulating 25-hydroxyvitamin D in infants, complicating accurate measurement and interpretation of vitamin D status. *Journal of Clinical Endocrinology and Metabolism*. **91**, 3055-3061.

Singh, R.J., Hines, J.M., Lopez, M.F., Krastins, B., Hoofnagle, A.N. 2015. Mass spectrometric immunoassay raises doubt for the existence of parathyroid hormone fragment 7-84. *Clinical Chemistry*. **61**, 558-560.

Snellman, G., Melhus, H., Gedeborg, R., Byberg, L., Berglund, L., Wernwroth, L., Michaelsson, K., 2010. Determining vitamin D status: a comparison between commercially available assays. *PloS One*. **5**, doi: 10.1371/journal.pone.0011555.

Souberbielle, J.C., Friedlander, G., Cormier, C., 2006. Practical considerations in PTH testing. *Clinica Chimica Acta.* **366,** 81-89.

Speeckaert, M., Huang, G., Delanghe, J., Taes, Y.E.C., 2006. Biological and clinical aspects of the vitamin D binding protein (Gc globulin) and its polymorphisms. *Clinica Chimica Acta*. **372**, 33-42.

St. Arnaud, R., 2010. CYP24A1-deficient mice as a tool to uncover a biological activity for vitamin D metabolites hydroxylated at position 24. *Journal of Steroid Biochemistry and Molecular Biology.***121**, 254-256.

Steen, H. & Mann, M., 2004. The ABC's (and XYZ's) of peptide sequencing. *Nature Reviews Molecular and Cellular Biology*. **5**, 699-711.

Stepman, H.C.M., Vanderroost, A., Stockl, D., Theinpont, L.M., 2011. Full-scan mass spectral evidence for 3-epi-25-hydroxyvitamin D(3) in serum of infants and adults. *Clinical Chemistry and Laboratory Medicine*. **49**, 253-256.

Stepman, H.C., Vanderroost, A., Van Uytfanghe, K., Theinpont, L.M., 2011a. Candidate reference measurement procedures for serum 25-hydroxyvitamin D3 and 25-hydroxyvitamin D2 by using isotope-dilution liquid chromatography-tandem mass spectrometry. *Clinical Chemistry*. **57**, 441-448.

Sturgeon, C.M., 2014. Common decision limits - The need for harmonised immunoassays. *Clinica Chimica Acta.* **432,** 122-126.

Sturgeon, C.M., Sprague, S.M., Metcalfe, W., 2011. Variation in parathyroid hormone immunoassay results-a critical governance issue in the management of chronic kidney disease. *Nephrology Dialysis Transplantation.* **26,** 3440-3445.

Su, Z., Narla, S.N., Zhu, Y., 2014. 25-Hydroxyvitamin D: analysis and clinical application. *Clinica Chimica Acta*. **433**, 200-205.

Svasti, J., Kurosky, A., Bennett, A., Bowman, B.H., 1979. Molecular basis for the 3 major forms of human serum vitamin D binding protein (group-specific component). *Biochemistry*. **18**, 1611-1617.

Synge, R.L., 1939. Experiments on amino-acids: the partition of acetamino-acids between immiscible solvents. *Biochemical Journal*. **33**, 1913-1917.

Tai, S.S-C., Bedner, M., Phinney, K. 2010. Development of a candidate reference measurement procedure for the determination of 25-hydroxyvitamin-D3 and 25-hydroxyvitamin-D2 in human serum using isotope-dilution liquid chromatography-mass spectrometry. *Analytical Chemistry*. **82**, 1942-1948.

Tai, S.S-C. & Nelson, M.A., 2015. Candidate reference measurement procedure for the determination of (24R),25-dihydroxyvitamin D3 in human serum using isotope-dilution liquid chromatography-tandem mass spectrometry. *Analytical Chemistry* **87**, 7964-7970.

Taniguchi, M., Tanaka, M., Hamano, T., Nakanishi, S., Fuji, H., Kato, H., Koiwa, F., Ando, R., Kimata, N., Akiba, T., Kono, T., Yokoyama, K., Shigematsu, T., Kakuta, T., Kazama, J.J., Tominaga, Y., Fukagawa, M., 2011. Comparison between whole and intact parathyroid hormone assays. *Therapeutic Apheresis and Dialysis*. **15**, S42-S49.

Tashjian, A.H., Munson, P.L., Ontjes, D.A., 1964.Alkylation and oxidation of methionine in bovine parathyroid hormone – effects on hormonal activity and antigenicity. *Biochemistry*. **3**, 1175-1182.

Thomas, A., Schänzer, W., Delahaut, P., Thevis, M. 2012. Immunoaffinity purification of peptide hormones prior to liquid chromatography-mass spectrometry in doping controls. *Methods.***56**, 230-235.

Torres, P.U., 2006. The need for reliable serum parathyroid hormone measurements. *Kidney International.* **70,** 240-243.

Touchstone, J.C., 1993. History of chromatography. *Journal of Liquid Chromatography*. **16**, 1647-1665.

Tswett, M., 1906. Adsorptionsanalyse und chromatographische methode. Anwendung auf die Chemie des Chlorophylls. *Berichte der Deutschen botanischen Gesellschaft.* **24**, 384-393.

Turner, C.T., Dalton, N, Inaoui, R., Fogelman, I., Fraser, W.D., Hampson, G., 2013. Effect of a 300,000-IU loading dose of ergocalciferol (vitamin D2) on circulating 1,25-(OH)2-

vitamin D and fibroblast growth factor 23 (FGF-23) in vitamin D insufficiency. *Journal of Clinical Endocrinology & Metabolism*. **98**, 550-556.

Van Deemter, J.J., Zuiderweg, F.J., Klinkenburg, A., 1956. Longitudinal diffusioin and resistance to mass transfer as causes of nonideality in chromatography. *Chemical Engineering Science*. **5**, 271-289.

van den Broek, I., Sparidans, R.W., Schellens, J.H.M., Beijnen, J.H.,2010. Quantitative assay for six potential breast cancer biomarker peptides in human serum by liquid chromatography coupled to tandem mass spectrometry. *Journal of Chromatography B.***878**, 590-602.

Vermeulen, A., 2004. Reflections concerning biochemical parameters of androgenicity. *The Ageing Male*. **7**, 280-289.

Vogeser, M., Kyriatsoulis, A., Huber, E., Kobold, U., 2004. Candidate reference method for the quantification of circulating 25-hydroxyvitamin D3 by liquid chromatgraphy-tandem mass spectrometry. *Clinical Chemistry*. **50**, 1415-1417.

Vogeser, M., 2010. Quantification of circulating 25-hydroxyvitamin D by liquid chromatography-tandem mass spectrometry. *Journal of Steroid Biochemistry and Molecular Biology*. **121**, 565-573.

Vogeser, M., Bacher, S., Seger, C., 2014. Challenges in describing vitamin D status and activity. *LaboratoriumsMedizin***38**, 1-10.

Vogeser, M. & Kirchhoff, F., 2011. Progress in automation of LC-MS in laboratory medicine. *Clinical Biochemistry.* **44**, 4-13.

Vogeser, M. & Seger, C. 2008. A decade of HPLC-MS/MS in the routine clinical laboratory – goals for further development. *Clinical Biochemistry*. **41**, 649-662.

Wagner, D., Hanwell, H.E., Schnabl, K., Yazdanpanah, M., Kimball, S., Fu, L., Sidhom, G., Rousseau, D., Cole, D.E., Vieth, R., 2011. The ratio of serum 24,25-dihydroxyvitamin D3 to 25-hydroxyvitamin D3 is predictive of 25-hydroxyvitamin D3 response to vitamin D3 supplementation. *Journal of Steroid Biochemistry and Molecular Biology.* **126**, 72-77.

Watson, D., Setchell, K.D.R., Ross, R., 1991. Analysis of vitamin D and its metabolites using thermospray liquid chromatography/mass spectrometry. *Biomedical Chromatography*. **5**, 153-160.

Wielders, J.P.M. & Wijnberg, F.A., 2009. Preanalytical stability of 25(OH)-vitamin D3 in human blood or serum at room temperature: solid as a rock. *Clinical Chemistry*. **55**, 1584-1585.

Wilm, M., 2011. Principles of electrospray ionization. *Molecular and Cellular Proteomics*. 10, p.M111.009407-M111.009407

Wolf, G., 2004. The discovery of vitamin D: the contribution of Adolf Windaus. *Journal of Nutrition*. 134, 1299-1302.

Wright, M., Couchman, L., Halsall, D.J., 2011. Turbulent flow liquid chromatography-tandem mass spectrometry for the analysis of bioavailable testosterone in serum. *Endocrine Abstracts*. **25**, 76.

Wright, M.J.P., Halsall, D.J., Keevil, B.G., 2012. Removal of 3-epi-25-hydroxyvitamin D3 interference by liquid chromatography-tandem mass spectrometry is not required for the measurement of 25-hydroxyvitamin D3 in patients older than 2 years. *Clinical Chemistry*. **58**, 1719-1720.

Wu, S.T., Xing, J., Apedo, A., Wang-Iverson, D., Olah, T., Tymiak, A.A., Zhao, N., 2004. High-throughput chiral analysis of albuterol enantiomers in dog plasma using on-line sample extraction/polar organic mode chiral liquid chromatography with tandem mass spectrometric detection. *Rapid Communications in Mass Spectrometry*. **18**, 2531-2536.

Xue, Y., He, X., Huan-De, L., Yang, D., Miao, Y., Hua-Lin, C., Mi-Mi, T., Rui-Li, D., Pei, J. 2015. Simultaneous quantification of 25-hydroxyvitamin D3 and 24,25-dihydroxyvitamin D3 in rats shows strong correlations between serum and brain tissue levels. *International Journal of Endocrinology.* Article number 296531, doi 10.1155/2015/296531 [Epub 2015, Dec 2].

Yalow, R.S. & Berson, S.A., 1960. Immunoassay of endogenous plasma insulin in man. *Journal of Clinical Investigation*. **39**, 1157-1175.

Yang, F., Brune, J.L., Naylor, S.L., Cupples, R.L., Naberhaus, K.H., Bowman, B.H., 1985. Human group-specific component (Gc) demonstrates striking homology with the albumin family of genes. *Proceedings of the National Academy of Sciences of the United States of America*. **82**, 7994-7998.

Yang, Y., Rogers, K., Wardle, R., El-Khoury, J.M., 2016. High-throughput measurement of 25-hydroxyvitamin D by LC-MS/MS with separation of the C3-epimer interference for pediatric populations. *Clinica Chimica Acta*. **454**, 102-106.

Yetley, E.A., Pfeiffer, C.M., Schleicher, R.L., Phinney, K.W., Lacher, D.A., Christakos, S., Eckfeldt, J.H., Fleet, J.C., Howard, G., Hoofnagle, A.N., Hui, S.L., Lensmeyer, G.L., Massaro, J., Peacock, M., Rosner, B., Wiebe, D., Bailey, R.L., Coates, P.M., Looker, A.C., Sempos, C., Johnson, C.L., Picciano, M.F., Vitamin D Roundtable on the NHANES monitoring of serum 25(OH)D:assay challenges and options for resolving them, 2010. NHANES monitoring of serum 25-hydroxyvitamin D: a roundtable summary. *Journal of Nutrition*. **140**, 2030-2045S.

Zahradnik, R.J. & Lavigne, J.R. 2011. Assay for the detection of phosphorylated PTH. US Patent Number 8,012,694, filed September 2006.

Zeng, W., Fisher, A.L., Musson, D.G., Qui Wang, A., 2004. High-throughput liquid chromatography for drug analysis in biological fluids: investigation of extraction column life. *Journal of Chromatography B*. **806**, 177–183.

Zerwekh, J.E., 2008.Blood biomarkers of vitamin D status. *Americal Journal of Clinical Nutrition*. 87, 1087-1091S.

Zhang, C.X., Weber, B.V., Thammavong, J., Grover, T.A., Wells, D.S., 2006. Identification of carboxyl-terminal peptide fragments of parathyroid hormone in human plasma at low-picomolar levels by mass spectrometry. *Analytical Chemistry.* **78,** 1636-1643.

Zhang, Y.V. & Rockwood, A., 2015. Impact of automation on mass spectrometry. *Clinica Chimica Acta*. **450**, 298-303.

Zhou, S., Zhou, H., Larson, M., Miller, D.L., Mao, D., Jiang, X., Naidong, W., 2005. High throughput biological sample analysis using on-line turbulent flow extraction

combined with monolithic column liquid chromatography/tandem mass spectrometry. *Rapid Communications in Mass Spectrometry*. **19**, 2144-2150.

Zimmer, D., Pickard, V., Czembor, W., Muller, C., 1999. Comparison of turbulent-flow chromatography with automated solid-phase extraction in 96-well plates and liquid-liquid extraction used as plasma sample preparation techniques for liquid chromatography-tandem mass spectrometry. *Journal of Chromatography A*. **854**, 23-35.

Zimmerman, M.K., Kumar, V., Maine, G.N., Sykes, E., 2012. Discrepant intact parathyroid hormone result by immunoassay. *Clinica Chimica Acta.* **413,** 344-345.

Zull, J.E., Smith, S.K., Wiltshire, R. 1990. Effect of methionine oxidation and deleted amino-terminal residues on the conformation of parathyroid hormone. Circular dichroism studies. *Journal of Biological Chemistry*. **265**, 5671-5676.